

T
482
GVP

PETROLOGY AND TECTONICS OF THE CENTRAL CRYSTALLINES BETWEEN BHAGIRATHI AND YAMUNA VALLEYS, GARHWAL HIMALAYA

A THESIS

Submitted in fulfilment of the

requirements for the award of the degree

of

DOCTOR OF PHILOSOPHY

University of Roorkee, Roorkee

Certified that the attached Thesis/
Dissertation has been accepted for the
award of Degree of Doctor of
Philosophy / ~~Master of Engineering~~

~~Earth Science~~ vide notification
No. Ex/12/E19 dated 10.4.1984

[Handwritten signature]

Asstt. Registrar (Exam)

[Handwritten mark]

By

SURINDER K. GUPTA



[Handwritten date]
20.7.84



DEPARTMENT OF EARTH SCIENCES
UNIVERSITY OF ROORKEE
ROORKEE-247667 (INDIA)

December, 1982



Candidate's Declaration

I hereby certify that the work, which is being presented in the thesis entitled "PETROLOGY AND TECTONICS OF THE CENTRAL CRYSTALLINES BETWEEN BHAGIRATHI AND YAMUNA VALLEYS, GARHWAL HIMALAYA" in fulfilment of the requirement for the award of the Degree of Doctor of Philosophy, submitted in the Department of Earth Sciences of the University, is an authentic record of my own work carried out during a period from April 1978 to October 1982 under the supervision of Dr. V. K. S. Dave, Professor and Dr. A.K. Jain, Reader.

The matter embodied in this thesis has not been submitted by me for the award of any other degree.

Candidate's signature

Handwritten signature of Surinder K. Gupta in blue ink.

(SURINDER K. GUPTA)

This is to certify that the above statement made by the candidate is correct to the best of my knowledge.

Signatures of Supervisors

Handwritten signature of V. K. S. Dave in blue ink.

(V. K. S. DAVE) PROFESSOR & HEAD

Department of Earth Sciences

University of Roorkee

ROORKEE-247672

Handwritten signature of A. K. Jain in blue ink.

(A. K. JAIN)

READER IN GEOLOGY

Department of Earth Sciences,

University of Roorkee,

ROORKEE-247672

Department of Earth Sciences
University of Roorkee
Roorkee-247667 (India)

ABSTRACT

The area under investigation forms a part of the Central Himalaya in Uttarkashi District along the Bhagirathi and Yamuna Valleys. The rocks exposed in the area belong to three distinct groups : the Garhwal Group, the Bhatwari Group and the Suki Group. The latter two have been considered as parts of the Central Crystallines.

The Garhwal Group is represented by the Gamri Quartzite lying below the Main Central Thrust (MCT) and the Banas and Janki Chatti Formations, which are tectonically involved slices of this Group with the Central Crystallines (migmatites and metasediments) within the Central Himalaya. The Banas Formation is comprised of thin to enormously thick ^(upto 850m) horizons of quartzite and quartz-sericite schist and bear a very strong similarity with the Gamri Quartzite in terms of lithology and heavy mineral assemblage. The Banas Formation is overlain by calc-schist of the Janki Chatti Formation with a gradational contact.

Immediately overlying the MCT, the Bhatwari Group reveals atleast one stage of deformation and metamorphism more than the rocks being referred to as the Suki Group. The Bhatwari Group is, thus, the oldest group in the area, as evidenced by petrographic and structural data and the Rb/Sr ^{whole rock} _^ isochron ages from the adjoining Bhillangana Valley (Chaili gneiss- 2150 my), The Bhatwari Group is separated from the Suki Group by the intervening tectonic slice of the low grade metamorphics of the Garhwal Group; the northern contact of which is marked by the Joti Bhandali Thrust (JBT).

The main rock types of the Bhatwari Group are chlorite schist, phyllonite, augen gneiss and schist, quartz-mica schist, garnetiferous mica schist, amphibolite and migmatite. The group is characterized by at least four phases of deformation, three phases of metamorphism and two phases of migmatization. The rocks belong mainly to the garnet grade and have undergone retrogressive metamorphism near the tectonic margins. The intensity of migmatization is maximum towards south and decreases gradually further northwards. The rocks are generally dipping due NE to NNE.

The Bhatwari Group is also characterized by the presence of several bands of amphibolite which represent the original basic sills. Various standard plots, indices and ratios were used to study the geochemistry of these amphibolites. Their parental nature was deciphered to be tholeiitic basalt resembling Karoo dolerite and occupy the position of middle differentiate. From the trace element studies, it is evident that the original rock was continental tholeiitic dolerite which could have crystallized at a depth of 40 to 50 km and that was far off from the primitive magma source.

The rocks overlying the JBT and extending upto Jhala in the Bhagirathi Valley and upto Yamnotri in the Yamuna Valley belong to the Suki Group. The Suki Group is characterized by an increasing grade of metamorphism from garnet grade near the JBT to sillimanite grade towards the top, thus representing an inverted metamorphic sequence. The degree of migmatization in the Suki Group similarly increases towards north.

Chemical data from the migmatite and the country rock of the Bhatwari Group and the Suki Group reveal that composition of anatectic melts producing these migmatites and formed during different periods of earth history was not significantly different, although ~~the~~ isochemical nature of transformations of country rocks into migmatite are decipherable. The normative mineral plots (Q-Ab-Or and An-Ab-Or) for migmatite fall near the cotectic lines when compared with experimental diagrams and reveal that the migmatite of both groups have been formed due to anatexis. The anatectic origin of migmatite is further supported from trace element data. Large variability in concentration with the intensity of migmatization indicates an external source of migmatizing fluids. Co/Ni and Sb/Bi ratios of these rocks also suggest a hydrothermal activity in the area.

Several traces of sulphide mineralization have been located in the Bhatwari Group. The mineralization is related to quartz and quartz-calcite veins. The main mineralization is pyrite + pyrrhotite \pm sphalerite \pm chalcopyrite \pm galena. A higher Co/Ni ratio in pyrite from Janki Chatti (average 1.09) and Banas (average 1.19) and low Sb/Bi ratio (average 0.46) in galena from Pindki indicates a relatively high temperature hydrothermal environment. Fluid inclusion studies of quartz from quartz sulphide veins reveal a minimum temperature of formation as 180-320°C.

On the basis of geological, petrological, structural, geochemical and radiometric data a tectonic model for the

geological evolution of the Central Himalaya has been postulated in the present work in which deformation of a Precambrian microcontinent has been postulated during the Himalayan Orogeny.

A C K N O W L E D G E M E N T

The present investigations were initiated under the UGC sponsored project "Integrated Earth Science Investigations in the Garhwal-Kumaun Himalaya" in 1978. Since January 1981, the research work was carried out while the author was awarded a UGC fellowship from the Department of Earth Sciences, University of Roorkee, Roorkee.

I express my deep sense of gratitude and indebtedness to Prof. V.K.S. Dave and Dr. A.K. Jain for their inspiring guidance, ceaseless encouragement and critical reading of the manuscript. Facilities for carrying out this work were generously provided by the Department of Earth Sciences, University of Roorkee, Roorkee for which I am grateful to Prof. R.S. Mithal, B.B.S. Singhal and V.K.S. Dave.

The geochemical analysis for chromium-determination was carried out at the Wadia Institute of Himalayan Geology. I am grateful to Dr. N.J. Singh for his untiring efforts and to Dr. K.C. Mittal (U.S.I.C.), Dr. G.C.S. Gaur (W.I.H.G.), Mr. R. Pant, Mrs. Neelima Gupta (U.S.I.C.) and Mr. Rakesh Bahuguna in chemical analyses and X-ray studies.

I express my sincere thanks to Prof. K.K. Nagpaul, Dr. Nand Lal, Dr. Kiran Bal and Mr. Pradeep Sharma of the Physics Department, Kurukshetra University, Kurukshetra for their help in fission-track dating of the samples from the Bhagirathi Valley.

I am thankful to the Director-General, Geological Survey of India for providing me the opportunity to complete this work by way of extending my joining period. The encouragement by Dr. S.S. Ghodke, Director, Maharashtra Circle West, Geological Survey of India, Pune in the completion of this work is highly appreciated.

My sincere thanks are due to Dr. S.K. Jaireth for helping me in ore-microscopy and fluid-inclusion studies. The epicentral map of microearthquakes was kindly provided by Prof. R. Chander and Mrs. I. Sarkar on the basis of the recordings done by various persons in the D.S.T. and U.G.C. sponsored projects. Discussions held with Dr. V.C. Thakur (W.I.H.G.), Prof. K.S. Valdiya (Kumaun University), Prof. S.K. Ghosh (Jadavpur University), Prof. K. Naha (I.I.T., Kharagpur), Dr. S. Kumar (W.I.H.G.), Dr. Alok Gupta and Dr. A.K. Awasthi during the course of the present work are highly appreciated.

Thanks are due to Mr. R. Sreedhar, Mr. K. Gohain, Mr. Ashwini Awasthi, Mr. B.C. Joshi, Mr. Vinod Bansal, Mr. D.K. Bharkatiya and Mrs. Nasreen Khan who helped me at various stages.

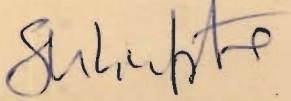
The affection and encouragement rendered to me by Dr. H. Sinval, Mr. Praveen Gupta, Mrs. Mamta Gupta, Mr. K.K. Dhagat and Mr. G.R.K. Nair during the course of the work is warmly appreciated.

I wish to record my warmest appreciation to Miss Margaret Dias for the pains she took in typing the manuscript. I also thank Mr. and Mrs. Dias and Miss. Mary Dias for their cooperation.

I wish to thank Mr. R.C. Punj and Mr. Ram Dal for their untiring assistance in preparation of thin and polished sections; Mr. Chahi Ram for the preparation of drawings and Mr. S.D. Sharma in the reproduction of photographs.

Constant encouragement made by my mother and brothers have provided me the necessary inspiration.

Lastly, I am grateful to all the members of the Earth Sciences Department who have helped me from behind the scene.


(SURINDER K. GUPTA)

C O N T E N T

	Page
CHAPTER I INTRODUCTION	
1.1 Survey of literature on the area ..	2
1.2 Scope of the present work ..	5
1.3 Methods of investigations ..	5
1.3.1 Field Investigations ..	5
1.3.2 Laboratory Investigations ..	6
CHAPTER II GEOLOGICAL SET-UP	
2.1 Lithotectonic framework ..	9
2.2 Garhwal Group ..	12
2.2.1 Gamri Quartzite ..	12
2.2.2 Banas Formation ..	13
2.2.3 Janki Chatti Formation ..	15
2.3 Central Crystallines ..	17
2.3.1 Bhatwari Group ..	18
2.3.2 Suki Group ..	28
2.4 Late phase magmatic and hydrothermal activities ..	33
2.4.1 Pegmatites ..	33
2.4.2 Meta-andesite ..	34
2.4.3 Metadolerite ..	35
2.4.4 Quartz and quartz-calcite veins ..	36
2.4.5 Quartz-tourmaline veins ..	36

	Page
CHAPTER III STRUCTURE AND TECTONICS	
3.1 Small scale structures ..	38
3.1.1 Structural elements ..	39
3.1.2 Mutual relationship between structures ..	46
3.1.3 Orientation of planar and linear structures ..	48
3.2 Large scale structures ..	53
3.2.1 Faults ..	53
3.2.2 Postulated lineaments between Yamuna and Bhagirathi Valleys ..	60
3.2.3 Folds ..	61
3.2.4 Thrusts ..	64
CHAPTER IV PETROGRAPHY	
4.1 Garhwal Group ..	73
4.1.1 Quartzite and quartz-sericite- chlorite schist ..	74
4.1.2 Heavy minerals from Banas Formation ..	76
4.1.3 Janki Chatti Formation ..	80
4.1.4 Other rock types ..	83
4.2 Bhatwari Group ..	86
4.2.1 Metasedimentaries ..	87
4.2.2 Cataclastic and retrograde metamorphism (strong) ..	97
4.2.3 Metamorphosed igneous rocks ..	99
4.2.4 Migmatite ..	105

	Page
4.3 Suki Group ..	115
4.3.1 Regionally metamorphosed (poorly migmatized) rocks ..	116
4.3.2 Rocks showing cataclastic and retrograde metamorphism ..	125
4.3.3 Igneous derivatives ..	127
4.4 Studies of feldspar ..	132
4.4.1 Triclinicity ..	134
 CHAPTER V GEOCHEMISTRY OF AMPHIBOLITE	
5.1 Analytical techniques ..	136
5.1.1. Major elements ..	136
5.1.2 Trace elements ..	137
5.2 Results ..	138
5.2.1 Magmatic nature of progenitor ..	139
5.2.2 Composition of progenitor ..	141
5.2.3 Intrusive or extrusive nature of the progenitor ..	146
5.2.4 Depth of source magma ..	147
5.2.5 Nature of source magma ..	148
5.2.6 Time of emplacement ..	151
5.3 Petrogenetic model ..	152
 CHAPTER VI PETROCHEMISTRY OF MIGMATITE	
6.1 Geochemistry ..	157
6.1.1 Techniques ..	157
6.1.2 Results ..	158
6.2 Trace elements distribution ..	161
6.3 Genesis of migmatite ..	166

	Page
6.3.1 Migmatite from the present area ..	169
6.4 P-T Conditions ..	181
CHAPTER VII SULPHIDE MINERALIZATION	
7.1 Mineralization at Janki Chatti ..	185
7.2 Mineralization at Benas ..	186
7.3 Mineralization at Pindki ..	187
7.4 Geochemistry and trace elements ..	188
7.4.1 Techniques ..	188
7.4.2 Results ..	189
7.5 Fluid inclusion studies ..	190
7.6 Decrepitation studies ..	192
7.7 Discussion and conclusions ..	192
CHAPTER VIII RADIOMETRIC DATING	
8.1 Rb/Sr ages in Garhwal-Kumaun Himalaya ..	195
8.1.1 Kumaun (Central Himalaya) ..	195
8.1.2 Bhillangana Valley (Central Himalaya) ..	196
8.1.3 Askot and Baijnath Crystallines ..	197
8.1.4 Kiodal Gneiss, Ramgarh (Lesser Himalaya) ..	198
8.1.5 Simla-Dudatoli-Almora belt (Lesser Himalaya) ..	198
8.2 Rb/Sr ages in Himachal Pradesh ..	199
8.2.1 Mandi-Dalhousie Granite ..	199
8.2.2 Nirath-Baragaon Gneiss ..	201

	Page
8.2.3 Bandal Granite and Manikaran Quartzite (Rampur Window) ..	202
8.2.4 Kulu-Manali-Rohtang-Jaspa Region (Salakhala/Central Gneiss) ..	202
8.3 Geological interpretation of Rb/Sr whole rock ages from the NW-Himalaya ..	204
8.4 Fission track dating ..	208
8.4.1 Experimental procedure ..	209
8.4.2 Results and discussion ..	211
8.4.3 Cooling and uplift rates ..	213
8.4.4 Cooling and uplift rates from the Bhagirathi Valley ..	215
CHAPTER IX DISCUSSION AND CONCLUSIONS	
9.1 The Main Central Thrust (MCT) ..	219
9.2 Deformation and metamorphism ..	220
9.3 Inverted metamorphism ..	222
9.4 Plate tectonics and evolution of the Central Himalaya ..	224
9,4,1 Type of geotectonic element ..	224
9.4.2 Timing and place of collision ..	226
9.5 Present Model ..	229

CHAPTER - I

INTRODUCTION

The term "Central Crystallines" was used by Heim and Gansser (1939) in Garhwal-Kumaun Himalaya to represent granites, migmatites and metamorphic rocks, thrust over the Lesser Himalayan metasediments along the Main Central Thrust (Auden, 1937). The Central Crystallines were earlier classified as Vaikrita System by Hayden (1904) in Himachal Pradesh. Later on various names were introduced in different parts of Himalaya for extensive crystalline rocks such as : Darjeeling gneiss in Darjeeling and Sikkim (Ray, 1947), Takhtsing Group in Bhutan (Gansser, 1964), Tibetan Slab (Bordet et al., 1972) and Himalayan gneiss zone in Nepal (Ohta and Akiba, 1973) and Siang Group in Arunachal Pradesh (Jain et al., 1974). Thakur (1980) suggested that this group forms a more or less continuous belt extending from Kashmir in NW to Siang Valley in Arunachal Pradesh.

The Central Crystallines in Garhwal-Kumaun Himalaya are distributed in the districts of Uttarkashi, Chamoli, Almora and Pithoragarh with probable tectonic slices in Pauri and Nainital districts. Present study relates to the petrology and tectonics of a part of Uttarkashi district, lying between latitude N $30^{\circ}43'$ to $31^{\circ}05'$ and longitude E $78^{\circ}15'$ to $78^{\circ}50'$ (Fig. 1.1) in Uttar Pradesh. The area is included in topographic sheets No.53 J/5, 53 J/9, 53 I/10 and 53 J/12 published by Survey of India in 1962.

The nearest rail heads are Rishikesh and Dehradun from where good all weather roads lead to the area. The best period for field seasons is April to June and September-October, when temperature is moderate and there is no heavy precipitation. Bhagirathi and Yamuna Rivers control the drainage system in the area.

Due to high relief, the intensity of mass movements is high and morphology shows a correlation with structure and lithology. The details on slope stability studies have not been included as a part of this thesis. The references may, however, be made to Gupta and Dave (1982) : Dave, Gupta and Singh (under publication) and Gupta (in preparation).

1.1 SURVEY OF LITERATURE ON THE AREA

The Central Himalaya (Strachey, 1851) in the Bhagirathi and Yamuna Valleys has unfortunately not attracted the attention of many geologists unlike several other sections of the Himalaya. Nevertheless, different opinions and terminology of various lithotectonic units have emerged on the basis of traverses between Uttarkashi-Gangotri and Barkot-Yamunotri by various workers. It would not be out of place to tabulate the various lithotectonic units observed by the author between Uttarkashi-Gangotri and Barkot-Yamunotri alongwith the localities where two lithotectonic units are in contact (Table 1.1).

The first reference to this area was made by Greisbach (1891) who took a few traverses in the Harsil area and classified the rocks into the Vaikrita system (metamorphics and

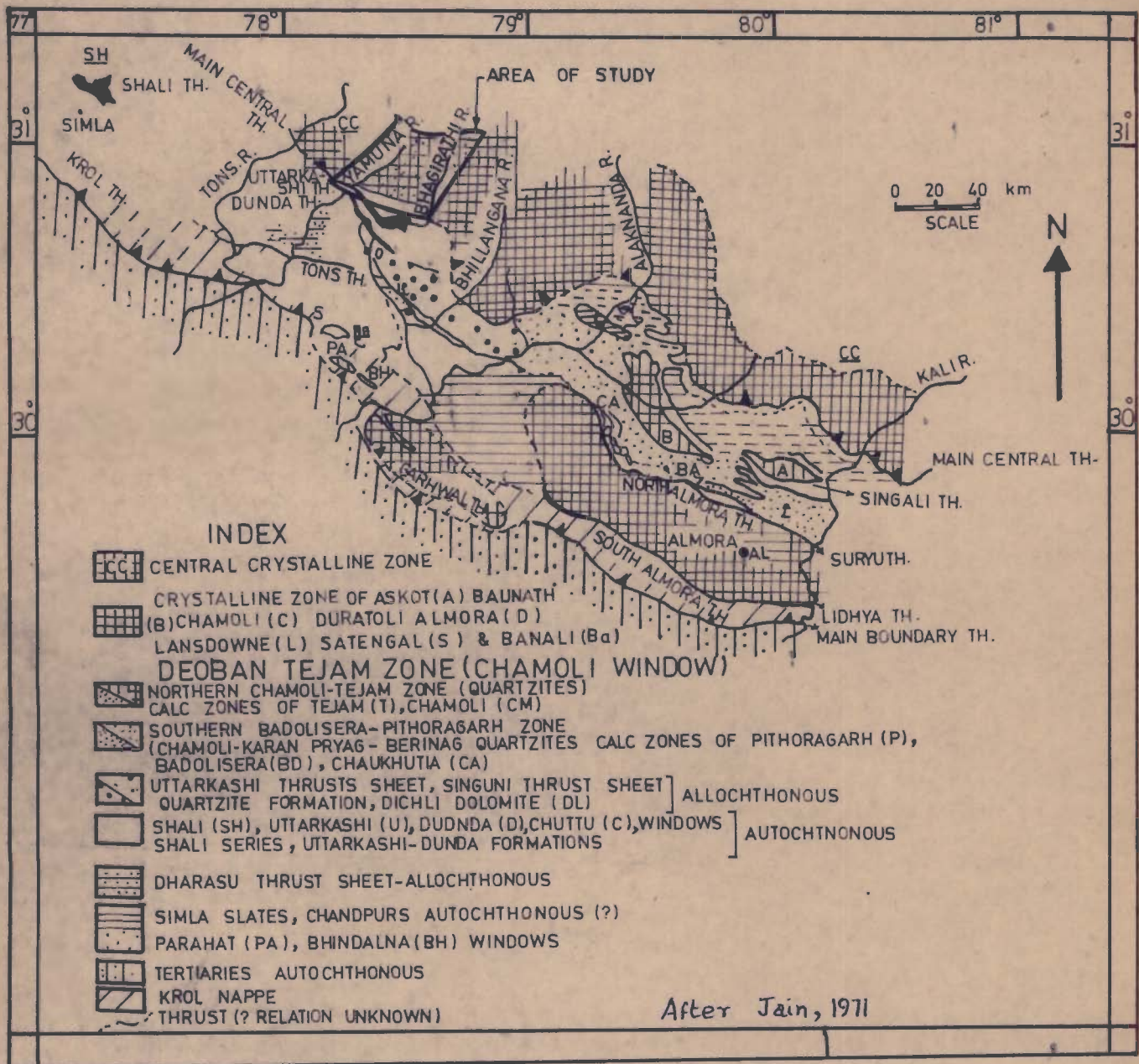


FIG.1.1-TECTONIC MAP OF LESSER HIMALAYAN REGION OF GARHWAL AND KUMAON U.P. [MODIFIED AFTER AUDEN(1937),HEIM & GANESSER (1939),VALDIYA (1962) & GANSSER(1964)], SHOWING THE AREA OF STUDY

TABLE 1.1 MAJOR LITHOTECTONIC UNITS OBSERVED BY THE AUTHOR

<u>Lithotectonic Unit</u>	<u>Main Locality</u>	
	BHAGIRATHI VALLEY	YAMUNA VALLEY
Tourmaline granite	Gangotari	

Porphyroblastic biotite granite	Dharali	

Metasediments of Harsil	Jhala	

Metamorphites and migmatites of Suki Group	JBT Joti	Bhandali Gad

Garhwal Group metasediment		
Metamorphites and migmatites of Bhatwari Group (with slices of Garhwal group metasediment)		

Quartzites and amphibolites of Garhwal Group	MCT Sainj	Wazari

granites) and the Haimanta System (phyllites and quartzites). Auden (1949) remapped the same area and considered that the Vaikrita System actually comprises of mesograde garnet-biotite granulite, garnet-biotite schist, staurolite schist and kyanite schist. He considered that the Haimanta System is lithologically correlatable to the 'Simla slates' and the Chandpurg. He also discovered the tectonic boundary between the Garhwal Group and the Central Crystallines near Sainj and named it as the Main Central Thrust (MCT).

Bhatt (1972) briefly discussed the geology of the Bhagirathi basin, which was the outcome of his 1963 expedition to Shri Kailas. Ranga Rao (1972) took traverses in the U.P. Himalaya and gave a brief account of the geology of the Bhagirathi and Yamuna valley sections. Further, he considered that the marbles exposed near Janki Chatti (author's Janki Chatti Formation) lithologically resemble the Deoban Limestone.

Tewari (1970) has not included present area in his study, although his contribution is of great interest. He regarded the contact between the Harsil metasediments (garnet-biotite schist and biotite schist, traversed by aplite and pegmatite veins and dykes) and the Gangotri granites (biotite granite, tourmaline granite, aplite and pegmatite) as tectonic one and named it as the Gangotri Thrust.

While working on the evolution of eastern Kumaun Himalaya, Mehdi et al. (1972) included the metasediments exposed on the northern side of Jhala bridge into the Martoli Formation. They postulated a tectonic contact near Jhala bridge between the 'green schist facies of rocks' (Martoli Formation) and almandine-amphibolite facies of rocks (Central Crystallines) exposed on the southern side of Jhala bridge. They referred this fault as the Dar-Martoli Fault.

Agarwal and Kumar (1973) carried out the traverse mapping of the Central Crystallines of the Bhagirathi and Yamuna Valleys (Fig. 1.2) and established the lithostratigraphy (Table 1.2). They assigned a pre-tectonic age to metabasic exposed near the MCT at Wazari and Sainj. They have also supported the existence of the Dar-Martoli Fault on the basis of U-shape valley and huge landslide recurrence at Suki.

On the basis of regional traversing in the Central Crystallines, Valdiya (1977, 1978, 1980) considered an abrupt change in grade of metamorphism and petrological character along a dislocation located much to the north of the MCT and called this thrust as the Vaikrita Thrust. Furthermore, Valdiya (1981) considers the latter thrust as the boundary between the Lesser and Central Himalayan subprovinces. Gupta and Dave (1979) have reported their initial findings on the Central Crystallines in these sections wherein a thrust passing through Joti was described. Valdiya (1980) extended his Vaikrita Thrust through this locality giving reference to abstracted structural and petrological evidences (Valdiya, 1973).

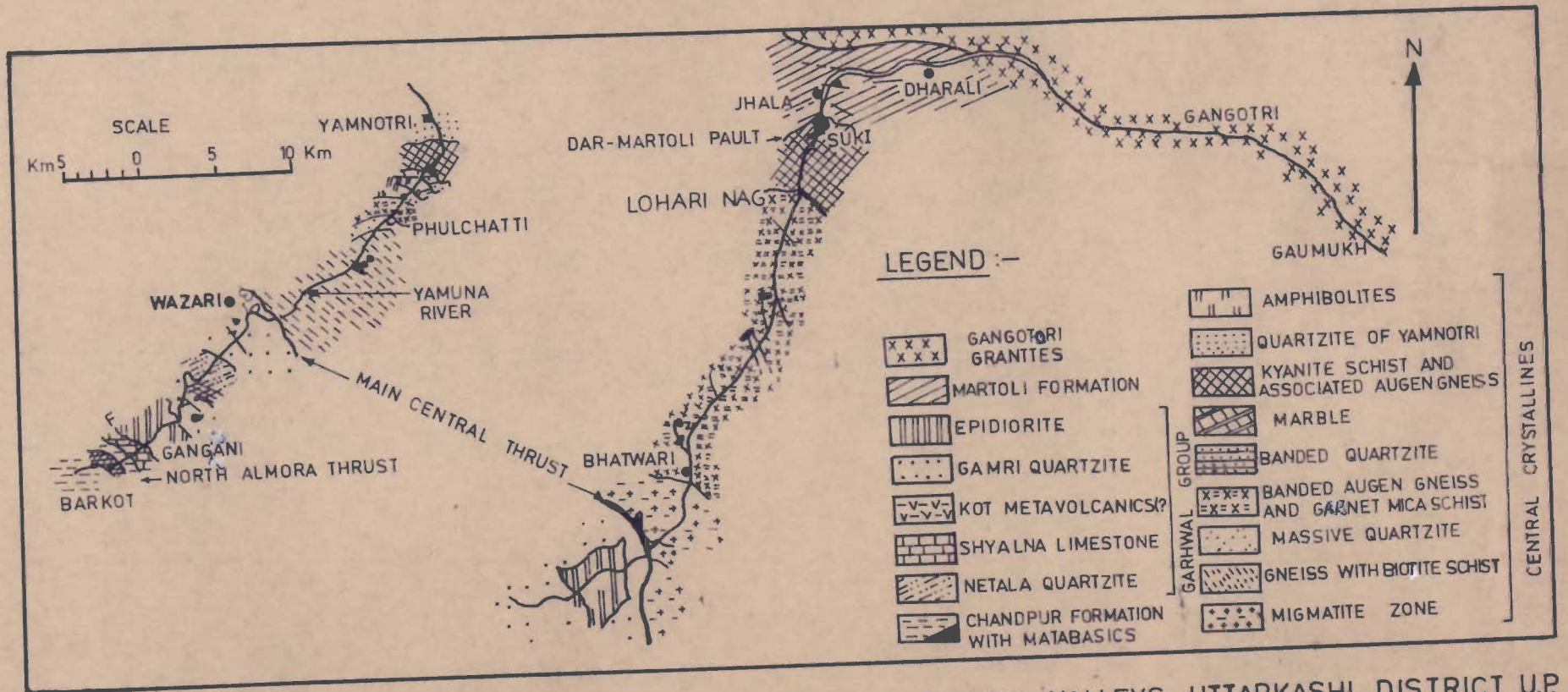


FIG.12-TRAVERSE GEOLOGICAL MAP OF UPPER YAMUNA & BHAGIRATHI VALLEYS, UTTARKASHI DISTRICT, U.P. (AFTER AGARWAL AND KUMAR, 1973)

TABLE 1.2 LITHOSTRATIGRAPHY OF CENTRAL CRYSTALLINES IN
BHAGIRATHI AND YAMUNA VALLEYS (after Agarwal and
Kumar, 1973)

Bhagirathi Valley	Yamuna Valley
Martoli Formation	
_____ Dar-Martoli Fault _____	
	Laminated quartzite near Yamotri temple
Banded augen gneiss	Augen gneiss with kyanite-garnet-mica schist containing tourmaline
Kyanite-garnet-mica schist and interbedded augen and porphyritic gneiss	
Banded augen gneiss and garnet-mica schist containing tourmaline	
Migmatite zone of mica schists gneiss, granite, marble/calc-silicate with amphibolite	Marble with quartzite Banded quartzite Biotite-quartz schist with amphibolite
	Garnet-mica schist Massive quartzite Gneiss with biotite schist
_____ Main Central Thrust _____	
Garhwal Group	

1.2 SCOPE OF PRESENT INVESTIGATIONS

From the previous work referred above, it would be apparent that no detailed study and relationship between various lithotectonic units have been carried out in this region regarding their geology, petrology and tectonics. The nature of contacts between several lithotectonic units forbids a direct correlation with other neighbouring regions of the Himalaya. Any such work would naturally aim at contributing to solve the problem of tectonics and origin of Himalaya. The petrology of individual rock types has been worked out in as much detail as feasible, including the geochemistry and correlation of mineral paragenesis with structural history of the rocks. The ultimate aim was to evolve a comprehensive model of the Himalayan Orogeny as may be applicable to this orogen in general and to this area in particular.

1.3 METHODS OF INVESTIGATIONS

In order to achieve the goal, the following studies were conducted in the field and laboratory.

1.3.1 Field Investigations

The field work was carried out for a period of 6-7 months in different field seasons since April, 1978. Due to inaccessibility and difficult terrain, the geological investigations were mainly confined to roads, mule tracks, foot paths and rivulets (nallah). The important traverses include Sairj-Harsil, Kaldiya-Dodital and Wazari-Yamnotri. These traverses were dealing with the following aspects:

- a. Detailed geological mapping of the area on a 1:50,000 scale.
- b. Collection and plotting of structural data.
- c. Collection of representative samples of all rock types including systematic sampling of amphibolites and migmatites for chemical analysis.

1.3.2 Laboratory Investigations

- a. A critical review of the relevant geological literature.
- b. Preparation of geological and structural maps, cross sections etc.
- c. Petrographic Studies : (i) Study of megascopic characters of all the rock samples. (ii) Mineralogical and textural study of nearly 350 representative thin sections. (iii) Modal analysis of 71 sections of various rock types. (iv) Heavy mineral analysis of 10 samples from quartz-sericite schist for the purpose of correlation. (v) X-ray analysis of 12 samples of feldspar from migmatites and 3 samples of amphibole bearing rocks. (vi) Microchemical staining of rock slabs and thin section with cobalt nitrate and trypan blue reagents to confirm the presence of cordierite.
- d. Chemical analysis of 32 rock samples (13 amphibolites and 19 migmatites and their country rocks).

- e. Separation of 14 sulphide mineral species from ten rock samples, their chemical analysis, ore microscopy and fluid inclusion studies.
- f. Fission track dating of 26 samples (13 apatites, 10 garnets and 3 zircons) was made available by the courtesy of Physics Department, Kurukshetra University, Kurukshetra.

The distribution of important samples used in modal analysis, chemical analysis, X-ray studies, fission track dating and heavy minerals has been shown in the outline geological map of the area (Fig. 1.3).

CHAPTER - II

GEOLOGICAL SET-UP

The problems of stratigraphy, structure and correlation of the crystalline sequences of the Central Himalaya have been a debatable matter. It has not been possible to settle the age of the Central Crystallines satisfactorily so far. These are mainly due to three reasons:

(i) insufficient geological information due to widely spaced traverses in the Central Himalaya, (ii) absence of mappable marker horizons (iii) scanty radiometric data from different sectors of the Himalaya. On the basis of geological and limited Rb/Sr data, Heim and Gansser (1939), Gansser (1964), Bhanot et al. (1975, 1977), Frank et al. (1976), Valdiya (1976), Thakur (1977, 1980), Acharyya (1980), Pande (1980) and Sinha Roy (1980) are of the opinion that the Central Crystallines form a part of the "Precambrian Basement" which has been reactivated during the Himalayan Orogeny (see Chapter 8). In the present study, some of these problems would be imminent as the region incorporates an important sector of the Central Crystallines in the Garhwal Himalaya. This chapter includes the distribution and field characters of different lithological and structural units recorded in the area (Fig. 2.1), while a generalized cross-sections along the Bhagirathi and Yamuna Valleys are shown in figure 2.2

2.1 LITHOTECTONIC FRAMEWORK

During the multidisciplinary project on the "Integrated geological and geophysical investigations in the Garhwal-Kumaon Himalaya" sponsored by the University Grants Commission, New Delhi to the Department of Earth Sciences, ^{Roorkee,} the Central Himalayan terrain between the Yamuna and Dhauliganga Valleys ~~have~~ ^{has} been traversed by a number of investigators. These investigations have clearly demonstrated a very complex lithotectonic setting of the Central Himalaya than hitherto known, (Figure 2.3). A generalised tectonostratigraphy of the Yamuna and Bhagirathi Valleys is described in Table 2.1.

The present area incorporates southernmost lithotectonic units of the Central Himalaya; the lithotectonic successions established for the Bhagirathi and Yamuna Valleys, have been given in Tables 2.2 and 2.3 respectively.

The rocks exposed in the area have been assigned to three groups namely, the Garhwal Group of the Lesser Himalaya, which forms the base over which the hitherto-called 'Central Crystallines are thrust along the Main Central Thrust. The Central Himalaya includes the following lithotectonic units, bounded by thrusts in the present area:

(a) A lowermost basal unit, here called as the Bhatwari Group which is thrust over the Lesser Himalayan Garhwal Group along the Main Central Thrust (MCT).

(b) Imbricate tectonic slices of the Banas Formation and the overlying Janki Chatti Formation of the Garhwal Group.

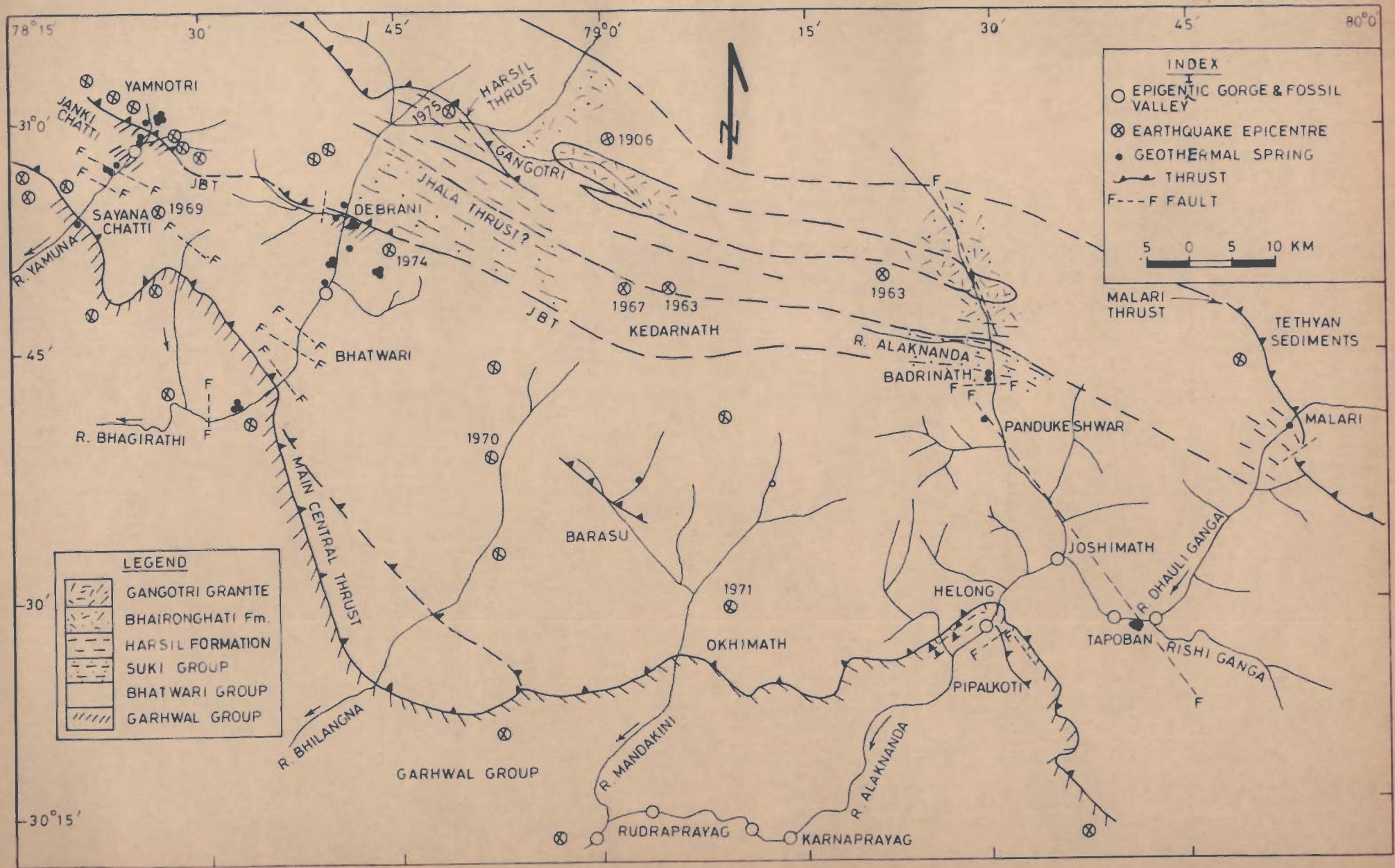


FIG. 23 - GEOLOGICAL MAP OF THE CENTRAL HIMALAYA BETWEEN YAMUNA AND DHAULI-

TABLE 2.1 TECTONO-STRATIGRAPHY OF THE CENTRAL HIMALAYA ALONG
YAMUNA-BHAGIRATHI VALLEYS

Malari Formation	Alternating sequence of phyllite-quartzite	
Gangotri Granite	Tourmaline-muscovite granite	
Bhaironghati granite-gneiss	Porphyroblastic granite-gneiss	
Tectonic Contact		
Harsil Formation	Schist showing normal progressive regional metamorphism, pegmatite intrusives.	
SUKI GROUP	Augen gneiss, migmatite, schist; inverted progressive metamorphism from garnet to sillimanite isograde	
Joti-Bhandali Thrust (JBT)		
Janki Chatti Formation	Calc-schist	
GARHWAL GROUP	Banas Formation	Quartz-sericite schist and amphibolite) Exposed as tectonic slices in the Central Himalaya
Tectonic Contact		
BHATWARI GROUP	Augen gneiss, migmatite, schist, amphibolite (garnet isograde)	
Main Central Thrust (MCT)		
GARHWAL GROUP	Quartzite and amphibolite	
(Gamri Quartzite)		

TABLE 2.2 LITHOTECTONIC SUCCESSION OF THE CENTRAL HIMALAYA
OF THE BHAGIRATHI VALLEY

Basic Intrusive (post MCT)	Metadolerite
	Quartz-muscovite-sillimanite gneiss with pargasite-ferrogedrite gneiss band
	Quartz-biotite-garnet-kyanite schist and gneiss containing 'anatectic portions'.
SUKI GROUP	Quartz-biotite-garnet-schist and gneiss; inter- banded with 'anatectic portions'; thin bands of mylonitic graphite schist
	_____ JBT _____
JANKI CHATTI FORMATION	Calc-schist; development of actinolite schist along tectonic planes
	_____ Tectonic Contact _____
	Amphibolite with 'anatectic portions'; development of hornblende-biotite schist and talc-chlorite schist along major tectonic zones.
BHATWARI GROUP	Garnetiferous-quartz-muscovite schist, cumming- tonite-biotite schist with 'anatectic portions'
	Augen gneiss with 'anatectic portions'
Phyllonite	_____ Main Central Thrust (MCT) _____
GARHWAL GROUP Gamri Quartzite	Massive quartzite and quartz-sericite schist, amphibolite, chlorite-actinolite schist

TABLE 2.3 LITHOTECTONIC SUCCESSION OF THE CENTRAL HIMALAYA
OF THE YAMUNA VALLEY

INTRUSIVES	Meta-andesite and metadolerite
SUKI GROUP	Quartz-biotite-garnet-kyanite schist and gneiss with 'anatectic portions'
	Quartz-chlorite schist, occasionally containing garnet
	_____ JOTI-BHANDALI THRUST (JBT) _____
G Janki A G Chatti R R Formation H O W U A P L	Calc-schist interbanded with quartzite and quartz-sericite schist
Banas Form- ation	Banded quartzite and quartz-sericite schist
	_____ Tectonic Contact _____
	Quartz-biotite-muscovite-garnet schist with 'anatectic portions'
	Quartz-muscovite-tourmaline schist with 'anatectic portions'
BHATWARI GROUP	Quartz-chlorite-biotite schist
	Augen gneiss and quartz-biotite schist with 'anatectic portions'
	Amphibolite and hornblende-biotite schists with 'anatectic portions'
	Mylonitised quartz-biotite schist and gneiss
	_____ MAIN CENTRAL THRUST (MCT) _____
GARHWAL GROUP Gamri Quartzite	Quartz-sericite schist

(c) the Suki Group metamorphics which are thrust over either the Bhatwari Group or the Janki Chatti Formation along the Joti-Bhandali Thrust (abbreviated in this work as the JBT).

Thus, the Bhatwari Group and the Suki Group constitute parts of the 'Central Crystallines'; the other lithotectonic units of 'Central Crystallines' are exposed further north of the present area of investigation. A distinction has been made in the present work between the Central Himalaya and the Central Crystallines, which have been previously used interchangeably by the investigators. The term Central Himalaya has been used in the physiographic sense in this sector of the Garhwal Himalaya, while the Central Crystallines constitute only the medium to high grade polymetamorphic rocks including the magmatic or anatectic derivatives. Thus, the Bhatwari Group, the Suki Group, the Banas Formation and the Janki Chatti Formation would constitute the southern parts of the Central Himalaya, whereas the former two lithotectonic units only would be considered as parts of the Central Crystallines, including the other lithotectonic units exposed in the north of the area. The contacts between the Bhatwari and the Suki Groups are tectonic; degree of metamorphism and migmatization are the other criteria for their separation. The rocks belonging to the Garhwal Group are the least metamorphosed and show no signs of migmatization.

In the Yamuna Valley section, there are several bands of quartzite, calc schist and crystalline limestone ranging in width from 10 to 850 m. The calc schist occurs in similar

manner in the Bhagirathi Valley, although the quartzite is not frequent. These rocks are intimately associated with the Bhatwari Group along the Yamuna Valley and occasionally with the Suki Group of rocks. The quartzite is massive to schistose in appearance similar to the Gamri Quartzite of the Garhwal Group exposed below the overthrust Bhatwari Group, whereas calc schist is similar to the Deoban Limestone (Ranga Rao, 1972). Due to their typical tectonic setting within the Central Himalayan terrain, a question arose if these were parts of the Central Crystallines occurring as imbricate slices of the Garhwal Group. A special effort was made, therefore, to investigate the heavy minerals of quartzite bands. On the basis of heavy mineral studies (Chapter 4), the author is convinced that bands of quartzite within the Central Himalaya of the Yamuna Valley are equivalents of the Gamri Quartzite and represent its imbricate slices. The presence of discrete fractures, strong development of crenulation foliation along the margins of quartzite bands and typical chlorite bearing quartzitic nature characterizing the Gamri quartzite are further evidences supporting above conclusion.

On the other hand, calc schist belonging to the Janki Chatti Formation reveals gradational contact with the overlying quartzite band at Bhaironghati in Yamuna Valley. Hence, the contact between calc schist and quartzite is normal whereas the contacts between any one of these low grade metamorphosed lithounits with migmatite and garnet grade metamorphics are sheared.

2.2 GARHWAL GROUP

The term Garhwal 'series' was introduced by Auden (1949) for extensively developed quartzite, limestone and amphibolite along the Bhagirathi Valley. Prior to this, these rocks were termed as the Barahat series by Auden (1939) and were exposed in the Chamoli Window. Jain (1971) reclassified these rocks into the Garhwal Group and subdivided it into many **formations**, which are essentially comprised of arenaceous sequences and carbonates. The arenaceous rocks have been earlier classified into the Gamri Quartzite along the Bhagirathi and Yamuna Valleys and form a part of Nagni Thank Formation (Agrwal and Kumar, 1973). This quartzite is comparable with the Hudoli Formation (Pachauri, 1972). In the present work, the term Gamri Quartzite has been retained for arenaceous rocks lying to the south of the Main Central Thrust in the Inner Lesser Himalaya along the Bhagirathi and Yamuna Valleys, while a new lithostratigraphic term - the Banas Formation has been introduced for the arenaceous rocks of the Central Himalaya. Calc-schist observed early by other workers but were not stratigraphically named, have been here classified as the Janki Chatti Formation.

2.2.1. Gamri Quartzite

The Gamri Quartzite is well exposed on southern side of Kumalti and Agora in the Bhagirathi Valley and extends further northwest to Wazari in the Yamuna Valley. The quartzite has been separated from the gneiss and schist of the Central

Himalaya by the Main Central Thrust (MCT).

In the vicinity of the MCT, the quartzite attains schistose character and is metamorphosed to quartz-sericite schist and friable schistose quartzite. Massive quartzite is white to greenish white, medium grained and poorly foliated. Schistose quartzite is grayish white, greenish white to greenish gray, fine to medium grained, thinly foliated and friable in nature. Greenish appearance of the quartzite is due to the presence of chlorite patches.

In the schistose quartzite, the foliation has been rendered prominent by mica flakes and quartz grains. The bedding surface is recognised by the presence of graded bedding and colour banding, which indicates right side up position of the Gamri Quartzite. NNW-SSE to NW-SE trending quartzite shows small deviations from this trend at a few localities. The quartzite dips 25-35° due NNE to NE, but its dip also changes to SSE or SE due to folding. The schistose variety at Kumalti contains black tourmaline aligned parallel to the foliation. Three sets of joints have been recorded in the quartzites which show large variation in spacing. In the massive quartzite they are widely spaced, whereas in the schistose quartzite they are closely spaced (1-3 cm).

2.2.2. Banas Formation

Predominantly quartzite and quartz-sericite schist outcrops within the Central Himalaya and occurring with the

Bhatwari Group and the Suki Group in the Yamuna Valley section have been designated as the Banas Formation by the author. In the entire section, these show tectonic contacts with the surrounding rocks. The contact between the Banas Formation and the Janki Chatti Formation is normal to gradational, indicating that both the formations belong to a single lithotectonic unit. The outcrop width of the Banas Formation varies from 10 to 850 m. ~~the~~ the main outcrop at Banas, ~~shows the maximum~~ ^{it} ~~width.~~ At this locality, the quartz ~~is~~ overlain by chlorite schist and underlain by the garnetiferous mica schist.

In the quartz-sericite schist, the foliation has been imparted by the sericite flakes and quartz grains. The bedding foliation is occasionally noticed in the schist by the presence of colour banding. The quartz-sericite schist is greyish white, greenish white to greenish grey, fine to medium grained and show variability in the development of foliation. Thin bands of quartz-sericite schist are highly sheared in comparison to thick horizons, which are mainly affected along the margins by tectonic movements. The extensive crushing of quartz-sericite schist at certain localities has led to the formation of gouges.

The quartz-sericite schist shows large deviations in its regional trend, particularly between Kupara and Phul Chatti indicating the presence of large scale folding of this lithotectonic unit. It dips 26-52° toward NNW or NE. At places, the dip changes toward SW or SE. Three sets of joints can be easily recognised in the schist. They are widely spaced in

the massive variety, whereas in more schistose variety they are closely spaced. The minor structures associated with schist are mineral lineation, slickenside, mesoscopic folds, crenulation cleavage, discrete fractures and shear planes. The slickensides are profusely developed near the tectonic contacts and plunge towards NE or SW.

2.2.3 Janki Chatti Formation

The Janki Chatti Formation encompasses the calc schist with minor amount of interbedded quartzite bands towards the top and thin amphibolite bands in the Yamuna Valley. In the Bhagirathi Valley and the Dodital section quartzite bands are absent, whereas small amphibolite bands do occur being associated with the lower calc schist outcrop.

(a) Calc-schist: In the Bhagirathi Valley, the southern outcrop of calc-schist occurs between Gangnani and Bhangel and is bounded by migmatite in south and garnetiferous mica schist in the north. At the northern contact, development of actinolite-tremolite schist is worth noting. A thin band of amphibolite occurs within the calc-schist at Gangnani. The northern outcrop of calc-schist lies above the garnetiferous mica schist with occasional development of graphite. The rock is more recrystallized often in this outcrop than in the southern one. The northern outcrop extends between Pala and Joti. At the latter locality, it comes in contact with the JBT.

In the Yamuna Valley, three outcrops of calc-schist have been mapped. The southern outcrop is well developed at Phul Chatti and is flanked by quartzite with a thin marginal chlorite schist. On the top of this outcrop lies feldspathized chlorite schist which extends well beyond Janki Chatti with overlying amphibolite and quartzite. In the second (middle) outcrop, the Janki Chatti Formation overlies the quartzite north of Janki Chatti and extends upto south of Bhandali Gad. The strong shearing of rock and formation of graphite at about 2 km north of Janki Chatti are notable features. The northernmost outcrop of the calc-schist in this valley, is comparatively thin and overlies the quartzite and underlies the JBT. The calc-schist shows narrow patches of graphite schist and development of gouge in numerous pockets.

The rock has been traversed by quartz-calcite veinlets. The middle outcrop contains disseminated pyrite mineralization (Chapter 7). Trace of pyrite-chalcopyrite mineralization is also associated with actinolite-tremolite schist at Gangnani. The calc schist is grey to white, fine grained hard and compact in which foliation is rather well developed due to preferred orientation of calcite and flaky sericite. At a few localities, original lithological layering is still preserved while the most prominent foliation is developed parallel to the layering. Most of the minor structures recorded in the Bhatwari Group or the Suki Group are also present in the calc-schist. The slickensides and mineral lineation are well developed along the tectonic zone and plunge towards NNE or NE.

(b) Amphibolite: Several concordant amphibolite bodies of 2-10 m wide have been recorded within the Gamri Quartzite and the Janki Chatti Formation. The thickest amphibolite has been mapped around Agora and trends NW-SE to N-S. The outcrop width in the central portion is 3.5 to 4 km, whereas in the marginal portion it is only about 500 m. Formation of hornblende biotite schist and chlorite schist has taken place along the shear zones.

The amphibolite has been folded along NE-SW trending antiform whose axis passes through the Kaldi Gad. Quartz (rarely calcite) veins and lenses are frequently seen in the schistose amphibolites. The mineral lineation has been marked by prismatic hornblende and biotite flakes. At Gajoli Gad (Kaldya), slickensides plunging 65-70° due SW are profusely developed indicating that the contact between the amphibolite and quartzite may be a tectonic.

2.3 CENTRAL CRYSTALLINES

As mentioned earlier, the Central Crystallines have been classified into two groups and have been mapped along three important sections in the area.

(i) Bhatwari Group

(ii) Suki Group

An account of their lithology, distribution and field characters is given below.

2.3.1. Bhatwari Group

The polymetamorphic and migmatized rocks exposed between the Main Central Thrust (MCT) and the Joti-Bhandali Thrust (JBT) have been classified ^{as} ~~as~~ the Bhatwari Group. The Bhatwari Group is characterized by the following features:

- (a) Development of intrafolial and rootless structures,
- (b) Extensive metabasic activity,
- (c) Garnet grade of metamorphism except in the areas of mylonitization,
- (d) Heterogeneity in lithology,
- (e) Absence of pegmatite bodies,
- (f) Strong retrogressive changes along tectonic zones and,
- (g) Multiplicity of deformational structures including rotation of porphyroblasts.

The Bhatwari Group comprises a varied lithology.

The major rock types are as follows:

- (i) Chlorite schist, (ii) phyllonite,
- (iii) mylonites, (iv) quartz-mica schist, (v) garnet-iferous mica schist, (vi) amphibolite
- (vii) migmatite, (viii) augen gneiss and schist.

(i) Chlorite schist: Chlorite schist is developed along tectonic zones due to the retrograde metamorphism of mica schist and metabasite during cataclasis. The best exposures of chlorite schist have been located at Kumalti, north of

Agora, Wazari, Sayana^aChatti, Banas, south of Janki Chatti and Bhandli Gad. The schist is pale greenish, fine grained, thinly foliated and is easily split along the foliation planes which give a soapy feel due to presence of talc and sericite. Talc-chlorite schist contains quartz-tourmaline (brown to blue) veins, which have been folded on mesoscopic scale at a few localities. In chlorite schist, tourmaline is either absent or poorly present. The outcrop width of schist in general varies from 1m to 15m. The best exposure of chlorite schist is seen south of Janki Chatti in the Yamuna Valley. The development of chlorite schist is related to the imbricate structure. The foliation in chlorite schist dips 25-52° due NNE to NE. Quartz veins and lenses are prominent. At Kumalti, the limonitic leaching has given slightly yellowish brown appearance to the rock. All the minor structures (such as folds, shears, lineations and crenulation foliation), formed during polyphase deformation, are well developed in schist.

(ii) Phyllonite: Narrow bands of phyllonite are developed in the vicinity of the MCT and JBT due to strong retrogressive changes caused by thrusting. A 15-20 m wide outcrop of phyllonite has been seen at Kumalti. The rock is greenish grey fine grained and poorly foliated. The phyllitic sheen is distinct on the foliation planes. The underlying chlorite schist imperceptibly grades upward into biotite-muscovite schist. The schistose rocks are overlain by mylonitic augen gneiss.

Fine grained biotite-muscovite schist with minor amount of chlorite and quartz possess preferred orientation of platy minerals which impart foliation to the rock. Numerous shear planes have been noticed in these rocks. The phyllonitic horizon has also been intruded by concordant metabasic ^{rocks} having a width of 2-3 m. The kinks and lineation are well developed in these rocks. The hinges of kinks, mineral lineations, intersecting lineation (S_1 and S_2) and slickensides plunge towards $20-25^\circ$ due NNE to NE.

(iii) Mylonite: There are several bands of rocks showing varying degree of mylonitization and growth of porphyroblasts. The rocks are associated with garnetiferous mica schist and amphibolite. In addition, these are also associated near outcrops of calc-schist and Banas Formation in the Yamuna Valley.

The mylonitic gneiss interbanded with mica schist is well developed in tectonic zone, however, its outcrop width varies in different sections. The mylonitic rocks are characterized by development of mylonitic foliation, S_{2a} . In all the sections near the MCT, large exposures of mylonitic rocks have been observed extending for more than one km in width, although the intensity of mylonitization decreases away from the thrust. The rocks exposed in the Bhatwari Group have been strongly mylonitized in comparison to the Suki Group of rocks. The mylonitic gneiss shows extensive recrystallization and can be comparable with blastomylonite

(Spry, 1969). The large scale mylonitization in the Yamuna Valley section is due to the presence of imbricate structure.

(iv) Quartz-mica schist: Quartz-mica schist occurs on the southern side of the JBT and is associated with migmatite and amphibolite. It is light grey, fine to medium grained having distinct foliation with strongly developed mineral lineation defined by mica flakes and plunging $15-20^\circ$ due NNE to NE. The width of outcrops varies between 5 to 20 m. It represents the remnant portions of the country rocks which were subjected to migmatization. Some good exposures of these rocks have been located at Bhatwari, north of Agora, Sayana Chatti, Nisni and Pindki. At Bhatwari, quartz-mica schist is faulted (North Bhatwari Fault) against the overlying hornblende-biotite schist, which is synformally folded. The faulting has resulted in crushing and fracturing of quartz grains and kinking of mica flakes. Hornblende-biotite schist, exposed on the southern side of Paper Gad Fault, shows large scale silicification, which might be related to faulting. The exact outcrop pattern of these rocks could not be traced between Malla and Bhatwari because the region is covered by pre-historic landslide. Structural features noticed in the field are minor folds, ptyctic folds, shears, crenulation foliation, quartz veins and lenses, rodding and slickensides. The minor folds plunge $12-25^\circ$ due NW or SE or NE. Slickenside is well developed near the North Bhatwari Fault and plunge towards NE at angle of $20-35^\circ$ (See Chapter 4).

(v) Garnetiferous mica schist: The garnetiferous mica schist occupies a large tract of the area, however, the width of outcrop and the size of garnet varies at different localities. It is closely associated with migmatite, amphibolite and hornblende-biotite schist. The contact with the overlying Banas Formation in the Yamuna Valley is tectonic with attended retrogression. The quartz grains have been fractured, crushed and even recrystallized. Numerous small scale shears and fractures have been recorded in the rocks. In the basal part, garnetiferous mica schist bands are almost indistinct, which could be due to strong mylonitization of the rocks.

The garnetiferous mica schist is greenish grey, medium to coarse grained and well foliated. Garnet is pink to brown and 0.1 to 0.5 cm in size except at one locality (south of Gangnani) where the rock contains garnet porphyroblasts of 0.8 to 1.2 cm in diameter. Garnet porphyroblasts contain inclusion of quartz. At 174/8 km stone (near Bhatwari), a thin band of garnetiferous mica schist is exposed which also contains minor amount of actinolitic hornblende and tourmaline. The rock is underlain by quartz-mica schist and overlain by hornblende-biotite schist. At several localities, thin bands of garnetiferous mica schist have been encountered within the migmatite, suggesting that these rocks represent non-migmatized portions of the country rocks. On the southern side of Gangnani, the rock has been synformally folded with migmatite in the core. At about 1 km north of Sunagar slip (near

Gangnani), a small antiform is seen within these rocks whose core is made up ^{of} metabasics.

The foliation commonly dips at an angle of 32-50° towards NE or NNE. At Banas, the strike of the formation changes from NW-SE to WNW-ESE. All the minor structures discussed earlier are also observed in these rocks.

North of Gangnani, garnetiferous mica schist has been exposed between two outcrops of the Janki Chatti Formation (calc-schist and crystalline limestone). The mica schist is highly sheared and controls an active landslide zone. Garnet is smaller in dimension (0.7 to 1.5 mm) than elsewhere and is embedded within quartz grains and schistose portion. The entire outcrop seems to be isoclinally folded.

(vi) Amphibolite: Isolated bands of amphibolite are exposed between the MCT and the JBT of varying dimension. About 25 to 30 such occurrences of amphibolite bands have been observed in the Bhatwari Group and most of them range in thickness from 1 to 4 m, hence smaller bodies have not been shown in the geological map (Fig. 2.2). Amphibolite bands are associated with other rock units of the Bhatwari Group, however, the frequency of occurrence **varies in different** sections. In the Bhagirathi Valley, these are more prominent in comparison to the Dodital or the Yamuna Valley sections. Their structural setting closely resembles with the country rocks. At places (e.g., Malla, Bhukki and Rana), the amphibolite shows evidences of migmatization in the form of ptygmatic folds,

veined and streaky structures. Along zones of dislocation, amphibolite has given rise to hornblende-biotite schist and chlorite schist. At Bhatwari, hornblende-biotite schist is synformally folded whose southern limb has been offset by the NW-SE trending **South Bhatwari fault**. All the minor structures, formed due to polyphase deformation, can be seen in these horizons. On the eastern side of Hanuman Chatti along the Yamuna Valley, amphibolite is exposed within the migmatite and has been subjected to superposed folding.

Amphibolite is dark green to greyish green with varying grain size ^(0.6 to 7 mm) and competence. Large bodies of massive amphibolite exposed along the road sections at Lata north of Bhatwari and Hanuman Chatti, are strongly foliated along the margins due to shearing. Their foliation usually dips towards NE to NNE at an angle of 25-50°. The foliation and lineation has been imparted to the rocks by preferred orientation of prismatic hornblende, platy biotite, and chlorite and occasionally by the presence of quartz grains. Quartz veinlets, lenses and small **boudins** are quite frequent in the schistose amphibolite and aligned parallel to the main foliation, S₂.

(vii) Migmatite: The outcrops of migmatite belonging to the Bhatwari Group can be best traced from Lata to Gangnani in the Bhagirathi Valley, Sayana Chatti to Banas in the Yamuna Valley and south of Dodital in the Kaldi Gad section. At several localities, migmatite comes in contact with the Gamri Quartzite of Garhwal Group along the tectonic contact

which is termed as the MCT. The migmatite of the Bhatwari Group is characterised by the presence of ptygmatic, phlebitic (vein) stromatic (banded), ophthalmitic (augen), nebulitic, schlieren, schollen and diktyonitic structures (cf., Mehnert, 1968).

Remnants of the country rocks are commonly recorded in the migmatite. The foliation attitude of migmatite is in concordance with the country rocks and their dip varies from 25-50° due NE to NNE. As has been described in Chapter 3, the migmatite of the Bhatwari Group reveals the earliest evidences of deformation and metamorphism in the area; ~~as~~ as the axial plane foliation of reclined folds, F_1 , is being isoclinally folded by second generation of folds and produce the most prominent foliation, S_2 .

The contact between host rocks and the migmatite is gradational. Rock units to which the migmatization has been restricted are garnetiferous mica schist, quartz-mica schist, gneiss and amphibolite. The amphibolite has been least migmatized. The size of the migmatized bands (excluding amphibolite) is much wider ^(30 to 400 m.) as compared to the host rocks (10 to 50 m).

On the basis of field characters, migmatite has been classified into foliated, banded (including subaugen migmatite) augen and streaky varieties. The migmatization is more prominent in the basal part of the Bhatwari Group and its intensity decreases as one proceeds upwards, thus indicating a normal metamorphic sequence in this group. The rocks, exposed in the Bhatwari group, generally belong to the garnet grade

of metamorphism. The rocks exposed close to the MCT are devoid of garnet, which may be due to the breakdown of mineral (garnet) during strong cataclastic metamorphism. Calc-schist has not been affected by the migmatizing fluids. In the Yamuna Valley, migmatitic horizons are also associated with the discordant metadolerite, quartzite and concordant metaandesite.

Migmatite is light grey, medium to coarse grained, hard and compact with distinct foliation. Augen and banded migmatites occupy a large track of the area. At places, banded character in the migmatite has been attained by the flattening of feldspar augen due to stretching. Some of the augen feldspar shows rotation, which might be related to shear deformation. Almost all the varieties of migmatite have been mylonitized to various degree depending upon the magnitude of the shear zones. Most of the structural features described in the country rocks are also present in the migmatite.

(viii) Augen gneiss and schist: The augen gneiss and schist cover a large part of the Bhatwari Group and show variance in the degree of feldspathization. At places, the augen gneiss gives the appearance of banded gneiss due to stretching of porphyroblasts. The gneiss exposed north of the MCT, contains pink to brown rotated garnet. These rocks have been subjected to varying degree of migmatization. At the basal part, it shows higher degree of migmatization as compared to similar rocks exposed further north. At few localities

(Wazari and near Banas), schistose portions predominate over the gneissose portion and the rock appears comparatively darker.

The rocks mainly contain augen of feldspar but rarely also of quartz, which are wrapped by mica flakes to give an 'eye' appearance to the rocks. ^{Some of} the feldspar augen are square in shape in which two sets of cleavage can be easily recognised, whereas quartz porphyroblasts are anhedral to subhedral in form. The size of augen ranges from 0.5 to 2 cm in length and 0.2 to 1 cm in width. The augen are mainly aligned parallel or subparallel to main schistosity, S_2 , and impart lineation to the rocks. Some of the feldspar porphyroblasts show rotation and are inclined to the foliation, S_2 . The gneiss contains numerous thin quartz (sometimes associated with tourmaline) veinlets (1.2 to 2 cm thick) and not exceeding a few cm in length (2-10 cm). The veinlets have been folded into small scale 'z' or 's' shaped folds; their axes plunging 15-30° due NW or SE. Development of pink to brown rhombododecahedral garnet, ranging in size from 0.5 to 3 mm is concentrated in the hinge portion of minor folds due to the folding of metamorphic layers.

Concordant amphibolite and meta andesite associated with these rocks are highly sheared along the margins producing, thereby, hornblende-biotite schist and chlorite schist. Augen gneisses have discordant relationship with metadolerite at Kumalti and south of Sayana Chatt. The foliation S_2 , in augen gneiss and schist generally dips towards NNE or NE at an angle of 25-50°. Strong jointing has resulted into

large blocks (1 to 5 m in length) causing landslide hazard in a few localities.

Minor structural features like folds, shears, faults, tension gash, mineral lineation, intersection lineation, rodding, boudinage and slickensides are usually recorded in these rocks. The linear features commonly plunge towards NNE or NE at gentle to moderate angle (10 to 35°). Slickensides plunging 20-35° due NE or 65-80° due SW have been profusely developed in augen gneiss near the vicinity of the MCT.

2.3.2 Suki Group

The Suki Group comprises the rocks exposed to the north side of Joti-Bhandali Thrust (JBT). The Suki Group differs from the Bhatwari Group in the following field characters:

- (a) Absence of intrafolial and rootless folds.
- (b) Very ~~few~~ or no metabasic occurrences.
- (c) Increase in the grade of metamorphism within a short distance from garnet to sillimanite grade.
- (d) Garnet porphyblasts showing little or no rotation.
- (e) Presence of aplitic and pegmatitic bodies.
- (f) Development of porphyroblastic migmatite.
- (g) Divergent inverted isograde pattern.
- (h) Homogeneity in lithology inspite of varying grade of metamorphism.
- (i) Poorly defined retrogressive metamorphic changes.

The rocks characterizing the Suki Group are as follows, whose field characters are given below,

(i) garnetiferous gneiss and schist, (ii) chlorite schist, (iii) amphibolite, (iv) kyanite schist and gneiss (v) quartz-sillimanite gneiss (vi) migmatite

(i) Garnetiferous gneiss and schist: Garnetiferous gneiss interbanded with schist and amphibolite has been thrust over the underlying calc schist of the Janki Chatti Formation along the JBT. The rocks have been mylonitized in the vicinity of the thrust. The chlorite schist has developed due to the retrogression of biotite schist. The garnetiferous schist is dark grey to greenish grey, medium to coarse grained with well developed foliation. Aplite and pegmatite veins of smaller dimension are commonly observed in these rocks and are aligned parallel to the main foliation, S_2 . The idioblastic garnet is pink to brown with size varying from 1 to 3 mm. The garnet shows poor rotation as is evident from the quartz inclusions, which are poorly present.

(ii) Chlorite schist: Narrow patches of chlorite schist associated with garnet and kyanite bearing rocks and amphibolite have been noticed north of Bhandali Gad. The chlorite schist has been formed due to the retrogression of biotite schist and amphibolite in the later stages of thrusting (JBT). A strong development of crenulation foliation, S_3 , has been recorded in the rock. The main foliation, S_2 , dips 40-55 towards NE or NNE.

(iii) Amphibolite: Concordant bodies of amphibolite are exposed north of Janki Chatti within the garnet and kyanite bearing schist and are subjected to varying degree of migmatization. Their outcrop width ranges from 5-25 m. True amphibolite has not been encountered in the Suki Group of the Bhagirathi Valley, although a band of gedrite-pargasite bearing schist does occur near sillimanite gneiss of Jhala.

The poor development of amphibolite in the Suki Group is a notable feature in comparison to the development of amphibolite in the Bhatwari Group. The megascopic characters resemble, to a large extent, with the amphibolite of the Bhatwari Group. These have produced hornblende or biotite or chlorite schist along weak zones. The effect of migmatization is rarely observed in the amphibolite. The foliations dip at an angle of 40-50° towards NE or NNE. A thin band of amphibolite (2-3 m in width) crops out north of Jhala bridge. It is associated with sillimanite gneiss and kyanite schist.

(iv) Kyanite schist and gneiss: Kyanite bearing schist and gneiss, which are exposed north of Debrani along the Bhagirathi Valley, cover comparatively large part of the Suki Group. They are associated with amphibolite and porphyroblastic migmatite. The rocks have been traversed by aplite and pegmatite veins of smaller dimension. The schist has attained somewhat banded appearance due to the enrichment of pegmatitic material along the foliation planes. The presence of kyanite bearing rocks on both side of sillimanite gneiss at Jhala, indicate a

divergent or inverted grade pattern in metamorphism in the area. These rocks are characterized by the development of augen to porphyroblastic migmatite of younger age. The size of blue kyanite blades increases from 0.2 to 2 cm northward, while the size of garnet reduces from 3 mm to 1.5 mm. Wherever large pegmatite bodies (0.5 to 1.5 m in width) have intruded the rocks, the size of kyanite blades has increased, (e.g., upstream of Son Gad, kyanite blades are 4-6 cm in length). Pink to brown garnet is idioblastic in nature. These rocks show various shades of grey colour and are medium to coarse grained. The kyanite schist is well foliated and the foliation dips 35 to 60° due NE or NNE.

(v) Quartz-sillimanite gneiss: It is exposed north of Jhala bridge and is localised in a narrow belt (100-150 m in outcrop width). It is flanked by kyanite bearing schist and gneiss on both sides. Tourmaline bearing aplite and pegmatite veins are rare in comparison to kyanite schist. Different mineral components show a strong tendency to segregate into lenticles and streaks.

The rock is light to purple grey, medium grained and massive in character. Sillimanite bearing horizon has not been encountered in the mappable areas of other sections. The rock exhibits granoblastic texture with a distinct foliation. The foliation dips 35-42° due NNE or NE.

(vi) Migmatite: The rocks belonging to the Suki Group have been subjected to varying degree of migmatization. The

enrichment of leucocratic material along foliation planes has given rise to banded and porphyroblastic migmatite. These migmatites appear to be younger in age as they are associated with tourmaline rich aplite and pegmatite bodies. Banded (including subaugen variety) migmatites are well exposed around Loharinag in the Bhagirathi Valley and south of Yamunotri in the Yamuna Valley. The excellent exposure of porphyroblastic migmatite has been recorded at Suki. The feldspar porphyroblasts are devoid of rotation unlike the Bhatwari Group. Their mode of occurrence is somewhat similar to the migmatite of the Bhatwari Group. The migmatite is least affected by dislocation metamorphism. The migmatite is characterized by the following features:

- (a) Distinct or indistinct nature of the original foliation
- (b) Size of the porphyroblasts giving rise to ophthalmitic (augen) structure.
- (c) Development of stromatic structure due to the elongated nature of the porphyroblasts.

The porphyroblastic migmatite grades into the foliated variety through augen and banded varieties. The gradual change of mica schist into porphyroblastic migmatite during metasomatism is **evidenced** from the following features:

- (a) Neosome (quartz-feldspar) encloses relicts of paleosome (schistose portion) with gradational or warty junction.

- (b) Structural continuity between paleosome and neosome.
- (c) Large grainsize variation from mica schist to porphyroblastic migmatite.

Northwards increase in the grade of metamorphism from garnet to sillimanite (from Debrani to Jhala), close association of migmatite with garnet, kyanite and sillimanite bearing rocks and presence of garnet and kyanite in migmatite indicate that these could have been formed due to anatexis. The appearance of blebs of quartz and feldspar in the garnet-kyanite schist and decrease in the intensity of migmatization from Suki to Jhala, probably suggest that anatectic zone ends here. The porphyroblasts show parallelism with the main foliation, which dips 40-52° due NNE or NE.

2.4 LATE PHASE MAGMATIC AND HYDROTHERMAL ACTIVITIES

2.4.1 Pegmatite

Several concordant pegmatite bodies of varying dimension are associated with the Suki Group of rocks and are excellently exposed in the Bhagirathi Valley section. Their size increases as one proceeds from Debrani towards Harsil (0.1 to 1.2 m). The pegmatite intrudes across as well as along the foliation planes and its contact with the surrounding rocks is irregular. It has been noticed that, wherever pegmatite has intruded the kyanite schist, development of large kyanite crystal has taken place.

Pegmatite is white to purple white, medium to coarse grained, hard, compact and undeformed. The pegmatite bodies are richer in black tourmaline. A large variation in size of tourmaline has been noticed, which could be the result of pegmatite zoning. Small veins of aplite, slightly elongated in shape are also seen. The aplite veins contain numerous minute crystals of tourmaline which are aligned in a particular direction, probably representing the direction of ^{pegmatitic fluid.} The field behaviour of pegmatite indicates that the bodies belong to the last granitic activity in the area. Muscovite books and biotite selvages are normally recorded in the pegmatite. Concordant pegmatite bodies dip $45-52^\circ$ due NNE or NE.

2.4.2 Meta-andesite

Meta-andesite outcrops for about 150-200 m at Banas and is associated with garnetiferous biotite schist and gneiss of the Bhatwari Group which is faulted against the overlying quartzite of the Banas Formation (Garhwal Group). The rock has been traversed by quartz-calcite veins and lenses, which are parallel to subparallel to the main foliation. Occasionally, the veinlets are inclined to the foliation. The veinlets show pinching and swelling. Due to strong shearing at the margins, meta-andesite and surrounding biotite schist have given rise to chlorite schist. The foliation is less prominent in the central portion in comparison to margins. The concordant meta-andesite dips 45° due NE. Sulphide mineralization

(containing pyrite and chalcopyrite) is associated with quartz-calcite veins and lenses. The adjoining chlorite schist also contains quartz veins and lenses but these are devoid of mineralization. In the other sections, meta-andesite has not been observed.

The rock is greenish black, fine to medium grained and hard with a distinct foliation. The foliation has been marked by the preferred orientation of mica flakes. Closely spaced joints have been developed at the margins. Several shears have been identified in the meta-andesite and surrounding rocks. The shears trend towards NW-SE to NNW-SSE. Quartz-calcite veins have been folded into small isoclines which show thickening in the hinge region.

2.5.3 Metadolerite:

Fine to medium grained, hard, compact and massive metadolerite has been discovered at Kumalti (Bhagirathi Valley) and Wazari (Yamuna Valley) having a discordant relationship with the surrounding rocks. At Kumalti, metadolerite has intruded both the Gamri Quartzite and the Bhatwari Group of rocks and cuts across the MCT, thus indicating its post-MCT nature. On the southern side of the MCT (at Kumalti), metadolerite is covered by the debris, therefore its exact outcrop pattern was not mappable. In the Yamuna Valley section, metadolerite belongs to the Bhatwari Group. The metadolerite occurs in the same manner, as in the Bhagirathi Valley.

Rocks, intruded by the metadolerite, are amphibolite, augen gneiss, migmatite and quartzite. At the margin, it is metamorphosed to chlorit  schist. The outcrop width varies from 100-300 m and extends for about 0.5 to 1 km. Metadolerite dips steeply (60-70°) towards NW, while the foliation in the metamorphosed country rocks dips at an angle of 30-35° due NE or NNE. At places, rock shows spheroidal weathering and the resulting boulders are dirty green in appearance.

2.4.4. Quartz and Quartz-calcite veins:

The quartz and quartz-calcite veins of late phase hydrothermal activity have been commonly recorded in the rock units belonging to the Bhatwari Group, the Suki Group and the Janki Chatti Formation. These mainly exhibit discordant relationship with the most prominent foliation of host rocks. At places, the veins show pinching and swelling character. The veins are 0.5 cm to 3 cm in width and 0.5 m to 10 m in length. The quartz and quartz-calcite veins associated with calc schist (at Janki Chatti), meta-andesite (at Banas) and migmatite (at Pindki) contain sulphide mineralization. The details of quartz-sulphide or quartz-calcite-sulphide veins are available in Chapter 7.

2.4.5 Quartz-tourmaline veins

The discordant tourmaline bearing quartz veins have also been noticed in almost all the rock units. Their

frequency of occurrence is less in the Bhatwari Group in comparison to the Suki Group. These contain crystals of black tourmaline, which at places, impart lineation to the rocks. The black tourmaline grains associated with pegmatite and other rock units show almost similar physical characters, indicating that the tourmaline is related to the late pneumatolitic phase. The quartz-tourmaline veins related with earlier pneumatolitic phase have been folded alongwith S_2 foliation.

CHAPTER - III

STRUCTURE AND TECTONICS

The diverse lithologies of the Central Himalaya along the Bhagirathi and Yamuna Valleys have undergone multiple structural deformation and metamorphism and also incorporate parts of the Lesser Himalayan metasediments. Multiple deformational structures are well displayed by interbanded psammitic gneiss and amphibolite within the pelitic sequences of the Bhatwari and Suki Groups on mesoscopic and microscopic scale.

In the present chapter, an attempt has been made to decipher some details of these multiple deformations followed by ^{the study of} macroscopic structures bounding the main lithotectonic units and their comparative analysis with similar studies in some sectors of the Himalaya.

3.1 SMALL-SCALE STRUCTURES

Small-scale structures are present throughout all the tectonic units of the Central Himalaya but are much better displayed at certain localities within the Bhatwari Group. The various structural elements recorded in the lithotectonic groups have been grouped into three categories

- (a) Planar structures
- (b) Folds
- (c) Other linear structures

Explanation for figures 3.1 and 3.2

Figure 3.1 Differentially weathered calc schist bands in the Janki Chatti Formation. S_1 lithological layers are isoclinally folded by F_2 folds plunging NW with development of S_2 axial plane foliation, coin's diameter is 2.5 cm.

Figure 3.2 Migmatite at the Bhatwari bridge with rotated quartzo-feldspathic boudins showing relict structures. Bhatwari Group. Pen is 15 cm in length.

Figure 3.2a Enlargement of boudin on left side. Relict S_1 foliation within the boudin is intersected by S_2 foliation in mica schist along which certain amount of translation is evident during D_{2a} deformation. Pen's cap is 5 cm.

Figure 3.2b Enlarged central part of figure 3 with relict F_1 folds and S_1 as axial plane foliation in extreme left and in central boudin; truncation of S_1 foliation along S_2 and S_{2a} foliations.

Figure 3.2c Enlarged quartzo-feldspathic boudin on extreme right in figure 3.2. Folded S_1 foliation in boudin by F_2 folds and wrapping of S_2 foliation around it.



3.1



3.2



3.2 a



3.2 b



3.2 c

3.1.1. Structural elements:

The mesoscopic structural elements observed in the above lithotectonic units have been classified into the planar and linear structures; most of them are penetrative except the joints and slickensides.

(a) Stratification (S_0): Stratification is mainly decipherable in the low grade metamorphic rocks of the Garhwal Group in which distinct sedimentary structures are still recognizable. Stratification is defined by colour and composition bands in the Garhwal Group, Banas Formation and the Janki Chatti Formation, while grain size variation is still seen in quartzite of the Garhwal Group. In calc schist of the Janki Chatti Formation, it is very distinct due to colour variation and differential erosion of calcareous rich bands (Fig. 3.1). However, recognition of stratification in schist lacking compositional bands is difficult in the Bhatwari Group because of multiple deformation, migmatization and profuse presence of amphibolite. In the Suki Group, it is faintly visible in the garnetiferous and kyanite mica schists but its gross configuration could not be worked out due to its transposition by other planar structure. A distinct bedding plane foliation can be observed in the Gamri Quartzite but its significance in relation to later deformational episodes is still not properly understood due to lack of good exposures revealing its relationship with later more pervasive foliations.



3·3



3·3 a



3·3 b



3·4

Explanation for figures 3.3 to 3.6

Figure 3.3 Hand specimen of refolded F_1 and F_2 folds by F_3 folds to produce mushroom structure in migmatite of the Bhatwari Group. Locality - Bhatwari College.

Figure 3.3a Enlarged view of hooked-shaped relict F_1 fold being coaxially folded by F_2 fold. Axial surface of F_1 fold is isoclinally folded by F_2 with the development of S_2 axial plane foliation. Quartzo-feldspathic band shows isoclinally folded S_1 foliation. Scale -2cm.

Figure 3.3b Central enlarged portion of mushroom fold revealing circular pattern due to F_1 and F_2 interference which was later on modified by F_3 folds.

Figure 3.4 Isoclinally folded migmatite of the Bhatwari Group, showing F_2 fold affecting migmatite layers along S_1 foliation S_2 foliation seen near fold closure. Layers subsequently deformed by inclined angular F_3 folds. Locality - Bhatwari bridge.

(b) Foliation: This term includes all penetrative s-surfaces of deformational origin and have been designated here in sequential order of their development in the deformational history of the Central Himalaya along the Bhagirathi and Yamuna Valleys. The foliations are designated here as S_1 , S_2 , S_{2a} and S_3 . From deformational point of view, they may be correlated with four distinct phases of deformation in the Bhatwari Group; the earliest deformation phase being absent in the Suki Group and probably also in the Garhwal Group.

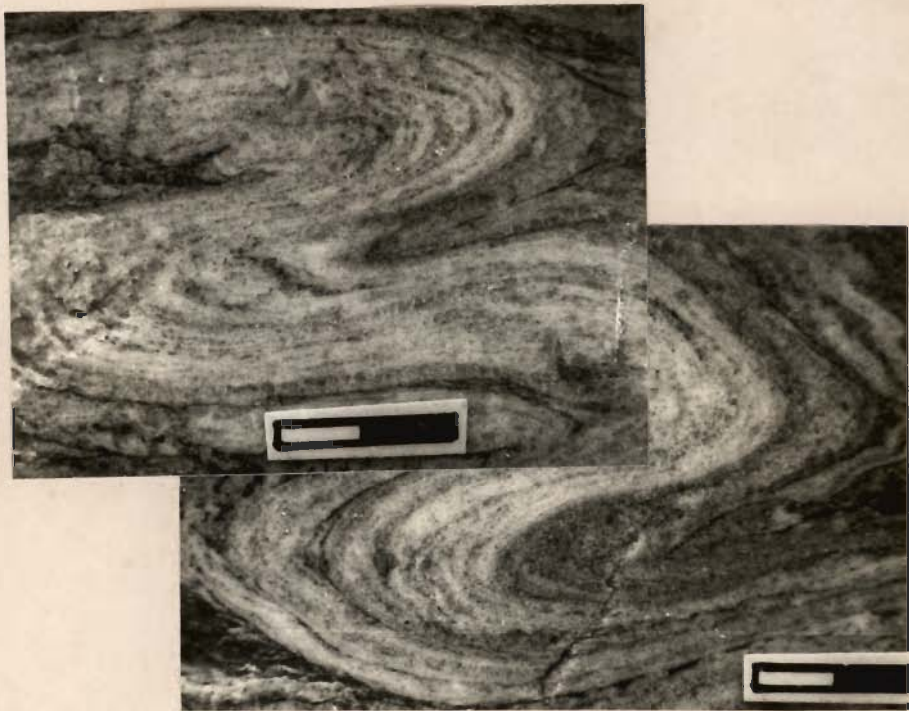
(i) S_1 foliation: In the Bhatwari Group, the earliest foliation has been observed as a relict foliation and is preserved either within the folded boudins (Figs. 3.2, 3.2 a-c) or could be seen along the hinge zones of refolded mushroom folds (Figs. 3.3, a-b). That S_1 foliation parallels the axial surfaces of very tight nearly isoclinal similar folds of Type IB (cf. Ramsay, 1967) is very clearly seen in migmatized biotite schist of the Bhatwari Group where such folds occur as hook-shaped relict structures (Fig. 3.2b). Within the folded boudins of mainly migmatite bands, the S_1 axial plane foliation is largely pervasive except in closures of relict structures (Figs. 3.2 a-c). Another evidence of the presence of an earlier S_1 foliation is very distinct and widespread occurrence of most prominent isoclinal folds affecting S_1 either on the metamorphic banding or migmatized layers within pelites of the Bhatwari Group. Thin sections, hand specimen and outcrops bear ample testimony to the above observations.

Figure 3.5 Migmatite layers in Bhatwari Group forming boudins at Bhatwari bridge. Isoclinally folded S_1 by F_2 folds and development of gently inclined S_2 foliation. Structure is subsequently folded by overturned tight to open F_3 folds with axial surfaces inclined towards right. Locality - Bhatwari Bridge.

Figure 3.6 Isoclinally folded S_1 migmatite layers by F_2 folds having S_2 as axial plane foliation. Migmatite from the Bhatwari Group. Locality - Agra, Bhagirathi Valley.



3·5



3·6

(ii) S₂ foliation: The most penetrative and widespread planar structure in both the Suki Group and the Bhatwari Group is the axial plane foliation which is coplanar to the S₁ foliation in the latter. It can be observed as axial plane foliation isoclinal folds which are developed on S₁ foliation in the migmatite, commingtonite-biotite schist of the Bhatwari Group (Figs. 3.4, 3.5, 3.6). In the Suki Group, S₂ foliation has been observed and developed over the poorly preserved stratification or on lithological bands as axial plane foliation. In the metasediments of the Garhwal Group, differentially weathered calc schist of the Janki Chatti Formation reveal the S₂ foliation as axial plane foliation of isoclinal folds which are developed on calcitic layers (Fig. 3.1).

Isoclinal nature of folds, tightly appressed limbs and large-scale transposition have been largely responsible for obliteration of S₁ foliation in the Bhatwari Group due to S₂ foliation which is invariably coplanar to the former except in hinge zone of these folds.

(iii) S_{2a} foliation: Increased deformation and transposition of structures along S₂ foliation has developed a rather discrete shear zones subparallel to S₂ foliation and reveals its mylonitic character in the major thrust zones. Transposition of S₂ into a new subparallel foliation, designated here as S_{2a}, indicates continued flattening during southerly movement to develop S_{2a} foliation (Figs. 3.7, 3.8) and also producing intrafolial folds with relict hinge zones as 'hooks' (Fig. 3.14).

Explanation for figures 3.7 to 3.10

Figure 3.7 Isoclinally folded migmatite layers in the Bhatwari Group by F_2 folds with S_2 axial plane foliation being transposed along a thrust plane, S_{2a} . Later F_3 inclined folds having S_3 axial plane foliation across S_2 and S_{2a} structures. Locality - Agra, Bhagirathi Valley.

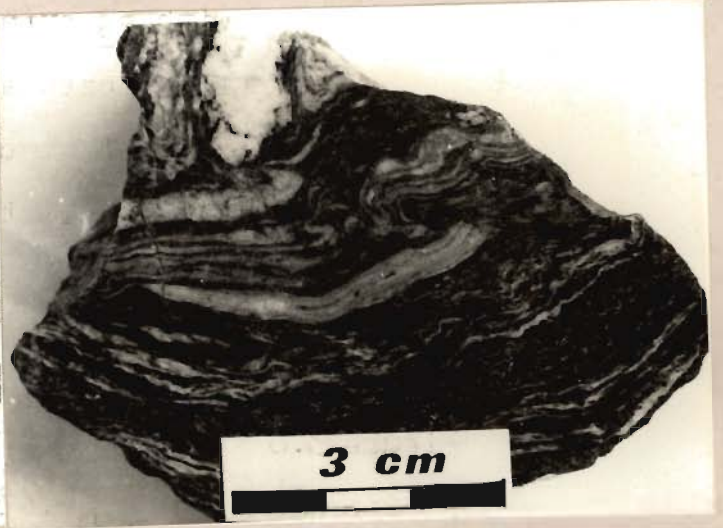
Figure 3.8 ~~isoclinally folded~~ Migmatite layers developed along S_1 foliation ^{disrupted} by S_{2a} surface. Isoclinally folded S_1 layers in western part by F_2 with axial plane foliation, S_2 , cut off obliquely by S_{2a} surface. Locality - Bhatwari College.

Figure 3.9 Migmatite layers in amphibolite of the Bhatwari Group showing development of boudin structure due to pinch and swell in upper layer, while main layer is disrupted by S_3 foliation to produce rhombio-shaped boudins. Locality - 2km south of Bhatwari.

Figure 3.10 Reclined folded silica layers in mica schist of the Bhatwari Group with F_1 folds having S_1 axial plane foliation. Locality - Bhatwari bridge.



3-7



3-8



3-9



3-10

Thin sections of chlorite schist, phyllonite, which have been detailed in Chapter 4, clearly reveal its transposed character from the S_2 foliation in the thrust zone and is well seen at Bhatwari, south of Dodital, around Syana Chatti, Nishni and north of Janki Chatti.

(iv) S_3 foliation: All foliations later than S_2 and S_{2a} foliation have been classified here as S_3 foliation which has a character of crenulation foliation (crenulation cleavage of Rickard, 1961; herring bone cleavage). Crenulation foliation is commonly seen as axial plane foliation of small scale folds on S_1 , S_2 and S_{2a} foliations affecting the previously developed metamorphic features like migmatitic and amphibolitic layers (Figs. 3.7, 3.8, 3.5) on mesoscopic and microscopic scales. At times, S_3 foliation produces rhombic-shaped boudins in migmatitic layers (Fig. 3.9). This structure has been observed in all the lithounits belonging to the Garhwal Group, the Bhatwari Group and the Suki Group. However, it is well developed in the latter two groups and more in pelitic sequences due to rheological variations. In its development, S_3 is defined by, preferred orientation of muscovite, biotite, quartz and sometimes chlorite and iron oxides either by rotation of previously existing minerals along S_2 and S_{2a} foliations or by new (growths of muscovite and biotite) (Chapter 4). Discrete fractures mark such foliations which are also sometimes intruded by tourmaline veins.

(c) Folds: On the basis of variation in style, orientation type of surfaces being folded and textural relationships, four

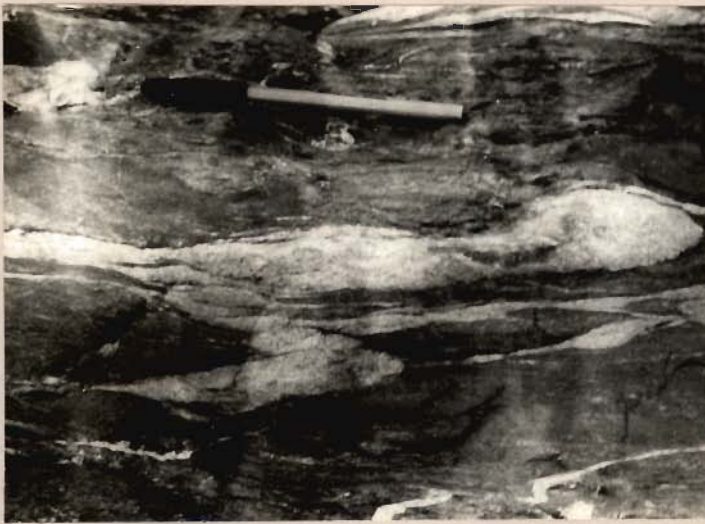
Explanation for figures 3.11 to 3.14

Figure 3.11 F_1 folds in migmatite layers of the Bhatwari Group with considerable flowage in hinge zones. Long attenuated limbs. Locality - Bhatwari bridge.

Figure 3.12 Reclined F_1 folds with S_1 axial plane foliation in mica schist of the Bhatwari Group. Locality - Bhatwari bridge.

Figure 3.13 Refolded isoclinal F_2 fold by inclined F_3 folds. Axial surface of F_2 fold is superimposed by axial surfaces of later folds having S_3 foliation. Locality - Bhatwari bridge.

Figure 3.14 Isoclinally folded and transposed S_1 foliation by F_2 folds showing rounded hinges and curving around of S_1 foliation in the Bhatwari Group. F_3 folds are coaxial to F_2 with axial surfaces dipping steeper to S_2 foliation. Locality - Bhatwari bridge.



3·11



3·12



3·13



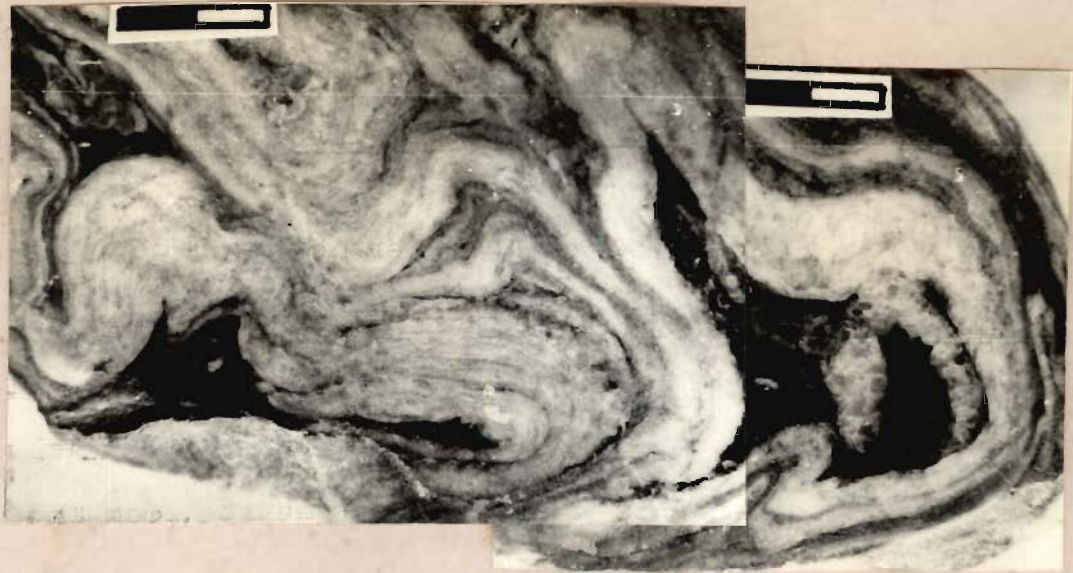
3·14

sets of folds, F_1 , F_2 , F_3 and F_4 have been identified in the rocks present in the area, of which the F_1 folds have been observed restricted mainly to the Bhatwari Group. Of these, F_1 folds possess hinge lines plunging nearly normal to F_2 folds, though both possess same style. The F_2 and F_3 folds have nearly same orientation of fold axes and hence are coaxial in character, while F_4 folds are transverse to F_2 and F_3 folds. These also represent four phases of deformation which affect the Bhatwari Group metasediments (D_1 to D_4) and are associated with three main phases of metamorphism and two phases of migmatization, besides post- D_3 pegmatitic activity in the area and syn- D_3 and post- D_3 pneumatolitic phenomena.

(i) F_1 folds: The Bhatwari Group of metasediments are characterized by some relict folds which are, at present, preserved either within the boudins or occur as rootless hook-shaped structures. These folds are very tight to isoclinal in sharp elongate hinges and very long drawn limbs (Fig. 3.3, 3.3 a-b, 3.10, 3.11, 3.12). Thickening of hinge zones and thinning on the limbs are common and is more accentuated with psammatic layers. F_1 has folded an earlier lithological layering S_0 which may even be of metamorphic origin; the evidences for which are not very distinct. Axial plane foliation is developed at high angles to S_1 layers in hinge zones (Figs. 3.3, 3.10, 3.11, 3.12). F_1 folds generally plunge either NE or SW and are reclined in nature with S_1 dipping at moderate angles towards NE or SW (Figs. 3.10, 3.12).

Explanation for figures 3.15 to 3.19

- Figures 3.15 Type 2 interference pattern due to F_1 and F_2 folds, in the Bhatwari Group. Axial surface of F_1 fold is isoclinally folded by F_2 fold and subsequently by open F_3 folds. Migmatite from the Bhatwari Group. Locality - Bhatwari College.
- Figure 3.16 Tight F_2 folds and isoclines in migmatite from the Bhatwari Group refolded by F_3 folds. Locality - Bhatwari bridge.
- Figure 3.17 Subhorizontal S_2 foliation paralleling the axial surfaces of F_2 folds on migmatite layers. S_3 crenulation foliation steeper to S_2 along axial surfaces of F_3 folds. Locality - Agra.
- Figure 3.18 Development of boudin due to excessive flowage of quartzo-feldspatic material in hinge zones of F_2 folds isoclinally folding S_1 foliation which is preserved within the boudin. Distinct S_2 foliation along axial surfaces of F_2 folds. Crenulation foliation, S_3 , runs



3-15



3-16



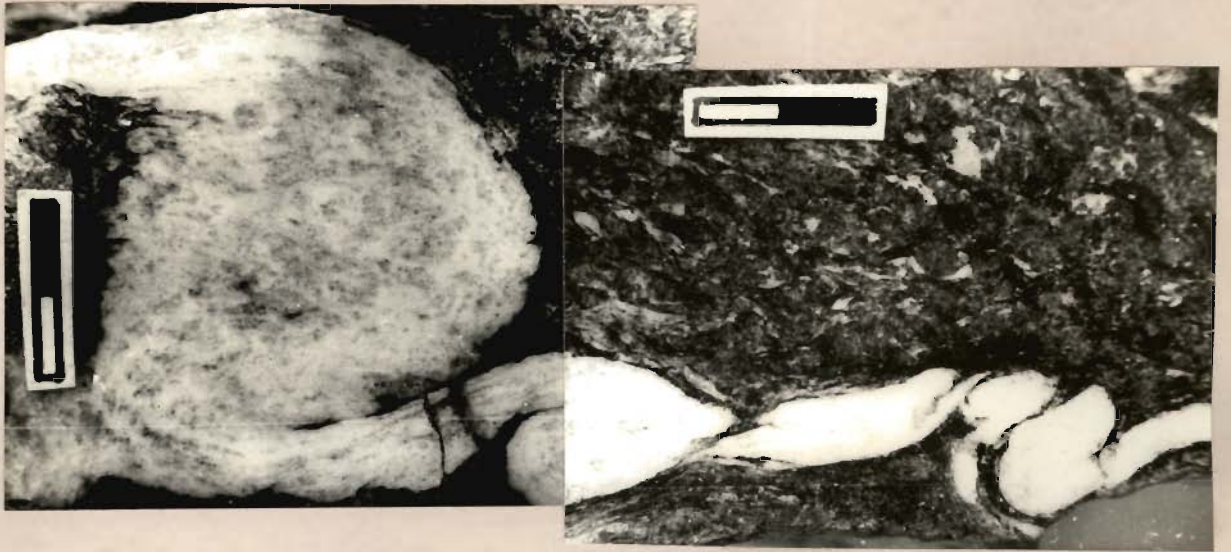
3-17

(ii) F₂ folds: Evidences for F₂ folds on an earlier metamorphic foliation S₁ are well distributed on mesoscopic and microscopic scales in the Bhatwari Group. In contrast, F₂ folds are seen affecting the lithological layering S₀ in the Suki Group and rocks of the Garhwal Group. F₂ folds are mostly isoclinal to very tight in character with interlimb angle not exceeding 20°. In most cases, it is generally 0-5° (Figs. 3.13, 3.14, 3.18, 3.20). Small scale F₂ folds are well displayed by contrasting lithologies e.g. amphibolite and migmatite layers in mica schists of the Bhatwari Group (Figs. 3.14, 3.18), calc schist layers of the Janki Chatti Formation (Fig. 3.1), the quartzose layers of the Gamri Quartzite and the Banas Formation and the psammite layers in the Suki Group. Interference of F₁ and F₂ folds produce Type 2 interference pattern with F₁ axial surface being isoclinally to tightly folded by F₂ axial surface (Figs. 3.3, 3.15, 3.20) and has even produced more complex mushroom type patterns with elliptical to circular outcrop patterns (Figs. 3.3b,). At other places, F₂ folds mainly affects the S₁ foliation in the Bhatwari Group (Figs. 3.17, 3.18, 3.20) and possess a coplanar S₂ axial plane foliation to the relict S₁ foliation. Because of coplanarity to S₁ and much more intense development, the Bhatwari Group reveals mainly the S₂ foliation.

(iii) F₃ folds: The F₃ folds are crenulation to tight folds in style and are well developed in all the lithotectonic units exposed along the two sections of the Central Himalaya. These folds are developed on long limbs of F₂ folds obliquely to F₂ folds and have steeper axial surfaces, though F₃ folds

obliquely to S_2 in the migmatite from the Bhatwari Group. Locality - Bhatwari College.

Figure 3.19 Relict F_1 fold with steeply dipping axial surface being refolded by F_2 folds. S_1 is isoclinally folded with the development of S_2 axial plane foliation which is being crenulated by F_3 folds with S_3 as axial plane foliation in the Bhatwari Group. Locality - Agra, Bhagirathi Valley.



3·18



3·19

are generally coaxial to F_2 folds (Figs. 3.4, 3.14, 3.16, 3.17). Interlimb angle of the F_3 folds, varies from 30 to 90° (Figs. 3.14, 3.17) and fall in the category of tight to open folds (Fleuty, 1964). F_3 folds have rounded hinges in ^apsmmite layers but are angular in case of pelitic layers (Fig. 3.17) and acquire the characters of crenulations (Figs. 3.18, 3.19). A small scale but prominent foliation S_3 parallels the axial surfaces of these F_3 folds in all the lithologies and sometimes shows minor displacements to produce rhombic boudins (Fig. 3.9) or small shears (Fig. 3.9). Rarely, tourmaline veins along the S_2 foliation are seen folded by F_3 structures.

(iv) F_4 folds: Cross-folding of certain lithotectonic units macroscopically along N-S or NE-SW trend of the axial surface produce F_4 open, symmetric to asymmetric folds which lack corresponding axial plane foliations.

(d) Other linear structures: Other linear structures of the Central Himalaya, besides the axes of F_1 , F_2 and F_3 folds, include mineral lineation, boudinage, mullions and slickensides. Mineral lineation is mainly developed due to the preferred orientation of phyllosilicates, equant quartz and feldspar grains and by prismatic to needle shaped grains of kyanite, sillimanite and amphibole. L_1 mineral lineation is developed only in the Bhatwari Group and parallels the F_1 folds which are mainly restricted to this group. In quartz-mica schist, L_1 is marked by preferred orientation of biotite and muscovite flakes, whereas in the garnetiferous mica schist and augen gneiss

L_1 is marked by preferred orientation of aggregates of muscovite, biotite and chlorite (retrograde after biotite) as well as quartz and feldspar. Another set of mineral lineation, L_2 , characterize all the lithotectonic units including the Garhwal Group and is well defined by preferred orientation of phyllosilicates but plunging NW or SE in contrast to the L_1 lineation which plunges NE or SW. Nevertheless, in the thrust zones and on the subthrust side of the MCT, this mineral lineation seems to be stretching lineation in NE direction in the Gamri Quartzite.

Boudins mark an important lineation in the rocks of the Bhatwari Group and are characterized by attenuation of more competent layers and concomittant flowage of material either into the hinge zones of the F_1 and F_2 folds or pinching and swelling of the limbs (Figs. 3.1, 3.17, 3.18). At times, boudins are also developed due to intersection of S_2 and S_3 foliations at moderate angle to produce shear displacement of migmatitic layers along S_3 (Fig. 3.11). At times, boudins seem to be considerably rotated due to F_2 folds and preserve earliest F_1 folds in them (Fig. 3.2a). Mullions are also associated with boudins due to intense F_2 folding. In Shearzone, widespread development of slickensides is seen on the S_2 foliation planes.

3.1.2. Mutual Relationship between structures

Different style and orientation of folds, their distribution in various tectonic units and their mutual relations to different S- surfaces indicate four phases of

deformation in the thick pile of the Central Himalaya; the earliest D_1 Deformation is restricted to the Bhatwari Group, while the younger three D_2 , D_3 and D_4 deformations affect all the lithotectonic units of the Central Himalaya.

- (i) Relict F_1 folds on first layers either of metamorphic or sedimentary origin (S_0) indicate widespread transposition and obliteration of structures of D_1 deformation in the Bhatwari Group. Reclined character of F_1 folds is evident from their fold axes lying in the direction of maximum dip of their S_1 axial plane foliation. Mineral lineation, L_1 , parallels the F_1 folds.
- (ii) The most widespread F_2 folds are isoclinal to nearly recumbent type and are developed on the S_1 foliation which is folded by F_2 folds. Coplanar S_2 axial plane foliation of the F_2 folds and trend of F_2 folds reveal their nearly orthogonal orientation to F_1 folds. D_2 deformation is therefore the most widespread in the Central Himalaya producing S_2 axial plane foliation of F_2 folds with mineral lineation L_2 paralleling the fold axes.
- (iii) Fold mullions and rodding have the same orientation as the axes of F_1 and F_2 folds and are therefore coeval to these deformational episodes.
- (iv) Subparallel transposition of S_2 foliation in the thrust zones into a mylonitic foliation and discrete small-scale development of fold nappe

structures are indications of continued deformation during D_{2a} phase with translation of the metasedimentary pile.

- (v) Early fold axes, F_1 and F_2 and mineral lineations, L_1 and L_2 , are folded by F_3 folds which possess S_3 axial plane foliation and a lineation; all as a result of D_3 deformation which macroscopically control configuration of lithological units.
- (vi) Cross folding along F_4 trends reveal the youngest D_4 deformation which has also produced fault zones, displacement of earlier thrust structures and joints.
- (vii) Mineral recrystallization and new mineral growth has been mostly synkinematic to D_1 , D_2 and D_3 deformational phases and have resulted in three metamorphic events, M_1 , M_2 and M_3 . Retrogression of certain higher grade metamorphic minerals has taken place during D_3 and post- D_3 deformational phase; while ubiquitous quartz has ultimately recrystallized in largely strain-free post- D_3 regime.

Relationship of deformational and metamorphic episodes are being elaborated in Chapter 4.

3.1.3 Orientation of Planar and linear structures:

For the structural analysis of planar and linear structures, individual lithotectonic units have been critically

examined from the Bhagirathi and Yamuna Valleys. Structural data from these valleys have been presented below for better understanding of deformational episodes.

(i) Bhatwari Group: Data on the S_1 foliation of the earliest folds are very scanty due to its transposition by later foliation. Mutual relationship of S_1 and S_2 reveals that S_1 axial plane foliation of F_1 folds is coplanar to S_2 and has same attitude as the latter foliation. A few F_1 fold axes indicate either a $N20^\circ$ plunge of these folds at 20° or towards SW on an average and falling on two great circles intersecting at very low angles towards SE (Fig. 3.20). Mineral lineation L_1 on the S_2 planes mainly plunges at $25^\circ N60^\circ$ and also reveals a submaximum towards SW (Fig. 3.21). Both the maxima fall on two great circles intersecting at $10^\circ N116^\circ$ which almost coincides with F_1 folds. It is likely to be a B-lineation parallel to earliest F_1 folds in the Bhatwari Group.

In contrast to F_1 folds, F_2 folds plunge either NW or SE at moderate angles and show considerable scatter along two great circles intersecting at $12^\circ N36^\circ$ (Fig. 3.22). This scatter seems to have resulted by their subsequent rotation as a result of F_3 folding. The corresponding S_2 axial plane foliation which is normally the most pervasive foliation in the Bhatwari Group mainly reveals a point maximum with two submaxima. S_2 planes strike $N295^\circ$ and dip $55^\circ N25^\circ$, while the two submaxima may indicate variation in orientation of S_2 planes due to later folding, (Fig. 3.23). Rather poorly

EXPLANATION OF FIGURES 3.20 to 3.25

Figure 3.20 - 45 F_1 fold axes from the Bhatwari Group lying on two great circles. Intersection plunges 5° N 125° .

Figure 3.21 - 102 L_1 mineral lineation from the Bhatwari Group lying on two great circles. Intersection plunges 10° N 116° .

Figure 3.22 - 80 F_2 fold axes from the Bhatwari Group lying on two great circles. Intersection plunges 12° N 35° .

Figure 3.23 - - diagram of poles to S_2 main foliation (91 observations) from the Bhatwari Group. Contours - 10 - 13.2 - 7.7 - 1.1%.

Figure 3.24 - 36 L_2 mineral lineation from the Bhatwari Group lying on two great circles. Intersection plunges 8° N 46° .

Figure 3.25 - - diagram of poles to S_3 crenulation foliation (65 observations) from the Bhatwari Group. Contours - 6 - 4.5 - 3 - 1.5%.

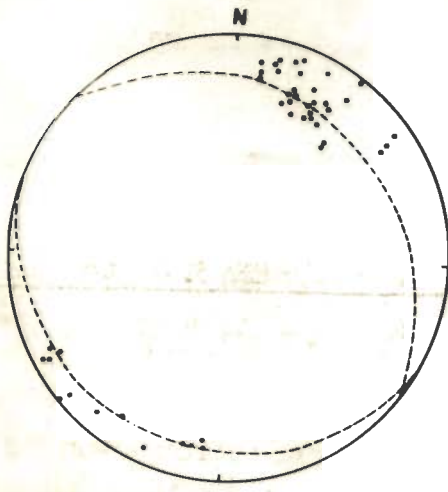


FIG. 3-20

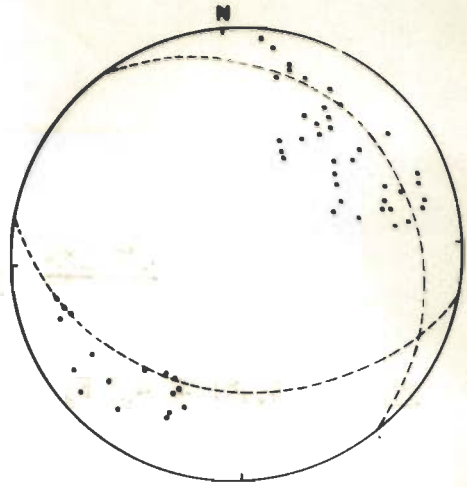


FIG. 3-21

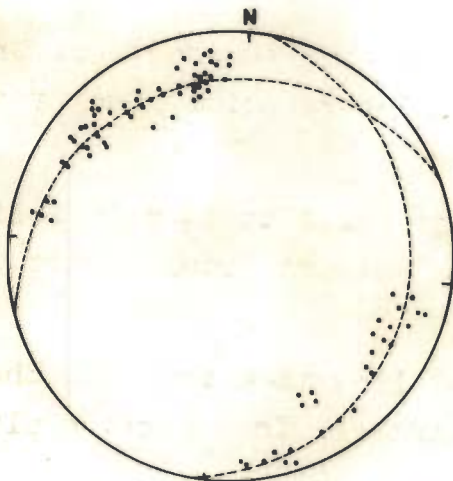


FIG. 3-22

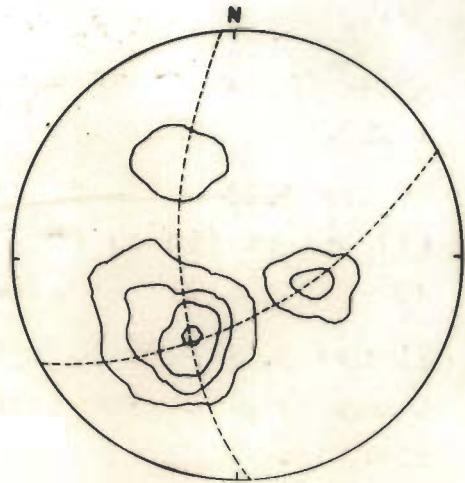


FIG. 3-23

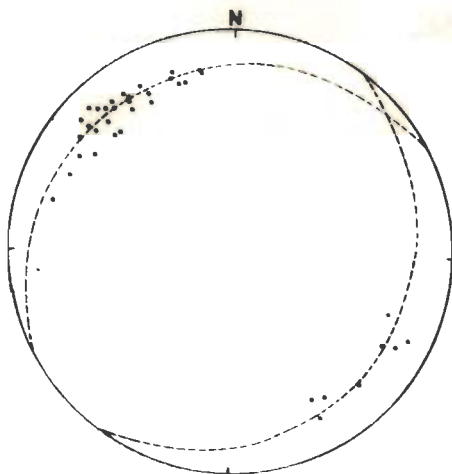


FIG. 3-24

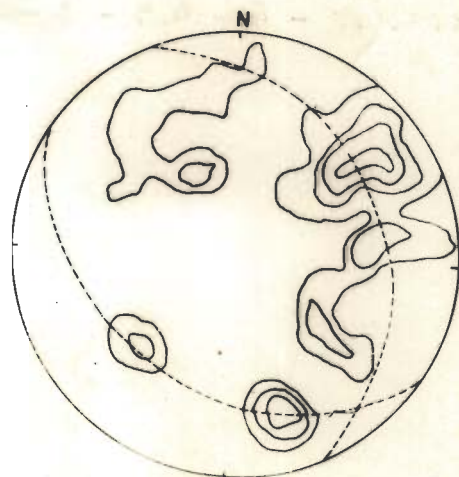


FIG. 3-25

developed L_2 mineral lineation on S_2 foliation also plunges either NW or SE like the F_2 folds and seems to be affected by subsequent folding. L_2 lineation defines two well developed girdles with considerable scatter as a result of later folding; the girdles intersect at $8^\circ N46^\circ$ (Fig. 3.24).

Though data on S_3 crenulation foliation in the Bhatwari Group is not sufficient to unravel a distinct trend because of wide scatter of observations, S_3 poles lie on two great circles trending $N338^\circ$ and $N304^\circ$ and intersect at $12^\circ N140^\circ$ (Fig. 3.25) indicating that S_2 foliations dip $65^\circ N230^\circ$ and $50^\circ N30^\circ$. S_3 planes dip steeper to S_2 foliation by approximately 25° and seem to correspond to macroscopic folds which control the distribution of lithological units and their map pattern. F_3 folds predominantly plunge $20^\circ N335^\circ$, though some of them also plunge towards SE at low angles (Fig. 3.26). F_3 folds lie on two great circles which intersect at $5^\circ N40^\circ$ probably indicating the effect of youngest NE plunging folds throughout the area (Fig. 3.27).

(ii) Suki Group: The most important and widespread S_2 foliation in the Suki Group makes a point maxima of its poles and strikes $N300^\circ$ with a dip of $40^\circ N30^\circ$ (Fig. 3.28). In comparison to the Bhatwari Group, S_2 foliation dips rather gentler by an amount of 15° probably indicating a more clockwise rotation of the Bhatwari Group along the strike of the S_2 planes due to frontal resistance offered by the overriding blocks and imbrication. F_2 folds in the Suki Group have considerable scatter in their NW or SE plunge directions

177759

EXPLANATION OF FIGURES 3.26 to 3.31

Figure 3.26 - 95 F_3 folds from the Bhatwari Group lying on two great circles. Intersection plunges 5° N 40° .

Figure 3.27 - 35 F_4 folds from the Central Himalaya (synoptic) showing ~~the~~ ^{sw-} the NE plunging folds.

Figure 3.28 - - diagram of poles to S_2 foliation (90 observations) from the Suki Group. Contours - 28.8 - 17.8 - 8.9 - 1.1%.

Figure 3.29 - 45 F_2 fold axes from the Suki Group lying on two great circles. Intersection plunges 5° N 36° .

Figure 3.30 - 24 L_2 mineral lineation from the Suki Group lying on two great circles. Intersection plunges 10° N 35° .

Figure 3.31 - 56 F_3 fold axes from the Suki Group lying on two great circles. Intersection plunges 6° N 46° .

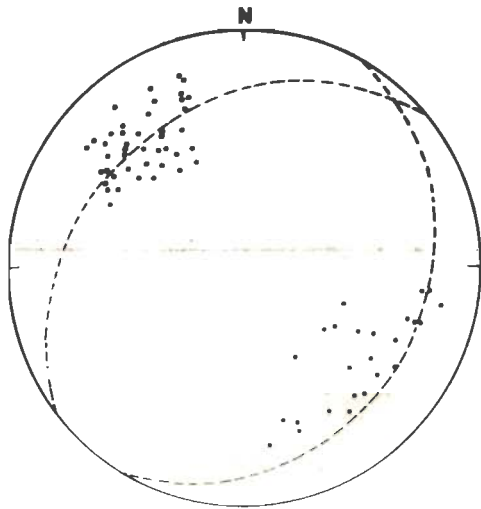


FIG. 3-26

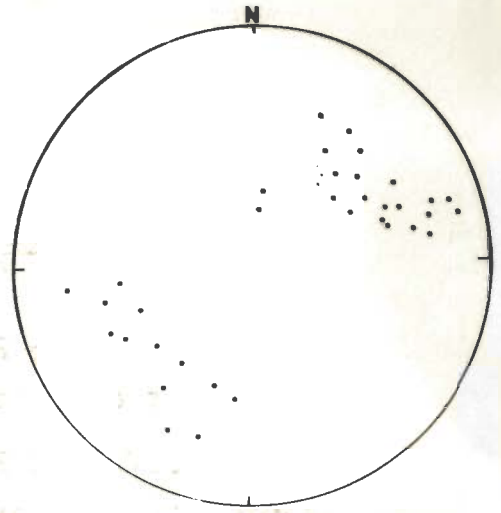


FIG. 3-27

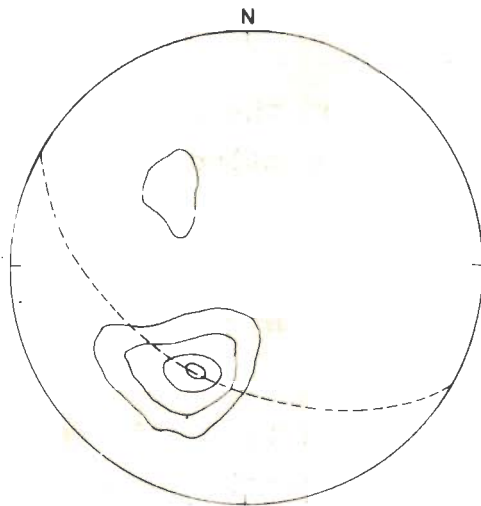


FIG. 3-28

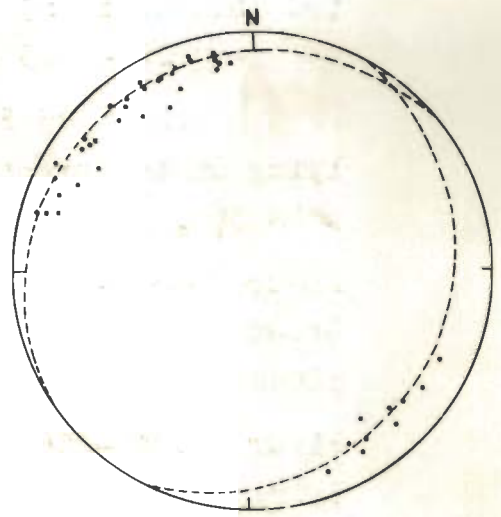


FIG. 3-29

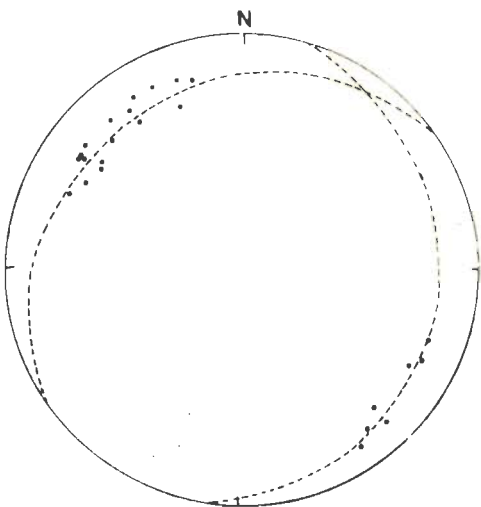


FIG. 3-30

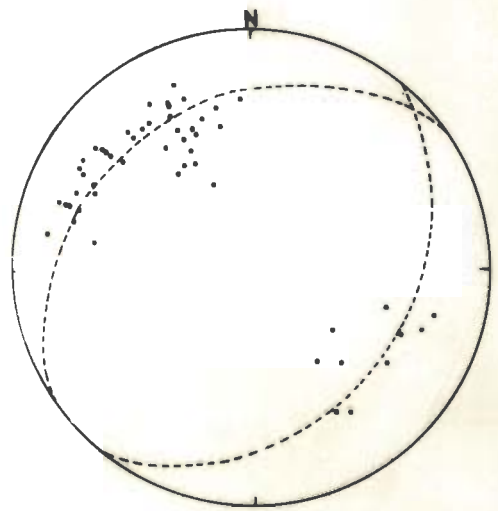


FIG. 3-31

at rather very low angles between 5 to 25°. Fold axes fall on two great circles intersecting at 5° N36° (Fig. 3.29) indicating their scattered distribution due to later F_3 and F_4 folds. Considering attitude of S_2 axial plane foliation of F_2 folds and their low plunge and style, these folds may be classified into moderately inclined - gently plunging isoclines. L_2 mineral lineation corresponds very well to the general orientation of F_2 folds and is a B-lineation parallel to the fold axes from the orientation diagrams as well as in outcrops. It plunges either NW or SE at low angles and seems to be folded along NE axes (Fig. 3.30).

F_3 folds in the Suki Group also plunge due NW or SE but at considerably steeper angle than the F_2 folds. Amount of plunge varies between 15 to 60° while F_3 folds trend between N200°-N360° and N105°-N150° (Fig. 3.31). Their crenulation foliation, S_3 , is considerably scattered with a common trend towards N340° and dips of 50°, SW (Fig. 3.32). Data from Suki and Bhatwari Group clearly demonstrates a common deformational pattern during D_3 phase.

(iii) Garhwal Group: The Garhwal Group is distributed in two lithotectonic units in this part of the Garhwal Himalaya; the Garhwal Quartzite sequence of the Lesser Himalaya constituting the frontal part over which the crystallines are thrust over along the MCT and the imbricate slices of the Banas Formation and the Janki Chatti Formation within the Central Himalaya.

EXPLANATION OF FIGURES 3.32 to 3.37

Figure 3.32 - - diagram of poles to S_3 foliation (40 observations) from the Suki Group.

Figure 3.33 - - diagram of poles to S_2 foliation (50 observations) from the Gamri Quartzite of the Garhwal Group. Contours - 46 - 30 - 14.2%.

Figure 3.34 - - diagram of poles to S_2 foliation (95 observations) from the Janki Chatti and Banas Formations of the Garhwal Group. Contours - 25 - 16.8 - 8.4 - 1%.

Figure 3.35 - 25 F_2 folds from the Janki Chatti and Banas Formations lying on two great circles. Intersection plunges 6° NE.

Figure 3.36 - 20 L_2 mineral lineation from the Janki Chatti and Banas Formation plunging NW and SE at low angles.

Figure 3.37 - 37 F_3 fold axes from the Janki Chatti and Banas Formation lying on two great circles. Intersection plunges 8° N 258° .

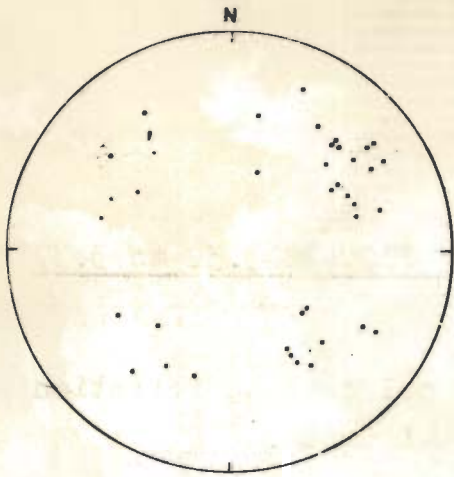


FIG. 3-32

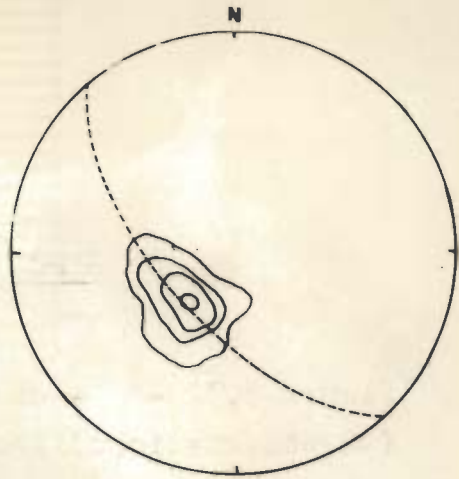


FIG. 3-33

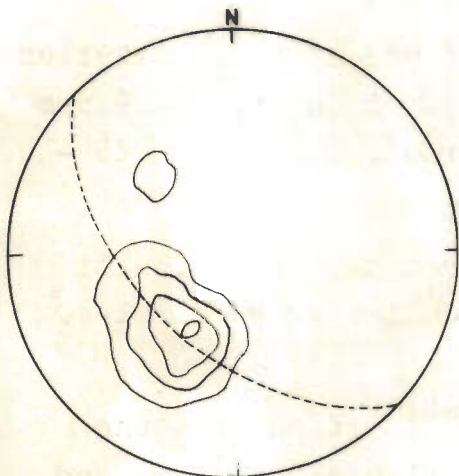


FIG. 3-34

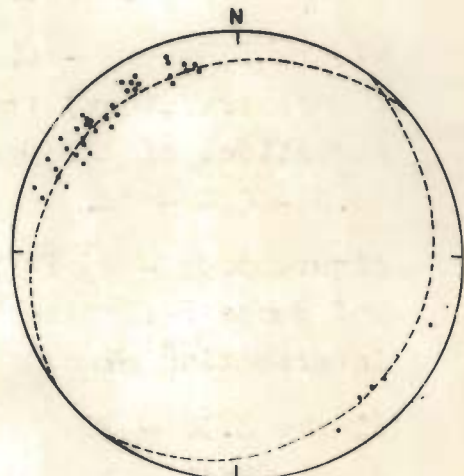


FIG. 3-35

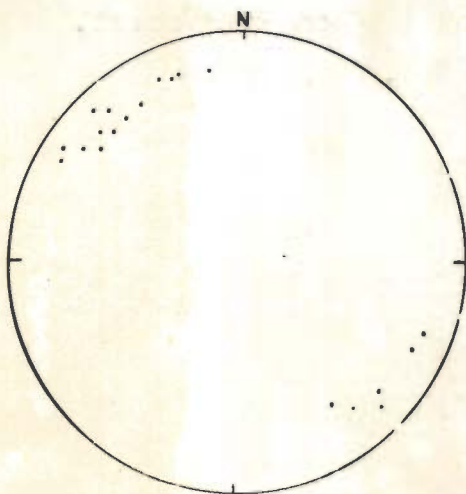


FIG. 3-36

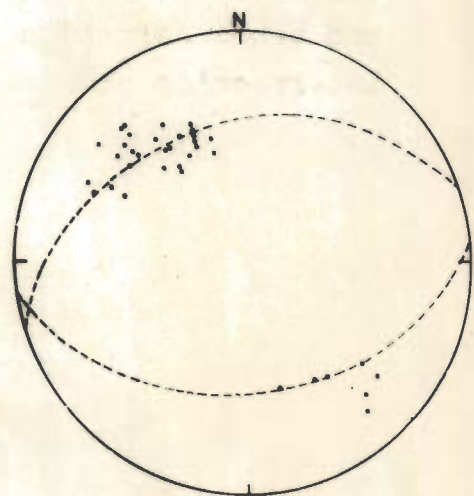


FIG. 3-37

The most prominent foliation, S_2 , in the Garhwal Group subscribes a very well defined point maximum in the Π - diagram and strikes $N320^\circ$ and dips 30° NE (Fig. 3.33). Likewise, S_2 foliation in the Janki Chatti Formation and the Banas Formation strikes $N315^\circ$ and dips 34° $N45^\circ$ and defines a well marked point maximum (Fig. 3.34). Mineral lineation, L_2 , in the latter two formations parallels the F_2 folds and is, therefore, the B -lineation. Both plunge at low angles NW and SE and show considerable scatter in their distribution (Figs. 3.35, 3.36). F_3 folds comparatively plunge steeply between 20 to 50° towards NW and SE (Fig. 3.37). while axial plane foliation, S_3 , corresponding to F_3 folds is widely scattered and dips either SW or NW/SE (Fig. 3.38).

(iv) Other small-scale structures: Other structures present in the Bhatwari, Suki and Garhwal Groups include slickensides, small-scale shear zones and joints. A synoptic orientation diagram of the slickensides present in these rocks reveal that two maxima of lineation plunge 65° $N220^\circ$ and 50° $N58^\circ$, while the submaxima are oriented towards 20° $N25^\circ$, 65° $N 25^\circ$, 20° $N44^\circ$, 50° $N58^\circ$, 40° $N310^\circ$ and 60° $N150^\circ$ (Fig. 3.39). An analysis of the available data on the shear zones in the rocks indicate that many slickensides are related to the shearing of rocks either in the thrust zones or along steeply dipping fault zones. The shear planes strike $N320^\circ$ and dip 50° $N50^\circ$, while also strike $N60^\circ$, $N 40^\circ$, N° and dip 40° SE, 40° NW and 50° W respectively (Fig. 3.40). It is likely that slickensides plunging $N 58^\circ$ and developed upon NE dipping

EXPLANATION OF FIGURES 3.38 to 3.41

Figure 3.38 - diagram of poles to S_3 foliation (29 observations) from the Janki Chatti and Banas Formations.

Figure 3.39 - 105 slickensides from all lithotectonic units of the Central Himalaya and Garhwal Quartzite. Contours - 8.6 - 6.7 - 4.8 - 2.9 - 0.95%.

Figure 3.40 - - diagram of poles to shear planes (85 observations) from all the lithotectonic units. Contours - 11.8 - 6.7 - 4.7 - 1.2%.

Figure 3.41 - - diagram of poles to joints (230 observations) from all the lithotectonic units. Contours - 6.5 - 5.2 - 3 - 1.3 - 0.4%.

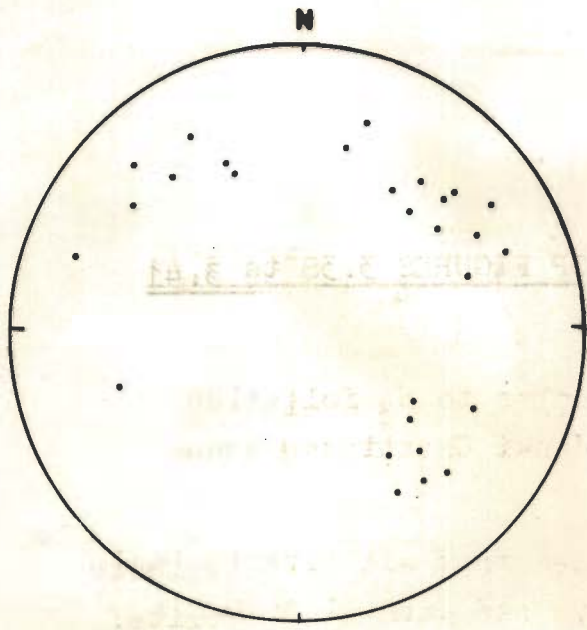


FIG. 3-38

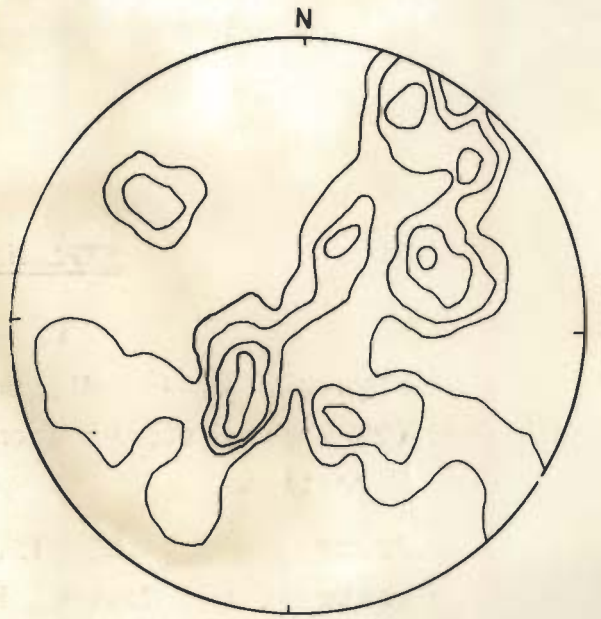


FIG. 3-39



FIG. 3-40

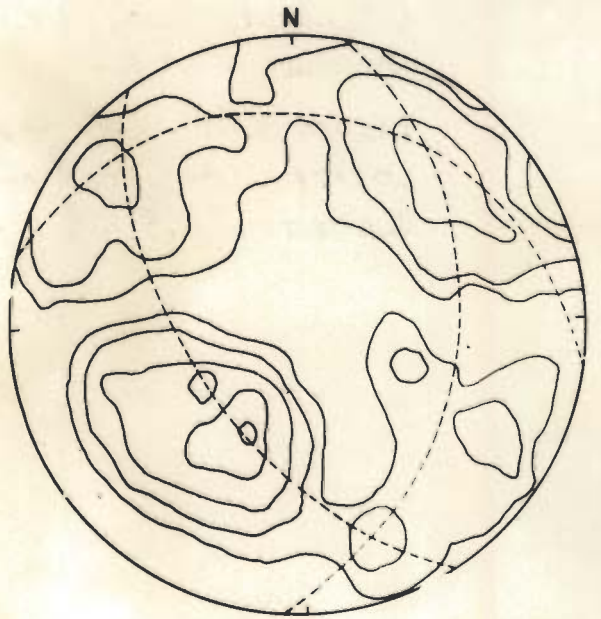


FIG. 3-41

shear zones are related to shear zones associated with the movements during D_{2a} deformation, when the thrust pile moved southward. N to NE trending shear zones dipping westerly and having westerly plunging slickensides seem to be related to the N or NE trending fault zones around Gangnani and Syana Chatti.

Joints distribution and attitude through various units reveal different maxima falling on three complete girdles (Fig. 3.41) and appear to be release joints subsequent to F_3 and F_4 foldings in the area.

3.2 LARGE SCALE STRUCTURES

Macroscopically, the Central Himalayan lithotectonic units are thrust-bound and are folded into open, gently plunging folds and are faulted controlling their distribution and map pattern. Some of these mappable structures are described below.

3.2.1. Faults: All the lithotectonic units of the Central Himalaya have undergone a phase of faulting which has also caused repetition of thrusts and underlying quartzite and calc schist of the Lesser Himalayan Garhwal Group, either concomittant to the piling of the metamorphics along thrusts or during late D_3/D_4 deformational phases. Some of these faults have the following characters, while other causing upthrusting of Garhwal Group rocks are dealt with the MCT and the JBT.

(i) Suparga Fault: The tectonic contact between amphibolite and migmatite about one kilometer south of Malla has been

renamed as Suparga Fault. It is a NW-SE trending fault dipping at moderately high angle ($55-60^\circ$) towards NE. It is characterized by shearing of amphibolite, mylonitization of migmatite, nearly straight course of a tributary and the presence of debris and slide zone.

(ii) Bhatwari Fault: A faulted contact has been traced along the Bhatwari Gad between migmatite and overlying amphibolite which is synformally folded with its southern limb offset by this structure. Its attitude coincides with the Suparga Fault. The presence of this fault is evident from the following evidences

- (a) Development of slickensides, shears and mesoscopic faults.
- (b) Large scale silicification of cummingtonite biotite schist and amphibolite.
- (c) Crushing and fracturing quartz grains and development of biotite due to the retrogression of hornblende during dislocation of metamorphism.
- (d) Offsetting of amphibolite on both sides of the Bhatwari Gad.

(iii) North Bhatwari Fault: The augen migmatite and associated amphibolite exposed north of Bhatwari have been antiformally folded and are offset by a fault along Paper Gad, which flows along the crest of the antiform. The fault plane strikes NW-SE and dips $50-60^\circ$ towards north. The crushing and fracturing of feldspar and quartz porphyroblasts, slickensides and active landslide zone are some of the features indicating

this structure.

(iv) Bygara Fault: During August, 1978, major landslides occurred in Kanuldia-Bygara area near the JBT thrust zone and later led to the Bhagirathi flash floods (Gupta and Dave, 1982). In western part of Joti, the JBT has been locally displaced by a NNW-SSE trending Bygara fault which dips at $55-58^{\circ}$ NE. It appears to be a neotectonic feature because of a major rockslide along this fault in August, 1978. The mylonitization of the garnetiferous gneiss, development of mylonitic graphite schist and association of slickensides, shears and mesoscopic faults are the notable features along the Bygara Fault.

In order to decipher the causes of landslides in the area, various structural data, such as foliation, shear planes and mesoscopic faults, joints and slickensides have been recorded in the thrust zone (JBT) and analysed (Figs. 3.42-3.45; Table 3.1). Relationship between the failure plane trending NNW-SSE and dipping at moderate angle towards NE along the Bygara Fault with different planar structures indicate that the failure has been caused mainly along joints and shear planes trending more northerly to the most prominent S_2 foliations in the rocks. The following fault parameters have been calculated geometrically for the Bygara Fault by the method proposed by Billings (1974) and shown in figure 3.46.

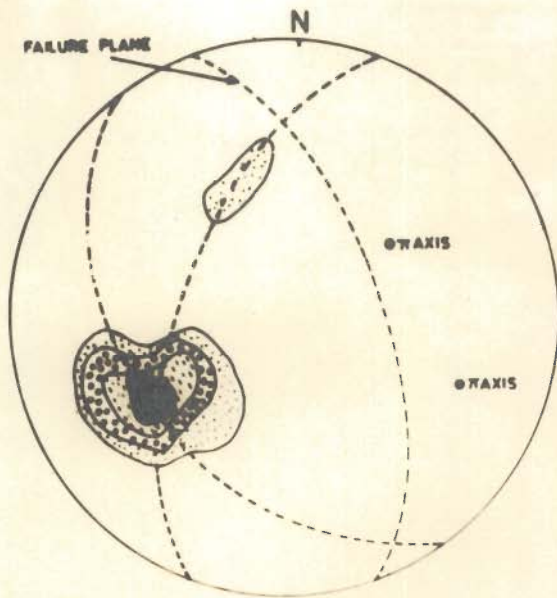


Fig 343-26 POLES OF SHEAR PLANES
CONTOURS 4 - 8 - 16 - 24%

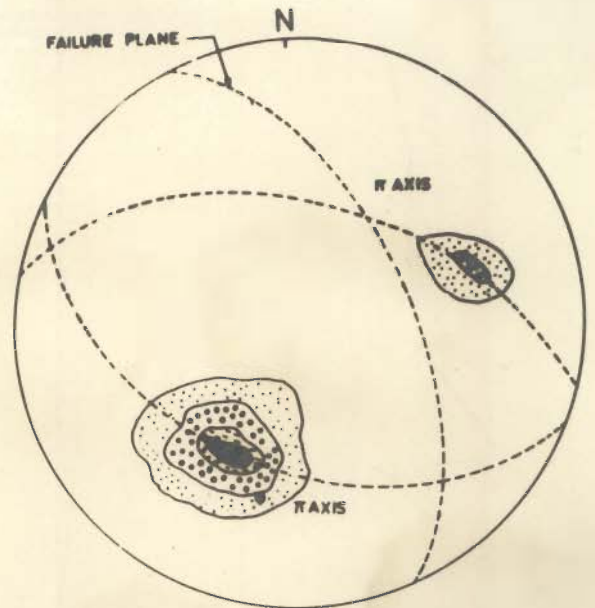


Fig 342-55 POLES OF FOLIATION
CONTOURS 3 - 8 - 11 - 15%

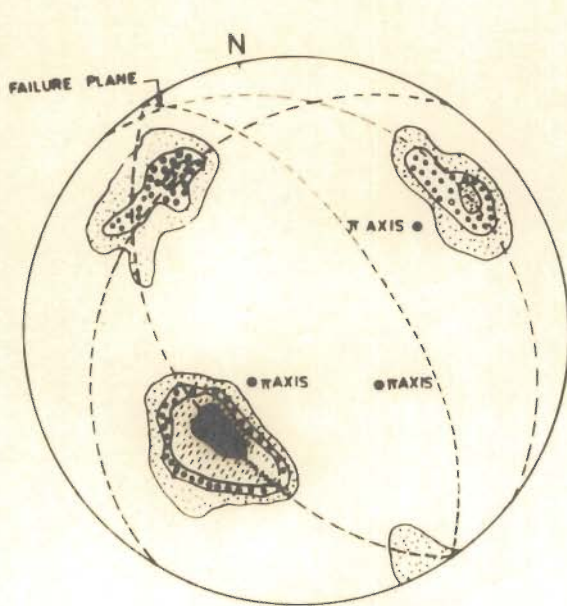


Fig 344-54 POLES OF JOINT PLANES
CONTOURS 3.5 - 7 - 10.5 - 14%

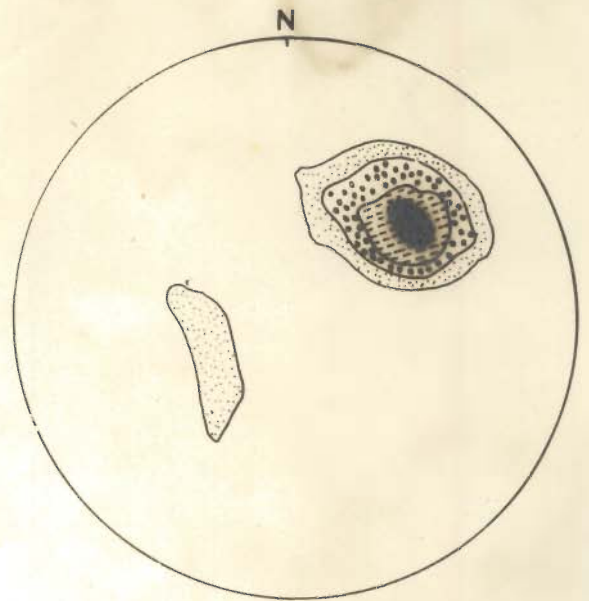
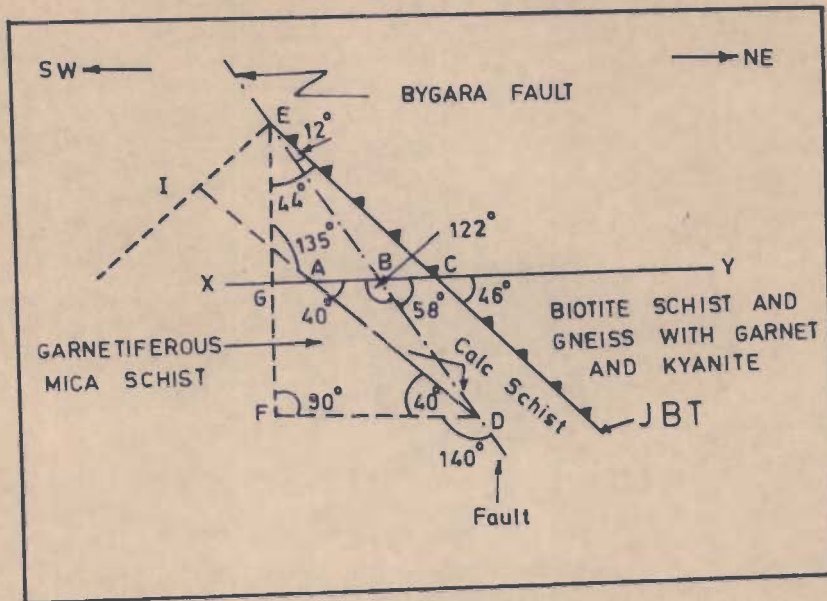


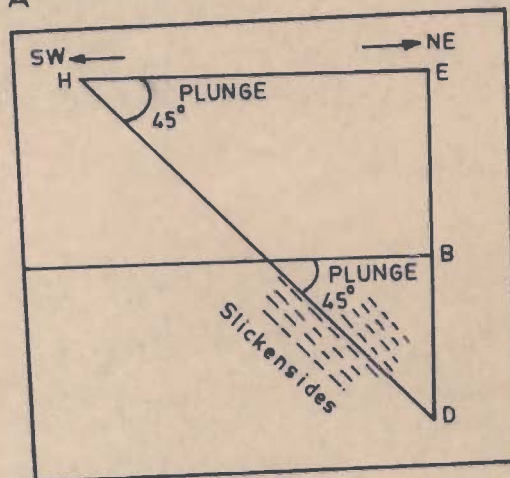
FIG 345-35 PLUNGE DIRECTION OF SLICKENSIDES
CONTOURS : 5.5 - 11.5 - 17 - 23 %

TABLE 3.1 ATTITUDES OF PLANAR STRUCTURAL FEATURES IN THE JBT AND BYGARA FAULT ZONES

Structural features	No. of observation plotted	Strike	Dip	Spacing from field observation (if any)	Distribution
<u>Foliation</u> (S ₂)	55	N 300° 45 45° N 30	--	--	Prominent
		N 285° 36° N 195	--		Less Prominent
<u>Shear Planes</u>	26	N 330 50° N 60	--	--	Prominent
		N 250 45° N 160	--		Less Prominent
<u>Joints</u>					
J ₁	50	N 325	40° N 55	0.2 to 0.3m	Prominent
J ₂		N 65	60° N 45	1.0 to 1.2m	"
J ₃		N 320	70° N 230	1.5 to 2m	"



A



B

FIG. 3-46 - TRIGONOMETRIC SOLUTION OF FAULT PROBLEMS.
 A - CROSS-SECTION OF KANAULDIA - BYGARA REGION.
 THE LITHOUNITS ARE DISPLACED ALONG THE
 BYGARA FAULT
 B - SLICKENSIDE PLUNGING 45° NE ALONG FAULT
 SURFACE

Computation of fault parameters from geometrical techniques

Fault parameters	Magnitude (in meters)
Dip slip	2522.5
Strike slip	2520
Net slip	3501
Throw	2139
Heave	1336
Stratigraphic separation	779.5
Vertical separation	1102
Horizontal separation	950

(v) Dar-Martoli Fault: Mehdi et al. (1972) and Agrawal and Kumar (1973) postulated the western extension of the Dar-Martoli Fault along the Bhagirathi Valley north of Suki and grouped the green schist facies rocks exposed north of Jhala into the Martoli Formation. They favoured the presence of this structure due to sudden change in valley profile from V to U-shape, huge landslides around Suki, presence of acid intrusive (pegmatite) in Martoli Formation only on northern side of Jhala bridge and break in the grade of metamorphism. However, on the basis of the following evidences, the existence of the Dar-Martoli Fault is not supported along the Bhagirathi Valley.

- (a) The rocks exposed beyond Jhala bridge show divergent metamorphic isograd pattern (Fig. 2.1) indicating that these rocks form a part of the Suki Group and do not belong to any distinct tectonic unit.

These are also subjected to almandine-amphibolite grade of metamorphism.

- (b) The acidic igneous activity (pegmatite veins and sills) has been recorded in the Suki Group much to the south, though the dimension of acidic intrusives increases from the JBT towards Harsil. Further, this is to be clarified that the pegmatite bodies exposed just north of Jhala bridge are wider in dimension (0.8 to 12 m in width) in comparison to those occurring south of Jhala bridge (0.1 cm to 0.5 cm). It seems probable that such small acidic intrusions, associated with the Suki Group in south between the JBT and Jhala, have not been recorded by Agrawal and Kumar (1973).
- (c) The broad U-shape profile around Jhala is not due to faulting but it is a result of fluvioglacial activity, as evident from the presence of fluvioglacial and glacial deposits around Jhala (Chibber, 1958).
- (d) The landslide zone occurring at Suki forms a part of the pre-slided mass. It is rock-debris fall zone which could have resulted due to steepened slope. Kyanite schist and porphyroblastic migmatite exposed around Suki are characterized by the presence of extensive joints and moderate angle of foliation which could have triggered the mass movement process in the past. Large scale road construction in the area may also be responsible for the reactivation of slipped mass.

The rocks exposed around Jhala show poor evidences of mylonitization and development of slickensides, shears and mesoscopic faults commonly recorded in the earlier described tectonic zones. Thus, it can be concluded that the rocks exposed beyond Jhala bridge form a part of the Suki Group of the Central Crystallines and, therefore, the possibility of western extension of the Dar-Martoli fault in the Bhagirathi Valley at this locality may be ruled out.

(vi) Gangnani Fault: It is N-S trending fault along the Bhagirathi River and has offset the JBT near Joti. The formations, which have been affected by this fault, are garnetiferous mica schist and kyanite schist of the Suki Group, calc schist of the Janki Chatti Formation, garnetiferous mica schist, amphibolite and migmatite of the Bhatwari Group. Along the fault, these rocks have been extensively sheared and crushed leading to rock debris slides. At Gangnani, the basic rock has been extensively sheared with the development of actinolite schist. Profuse development of slickensides and occurrence of geothermal springs at Joti, Gangnani and Sunagarh are notable features. The presence of active landslide zones along the fault also indicate that it is probably an active fault zone.

In Dangal region, severe landslips have occurred in puckered, highly sheared and crushed garnetiferous quartz-mica schist and gneiss. Most of the axial planes of these folds dip towards NE or NW with varying amount, as recorded in the field. At many places, offsetting of the lithounits,

as a result of drag along the axial planes is quite conspicuous^{CU}. Intense folding in garnetiferous-quartz-mica schist, dragging of the lithounits along the axial plane of mesoscopic folds and subsequent dislodging of rocks coupled with intense crushing and fracturing are the main causes for landslide in this particular area. The disturbance in angle of repose during road construction, might have triggered the intensity of land-sliding along the road.

As mentioned earlier, the JBT has been offset by the Gangnani fault and the Bygara fault. Along these faults, slickensides are profusely developed and plunge 45° N 50° (prominent) and 60° N 255° (less prominent) along probable direction of net slip of movement (Fig. 3.45).

(viii) Agora Fault: About 4km north of Agora, a faulted antiform has been seen within the migmatized zone along the Kaldya Gad. The rocks affected by this fault are chlorite schist and migmatite. It is a NW-SE trending structure dipping at moderate angle towards north. Formation of retrograde chlorite schist from amphibolite, mylonitization of migmatite and association of slickensides are recognizable criteria for this fault.

(ix) Rana Fault: A NW-SE trending fault has been observed within the migmatite zone south of Rana village along the Yamuna Valley. The rock units affected by this structure are gneiss, migmatite and garnetiferous mica schist of the Bhatwari Group and quartz-sericite of the Banas Formation, occurring as a tectonic slice of the Garhwal Group with the

Bhatwari Group. The fault dips at an angle of 50-55° NE. Lithological displacement, mylonitization of surrounding rocks, development of slickensides, shears and mesoscopic faults are favourable evidences for this structure.

(x) Banas Fault: A faulted contact has been located at Banas and offsets the garnetiferous mica schist and migmatite of the Bhatwari Group. The meta-andesite sill is closely associated with this fault. The other notable evidences for the existence of this structure are mylonitization of the surrounding rocks and association of minor structures as observed in Rana Fault, silicification of garnetiferous mica schist and meta-andesite. The association of sulphide mineralization of hydrothermal origin with meta-andesite also support the existence of this structure.

3.2.2. Postulated lineaments between Yamuna and Bhagirathi Valleys:

Two important NE-SW trending lineaments seem to exist between the two valleys, whose sinistral strike-slip fault character is evidenced by considerable displacement of the traces of important lithounits and thrusts. Of these, the transverse lineament near the Yamuna Valley seems to be more important, as it appears to displace sinistrally the surface trace of the MCT by about 10 km. Considering the northwesterly projects of the calc schist bands of the Janki Chatti Formation between the Kaldya Gad and Yamuna Valley, this displacement is considerably less and amounts to about 3.5km. This

extrapolated lineament has been termed as the Upper Yamuna Lineament whose surface trace seems to extend for more than 25km hence it is an important transverse lineament with sinistral sense of displacement across the Central Himalaya.

Another such transverse sinistral lineament is postulated between the Kaldya Gad and the Bhagirathi Valley and displaces most of the lithounits of the Bhatwari Group by about 4km. This lineament has been termed as the Kaldya Gad Lineament which can be traced for atleast 25km.

It is therefore evident that the Bygara and Gangnani Faults along the Bhagirathi Valley are the conjugate dextral strike-slip faults of this fault system which seems to have resulted from maximum principal stress (σ_1) oriented approximately N-S in this part of the Central Himalaya with intermediate principal stress (σ_2) being vertical and minimum principal stress (σ_3) being horizontal and oriented approximately E-W. Microseismic clustering of numerous earthquake events in this part of the Lesser and Central Himalaya (Fig. 3.47, Sarkar, personal communication) in the region falling south of the MCT indicate seismically active character of this fault system as a result of ongoing deformation in the Himalaya.

3.2.3. Folds: The different lithounits exposed in the area have been mainly subjected to isoclinal folding on the mesoscopic scale, though macroscopic isoclinal folds are difficult to map. Therefore, various synformal and antiformal structures in the area are mostly gently plunging open upright to

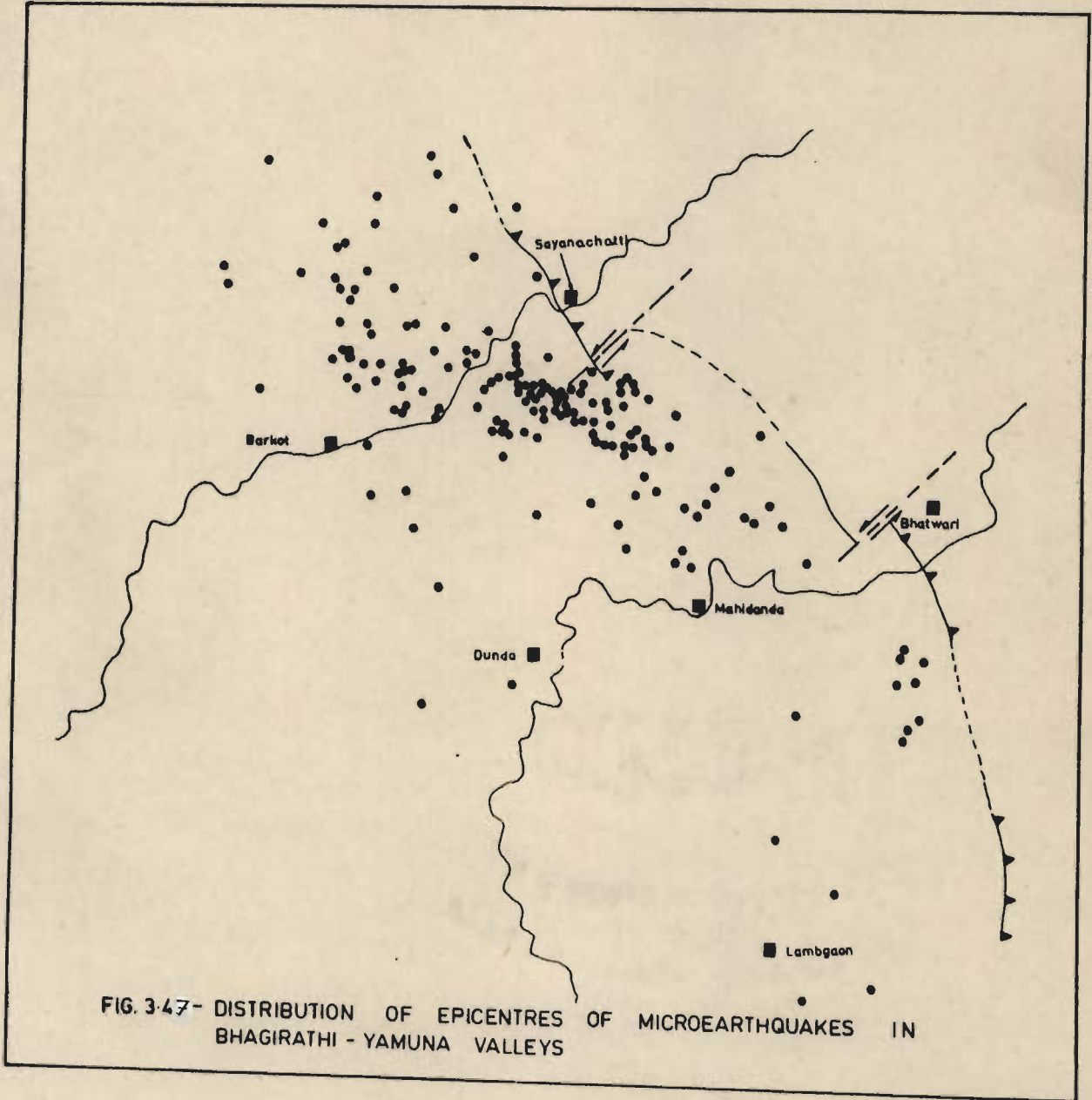


FIG. 3-47- DISTRIBUTION OF EPICENTRES OF MICROEARTHQUAKES IN BHAGIRATHI - YAMUNA VALLEYS

asymmetric folds of D_3 and D_4 deformational phases affecting mostly the main foliation, S_2 . Though some repeated amphibolite and migmatite bands may be considered as limbs of large isoclinal folds, a very few such closures of folds could be worked out due to rather inaccessible regions between the two adjacent valleys. Some of these structures are described below.

- (i) Malla Antiform: The migmatized rocks exposed at Malla are folded into a small antiform (Fig. 2.1), as evident from the change in dip of foliation from $25-30^\circ$ SE to $25-35^\circ$ NE around Malla. The structure has been recognized to be a F_3 -fold; the southern limb of which has been offset by the Suparga Fault.
- (ii) Bhatwari Synform: Thick amphibolite band near Bhatwari, underlain by migmatite has been subjected to an upright F_3 , NW-SE trending synformal structure. The core of the Bhatwari Synform is occupied by another small outcrop of migmatite. The southern limb of the fold dips at $20-25^\circ$ NE, whereas the northern limbs at $25-30^\circ$ SW. Both the limbs of the synform have been affected by the Bhatwari Fault and North Bhatwari Fault. The trace of the axial surface of the fold is nearly parallel to the Bhatwari Gad.
- (iii) Bhatwari Antiform: To the north of Bhatwari, amphibolite along with augen migmatite have been folded into an antiform, along the Paper Gad. This structure appears to be related to D_3 -deformation (i.e., F_3 -fold). The core of the fold is occupied by augen migmatite. The trace of axial surface of the antiform

runs parallel to Paper Gad and is offset by NW-SE trending North Bhatwari Fault. The S_2 foliation on southern limb of the fold dips at an angle of $25-30^\circ$ SE and on the northern limb at $20-35^\circ$ NE.

- (iv) South Gangnani Synform: About 2.4 km south of Gangnani the garnetiferous mica schist, migmatite and amphibolite of the Bhatwari Group have been folded into a symmetrical synform whose trace of axial surface is approximately parallel to the course of Mamlapani Gad. S_2 foliation on southern limb of the synform dips $40-45^\circ$ NE, while on the northern limb, it dips at an angle of $50-55^\circ$ SW. The core of this synform is seen near Sunagar and exposes the migmatite.
- (v) North Agora Antiform: About 4 km north of Agora, the chlorite schist (a retrograde product of amphibolite) exposed within the augen migmatite of the Bhatwari Group is folded probably into an isoclinal antiform. The foliation dips from $35-40^\circ$ NE on the limbs of the antiform, while trace of axial surface of the antiform has been affected by NW-SE trending Agora Fault.
- (vi) Bhankoli Antiform: The metabasic sill associated with the Gamri Quartzite in Kaldya Dodital section has been deformed into an open fold. The trace of axial surface of the antiform trends ENE along the Kaldi Gad. S_2 foliation in metabasic, exposed on the western side of Kaldi Gad, dips $20-25^\circ$ NE and, on the eastern side dips $20-25^\circ$ SE. The fold seems to be a structure of F_4 phase of deformation.

(vii) Hanumanchatti Fold: The amphibolite sills associated with migmatite around Hanumanchatti have been subjected to cross folding of F_4 phase, as it is evident from the outcrop pattern (Fig. 3.1). In the first instance, the amphibolite is folded along NW-SE trend during D_3 deformation and later on to cross-folding by D_4 deformation, producing F_4 cross fold. The trace of axial surface of the F_4 fold runs in the NE-SW direction, while axis plunges towards NE.

(viii) Rana Antiform: The rocks exposed around Rana in the Yamuna Valley section and forming a part of the Bhatwari Group and Garhwal Group (Banas Formation) have been folded into an open antiform plunging NW. The folding is better reflected by the trace of thrust plane and its trend which varies from NW-SE to E-W in northwestern parts of Rana and Banas villages. The rocks involved in folding are quartz-sericite schist (the Banas Formation) and migmatite, augen gneiss, amphibolite and garnetiferous mica schist (Bhatwari Group). The trace of the axial surface passes through Rana and has been offset by the Rana Fault. The northern limb of the antiform has also been affected by NW-SE trending Banas Fault.

3.2.4 Thrusts:

(i) Main Central Thrust (MCT): Heim and Gansser (1939) originally introduced the term "Main Central Thrust" in the Kumaon Himalaya as a tectonic boundary between the Lesser Himalayan sediments and medium grade metamorphics constituting the basal part of the Central Crystallines.

The Main Central Thrust in the Uttarkashi area along the Bhagirathi Valley was first located near Sainj by Auden (1937) and thereafter, several workers confirmed its existence along the Yamuna and Bhagirathi Valleys (Jain, 1971; Pachauri, 1972; Ranga Rao, 1972; Mehdi et al., 1972, Agarwal and Kumar, 1973; Valdiya, 1976, 1978). All these authors mark the MCT between the almandine-amphibolite facies of rocks belonging to the Central Crystallines and lower green schist facies of rocks of the Garhwal Group (Gamri Quartzite). However, Valdiya (1978) renamed this thrust as the Munisari Thrust and opined that the true MCT, now designated as Valdiya's MCT or MC (Vakirita) Thrust, lies further northward throughout the length of the Central Himalaya Valdiya (1980). In the present work, the original status and position of the MCT has been retained, as no convincing evidences have been found for the change in its nomenclature.

During the detailed geological investigations along these valleys and in thrust zones, it has been observed that the MCT is not a simple clean shear plane along which huge pile of crystalline rocks ^{has been} thrust southward, as has been shown by earlier workers in their maps and sections of this area (Ranga Rao, 1972; Pachauri, 1972, 1980; Agrawal and Kumar, 1973; Valdiya, 1976, 1980). The imbricate nature of the MCT is very well evidenced by the occurrence of quartz-sericite schist bands of the Banas Formation and low grade calc schist of the Janki Chatti Formation belonging to the Garhwal Group within the Bhatwari Group of the Central Crystallines. The

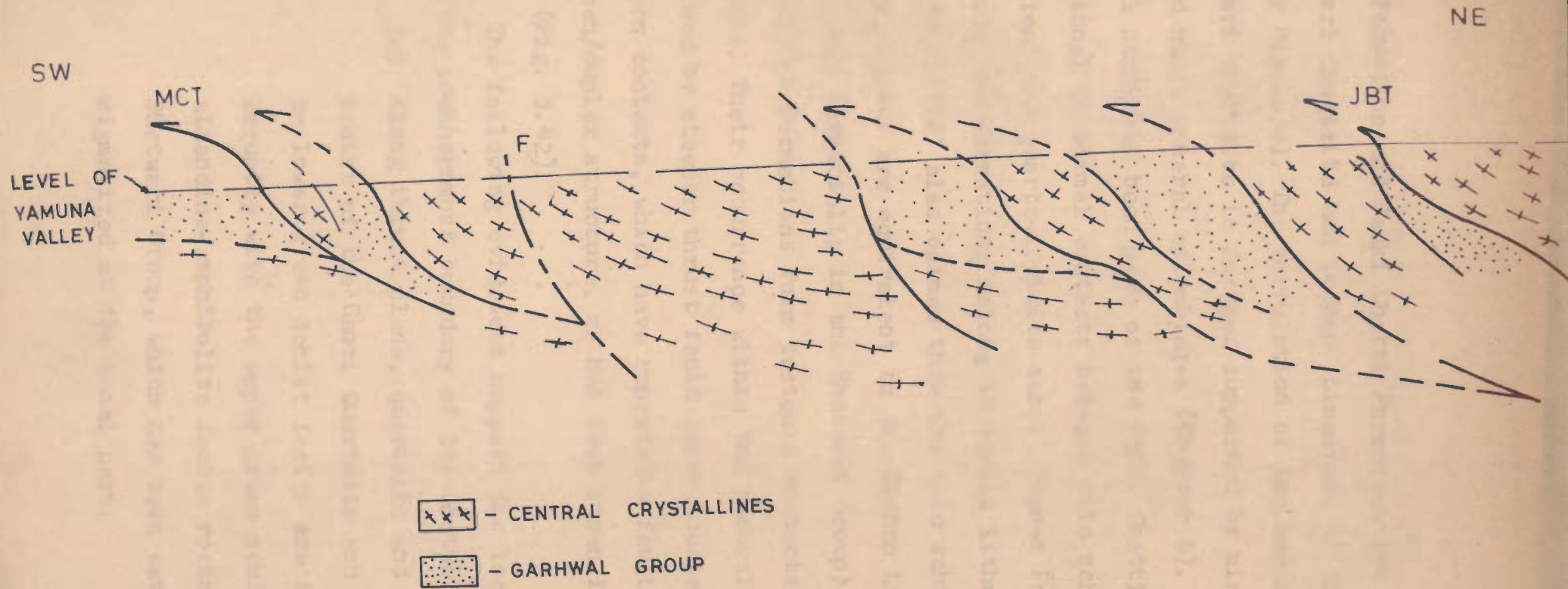


FIG. 3.42- SCHEMATIC CROSS-SECTION SHOWING EVOLUTION OF IMBRICATE THRUST SLICES ALONG THE YAMUNA VALLEY

Banas Formation and Janki Chatti Formation are correlative ^{with} the Gamri Quartzite and Deoban Limestone of the Garhwal Group (Lesser Himalaya). The correlation of the Banas Formation with the Gamri Quartzite is further supported by microscopic characters and heavy mineral assemblages (Chapter 4). Although, no special study has been made of the Janki Chatti Formation, gradational to normal contacts between calc schist (Janki Chatti Formation) and quartz-sericite schist (Banas Formation) indicate that both the formations belong to single lithotectonic unit. Ranga Rao (1972) also opined that the calc schist and marble at Janki Chatti are equivalent to the Deoban Limestone. In the entire area (especially in the Bhatwari Group), the Banas and Janki Chatti Formations form tectonic contacts with the surrounding rocks. Their occurrence within the Central Himalaya has been explained by steeper thrust fault zones located along their southern contacts, which have repeatedly faulted the MCT as a schuppen/duplex structure, as has been shown in the schematic model (Fig. 3.42).

The following evidences support the location of the MCT along the southernmost boundary of the Bhatwari Group:

- (a) Along thrust plane, quartzite and quartz-sericite schist of the Gamri Quartzite and metamorphosed to lower green schist facies are in contact abruptly with the upper green schist to almandine-amphibolite facies rocks of the Bhatwari Group, which has been extensively migmatized at the basal part.

- (b) Variation in the degree of deformation and metamorphism. The evidences of four phases of deformation and three metamorphism are seen in the Bhatwari Group, while the Lesser Himalayan metasediments have undergone only three phases of deformation.
- (c) Development of a wide zone of mylonitization and shearing along the MCT.
- (d) Retrograde metamorphism of basic rock to actinolite-talc-chlorite schist showing strong mylonitic foliation.
- (e) Stretching and rotation of feldspar porphyroblasts defining a lineation in augen gneiss.
- (f) Profuse development of slickensides plunging 25-30° NE or SW.
- (g) Formation of unconsolidated powdered material due to reduction in grain size and rocks strength during thrusting.
- (h) Transposition of F_1 and F_2 fold structures and development of transposed foliation, S_{2a} . The other associated transposed structures (shear zones and mesoscopic faults) along low dipping axial surfaces of F_2 folds dip 25-50° NNE or NE and strike NNW-SSE or NW-SE. At places, these structures occur within the Schuppen zone. The above behaviour of mesoscopic shears associated with F_2 folds in the thrust sheet

indicate that thrusting (MCT) could have been initiated in the late stages of D_2 deformation and has been considered as D_{2a} phase of deformation.

- (i) i, The occurrence of metadolerite dykes at Kumalti and Wazari and meta-andesite sill at Banas in the tectonic zones also confirm the existence of these structures. The metadolerite dyke at Kumalti is cuts ~~the~~ the MCT.
- (j) Retrogression of mica schist and amphibolite to chlorite or chlorite-talc-schist and development of phyllonite along the thrust zone.
- (k) Association of sulphide mineralization of hydrothermal origin (Chapter 7) with quartz-sericite schist (Garhwal Group) NW of Gorsali and with meta-andesite sill at Banas.
- (l) Strong silicification and development of tension gashes along the tectonic planes.

(ii) Joti-Bhandali Thrust (JBT): The Joti Bhandali Thrust (JBT) has been discovered as a major structural feature within the Central Crystallines by the author. It separates the Bhatwari Group from the Suki Group, although former does not come directly in contact with the Suki Group due to the presence of the Janki Chatti Formation, in the Schuppen zone of the MCT. The topmost calc schist band (Janki Chatti Formation) can be taken as marker horizon for this thrust. The JBT passes through Joti in the Bhagirathi Valley and

follows Bhandali Gad ($2\frac{1}{2}$ km north of Janki Chatti) in the Yamuna Valley. The position of this structure could not be traced in Dodital section due to inaccessibility. The thrust dips at an angle of $40-50^{\circ}$ NE.

The presence of this thrust in the Bhagirathi Valley was first reported by Gupta and Dave (1979). Valdiya (1980) extended the limit of the MC (Vakirita) Thrust to this area, which also passes through Joti. He considered abrupt change in the grade of metamorphism (appearance of kyanite zone) as the main basis for the existence of this structure. Further, he opined that this structure defines the upper limit of the Lesser Himalayan sediments and metasediments.

The supporting evidences, recorded by the author, for the presence of the JBT in the area are:

- (a) Large variation in lithology in the thrust zone particularly in the Yamuna Valley section, where in a narrow zone of about 100-150m calc-schist, amphibolite, quartz-sericite schist, chlorite schist, garnetiferous mica schist and porphyroblastic migmatite are exposed.
- (b) Very poor or no basic igneous activity in the Suki Group in comparison to the Bhatwari Group which has undergone profuse activity.
- (c) No evidence of the first phase of deformation, metamorphism and migmatization has been observed in the Suki Group, indicating that two groups

belong to different tectonic unit (Chapter 2, 4). This is also evidenced from the fact that the Bhatwari Group show normal metamorphic sequence, whereas the Suki Group is characterized by inverted metamorphic sequence. It has also been observed that garnet and feldspar porphyroblasts show strong rotation in the upper part of the Bhatwari Group. On the other hand, porphyroblasts in Suki Group do not show much rotation. Transposition of S_2 foliation and development of mylonitic foliation, S_{2a} , in the thrust zone are noticeable features.

- (d) Formation of gouge, mylonitic graphite schist, and chlorite schist due to thrusting.
- (e) Association of sulphide mineralization of hydrothermal origin (Chapter 7) with topmost horizon of the calc schist (Janki Chatti Formation) occurring along the basal part of the JBT.
- (f) Presence of slickensides, shear planes and mesoscopic faults are indicative of tectonic movements.
- (g) Association of geothermal springs in the thrust zone. Dave et al. (1981) plotted geothermal springs and epicentral data of recent earthquake on a tectonic map of the area and found a good correlation. The epicenters have a linear distribution along the JBT, particularly, in the Yamuna Valley, indicating a seismically active nature of the thrust.

They also noticed that the frequency of occurrence of landslides in the thrust zone is quite high, and are mainly controlled by structural elements. The active nature of this thrust and associated faults is also evident from major landslides which took place during August, 1978 in the area (Gupta and Dave, 1982).

- (h) The Suki Group is characterized by divergent inverted type of metamorphic isograde pattern, which is well observed in the Bhagirathi Valley section. In the northern side of the JBT, a narrow band of garnetiferous gneiss is overlain by a wide zone of kyanite schist, (cf. Valdiya, 1980). At Jhala, kyanite schist is overlain by sillimanite gneiss. From north of Jhala sillimanite grade decreases to garnet through kyanite grade in a narrow zone. The garnet grade extends to Harsil and further north of this locality, it changes to biotite grade and finally to phyllite and slate. The above behaviour of metamorphic isogrades in the Suki Group show that the rocks exposed between the JBT and Jhala are characterized by inverted metamorphic sequence, whereas the rocks exposed on northern side of Jhala (around Harsil) are characterized by a normal metamorphic sequence. In normal case, the lower grade metamorphic rocks exposed around Harsil should be repeated near the basal part of the Suki Group due to

CHAPTER - IV

PETROGRAPHY

This chapter deals with the petrographic descriptions of various lithological units of the Garhwal Group, Bhatwari Group and Suki Group and incorporates

- (i) the megascopic and microscopic characters of representative specimens belonging to the above mentioned groups, including the detailed micro-textural relationship of main minerals with structural elements to decipher relationship between mineral growth, metamorphism and deformation phases;
- (ii) the heavy mineral analysis of arenites from the Banas Formation for comparison with those of the Gamri Quartzite;
- (iii) the modal analysis of selected specimens of amphibolite, meta-andesite and metadolerite.
- (iv) the modal analysis of selected specimens of migmatite and country rocks of the Bhatwari and Suki Groups (details in Chapter 6);
- (v) the X-ray studies of feldspar of the Bhatwari and Suki Groups.

4.1 GARHWAL GROUP

Arenaceous component of the Garhwal Group is comprised of the Gamri Quartzite and the Banas Formation belonging to

two distinct tectonic regimes (Chapters 2 and 3), while the carbonates have been classified as the Janki Chatti Formation. The rock types belonging to the Garhwal Group are:

- (i) Quartzite
- (ii) Quartz-sericite-chlorite schist and Banas Formation
- (iii) Calc. schist
- (iv) Actinolite schist
- (v) Amphibolite
- (vi) Chlorite-actinolite-talc schist

4.1.1 Quartzite and quartz-sericite-chlorite schist:

A gradual textural evolution has been observed in the Gamri Quartzite from unmetamorphosed orthoquartzite to quartz-sericite schist in the thrust zone (Jain, 1972) while the Banas Formation reveals mostly schistose varieties.

Quartz-sericite-chlorite schist is characterised by abundant quartz (80-95%) showing subpolygonal to strongly preferred oriented grains. The foliation is conspicuous by chlorite-sericite (occasionally muscovite) flakes. At times, patches of chlorite are seen. Grains of zircon, tourmaline, apatite, sphene, ilmenite and rutile occur as minor detrital minerals. The foliation is more prominent near the tectonic zones.

Microtextures of quartz:

A sequential microtextural evolution in quartz characterize these rocks. In low grade metamorphic

environment, slightly deformed, detrital lensoidal porphyroclasts (quartz I) remain mostly unrecrystallized and are even marked by strongly undulose extinction with deformation lamellae with misoriented bands (Fig. 4.1 - central grain) and incipient recrystallization along grain margins (Fig. 4.1 - second grain in centre). Their axial ratio rarely exceeds 3. Relict porphyroclastic microstructures are common indicating evolution of subgrains due to recrystallization (Fig. 4.1). Due to recovery, new quartz II grains are most abundant and well developed with strain free straight extinction. ^{These also reveal} numerous inclusions of chlorite-sericite flakes of the foliation without any deflection (Si = Se) and triple junction, with nearly straight grain boundaries (Figs. 4.1-2).

Two foliation configuration marks the main foliation plane (XY plane) in these quartzite and schist throughout in the thrust zone of the MCT and in the Banas Formation (Figs. 4.1-2). Similar characters of foliation have been extensively observed in the MCT zone of the Nepal Himalaya within the Tibetan sedimentary cover rock and the Midland Formations (Pecher, 1977; Bouchez and Pecher, 1981). In the XZ section of the foliation, two-foliation configuration is characterized by discrete shear zones marked by recrystallized phyllosilicates and quartz II producing lozen^{ge}/almond-shaped domains from quartz I having an angular relation of about 30°. These represent "finite strain cleavage" and "shear cleavage" of Bouchez and Pecher (1981) or those described

EXPLANATION OF PHOTOMICROGRAPHS:

FIGURES 4.1 to 4.6

Figure 4.1 - Quartz-sericite schist showing micro-texture in quartz. Porphyroclastic quartz in centre with deformational bands and strong undulose extinction-having serrated margins.

Almond shaped S_2 foliations intersection at low angles. Gamri Quartzite of the Garhwal Group. Locality - south of Kumalti Gad Bhagirathi Valley (D₂₇/698). Crossed X55.

Figure 4.2 - Quartz-muscovite schist with intrafolial isoclinal F_2 folds having phyllosilicates aligned parallel to S_2 foliation, which is crenulated by F_3 folds. Post-tectonic granoblastic quartz II and muscovite I and II oriented along S_2 and S_3 respectively. Gamri Quartzite of the Garhwal Group. Locality - south of Kumalti Gad (BH₃). Crossed X110.

Figure 4.3 - Calc schist with preferred orientation of muscovite and calcite along axial plane foliation, S_2 , of isoclinal to tight F_2 folds. Janki Chatti Formation. Locality --Janki²Chatti (D₂₇/791). Crossed X55.

Figure 4.4 - Quartz-chlorite-actinolite schist with preferably oriented chloritized actinolite along S_2 foliation cut by randomly oriented fractured tourmaline after D_2 deformation. Gamri Quartzite. Locality - Kumalti²Gad (D₂₇/446). Plane X55.

Figure 4.5 - Cummingtonite-biotite schist with biotite oriented along S_2 foliation which is crenulated by F_3 folds with development of biotite, chlorite along S_3 foliation. Post- D_3 helicitic quartz in hinge zone of F_3 folds containing inclusions of biotite, muscovite and iron oxide. Bhatwari Group. Locality - East of Hanuman Chatti (D /737). Crossed X110.

27

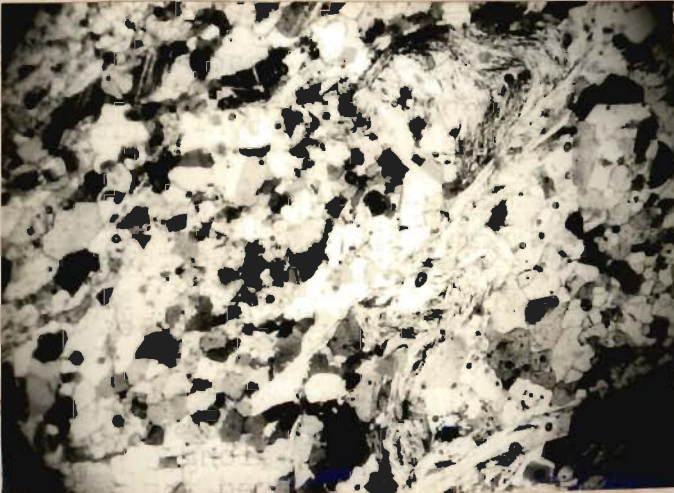
Figure 4.6 - Quartz-mica schist with preferably oriented phyllosilicates along S_2 foliation being crenulated by F_3 folds. New growth of muscovite along S_3 foliation due to syn- to late M_3 metamorphism. Bhatwari Group. Locality - South of Dodital (D₂₇/680). Crossed X110.



4.1



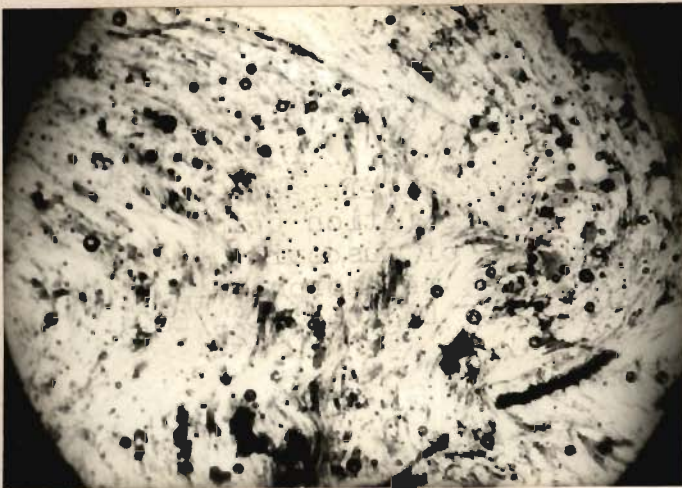
4.2



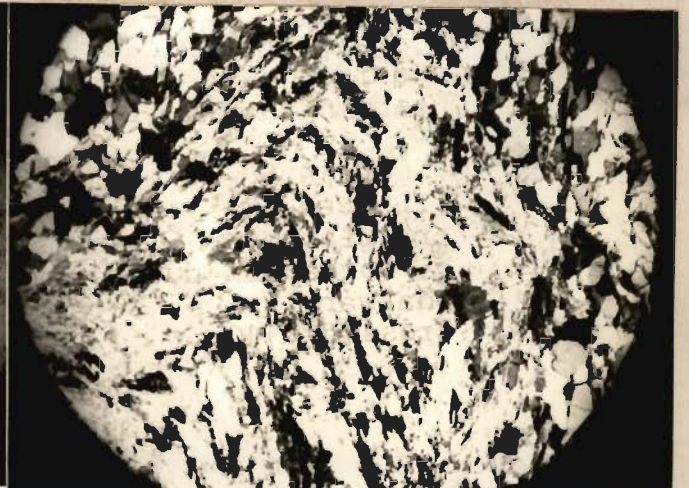
4.3



4.4



4.5



4.6

by Berthe et al. (1979) in South American Shear Zone and from mylonites of the Bergen Arc (Sinha Roy, 1977). Their conjugate disposition changes with orientation in the MCT zone along the Bhagirathi Valley from steeper orientation to gentler sinistral sense of movement parallel to the listrically disposed MCT (Jain, personal communication).

In the pelitic rich bands, sequential evolution of foliations is very distinct and is characterized by syntectonic growth of quartz and phyllosilicates (M_1) along relict S_1 which is subsequently crenulated into tightly appressed intra-folial folds and developing into the most prominent foliation S_2 having syntectonic mineral growth (M_2 -Fig. 4.2). Later slips and recrystallization along slightly oblique foliation S_{2a} produces the fish-scale textures in phyllosilicates and may correspond to two-foliation configuration in quartz-sericite schist. Such structures are commonly observed in phyllonite of the major thrust/shear zones (Roper, 1972; Gupta, 1978) due to multiple shear deformation and recrystallization (M_{2a}). Still later phase of D_3 deformation associated with M_3 metamorphism crenulates S_2/S_{2a} foliation discretely with new phyllosilicate growth along the axial surfaces (Fig. 4.2).

4.1.2 Heavy minerals from Banas Formation

Heavy minerals in sedimentary and metamorphic formations have been widely used in solving problems of correlation, provenance and paleogeography (Milner, 1962). Quartz-sericite schist of the Banas Formation was, therefore, analysed for

its heavy mineral assemblage to know whether it constitutes a part of the lithologically similar Gamri Formation of the Garhwal Group (see Chapter 2) or else belongs to the Central Crystalline metamorphics. Standard crushing method for heavy mineral separation from indurated rocks (Henningsen, 1967; Jain, 1972) has been followed for 10 samples selected from different quartz sericité schist bands from the Yamuna valley. A comparatively richer fraction between -100 and +120 mesh size was mounted for qualitative and quantitative analysis of heavy mineral residue obtained after bromoform separation (Table 4.1).

Zircon: It is colourless to yellowish brown and forms the main constituent of the residue. Two important varieties of zircon have been identified on the basis of roundness:

- (i) Subrounded to rounded or sometimes globular to ellipsoidal grains probably having a distant source of detritus or multicycling.
- (ii) Subangular to angular exhibiting generally prismatic habit indicating a nearby provenance

Most of the prismatic and rounded zircon appear turbid and brownish in transmitted light. Invariably, all coloured varieties show clouding. Several unidentifiable inclusions have been noticed in zircon giving it a pitted appearance. Some of zircon grains show zoning due to successive addition of light and darker material.

TABLE 4.1 PERCENTAGE OF MEAVY MINERAL COMPONENT IN BANAS FORMATION
AND THEIR CORRELATION WITH LESSER HIMALAYAN QUARTZITES

Sample No.	Rounded	Zircon Prismatic	Total	Tourmaline	Rutile	Garnet	Staurolite	Kyanite	Sillimanite	Hornblende	Others	ZTR*
677	60.14	28.10	88.24	-	3.53	-	-	1.18	-	-	7.06	91.77
693	62.40	17.60	80.0	5.56	6.67	-	-	-	-	-	13.33	86.67
704	61.33	22.00	83.33	2.20	-	-	-	2.78	-	4.17	4.16	88.89
838	64.31	21.40	85.71	2.89	3.30	2.19	-	4.30	-	-	2.19	91.21
851	66.38	24.20	90.58	2.37	2.17	-	-	1.45	-	-	2.90	95.64
760	62.45	23.35	85.80	3.78	2.96	1.79	1.18	1.78	-	-	4.14	91.13
879	62.31	23.10	85.41	0.56	2.70	1.08	1.09	1.08	-	2.71	2.16	91.89
793	66.58	21.08	87.64	8.89	2.81	1.12	-	1.13	-	5.62	1.12	91.01
765	52.16	21.18	73.33	-	6.67	-	-	4.44	2.22	-	4.45	88.89
809	60.31	25.40	85.71	-	3.57	2.38	-	1.19	-	-	8.33	89.28
Average of 22 samples of quartzite from North of Dunda (After Jain, 1969)	76.96	8.74	85.70	5.64	1.70	0.61	-	0.42	-	-	0.88	93.04

*ZTR = Zircon + Tourmaline + Rutile %

Tourmaline: It exhibits prismatic, rounded, globular to ellipsoidal habits with colour varying from greenish brown to brown and occasionally blue. A few grains are highly fractured and displaced along irregular planes. Tourmaline is mainly devoid of inclusions.

Rutile: A few grains of rutile are yellowish brown to reddish brown, rounded, equidimensional to elongated prismatic in habit. Rarely, a faint pleochroism in reddish tinge is noticed in these grains.

Staurolite: It is colourless to straw yellow and is faintly pleochroic. The staurolite grains are restricted to a few sections showing prismatic to subrounded character and exhibit patchy extinction.

Kyanite: Most of the sections contain colourless, elongated, bladed and prismatic kyanite. The grains show two sets of prominent cleavages at right angles. Blades are slightly rounded along edges indicating some transportation.

Garnet: A few rounded grains of pink to brown garnet have been noticed and contain rounded quartz and other unidentifiable inclusions.

Hornblende: Green to brown hornblende occurs in a few sections. It is pleochroic and prismatic in nature. Occasionally, it contains inclusions of opaques and quartz.

Chlorite: Chlorite plates are commonly seen in these sections with varying amount (2-3%). It has a scaly habit and is slightly pleochroic. The presence of chlorite plates in the quartz-sericite schist indicates that it could be lithologically

equivalent to the Gamri quartzite. The chloritic material could have formed due to diagenesis and metamorphism of argillaceous intercalations.

Other Minerals: Besides these mineral component, other traceable minerals are sillimanite needles (present in one section), zoisite and opaques such as ilmenite, hematite, magnetite and pyrite.

The heavy mineral assemblage of the Banas Formation suggests that it could have been derived from low to medium grade metamorphics and granitized rocks.

Comparison with the Gamri Quartzite:

Heavy mineral assemblage of the Banas Formation closely resembles the Gamri Quartzite of the Garhwal Group exposed to the south of the MCT indicating that the former is lithologically similar to the latter. The similarities and dissimilarities found in the heavy mineral components of the Banas Formation and that detailed for the Gamri Quartzite by Jain (1972) are highlighted below.

Zircon: The Banas Formation contains 61.84% rounded zircon and 22.84% prismatic zircon, while the Gamri Quartzite has 76.96% rounded zircon and 8.74 prismatic zircon. The higher percentage of prismatic zircon in the Banas Formation may probably be due to its nearness to the source and less abrasion. It may represent the topmost portion of the Gamri Quartzite.

Tourmaline: The Banas Formation contains 2.65% of tourmaline, whereas its percentage is slightly higher in the Gamri Quartzite

(5.64%).

Rutile: Slight decrease in the percentage of rutile has been noticed from the Banas Formation towards the Gamri Quartzite. It is 3.44% in the Banas Formation and 1.70% in the Gamri Quartzite.

Other minerals: The percentages of garnet, staurolite, kyanite and sillimanite is very poor to almost absent either in the Banas Formation or the Gamri Quartzite. Jain (1972) reported 0.61% garnet and 0.42% kyanite while the other medium to high grade minerals are absent in the Gamri Quartzite. On the other hand, the Banas Quartzite has 0.87% garnet, 0.28%, staurolite, 1.93%, kyanite and 0.22% sillimanite, thus indicating nearness to the metamorphic source.

ZTR: This ratio (zircon + tourmaline + rutile%) in the Banas Formation (90.64) closely resembles with the Gamri Quartzite (93.04) indicating that the Banas Formation may form a part of the Gamri Quartzite and is presently involved in the Central Crystallines due to Schuppen structure.

4.1.3 Janki Chatti Formation

Calc schist: The schist is light grey to grey, fine grained (occasionally medium grained) and compact with distinct foliation defined by lensoidal calcite, talc and muscovite flakes. In hand specimens, it appears to be dolomitic limestone or crystalline limestone, showing gradational contacts with quartz-sericite schist of the Banas Formation. In a few specimens, mineral lineation is defined by talc or muscovite

flakes. The concordant quartz-calcite veins exhibit pinch and swell structure. Other important mineral components in the rock are quartz, plagioclase, tremolite, zoisite and occasionally biotite. Apatite, tourmaline (brown), sphene, ilmenite and pyrite are the accessory minerals.

Calcite I forms the main constituent of the rock and occurs as lensoidal, inequant grains with irregular denticulate interlocked sutured aggregates to straight grain boundaries aligned along the main foliation. Lamellar twinning is commonly developed in strained calcite grains, which could be the result of twin gliding during plastic deformation. The twin angle generally varies from 49 to 52° and occasionally it is greater than 85° . Wherever the twin angle is obtuse the twin lamellae have been formed along the cleavages. Some of the sections contain relicts of sedimentary calcite thereby suggesting a very low grade metamorphism. The vein calcite is medium grained and cuts the main foliation.

Quartz I shows undulatory extinction and is closely associated with calcite I. In the groundmass, it replaces Calcite I indicating that quartz I has grown later to calcite I. Quartz II is fine to medium grained unstrained and post-tectonic in character.

Talc and/or muscovite along intergranular boundaries of quartz-calcite grains show kinking and development of transposed foliation (S_2). Flakes are bent and slipped having sharp margins in hinge zones, while new phyllosilicates

synkinematically grow along S_2 foliation with helicitic textures (Fig. 4.3). These contain numerous relict folded iron oxide inclusions of D_2 generation. Many deformational textures observed along crenulation have been described by Williams et al. (1977), Vernon (1977) and Glen (1980) in phyllosilicates.

Other accessory minerals like tremolite exhibit prismatic to acicular habit and associated with calcite. Albite grains are fractured and slightly sericitized. Deep brown biotite in one section is intimately associated with quartz-feldspar portion. Biotite also occupies the fractures and cracks in calcite I. At places, it is interlayered with muscovite along S_2 . The unstrained to slightly strained mica porphyroblasts indicate their ^{growth} mainly in the strain free environment along S_2 . Minor amount of zoisite or epidote is associated with quartz.

Actinolite schist: It is greenish and fine grained with prominent foliation (S_2) defined by actinolite and intimately associated tremolite oriented along mineral lineation (L_2). These exhibit flaky, fibrous habits to μ kiloblastic character containing inclusions of clinozoisite, zircon, sphene, ilmenite and occasionally apatite and tourmaline. Kinking of actinolite flakes develops transposed and crenulation foliation (S_3). At times actinolite is degenerated into chlorite. Slickenside is profusely developed on foliation planes near fault zones.

Sphene (pinkish to greyish brown), as granular aggregates to lozenge shape crystals is rimmed by ilmenite. It is closely associated with actinolite and has formed later as evidenced from their μ kiloblastic shape.

The actinolite schist is in contact with pegmatite (described later) near Gangnani and shows banded character and mixing of pegmatitic material. At the contact, large amount tremolitic asbestos is developed. In actinolite schist of contact zone, xenoblastic quartz replaces actinolite and shows helicitic texture, thereby confirming its post-tectonic growth (post D_3). It also occurs along cleavage and fracture in actinolite indicating its later growth.

4.1.4 Other rock types

Amphibolite: The rock comprises of actinolite, hornblende, plagioclase, quartz, chlorite, sphene, clinozoisite or epidote, ilmenite, rutile and leucoxene. In the tectonic zones it is mylonitized and changes to chlorite schist. Actinolitic hornblende occurs as nematoblastic, prismatic to small radiating fibrous grains along foliation (S_2) and ^{also} produce a prominent mineral lineation (L_2). It is the most common variety and occasionally encloses brown porphyroblastic hornblende containing inclusions of ilmenite, quartz and sphene. Along the fractures and cleavages, it has broken down into biotite or chlorite.

At place, actinolitic hornblende retrogrades into clinozoisite or epidote. Actinolitic hornblende shows kinking and formation of crenulation foliation (S_3). Plagioclase are fine to medium grained and xenoblastic to sub-idoblastic in nature. The margins are ill defined and crowded near the actinolitic hornblende due to the reaction. Some of the plagioclase shows undulose extinction.

Plagioclase is mainly albite, though certain grains are also andesine to labradorite in composition, probably representing the original plagioclase of the rock. At places, plagioclase grains are sericitized and saussuritized, thereby developing sercite, clinozoisite/epidote and calcite. Chlorite (pennⁿite) as well as biotite are important constituent of some thin sections along fractures, cleavage and margins of actinolitic hornblende due to retrograde metamorphism. Xenoblastic quartz is closely associated with plagioclase and clinozoisite which clusters along (i) laths of plagioclase and (ii) also along the contacts of actinolitic hornblende with ilmenite. The latter is associated with sphene and appears to be a reaction product of actinolitic hornblende and ilmenite because it shows irregular boundaries with sphene. Late phase calcite veins cut across foliation (S_2) and replace actinolite flakes. The presence of actinolitic hornblende, albite, epidote/clinozoisite and chlorite indicate metamorphism of basic rocks upto green schist facies.

Chlorite-Actinolite-Talc schist:

Chlorite-actinolite-talc schist marks the MCT in the Bhagirathi valley. Towards the south, the schist contains of quartz and tourmaline of late phase (related to the pegmatitic activity in the Central Crystallines), thereby imparting banded character to the rock. Apatite, zircon, rutile and magnetite are the minor mineral of the rock. The formation of mylonitic foliation and transposition of an earlier structure are the notable features.

Chlorite is associated with actinolite along the main foliation (S_2) as the main constituents of the rock. Chlorite-actinolite bands alternate with quartz or tourmaline-quartz rich bands of variable thickness. Chlorite-actinolite grains also shows transposition of the main foliation (S_2) into a subparallel mylonitic foliation (S_{2a}) due to which these are rotated obliquely to S_2 . Small amount of chlorite occurs as pseudomorphs after actinolites. A few prismatic grains of tremolite show inclined relationship to S_2 foliation due to their later growth along the S_3 foliation. Talc occurs in small proportion and is closely associated with chlorite, actinolite and quartz. Occasionally it shows kinking. Quartz I is fine grained and occurs as inclusion in chlorite-actinolite.

Chlorite-actinolite-talc assemblage indicate its probable derivation from the mafic or ultramafic rocks.

Quartz-II is coarse grained with straight to curved margins and shows least strain effect. It also contains inclusions of chlorite and actinolite. At places, it occupies the intragranular spaces of chlorite and actinolite. It shows helicitic texture or replacement texture with chlorite-actinolite indicating its post-tectonic recrystallization.

Sch~~o~~rlite is closely associated with quartz II in the MCT zone as a part of quartz-tourmaline vein of post-tectonic stage. Sch~~o~~rlite is irregularly fractured and randomly oriented across S_2/S_{2a} indicating post- D_2/D_{2a} pneumatoliticization of the Gamri Quartzite along the MCT (Fig. 4.4).

4.2. BHATWARI GROUP

The Bhatwari Group is comprised of polymetamorphic rocks of sedimentary and igneous parentage and has undergone migmatization ~~to various degrees~~ to various degrees. The highest grade of metamorphism achieved by the Bhatwari Group is garnet grade corresponding to the almandine-amphibolite facies. Some rocks have undergone large scale retrogression during cataclastic metamorphism along tectonic zones especially near the MCT. On the basis of possible parentage, the rock types of the Bhatwari Group have been categorised as follows and being described accordingly.

A. Metasedimentaries (poor migmatization)

I. Retrograde metamorphism (not strong)

- (i) Quartz mica schist
- (ii) Cummingtonite-biotite schist
- (iii) Garnetiferous mica schist

II. Cataclastic and retrograde metamorphism (strong)

- (i) Phyllonite
- (ii) Quartz-chlorite schist

B. Metamorphosed igneous rocks (poor or no migmatization)

- (i) Amphibolite
- (ii) Meta-andesite
- (iii) Metadolerite

C. Migmatites (migmatized metasediments and amphibolite, mylonitized along tectonic contacts)

- (i) Augen migmatite
- (ii) Streaky migmatite
- (iii) Mylonitic augen gneiss

Late stage quartz-aplitic veinlets, quartz-tourmaline veins and quartz-feldspar injections are not widespread in the Bhatwari Group, although these occasionally become conspicuous.

4.2.1 Metasedimentaries:

The Bhatwari and Suki Group have undergone polyphase metamorphism, deformation and migmatization which have led to extensive obliteration of earlier texture and structure. However, bedding plane foliation can be occasionally recognised due to colour banding and grain size variation. Further, mineral assemblages of these formations reveal their psammitic, semi-pelitic and pelitic metasedimentary character.

(i) Quartz-mica schist: Light grey to dark grey, fine to medium grained schist is mainly comprised of lepidoblastic muscovite and biotite in varying proportions of quartz and feldspar along the main foliation with tourmaline, apatite, ilmenite, sphene, rutile and zircon as accessory minerals.

Quartz forms the major constituent in most of the thin section and belongs to two generation. Quartz I occurs in the groundmass as well as inclusion in mica flakes and feldspar

porphyroblasts. Quartz I is strained and shows serrated, ~~sutured~~ and occasionally diffused margins. Subsequent, elongate quartz II is mostly unstrained showing straight to very mild undulose extinction with grain boundaries being mostly straight and forming triple junction (Fig. 4.5 and 4.6). Quartz II replaces muscovite and biotite and contains helicitic inclusions of mica with post- S_3 porphyroblastic growth in strain-free environment indicating a very prolonged recrystallization of quartz even after the main deformational phases - D_3 (Fig. 4.5). Some of quartz porphyroblasts II are fractured and these fractures are oriented in a random or step like pattern. Albite shows the development of sericite along the twin planes and fractures. Orthoclase is occasionally seen and is being replaced by albite.

Muscovite and biotite of two generations have been identified in quartz-mica schist. Muscovite I and biotite I are interlayered, fine grained having ^{indistinct} grain boundaries and define the main foliation, S_2 . Biotite I, at places, retrogrades into chlorite. On the other hand, muscovite II and biotite II occur as porphyroblasts either subparallel to the main foliation, S_2 , on limbs of crenulations, F_3 , or at very high angle to S_2 in the hinge zone of F_3 folds, where these new mica impart the new foliation, S_3 (Fig. 4.6). Muscovite II occasionally contains inclusions of biotite II, particularly along the cleavages indicating that some of the muscovite could have been derived from biotite II. Muscovite porphyroblasts also contain inclusions of quartz in the intragranular spaces. Muscovite II and biotite II sometimes show undulatory extinction. Syntectonic

mica flakes along the main foliation, S_2 , show bending, kinking and breaking.

Based on the relative proportions of the micas in these schists, the two types of quartz mica schist have been recognized:

- (a) Quartz-muscovite-biotite schist
- (b) Quartz-biotite-muscovite schist

(ii) Cummingtonite-biotite schist: Synformally folded cummingtonite-biotite schist at Bhatwari is dark grey, brownish grey to greenish grey, medium grained, hard and well foliated. Alternate biotite and amphibole rich bands impart main foliation, S_2 , and also contains quartz, cummingtonite, anthophyllite, muscovite, plagioclase and K-feldspar and accessory amount of tourmaline, zircon, apatite, sphene, rutile, ilmenite and clinzoisite. Quartz-tourmaline and quartz-feldspar veins, folded along with the foliation, traverse these schists at times.

Varying amount of cummingtonite is characterized by an extinction angle $C\lambda Z = 15-20^\circ$, lamellar and intergrowth twinning. Along cleavages, margins and fractures, it shows breaking into biotite and iron oxides indicating a ferruginous character of the original amphibole. It is often surrounded by biotite which, at places, abuts against cummingtonite indicating that the latter has grown earlier to biotite. At times, cummingtonite contains coaxial patches and bands of anthophyllite which may reflect the original anthophyllitic

character of the cummingtonite. X-ray studies of amphibole-rich portion of samples nos. D27/522 and D27/471 also confirm presence of both varieties of amphibole.

Biotite shows phlogopitic character (pink to brown) and occurs with muscovite flakes. It also encloses grains of ilmenite, rutile, sphene, zircon, apatite and tourmaline. Cummingtonite, biotite and muscovite show preferred orientation along the earliest detectable foliation, S_1 , in thin sections, which is subparallel to the axial surface of the nearly isoclinal folds, F_1 (Fig. 4.7). Prismatic cummingtonite is subparallel to the metamorphic banding marked by quartz-rich and mica-rich layers, while in hinge zones of F_1 folds, biotite and cummingtonite converge to define the S_1 foliation. Interestingly, S_1 foliation is again isoclinally folded by later folds, F_2 , in which distinct rounded hinge zones and folding of S_1 foliation is evident (Fig. 4.8). Coplanar S_2 foliation, marked by elongate quartz, cummingtonite and biotite parallels the axial surface of F_2 folds (Figs. 4.8, 4.9, 4.10). Some mica is also recrystallized as tiny distinct flakes along axial surfaces of later close folds, S_3 (Figs. 4.9, 4.10).

Quartz occurs as xenoblastic to elongate grains along S_1 and S_2 foliations and show nearly straight boundaries and extinction. Many grains are tabular in character with long dimension preferably oriented along S_1 foliation (Figs. 4.8, 4.11, 4.12) where alternating coarse elongate grains alternate with fine grained mylonitic quartz revealing

EXPLANATION OF PHOTOMICROGRAPHS:

FIGURES 4.7 to 4.12

Figure 4.7 - Cummingtonite-biotite schist having F_1 relict fold with preferred orientation of biotite and cummingtonite along S_1 foliation. Bhatwari Group. Locality - Bhatwari College (D₂₇/810). Crossed X 55.

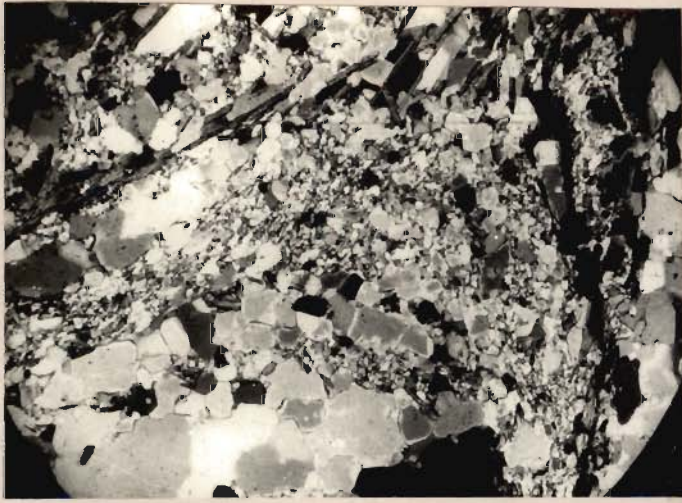
Figure 4.8 - Quartz-biotite-cummingtonite schist showing alternating coarse and fine quartz along S_1 foliation. Grain size reduction and annealing of fine quartz. Isoclinally folded S_1 foliation having dimensionally oriented quartz by F_2 folds with nearly zero interlimb angle. Also affected by F_3 folds in right hand corner with quartz II along S_3 foliation. Bhatwari Group. Locality - Bhatwari College (D₂₇/818). Crossed X 55.

Figure 4.9 - Migmatized cummingtonite-biotite schist having K-feldspar grains preferably oriented along S_1 on limbs of F_2 folds and syn- to late D_1 with helicitic texture. S_1 is isoclinally folded by F_2 folds. Bhatwari Group. Locality - Bhatwari (D₂₇/817). Crossed X55.

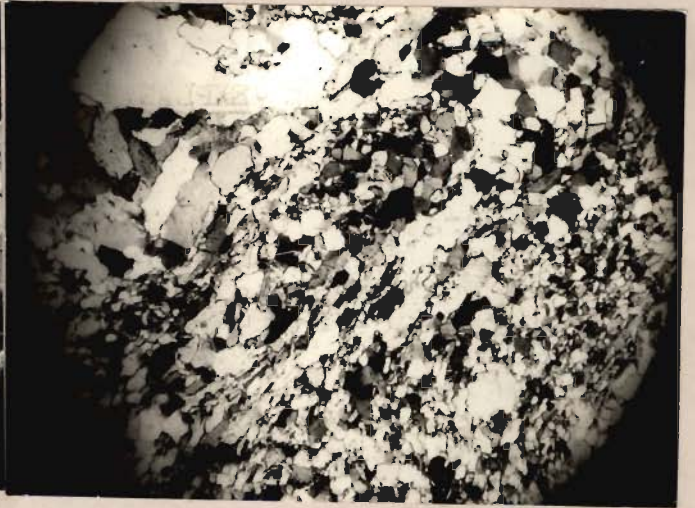
Figure 4.10 - Cummingtonite-biotite-schist having helicitic K-feldspar with phyllosilicates as inclusions (S_1), which is folded with F_3 folds. Bhatwari Group. Locality - Bhatwari (D₂₇/817). Crossed X110.

Figure 4.11 - Cummingtonite-biotite schist with alternating coarse granoblastic quartz having triple junctions with fine quartz along S_1 foliation. Annealed serrated grain boundaries in fine quartz are indicative of its mylonitic character. Bhatwari Group. Locality - Bhatwari (D₂₇/817). Crossed X110.

Figure 4.12 - Cummingtonite-biotite schist revealing F_2 isoclinal fold having zero interlimb angle. Recrystallized phyllosilicates and cummingtonite along S_2 foliation paralleling axial surface of F_2 fold. Bhatwari Group. Locality - Bhatwari College (D₂₇/810). Crossed X55.



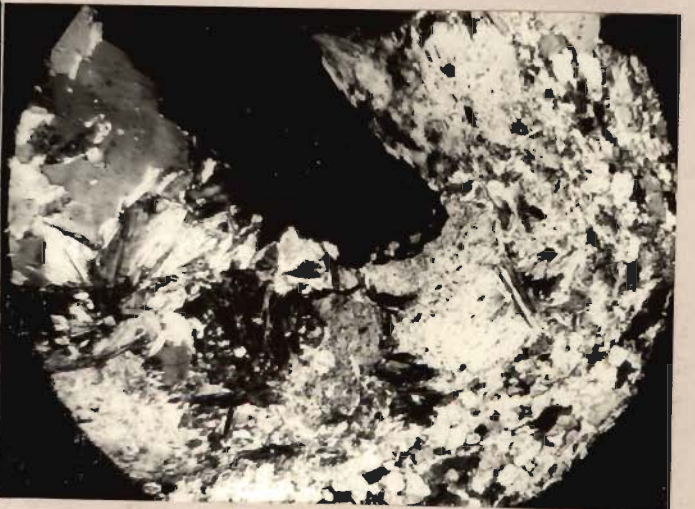
4.7



4.8



4.9



4.10



4.11



4.12

annealing and grain size reduction (Fig. 4.11) - a typical overall character of the Bhatwari Group. Coarse quartz rich bands probably represent veins which might have permeated synkinematically during D_1 deformation which has produced F_1 folds and S_1 foliation. Individual grains are even bent in hinge zones of F_2 folds (Fig. 4.8), while others are even affected by later asymmetric close folds, F_3 (Figs. 4.8, 4.9).

Plagioclase ranges in composition from An_7 to An_{16} and is associated with subidioblastic K-feldspar along the S_1 foliation which is folded later on by F_2 folds (Figs 4.9, 4.10). In hinge zones, K-feldspar reveals curved grain boundaries and is helicitic in character with inclusions of quartz, biotite and muscovite (Fig. 4.10). K-feldspar has distinctly grown synkinematically to D_1 deformation along S_1 foliation and hence it is termed as K-feldspar I. Some of plagioclase grains are fractured and sericitized.

Schorlite is found in a few sections in variable amount. It is generally associated with quartz and, at times, with feldspar. Schorlite grains show irregular fractured and cross-cut relationship with the main foliation, S_2 and contain inclusion of quartz. At places, green to yellowish brown tourmaline grains have been folded along with S_2 foliation indicating their syn- D_3 relationship.

(iii) Garnetiferous mica schist and gneiss: The garnet bearing mica and gneiss schist cover comparatively wider zone of the Bhatwari Group and contain varying amount of muscovite and

biotite which impart a lepidoblastic foliation. The biotite rich schist is darker in colour, whereas muscovite rich schist and gneiss are lighter in shade. At places, garnetiferous biotite schist has a greenish tint due to the development of retrograde chlorite. The schist is medium to coarse grained, well foliated and shows variability in competence. At certain localities, it is closely jointed and friable in character. Kinking of mica flakes, formation of crenulation foliation, association of quartz veins and lenses or small scale boundaries parallel to the foliation and development of lineation are the common features. Quartz, muscovite, biotite and garnet are the important constituents in schist and gneiss with small proportions of plagioclase, K-feldspar, hornblende, chloritoid and chlorite. Ilmenite, tourmaline, apatite and zircon are the accessory minerals.

Quartz forms an important constituent in most of the thin sections and exhibits granoblastic to porphyroblastic texture. Undulose extinction and sutured margins are characteristic. Tiny quartz grains occur as inclusion in garnet, biotite, muscovite and plagioclase. Two generations of biotite and muscovite have been observed in these rocks. Biotite I and muscovite I of the first generation are seen along axial surfaces of F_2 folds and define the most prominent lepidoblastic foliation, S_2 (Figs. 4.13, 4.14).

Biotite II and muscovite II of later generation are also seen along axial surfaces of F_3 crenulation folds and

EXPLANATION OF PHOTOMICROGRAPHS:

FIGURES 4.13 to 4.18

Figure 4.13 - Garnetiferous mica schist with F_2 isoclinal folding garnet I along relict S_1 foliation. Axial plane foliation, S_2 , prominent due to recrystallized quartz and phyllosilicates. Bhatwari Group. Locality - South of Bhatwari ($D_{27}/416$). Crossed X110.

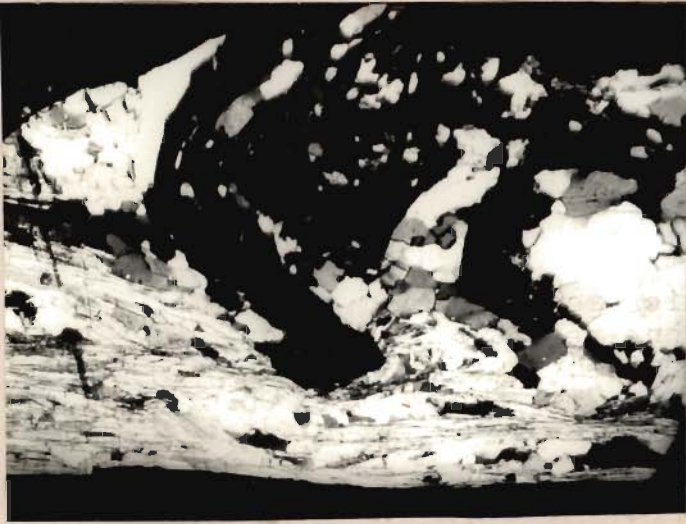
Figure 4.14 - Garnetiferous mica schist with incipient garnet II crystallizing in pressure shadow zone marked by granoblastic quartz. Wrapping of S_2 foliation with slight foliation - parallel anticlockwise rotation during M_2 metamorphism. Cross biotite II across S_2 foliation represents M_3 metamorphism. Bhatwari Group. Locality - NW of Joti ($D_{27}/643$). Crossed X55.

Figure 4.15 - Garnetiferous mica schist with syntectonic nuclei of garnet II having inclusions with peripheral inclusion-free garnet II across S_2 foliation. Development of S_3 foliation along axial surfaces of F_3 folds with growth of new muscovite and iron oxide representing M_3 metamorphism. Bhatwari Group. Locality - NW of Joti ($D_{27}/646$). Crossed X55.

Figure 4.16 - Garnetiferous mica schist with helicitic rhombic biotite II across S_2 foliation and containing S_1 parallel to S_e . Growth of biotite II is post- D_2 deformation and represent M_3 metamorphism. Bhatwari Group. Locality - NW of Joti ($D_{27}/643$). Crossed X110.

Figure 4.17 - Garnetiferous mica schist having syntectonic snowball garnet II with S_1 obliquely oriented to S_e . Rotation of about 90° is indicated by S-shaped S_1 trails of quartz and iron oxide. Retrograde chlorite along lower margin. Bhatwari Group. Locality - North of Gangnani ($D_{27}/559$). Crossed X55.

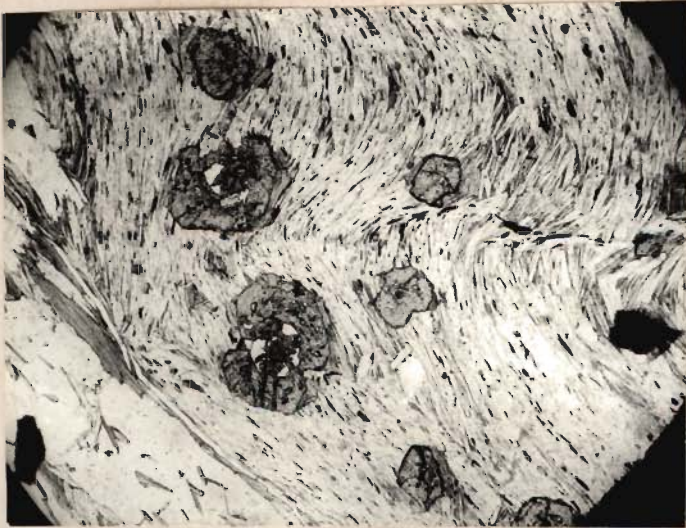
Figure 4.18 - Garnetiferous mica schist showing two snowball garnet II with considerable rotation amounting to about 540° . S_1 parallels S_e of S_2 foliation along margins indicating their syntectonic growth during M_2 metamorphism. Biotite II grows across two garnets as cross mica during M_3 metamorphism. Bhatwari Group. Locality - NW of Joti ($D_{27}/643$). Crossed X110.



4 · 13



4 · 14



4 · 15



4 · 16



4 · 17



4 · 18

mark their crenulation foliation, either due to rotation of earlier biotite I and muscovite I or due to new mica growth transecting the S_2 foliation (Figs. 4.14, 4.15). Many Biotite II flakes are well defined as elongate distinct grains, which, at times are rhombic in shape containing earlier S_2 foliation as helicitic inclusions (Fig. 4.16). Gregg (1980) has recently described similar looking cross-micas in rocks by schistosity-parallel displacement, but evidences for such shear displacements are lacking in biotite II of the Bhatwari Group.

Most important textures in the garnetiferous mica schist are revealed by garnet crystals. Three generations of garnet have been identified from the Bhatwari Group; garnet II and III are common to the Suki Group garnetiferous mica schist, while garnet I is restricted to the Bhatwari Group garnetiferous schist and gneiss. Garnet I occurs as elongate stringers along relict S_1 foliation with quartz (Fig. 4.13) and is dark brown to turbid having iron oxide inclusions in contrast to pink clear almandine of the second and third generations. Stringers of garnet I are folded as intrafolial close folds with curved quartz inclusions trending parallel to S_1 foliation; both garnet I and quartz elongate grains are aligned at high angles to axial plane foliation of these F_2 folds in chloritoid bearing garnetiferous mica schist (Fig. 4.13).

Garnet II is distinctly transparent pink subidioblastic, xenoblastic to elongate skeletal along S_2 foliation and reveals considerable amount of syntectonic rotation near the

Joti-Bhandali Thrust Zone (JBT). Incipient xenoblastic garnet II starts growing synkinematically to D_2 deformation with the development of S or Z shaped pressure shadow (Fig. 4.14). Large rotation through 90° as revealed from S-shaped sigmoidal quartz, mica and ilmenite inclusions causes truncation of Se along idioblastic almandine grains so that Si \nparallel Se relationship characterize such grains along the JBT (Fig. 4.17). Wrapping and bowing out of Se is also distinct along longest dimension of grains (Fig. 4.17). On the other hand, Si \parallel Se relation persists even after a rotation by an amount of 540° in the thrust zone where muscovite II and biotite II imperceptibly grade into garnet II (Fig. 4.18). Outside the thrust zone, garnet II is characterized by idioblastic grains with Si \parallel Se relationship having evidences of syntectonic growth due to which intergranular space between two large garnet II grain show evidences of compression of S_2 foliation into grenaulation (Fig. 4.19). Such Si Se relations are distinct in stringer and skeletal growth of garnet II where it extends parallel to S_2 foliation and along straight grain boundaries of xenoblastic quartz (Fig. 4.20). Kinking of such stringers and ilmenite inclusions clearly indicate its pre- D_3 growth due to which garnet II is folded into open to tight folds and fractured along crest of such folds (Figs. 4.20, 4.21).

Nevertheless, garnet III is subidioblastic in character and also devoid of quartz inclusions (Figs. 4.15, 4.22). Rarely, it reveals undisputed evidences of helicitic inclusions of Se passing uninterruptedly across garnet III grains indicating

EXPLANATION OF PHOTOMICROGRAPHS:

FIGURES 4.19 to 4.24

Figure 4.19 - Porphyroblastic growth of idioblastic garnet II displacing groundmass rich in phyllosilicates and causing crenulation of S_2 foliation. Garnetiferous mica schist of the Bhatwari Group. Locality - south of Gangnani (D₂₇/834b). Crossed X110.

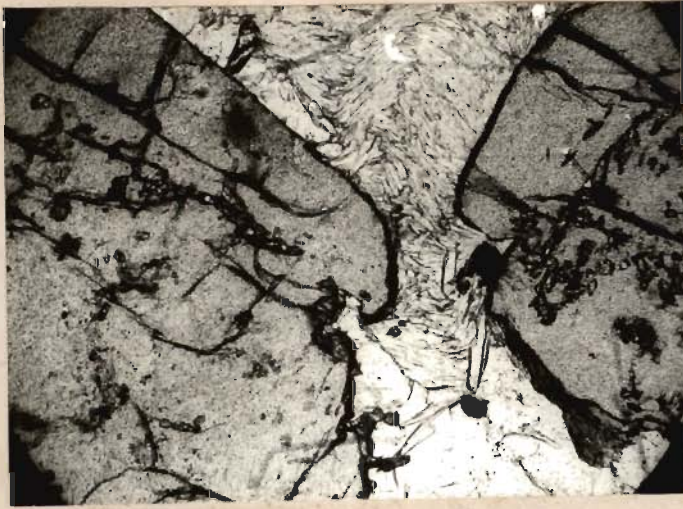
Figure 4.20 - Synkinematic growth of garnet II along S_2 foliation and in intergranular spaces between quartz and subsequent folding by F_3 folds. Fractures along axial surface of F_3 fold in garnet II. Garnetiferous mica schist of the Bhatwari Group. Locality - south of Gangnani (D₂₇/830). Crossed X55.

Figure 4.21 - Same garnet II porphyroblast as in figure 4.20 revealing openly folded helicitic inclusions of ilmenite needles due to F_3 fold. Fractures converging towards the trace of axial surface. Crossed X55.

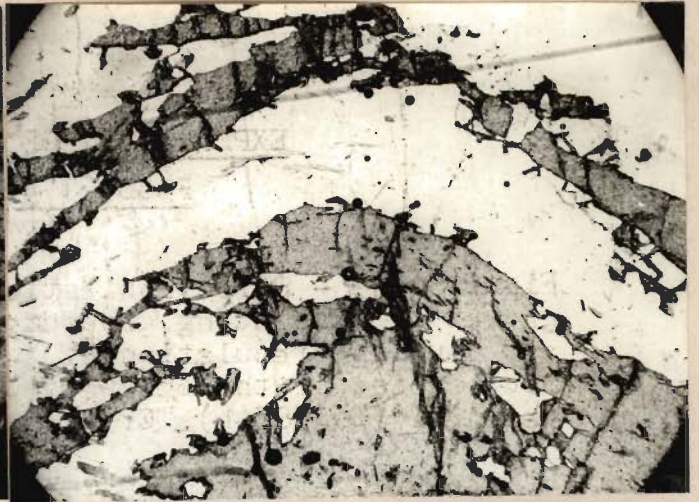
Figure 4.22 - Development of post- D_2 helicitic garnet III porphyroblast with superimposed texture of S_2 foliation, defined by biotite, passing uninterrupted through the porphyroblast. Garnetiferous mica schist of the Bhatwari Group. Locality - north of Gangani (D₂₇/559). Crossed X220.

Figure 4.23 - Intrafolial F_2 isoclines showing curving of quartz and phyllosilicates crystallized along S_1 foliation in the hinge zone and development of S_2 foliation along the axial surfaces. Obliquely trending discrete dark bands of finely granulated mass along mylonitic foliation, S_{2a} . Extensive retrograde metamorphism and fine grained texture. Quartz-chlorite schist of the Bhatwari Group. Locality - Dodital section near the MCT. (D₂₇/661). Crossed X55.

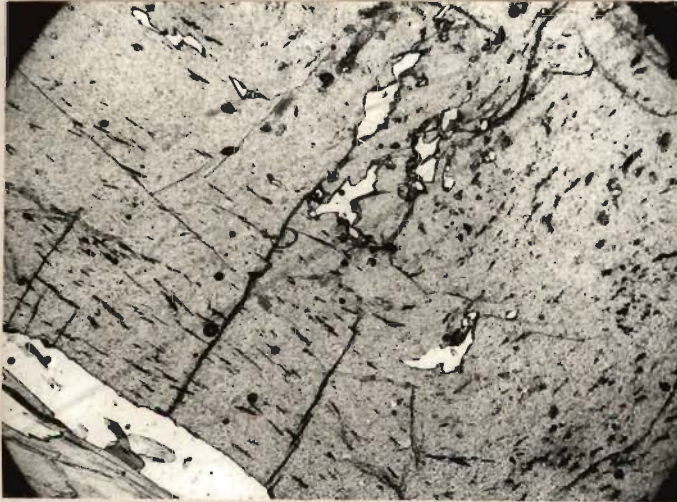
Fig. 4.24 - Granoblastic quartz and phyllosilicates along the S_2 foliation are cut obliquely by S_{2a} mylonitic foliation to produce almond-shaped structures or button textures. Crenulations (F_3 folds) trend obliquely to S_2 and S_{2a} foliations. Quartz-chlorite schist of the Bhatwari Group. Locality- Dodital section near the MCT (D₂₇/661). Crossed X110.



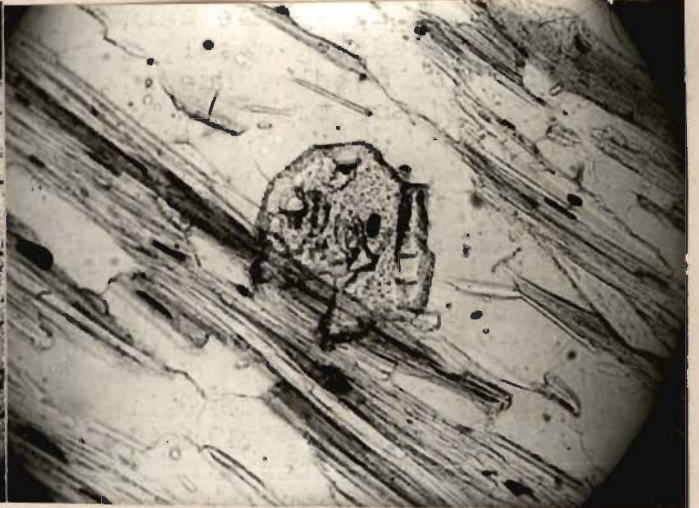
4 · 19



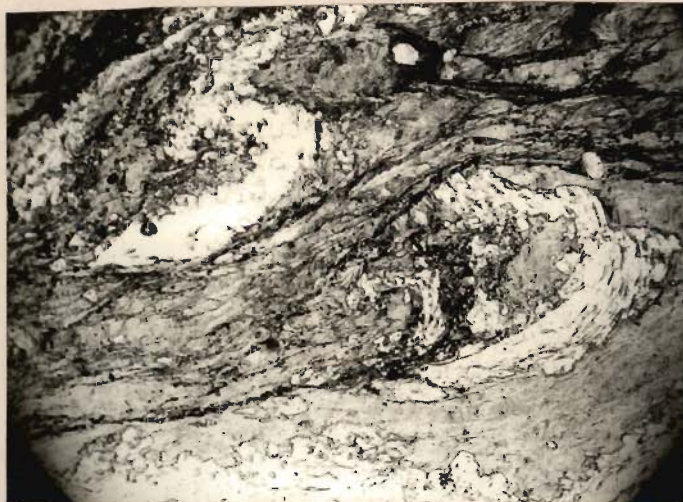
4 · 20



4 · 21



4 · 22



4 · 23



4 · 24

its post- D_2 growth (Fig. 4.22) probably during D_3 deformation which has produced widespread crenulation of the mica schist (Fig. 4.15):

Kinematically, garnets from the Bhatwari Group reveal different relations with the foliation of the garnetiferous mica schist. While bowing out of foliation in the matrix mark the snowball garnets of second generation, imperceptible garnet growths without any effect on the foliation characterize both the garnet II and garnet III. Misch (1971) interpreted bowing out of foliation as unequivocal proof of mechanical displacement due to crystal growth (also Harris, 1977). Nevertheless, other interpretations include the following:

- (a) flattening of schist during or subsequent to growth of porphyroblast (Shelley, 1972),
- (b) diffusion of material and reduction of volume immediately around the growth site (Shelley, 1972),
- (c) production of foliation during F_1 , followed by post-tectonic growth of porphyroblast, then distortion of foliation accompanying differential thinning, flowage and recrystallization of the matrix due to flattening during F_2 (Spry, 1972).

In the Bhatwari Group, it is therefore evident that different mechanisms of garnet growths were probably operative for various generations of garnet. Stringers of garnet II along the main foliation S_2 as well as along grain boundaries clearly envisages growth of garnet with displacement in

intergranular spaces (Fig. 4.20), which is also evident from two nearby growing porphyroblasts displacing the matrix and crenulating it to a great extent (Fig. 4.19). Mechanical displacement by the growing and rotating garnet porphyroblast is again evident by parallelism of Si with Se from two nuclei of garnet grains which ultimately become a single grain.

A narrow band of chloritoid-bearing garnetiferous mica schist occurs within the migmatite south of Bhatwari. Besides, showing all the textures of quartz, muscovite, biotite and garnet described above, the schist contains tabular, lenticular to elongate prisms of chloritoid which is aligned parallel to the S_2 foliation. The grains rarely contain inclusions of muscovite I and quartz which are smaller in size than those present in the matrix. Chloritoid grains are optically length-slow, pleochroic and show intergrowth, twinning and zoning. The extinction angle varies from $15 - 16^\circ$. Some of the chloritoid grains are strained. Rarely, chloritoid grains are slightly inclined to the main foliation indicating their development even after the D_2 deformation. At places, chloritoid has given rise to chlorite.

Plagioclase ($Ab_{92} An_8$ or $Ab_{86} An_{14}$) has been sericitized along the twin planes and fractures. K-feldspar occurs in minor amount and, wherever K-feldspar and plagioclase coexist, the former is being replaced by the latter. Prismatic hornblende grains have been recorded in single section where these are aligned parallel to the S_2 foliation. Ilmenite

needles are closely associated with garnet II (Figs. 4.20, 4.21) or retrograde chlorite which develops along margins of idioblastic garnet II due to retrograde metamorphism (Fig. 4.17). It appears that some amount of ilmenite has been liberated during degeneration of garnet II. Schorl~~ite~~ is associated with vein quartz and appears to be a part of quartz-tourmaline vein.

The following mineral assemblages have been observed in the garnetiferous mica schist.

- (a) Quartz + muscovite \pm biotite + almandine \pm plagioclase
(Ab₉₂ An₈ or Ab₈₆ An₁₄) \pm K-feldspar
- (b) Quartz + biotite \pm muscovite + almandine +
plagioclase (Ab₉₂ An₈ or Ab₈₆ An₁₄) + K-feldspar
- (c) Quartz + biotite + muscovite + hornblende +
almandine + plagioclase (Ab₈₆ An₁₄) + K-feldspar
- (d) Quartz + muscovite + biotite + chloritoid + chlorite
+ garnet.

4.2.2 Cataclastic and Retrograde Metamorphism (Strong)

(i) Phyllonite: Phyllonite occurs along the MCT and the JBT as thin lenticular bands. It is fine grained, dark grey to greenish grey, thinly foliated and phyllitic in character. Kinking, bending and breaking of mica flakes and profuse development of slickensides are the common features. The phyllonite is characterized predominantly by cataclastic textures and attendant retrogressive changes. It consists of a very strongly foliated, fine grained aggregate of biotite,

muscovite, quartz, chlorite, magnetite and ilmenite. Biotite is abundant and contains inclusions of tourmaline, zircon and apatite and also shows alternation to a finely foliated mass of chlorite. Tiny grains of magnetite are confined to the biotite flakes indicating that they are the product of the degradation of biotite. Muscovite occurs as streaks and the flakes often show kinking. Quartz grains have been intensely fractured, crushed and arranged in streaks parallel to the foliation. Tourmaline grains are fractured and ilmenite has been altered to leucocene.

(ii) Quartz-chlorite schist: The chlorite bearing schist has also developed along the thrust zones and fault planes due to the strong retrogression of biotite schist or amphibolite. It is strongly crenulated and the chlorite flakes exhibits streaky habit. The main mineral components of the schist are: quartz, chlorite, biotite, muscovite, plagioclase, K-feldspar with some amount of tourmaline, apatite, ilmenite and magnetite.

Quartz I occurs both as fine grained mass largely having serrated margins and mildly undulose extinction with annealing effects (Spry, 1969). Quartz II is least strained with straight to curved boundaries and show porphyroblastic post-tectonic growth. Both the varieties of quartz occur along limbs of relict intrafolial folds, F_2 which isoclinally folds the oldest visible foliation S_1 in the quartz-chlorite schist (Fig. 4.23). Muscovite and biotite along with retrograde chlorite define the main foliation, S_2 , in the rock, where

phyllosilicates are mostly very fine grained with indistinct gradational boundaries. Alternate quartz and phyllosilicate layers along S_2 foliation are cut across by discrete bands trending at $15 - 30^\circ$ to S_2 in phyllosilicate layers and define the mylonitic foliation S_{2a} . Recrystallized quartz and chlorite characterize S_{2a} foliation; the low angle intersection of which with S_2 produces the button texture in layers (Fig. 4.24; Roper, 1971). Buckling of S_2 and S_{2a} foliations is clearly visible in these rocks causing development of F_3 folds having axial plane foliation S_3 (Fig. 4.24).

Plagioclase ($An_7 Ab_{93} - An_{14} Ab_{86}$) occurs in small amount. The plagioclase porphyroblasts are fractured and sericitized. The plagioclase replaces K-feldspar. Buff coloured tourmaline has been folded along with S_2 foliation indicating that some of tourmaline veins permeated along S_2 are folded during the D_3 deformation. Ilmenite is closely associated with chloritized biotite flakes. Two generations of opaque have been identified. Opaques of first generation are aligned parallel to the S_2 foliation and subjected to folding, whereas opaques of second generation are aligned parallel to the new foliation S_{2a} (Fig. 4.23).

4.2.3 Metamorphosed igneous rocks:

The metamorphosed igneous rocks in the Bhatwari Group occur as amphibolite, meta-andesite and metadolerite. Amphibolite and meta-andesite show concordant behaviour with the

country rocks, whereas metadolerite is discordant with the country rocks and also the Main Central Thrust. The megascopic and microscopic characters of these rock types are discussed in the following pages.

(i) Amphibolite: Several bands of amphibolite of varying dimension have been recorded within the Bhatwari Group. The amphibolite is dark green, fine to medium grained, compact and well foliated. Hornblende prisms impart nematoblastic foliation, S_2 , to the rocks. At places, the amphibolite is affected by late phase quartz-feldspar and quartz-calcite veins, giving lighter appearance to the rocks. Along the weak zones, amphibolite has produced hornblende-biotite schist or chlorite schist. Bending and breaking of hornblende prisms and flakes in more foliated variety are commonly observed. The main constituents of amphibolite are hornblende, plagioclase and quartz with varying amount of chlorite, biotite, clinozoisite or epidote, sphene, and ilmenite. (Table 4.2)

Hornblende occurs as yellowish green normal hornblende and bluish green (actinolitic hornblende) prisms and cross sections along nematoblastically developed S_2 foliation in amphibolite (Fig. 4.25). Hornblende prisms are mostly subidioblastic in nature, in which cross fractures are quite common. These are prismatic to acicular in habits. Although the mineral commonly shows dimensional orientation in foliated variety, but there are few grains, bearing angular relationship to the main foliation (Fig. 4.25). Some crystals of hornblende

TABLE 4.2 MODAL ANALYSIS OF AMPHIBOLITE OF THE BHAGIRATHI VALLEY

Sample No./ Mineral Component	404	411	508	456	457	417	525	474	436	567	541	543	517
Quartz	10.75	16.69	14.50	12.99	18.65	23.64	23.82	24.92	20.78	21.75	24.25	26.16	21.15
Hornblende	34.30	65.35	62.33	54.81	49.55	33.59	38.65	35.52	46.96	53.32	38.75	48.05	54.25
Actinolite- Tremolite	9.75	-	-	-	-	-	-	-	-	-	-	-	-
Plagioclase	26.95	11.61	12.68	18.96	17.73	7.41	7.49	7.64	18.75	19.45	20.37	7.96	10.66
Augite	6.24	-	-	-	-	-	-	-	-	-	-	-	-
K-feldspar	-	-	-	-	4.52	-	-	-	-	-	3.50	-	-
Biotite	1.30	0.45	0.18	1.73	0.25	21.28	18.01	20.48	2.64	0.21	6.75	11.03	8.61
Muscovite	0.17	-	-	-	-	1.40	0.86	1.37	-	-	-	0.85	-
Chlorite	0.46	1.30	0.91	0.98	0.45	1.30	0.95	0.45	0.69	0.23	0.21	0.45	0.11
Epidote/clino- zoisite	4.80	1.56	3.76	4.22	3.55	2.65	2.72	1.95	2.98	2.96	1.65	1.25	0.85
Sphene	1.32	0.74	1.61	3.34	2.68	2.94	3.88	3.62	2.85	0.63	2.35	0.78	0.75
Calcite	-	-	-	-	-	-	-	-	-	-	-	-	-
Other min- erals (iron oxides, apatite, zircon tourmaline etc.)	4.26	3.23	4.03	3.77	2.62	4.64	3.62	4.15	4.35	2.45	2.31	3.47	2.62

404 - Metadolerite
411 to 517 - Amphibolites

TABLE 4.2 MODAL ANALYSIS OF AMPHIBOLITES AND METAANDESITES OF THE YAMUNA VALLEY

Sample No./ Mineral Component	797	702	751	743	749	756	876	736	725
Quartz	12.48	5.96	6.83	16.65	18.32	12.45	11.97	13.76	10.30
Augite and tremolite	-	43.65	-	-	-	-	-	-	-
Hornblende	43.83	-	39.69	40.29	59.74	-	-	57.76	58.34
Plagioclase	23.75	36.07	26.26	25.26	13.61	30.56	28.54	8.53	12.95
Biotite	7.04	-	13.90	4.38	2.08	29.70	27.84	5.43	7.58
Corianderite	-	-	-	-	-	2.54	2.40	-	-
Muscovite	0.55	0.74	-	-	-	0.85	0.99	-	-
Chlorite	0.73	0.44	0.88	0.56	0.92	3.36	5.58	0.75	0.69
Epidote/ Clinzoisite	4.03	6.04	4.49	6.85	2.28	6.15	6.29	3.67	4.23
Sphene	3.75	2.0	2.65	1.97	1.69	2.65	1.70	5.51	3.64
Calcite	-	-	-	-	-	7.85	11.07	-	-
Accessaries (ilmenite, apatite, zircon etc.)	3.84	5.10	5.30	4.14	2.36	3.89	3.62	4.61	2.27

797, 751, 743, 749, } Amphibolites
736, 725

702 - Metadolerite

756, 876 - Meta andesite

Quartz is xenoblastic in character with serrated margins, except a few grains which show straight to curved margins. Majority of the quartz grains show undulose extinction. Vein quartz occurs along the foliation and is characterized by straight and curved boundaries and occasionally show helicitic texture. Biotite is confined to a few thin sections and develops due to the breaking of hornblende, as it occupies the cleavage plane, fractures and margins of latter. Biotite is pink to brown and usually oriented parallel to the main foliation except a few grains. It is interesting to note that in those rocks where hornblende has come in contact with leucocratic material, it has produced varying amount of brown biotite.

Clinozoisite is idioblastic and does not show any orientation except a few clinozoisite grains which are elongated parallel to hornblende and plagioclase forming the foliation. At places, epidote is also associated with quartz. Sphene is subidioblastic to xenoblastic in nature associated with hornblende, plagioclase, clinozoisite and ilmenite. Chlorite is a retrograde product of hornblende and biotite. Accessory minerals in the form of ilmenite, magnetite, apatite and zircon are also present. Opaques are aligned along the main foliation suggesting that they are synkinematic in growth.

Vein calcite occupies the fractures in plagioclase and is of post-tectonic origin. Amphibolite is characterized by the following mineral assemblages:

- (1) Hornblende + albite or andesine + quartz +
+ biotite + clinozoisite + ilmenite + sphene

(2) Hornblende + albite or andesine + quartz +
cummingtonite + clinozoisite + ilmenite + sphene

(ii) Meta-andesite: Meta-andesite crops out at Banas and occurs as sill along the fault plane. The rock is greenish dark, medium grained, hard, compact and well foliated. Quartz-calcite veins and lenses are frequently observed. The rock is mainly composed of plagioclase, biotite, quartz, cordierite, calcite, chlorite, clinozoisite/epidote and sphene. (Table 4.2). Under the microscope the rock shows a blastoporphyritic texture.

Andesine is poikiloblastic sub-idiomorphic in character and shows extensive inclusions of biotite, sericite and quartz. Clinozoisite or epidote and calcite assemblage suggest the possibility of saussuritization at the contact with surrounding biotite. Biotite occurs as short stubby randomly oriented flakes, but still showing faint parallelism with the S_2 foliation. The laths are intimately associated with plagioclase, both as inclusions and as surrounding mass. It however, does not envelop the plagioclase grains. It appears, therefore, grown out of the recrystallization of glass or original fine grained ground mass, which is totally recrystallized to biotite. Chlorite has developed along cleavages, fractures and margins of biotite, giving greenish appearance to the rock.

Quartz is xenoblastic (mainly vein quartz) in nature and is associated with calcite grains. Strained quartz grains possess sutured to serrated margins. Quartz also occurs as inclusions in plagioclase. Cordierite occurs as

subhedral porphyroblasts showing distinct zonal or patchy parallel twins. The grains were initially identified by optical properties and staining tests. The thin sections were also sent to Dr. R.K. Lal, Banaras Hindu University, who also doubted the presence of cordierite on the basis of large axial angle. Further confirmation was carried out by micro-staining tests. Clinozoisite or epidote is idioblastic in character and associated with plagioclase-quartz portion. Calcite mainly occurs as vein, but is always associated with isolated grains of epidote, sphene, quartz etc. Sphene is associated with chloritized biotite and plagioclase. Ilmenite, apatite and zircon are present in varying proportions. Ilmenite is mainly associated with chloritized biotite and sphene.

(iii) Metadolerite: Metadolerite dykes are exposed at Kumalti (Bhagirathi Valley) and Wazari (Yamuna Valley) and are dark green, compact, hard and poorly foliated. These are mainly composed of augite, plagioclase, tremolite, hornblende, quartz, clinozoisite or epidote, sphene and ilmenite. (Table 4.2) Under the microscope, the dykes exhibit blasto-ophitic texture.

Augite occurs as subhedral grains and is characterized by an extinction angle of 35-37°. Along the fractures and margins, tremolite and actinolitic hornblende are developed, though actinolitic hornblende also occurs as pseudomorphs after pyroxene. Plagioclase (Ab₃₈An₆₂) occurs as aggregate of laths with blastophitic to blastosubophitic texture. Some of the plagioclase grains are fractured which are occupied

by quartz. The plagioclase encloses ~~augite~~ indicating a typical character of dolerite. Plagioclase shows alteration to clinozoisite of epidote, chlorite, sericite, quartz and albite. Plagioclase also contains inclusions of apatite, tourmaline and rutile. It also shows zoning, development of myrmekitic intergrowth and pericline twin.

Quartz is xenoblastic in character and mainly associated with plagioclase. Clinozoisite is associated with plagioclase, along twin planes, fractures and margins and seems to be the altered product of latter. A few grains of epidote are associated with augite, plagioclase, magnetite and ilmenite indicating its probable development due to reaction of ilmenite with pyroxene. Minor amount of apatite, tourmaline and rutile is also present.

4.2.4 Migmatite

Migmatite forms an important constituent of the Bhatwari Group and is characterized by schollen, phlebitic, stromatic, ptygmatic, ophthalmitic (augen), schleieren and occasionally nebulitic structures (Mehnert, 1968). The migmatitic rocks show variation in neosome content and contain relict paleosome with gradational contacts. All the structural elements of migmatite are in concordant with the country rocks. These features suggest that migmatite has formed due to the introduction of leucocratic material from the external source. Late phase quartz-tourmaline and quartz-aplitic veins are commonly associated with these migmatitic rocks. On the basis of structure, texture and

mineralogy these rocks have been classified into the following varieties:

1. Streaky migmatite
2. Augen migmatite
3. Mylonitized augen gneiss

Streaky migmatite shows the least migmatization, whereas augen (granitoid) migmatite, exposed near the MCT, has undergone maximum migmatization.

(i) Streaky migmatite: In certain localities amphibolite shows evidences of migmatization in form of ptigmatic, veined and streaky structures with the enrichment of leucocratic material along the foliation. The neosome (quartz-feldspar) contains remnants of paleosome (hornblende) of varying dimension.

Mineralogically, the streaky migmatite contains a higher amount of quartz-feldspar and lesser amount of hornblende in comparison to amphibolite. Quartz occurs both as fine grained mass and porphyroblasts. Potash feldspar porphyroblasts are represented by the orthoclase containing plagioclase inclusions more frequently in their central portions. Quartz is more common near the peripheral region. Myrmekitic intergrowth is commonly seen near the contacts between plagioclase and fine grained quartz of the groundmass. Perthitic intergrowths are quite common. Small laths and large porphyroblasts of plagioclase is of albite composition and grows by replacing the groundmass. The grains have sutured and embayed margins and

contain inclusions of hornblende, quartz, tourmaline, apatite and iron oxides. Plagioclase, in turn, is replaced by potash feldspar, which partly or completely encloses it.

Plagioclase grains are fractured and sericitized along the twin planes. A few fresh plagioclase grains occur either as inclusion in the sericitized plagioclase or present as a separate grain with crowded margins. The latter plagioclase seems to be younger in age and is related to the pegmatitic activity in the area. The plagioclase porphyroblasts enclose hornblende of the main foliation, S_2 , indicating that these have grown later during the late D_2 deformation. The fractures within the plagioclase are occupied by calcite vein of later origin. Some amount of calcite and clinozoisite have been formed due to saussuritization. Clinozoisite is well developed along the fractures and twin planes. Minor amount of biotite is developed due to the reaction between leucocratic material with amphibole.

(ii) Augen migmatite: Augen migmatite is light grey, medium to coarse grained, compact and foliated. The S_2 foliation is imparted by lepidoblastic biotite and muscovite flakes. The size, shape and disposition of augen show little variation in the Bhagirathi Valley and is related to growth of feldspar and quartz porphyroblasts, wrapped around by sheaths of mica. The feldspar augen are rectangular to ellipsoidal in shape and aligned parallel or subparallel to the main foliation, S_2 , with occasional rotation. The S_2 foliation in such augen migmatite is well defined due to alternate dark and light

coloured bands. Sometimes, it is less conspicuous due to the increasing augen size.

When augen are very small or micas too prominent, the migmatite has been referred to as 'foliated migmatite' showing least degree of migmatization, nearly uniform grain size of neosome and variable size of paleosome. Most of the original characters of paleosome are well preserved within the neosome. At times, augen are flattened or the micas do not wrap around them. The neosome are made up of quartz-feldspar, in such cases, is characteristically stromatic. Such migmatite has been referred to as 'banded migmatite' showing comparatively higher degree of migmatization due to the thickening of paleosome along the foliation plane.

In the Yamuna Valley, another variation of migmatite is seen near the MCT. The migmatite has a granitoid look with indistinct foliation in hand specimen. Such migmatite has been called as granitoid migmatite which represent highest degree of migmatization in the Bhatwari Group, exposed around Sayana Chatti in the Yamuna Valley.

In all the varieties of migmatite, the paleosome is represented by relicts of country rocks comprising mainly of quartz, biotite, muscovite and garnet, whereas the neosome contains feldspar, quartz and subordinate mica. The mineralogy of migmatite is more or less similar, except that an enrichment of feldspar and depletion of quartz content has taken place from foliated to granitoid varieties. Occasionally, the migmatite

contains minute grains of garnet enclosed within the neosome indicating a garnet grade of metamorphism of the country rocks. The garnet is, however, absent from migmatite showing intense migmatization or a strong mylonitization. Quartz, K-feldspar, plagioclase, biotite and muscovite are the main mineral component of migmatite. Garnet, chlorite and calcite occur in minor amount. Apatite, tourmaline and zircon are associated with neosome, whereas rutile, sphene and ilmenite are forming a part of the paleosome. The migmatite varieties are characterized, by porphyroblastic texture and lepidoblastic foliation marked by biotite and muscovite flakes.

Quartz occurs as lensoidal porphyroblasts and fine grained mass and seems to be atleast of two generations along the foliation plane, besides that occurring along the fractures. Quartz I occurs as elongate to tabular grains of medium size having nearly straight grain boundaries and straight extinction (Figs. 4.26, 4.27). These grains are developed along isoclinally folded S_1 foliation which alternates with foliation revealing grain size reduction, serrated margins, fine elongate dimensionally oriented quartz grains and phyllosilicate rich layers (Fig. 4.27). Mylonitic character of fine quartz I is distinct in such foliation which is isoclinally folded by F_2 folds. Quartz I also occurs as inclusions within plagioclase I aligned along S_1 foliation (Fig. 4.26).

Quartz II shows serrated, sutured and diffused margins inequigranular porphyroblastic character and is associated with mica flakes preferably oriented along S_2 foliation in the core

EXPLANATION OF PHOTOMICROGRAPHS:

FIGURES 4.25 to 4.27

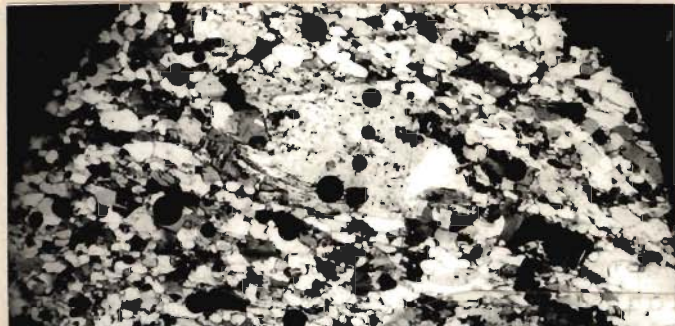
Figure 4.25 - Migmatization of amphibolite. Hornblende prisms preferably oriented along S_2 foliation have uneven contact with quartz and feldspar band along S_2 foliation. Streaky migmatite of the Bhatwari Group. Locality - Malla ($D_{27}/457$). Crossed X55.

Figure 4.26 - Mosaic showing plagioclase I porphyroblasts with quartz inclusions occurring along S_1 foliation with phyllosilicates and quartz. S_1 foliation is isoclinally folded during D_2 deformation. Incipient crystallization of plagioclase II along axial plane of F_2 fold along S_2 foliation in right hand side. Migmatite of the Bhatwari Group. Locality - Agra ($D_{27}/516$). Crossed X55.

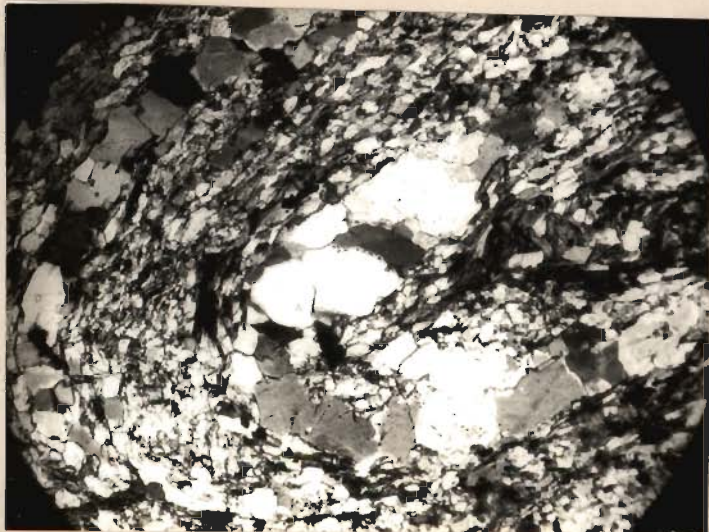
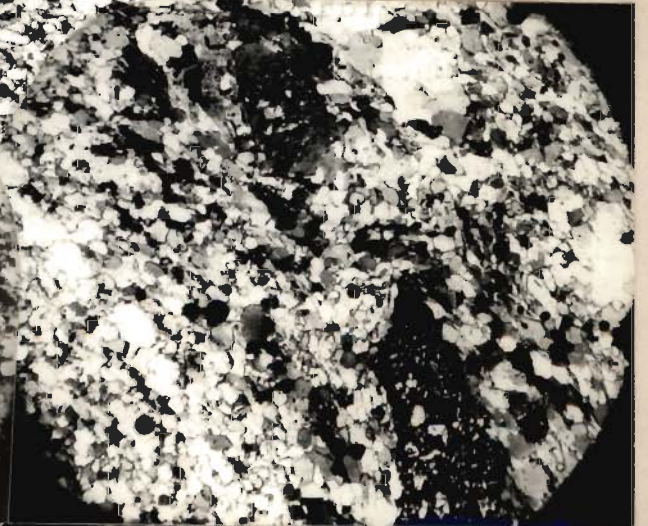
Figure 4.27 - Alternating xenoblastic annealed fine quartz and phyllosilicates along S_1 being isoclinally folded by F_2 fold having S_2 as the axial plane foliation. Cummingtonite biotite schist of the Bhatwari Group. Locality - Bhatwari College ($D_{27}/810$). Crossed X55.



4.25



4.26



4.27

and hinge zones of F_2 folds. At least one more younger generation of quartz is indicated in the migmatite and occurs as strain-free veinlets along fractures in groundmass and feldspar (Fig. 4.28). Presence of fluid inclusions within this variety of quartz indicates that it has formed due to hydrothermal activity in the area. Quartz II shows replacement textures with quartz I, plagioclase I and K-feldspar II. At the junction of quartz-plagioclase-K-feldspar, myrmekitic or graphic intergrowth is commonly seen.

One of the most interesting aspect of the migmatite of the Bhatwari Group is two distinct phases of migmatization during D_1 and D_2 deformational episodes. First migmatization is characterized by preferred orientation of K-feldspar I and plagioclase I along the isoclinaly folded S_1 foliation by F_2 folds (Fig. 4.26). In this phase, K-feldspar I is rather uncommon and occurs as subidioblastic grains with occasional twinning either as separate grains or as completely enclosed inclusions in sericitized plagioclase-I. This indicates that plagioclase I has formed later to K-feldspar during the first phase of migmatization. Plagioclase I is subidioblastic to elongate xenoblastic in shape showing serrated indistinct grain boundaries with the groundmass and containing numerous xenoblastic quartz inclusions of S_1 foliation (Fig. 4.26). Complete grains are either sericitized or extensive sericitization is mainly confined to twin and fracture planes, thus making composition determination difficult (Fig. 4.28).

EXPLANATION OF PHOTOMICROGRAPHS:

FIGURES 4.28 to 4.33

Figure 4.28 - Highly sericitized plagioclase I (left side) is surrounded by a thin rim of fresh plagioclase II showing albite twins. K-feldspar II cut across by quartz III along veins and is in contact with plagioclase I and plagioclase II. Granoblastic quartz and phyllosilicates of the groundmass to the right. Granitoid migmatite of the Bhatwari Group. Locality - Syana Chatti (D₂₇/744). Crossed X55.

Figure 4.29 - Inclusions of rounded blebs of quartz, subidioblastic chloritized biotite and highly sericitized plagioclase I in perthitic K-feldspar II. Granitoid migmatite of the Bhatwari Group. Locality - Syana Chatti Crossed X55.

Figure 4.30 - Plagioclase I subhedral grains as inclusions in K-feldspar II porphyroblasts. At margins, intergrowth with plagioclase II. Mylonitized quartz-phyllosilicates along S₂ foliation. Granitoid (augen) migmatite of the Bhatwari Group. (D₂₇/705). Crossed X55,

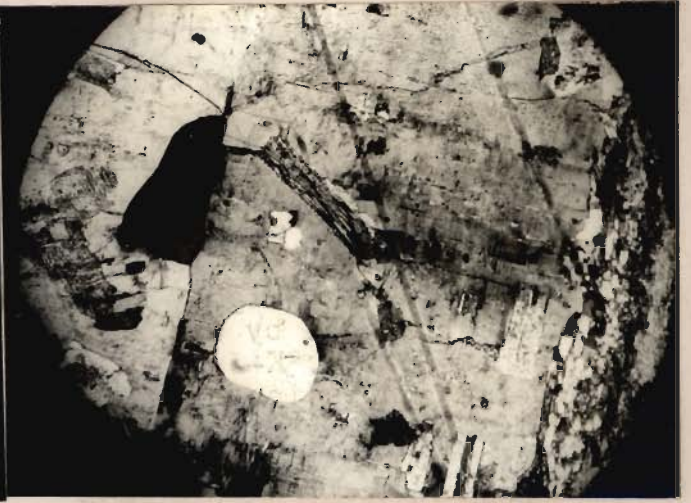
Figure 4.31 - Migmatization along S₁ foliations during D₁ deformation with sericitized plagioclase I occurring along the foliation as well as inclusions in K-feldspar II. Porphyroblastic growth of K-feldspar II during D₂ deformation along the S₂ foliation. Granitoid (augen) migmatite of the Bhatwari Group. Locality - Syana Chatti (D₂₇/705). Crossed X55.

Figure 4.32 - Subidioblastic yellowish to dark brown garnet I grains along relict S₁ foliation being isoclinally folded by F₂ folds having phyllosilicates along axial plane foliation S₂. Migmatite of the Bhatwari Group. Locality - Agra (D₂₇/540). Crossed X55.

Figure 4.33 - Subidioblastic fractured garnet II with inclusions of quartz and biotite surrounded by inclusion-free garnet III. Wrapping of the grain by S₂ foliation. Garnetiferous kyanite-biotite gneiss of the Suki Group. Locality - Debrani (D₂₇/837). Crossed X55.



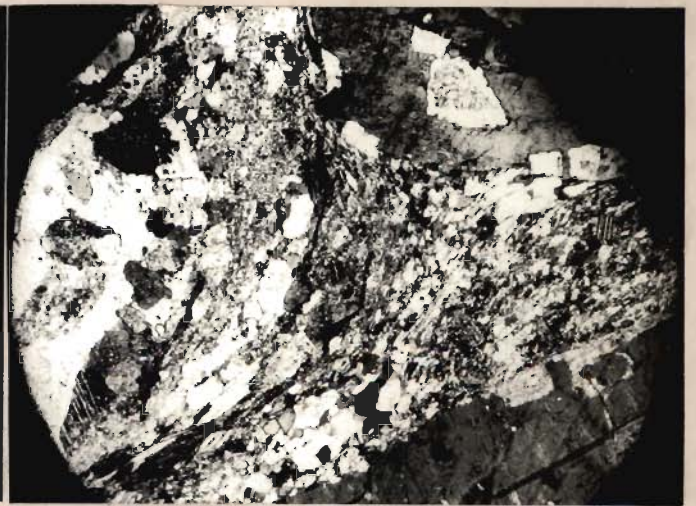
4.28



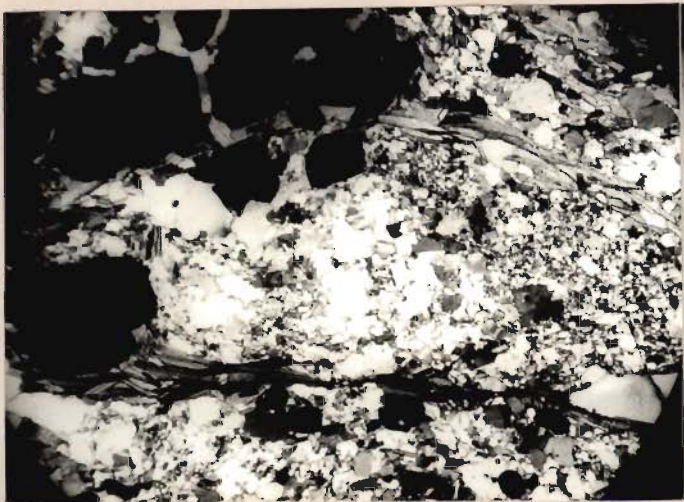
4.29



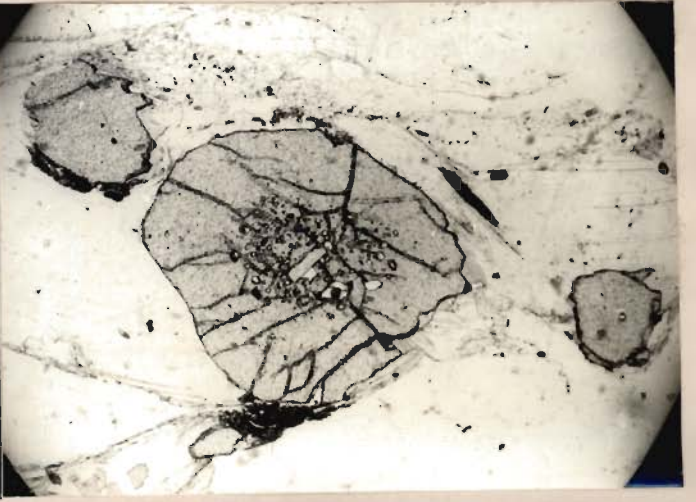
4.30



4.31



4.32



4.33

In a few grains, composition of plagioclase I is albite or oligoclase. Plagioclase I grains are fractured and their twin lamellae have been deformed. The fractures are filled up by quartz and mica. Plagioclase I also contains relicts of ground-mass mainly tiny grains of quartz and mica. At places, it is saussuritized producing clinozoisite or epidote, calcite and chlorite. Paragenetically, plagioclase I has been observed to occur either as inclusion in plagioclase II and K-feldspar II or along their slightly corroded margins (Fig. 4.28).

During the second phase of migmatization, it has been observed that K-feldspar II has developed paragenetically later than plagioclase II. Plagioclase II is fresh, and is of albite in composition with minimum sericitization. It occurs as inclusion in K-feldspar II or as a separate grain or forming a rim round plagioclase I, especially when in contact with K-feldspar II (Fig. 4.28). Plagioclase II grains are subidioblastic and, at times, show zoning. Some of the plagioclase II grains are also strained.

K-feldspar II porphyroblasts are mostly subidioblastic in shape and have irregular margins (Fig. 4.29). The porphyroblasts contain inclusion of subrounded to subhedral plagioclase I (Figs. 4.29, 4.30) or subhedral plagioclase II (Fig. 4.30). Along the cleavage, vein, stringer and film perthites are well developed (Fig. 4.29) and have formed later to patchy perthite.

In K-feldspar II, microcline twins are visible in patches indicating that microcline could have formed due to

the structural state transformation of orthoclase. Occasionally, K-feldspar-II porphyroblasts are zoned. The formation of myrmekite at the outer margins of perthitic K-feldspar II suggests that the process of myrmekitization is probably related to the development of vein, stringer and film perthites. The K-feldspar-II porphyroblasts contain the inclusion of chloritized biotite, oriented parallel to the S_2 -foliation (Fig. 4.29) or other phyllosilicates (Fig. 4.31) indicating that K-feldspar II porphyroblasts have crystallized synkinematically to the development of S_2 foliation. At times, ilmenite, tourmaline, zircon and apatite occur as inclusions in K-feldspar II. At places, K-feldspar II also shows intergrowth with plagioclase II indicating their simultaneous crystallization for certain period of time.

Biotite I and muscovite I with quartz define the S_2 foliation (Figs. 4.26, 4.27) also wraps around or abuts against the feldspar porphyroblasts indicating their syn-to late tectonic growth (Fig. 4.31). Though an still older generation of mica define S_1 foliation along with quartz and is isoclinally folded by F_2 folds having S_2 as axial plane foliation, biotite I and muscovite I do not texturally differ from this mica hence being described together. Mica I also occurs as inclusion within the feldspar porphyroblasts. Muscovite II and biotite II porphyroblasts are sometimes randomly oriented. Most of the mica II grains are inclined to S_2 foliation indicating their post- D_2 growth. However, some of the muscovite II porphyroblasts are also aligned parallel to S_2 foliation but are crenulated

with axial plane foliation, S_3 . The strain effect is restricted only to some of the mica II porphyroblasts. Muscovite II also occupies fractures and cracks in feldspar porphyroblasts. Some of the deformed mica flakes show undulose extinction. Chlorite has been formed due to the breakdown of biotite.

Interestingly, augen migmatite also contains garnet of the first generation. Garnet I is yellowish to dark brown, subidioblastic and contains very fine grained quartz and ilmenite inclusions. Garnet I is essentially developed along S_1 foliation and occurs in a string which is isoclinally to very tightly folded into F_2 folds (Fig. 4.32). The association of schorlite with leucosome indicates the pneumatolytic phase related to hydrothermal activity.

The presence of two generations of plagioclase coupled with K-feldspar in the migmatite along with other textural criteria suggests that the Bhatwari Group has undergone two stages of migmatization. Further, it has been noticed that the amount of K-feldspar reduces from south (near the MCT) towards north (near the JBT), indicating that the potash metasomatism was prominent only in the basal part. The presence of plagioclase in all the thin sections of migmatite in variable amount indicates that the soda metasomatism has affected the entire area.

(iii) Mylonitic augen gneiss: The mylonitic augen gneiss interbanded with mylonitic augen schist are well developed along the tectonic zones, particularly in the Bhatwari Group.

The mylonitic gneiss is light grey, medium grained and, at places, gives greenish tint due to the development of retrograde chlorite. The schistose portions are strongly crenulated and their axial surfaces are occupied by quartz vein of late phase. The extensive tectonic movement has led to the development of slickenside and even smoothing of the surface.

In general, these exhibit cataclastic structure with later recrystallization and can be compared with blastomylonite (Spry, 1969). Quartz, plagioclase, orthoclase, biotite and muscovite are the main constituents of rocks. Occasionally, garnet is present.

Quartz occurs both as fine grained mass and lensoidal porphyroclasts, showing serrated margins, microfractures and strong undulose extinction. Feldspar (albite and orthoclase) occur as prophyroblasts. The crystals are generally subhedral and have displaced S_2 foliation, so that the latter wraps around the former.

The feldspar crystals are extensively fractured and altered. Around many lenticular porphyroblasts, pressure shadows have developed. Occasionally, the feldspar porphyroblasts abut against the S_2 foliation suggesting that the crystals have grown by replacing the groundmass consisting of quartz and micas.

Two generations of biotite and muscovite have been observed. Biotite I and muscovite I define the S_2 foliation plane, whereas biotite II and muscovite II define the S_3 foliation plane. Chlorite is developed along the margins of biotite I.

Mica II flakes are bent and show undulatory extinction, indicating that the deformation continued after their recrystallization. Apatite, tourmaline, ilmenite and rutile are the accessory minerals.

4.3 SUKI GROUP

The rocks of the Suki Group have been progressively regionally metamorphosed from garnet to sillimanite grade and have undergone varying degree of migmatization and late phase pegmatitic activity. This group reveals inverted metamorphic isograde pattern which has been recently reinterpreted as the divergent type (Thakur, 1977, 1980). This pattern has been well established around Jhala in the Bhagirathi Valley. The mylonitic effects in these rocks are less prominent unlike the Bhatwari Group, except along the JBT, where they show strong cataclastism and retrograde metamorphism. Kyanite zone covers considerable area, whereas sillimanite is locally developed at Jhala. At places, relict bedding (S_0) can still be traced in the field inspite of strongly superimposed foliation (S_2). Petrographically, the Suki Group is characterized by metamorphic textures of progressive regional metamorphism, present of syn- and post- tectonic garnet II and III respectively, poor rotation of garnet porphyroblasts, absence of first phase of migmatization as well as the earliest foliation (S_1) which characterize the Bhatwari Group. All these evidences indicate that the Suki Group has not undergone the first phase of progressive regional metamorphism of the Bhatwari Group,

The Suki Group is comprised of the following rock types:

A. Regionally metamorphosed rocks (poorly migmatized)

- (i) Quartz-muscovite-biotite-garnet schist
- (ii) Quartz-biotite-garnet-kyanite schist
- (iii) Quartz-muscovite-sillimanite gneiss
- (iv) Pargasite-ferrogedrite-muscovite gneiss

B. Rocks showing cataclastic and retrograde metamorphism

- (i) Mylonitic graphite schist
- (ii) Quartz-chlorite schist

C. Igneous derivatives

- (i) Pegmatite
- (ii) Amphibolite
- (iii) Porphyroblastic migmatite

4.3.1 Regionally metamorphosed (poorly migmatized rocks):

(i) Quartz-muscovite-biotite-garnet schist: The garnetiferous mica schist is greyish, medium grained and well foliated due to lepidoblastic biotite and muscovite flakes. Mica is associated with quartz and garnet and small amount of chlorite, hornblende, plagioclase and K-feldspar. Tourmaline, apatite, sphene, ilmenite and rutile occur as accessories. Along the JBT, it shows cataclastism and profuse development of slickenside. At places, the pegmatite veins occur along the foliation and gives banded appearance to the rock. Kinking of mica flakes,

formation of mineral lineation and association of quartz aplitic, quartz-tourmaline veins are some of the notable features.

As a dominant constituent in most of the thin sections, quartz is elongate, granoblastic to porphyroblastic in character having straight or serrated boundaries and commonly with triple junction boundaries. Most quartz is strained-free with straight extinction having helicitic mica inclusions (Fig. 4.33), though it is affected by strain during D_3 deformation. Tiny quartz inclusions occur in poikiloblastic, biotite, muscovite, garnet and plagioclase indicating its limited metamorphic growth, while it has continuous growth during D_2 and D_3 deformations.

Two generations of biotite and muscovite have been observed in these schists. Biotite I and muscovite I impart lepidoblastic foliation (S_2) and have grown rather simultaneously along S_2 . These have gradational interfoliated contacts and are subsequently kinked due to F_3 folds (Fig. 4.34). Biotite I occasionally retrogrades to chlorite. Biotite II and muscovite II are oblique to S_2 when present as a result of rotation of biotite I or new mica growth along axial surfaces (S_3) of later angular folds or kinks (F_3). Fig. 4.34 reveals many such textures of new biotite II and muscovite II along S_3 resembling textures of the deformational zones in mica described by Vernon (1977) from deformed pegmatite (also, Glen, 1980). Minor amount of biotite is also formed due to the retrogression of garnet and hornblende along fractures and margins probably during the D_{2a} deformation.

EXPLANATION OF PHOTOMICROGRAPHS:

FIGURES 4.34 to 4.39

Figure 4.34 - Subidioblastic tourmaline along S_2 foliation during or late D_2 deformation. Kinking, bending and slippage of lepidoblastic biotite due to F_3 folds. Prograde textures predominant. Kyanite-garnet mica schist of the Suki Group. Locality - Jhala ($D_{27}/606$). Plane X55.

Figure 4.35 - Porphyroblastic sodic plagioclase II along S_2 foliation causing its bending during growth. Kyanite bands and biotite wraps around plagioclase indicating syntectonic migmatization during D_2 deformation. Kyanite schist of the Suki Group Locality - near Suki ($D_{27}/571$). Crossed X55.

Figure 4.36 - Syntectonic porphyroblastic kyanite growth with rotation during D_2 deformation. Garnetiferous kyanite-biotite gneiss of the Suki Group. Locality - Debrani ($D_{27}/837$).

Figure 4.37 - Fibrolite variety of sillimanite developing from muscovite along S_2 foliation. Quartz-muscovite-sillimanite gneiss of the Suki Group. Locality - Jhala ($D_{27}/616$). Plane X220.

Figure 4.38 - Radiating cluster of nematoblastic needles of fibrolite from the same thin section as shown in figure 4.38. Plane X55.

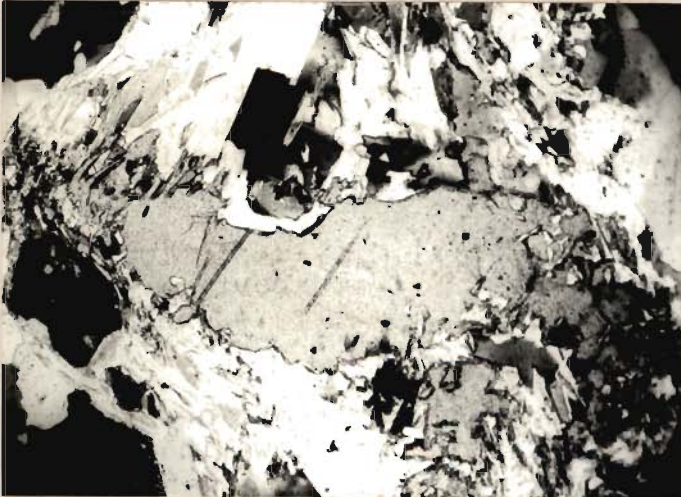
Figure 4.39 - Ferrogedrite breaking into nematoblastic talc along S_2 foliation. Xenoblastic quartz with triple junction and straight extinction. Pargasite-ferrogedrite-muscovite gneiss of the Suki Group. Locality - Jhala. ($H_8/79$). Crossed X55.



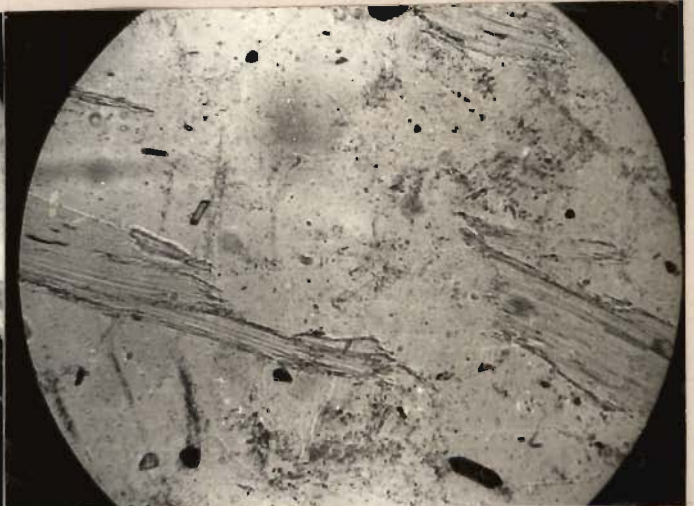
4-34



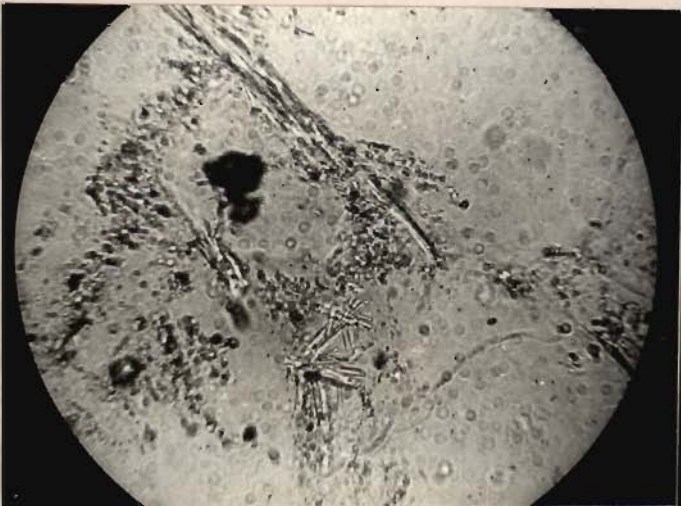
4-35



4-36



4-37



4-38



4-39

Garnet (almandine) occurs as pink, fine to medium, idioblastic or subidioblastic grains enveloped by the bent S_2 foliation as well as revealing superimposed fabric (Fig. 4.33). Two distinct garnets have the following characters:

- (i) An older generation of almandine (garnet II; chronology for comparison with garnets of the Bhatwari Group) defined by profuse tiny quartz, biotite and ilmenite inclusions (Fig. 4.33).
- (ii) Inclusion-free, peripheral garnet III either over the garnet II nuclei or as tiny subidioblastic grains across the foliation S_2 which is not deflected around them (Fig. 4.33).

The above behaviour of two generations of garnet indicate a syn- to post-tectonic growth for garnet II and garnet III respectively and can be comparable with those of the Bhatwari Group. At places, distinction between syntectonic core of garnet II and post-tectonic margin of garnet III has been made by ilmenite grains and the presence of fractures near the JBT. Along fractures and margins garnet occasionally retrogrades to biotite and chlorite. Most of the sections contain inclusion free subidioblastic garnet of post-tectonic growth (garnet III) along with syn-to post-tectonic garnet III. As has been briefly described, many Lesser Himalayan and Central Himalayan crystalline sequences reveal two stages of the garnet growths which have been correlated to two metamorphic events during the Himalayan Orogeny (Das and Pande, 1963-64; Bisaria, 1972; Kumar, 1975; Das, 1978a,b; Mehta, 1976; Mehta and Pande, 1977; Lal et al., 1981; Merh and Vashi, 1965).

Prismatic hornblende has been noticed in one thin section (D₂₇/799) parallel to the S₂-foliation where retrogression along the fractures and margins has also resulted in smaller amount of chlorite. Plagioclase (Ab₈₆, An₁₄), at times, has been sericitized along the twin planes and fractures. K-feldspar is rarely recorded, and whenever it is present with plagioclase, the former replaces the latter.

Two generations of tourmaline has also been identified, Tourmaline I (albite) occurs as subidioblastic, fractured grains with their long prismatic faces along the foliation S₂ as a result of their synkinematic growth during D₂ deformation (Fig. 4.34) and is affected by crenulation of the D₃ deformation (Fig. 4.34). Tourmaline II (schorlite) is closely associated with quartz or quartz or feldspar portion. At places, it is oriented obliquely to S₂-foliation, thereby indicating a post-tectonic crystallization after D₂ deformation which could relate to the post- D₃ deformation late phase pegmatitic activity in the area like along the MCT.

The following mineral assemblages have been observed in the schist:

(i) Quartz + biotite + muscovite + almandine + plagioclase (Ab₉₂) ± K-feldspar.

(ii) Quartz + biotite + muscovite + almandine + plagioclase (Ab₈₆) + hornblende.

(ii) Quartz-biotite-garnet-kyanite schist: The kyanite bearing garnetiferous mica schist covers comparatively

wider area of the Suki Group and is mostly light to dark grey, medium to coarse grained and well foliated. At places, it shows banded character due to pegmatite veins parallel to the foliation and develops larger kyanite blades. Kinking of mica flakes, development of mineral lineation and association of quartz veins, lenses and small scale boundins are other common structures. The main constituents of the schist are quartz, biotite, muscovite, garnet, staurolite, kyanite and plagioclase with minor amounts of cordierite, tourmaline, apatite, zircon and rutile.

Quartz occurs both as porphyroblast as well as xenoblastic inclusions in biotite, garnet, kyanite and plagioclase. Majority of quartz grains are unstrained, however, some of the strained quartz grains show undulose extinction. Quartz grains are characterised by curved, straight and sutured margins indicating predominantly post- D_3 recrystallization.

Biotite I is interlayered with muscovite I and imparts lepidoblastic schistosity (S_2) to the rocks. Biotite I is yellowish brown and occasionally shows undulose extinction. The textural behaviour of biotite I shows that it is synkinematic in growth. Biotite II is pinkish brown and occurs as porphyroblasts, grown obliquely the S_2 foliation, suggesting a late stage crystallization of biotite II. The orientation of biotite II defines the S_3 foliation. The behaviour of muscovite I and muscovite II is similar to biotite I and biotite II but muscovite occurs in lesser amount in comparison to biotite.

Plagioclase ($Ab_{84}An_{16}$; occurs as porphyroblasts wrapped by synkinematic mica flakes. Some of the plagioclase

grains are fractured and least sericitized. The fractured plagioclase contains inclusion of quartz, apatite, zircon, tourmaline and rutile.

Garnet (almandine) is syn- to post-tectonic in relation to S_2 -foliation and shows similar characters as in garnetiferous mica schist.

Kyanite occurs as bladed to elongate laths, which are oriented parallel or sub-parallel to the S_2 foliation (Fig. 4.35). Kyanite blades show sieve structure with inclusion of quartz and iron oxides revealing frilled margins and slight synkinematic rotation of porphyroblastic blades (Fig. 4.36). The concordant to discordant behaviour of kyanite with S_2 -foliation suggest that the crystallization of kyanite laths continued sometimes even in late D_2 deformation.

Staurolite occurs as porphyroblast and contains inclusion of quartz. However, there are certain staurolite grains which do not contain inclusion. It appears that staurolite started crystallizing in late phase of tectonism. K-feldspar porphyroblasts contain inclusions of quartz, apatite, zircon and tourmaline and show replacement relationship with the plagioclase. At places, K-feldspar grains contain randomly oriented fractures. Cordierite occurs as pokiloblastic grains having inclusions of quartz, apatite, tourmaline, rutile and biotite. It is characterized by high 2V angle and faint lamellar twinning. Cordierite has also been confirmed by microstaining test.

The schist is characterized by the following assemblage.

Quartz + biotite + muscovite + plagioclase + K-feldspar
 + garnet + kyanite + staurolite + cordierite

(iii) Quartz-muscovite-sillimanite gneiss: It is exposed north of Jhala bridge and is localised in a narrow belt flanked by rocks containing kyanite on both sides. Tourmaline bearing aplite and pegmatite veins are quite common. Different mineral components show a strong tendency to segregate into lenticles and streaks. The gneiss is light grey, medium to coarse grained, compact and show poor development of foliation which is defined by muscovite flakes. These occasionally show bending and breaking. In thin sections, it exhibits lepidoblastic texture. Quartz, muscovite, sillimanite and plagioclase are the main constituents of the rock with minor proportion of K-feldspar, tourmaline, apatite, zircon and rutile.

Most of the quartz grains are unstrained, however, a few of them are strained and show undulose extinction. Some of the quartz grains have rounded margins whereas in other grains triple junction is quite sharp. Majority of the oligoclase grains are subhedral, unaltered and have serrated boundaries with adjacent feldspar and muscovite grains. Most of the sillimanite is of fibrolite variety as is evident from the tiny fibrous needle character. Fibrolite occurs as very fine grained nematoblastically oriented needles along muscovite flakes in S_2 foliation, which have developed a frilled character due to its breakdown (Fig. 4.37). Also, radiating fibrolite cluster around a nuclei and reveals helicitic texture within granoblastic

quartz (Fig. 4.38). Most of fibrolite textures are characteristic of the prograde regional metamorphism and represent highest metamorphic zone at Jhala Bridge. Rutile, zircon, apatite and tourmaline are the accessory minerals.

(iv) Pargasite-ferrogedrite-muscovite gneiss: A narrow band (4-5m in width) of pargasite-ferrogedrite-muscovite gneiss occurs just east of Jhala bridge and is underlain by quartz-muscovite-sillimanite gneiss; garnet-kyanite schist overlies the former. This gneiss is greyish green to brownish green, medium to coarse grained having poorly developed thin alternating bands of amphibole and quartz feldspar along gneissosity. Small veinlets of pegmatite are commonly associated with gneiss. Quartz, pargasite, ferrogedrite, muscovite, plagioclase are the main constituents with minor amount of biotite and K-feldspar. Sphene, rutile, apatite, zircon, ilmenite and tourmaline are the accessory minerals.

X-ray diffractogram peaks of sample No. D₂₇/615 indicate main amphibole to be pargasite of subhedral character having fairly good pleochroism from colourless to greenish yellow colour. It is characterized by an extinction angle of CAZ -28° . Pargasite commonly shows the development of intergrowth twinning. It usually breaks into a fine grained mixture of fibrous talc and iron oxide when in contact with quartz or plagioclase (Fig. 4.39) and defines well developed foliation, S₂. At times, pargasite contains fibrous to flaky patches of ferrogedrite showing poor pleochroism. Some of these patches show optical

EXPLANATION OF PHOTOMICROGRAPHS:

FIGURES 4.40 to 4.45

Figure 4.40 - Intergrowth of pargasite and lepidoblastic ferrogedrite. Pargasite-ferrogedrite muscovite gneiss of the Suki Group. Locality - Jhala (D₂₇/615). Crossed X55.

Figure 4.41 - Localized isoclinal folding of S₂ foliation having chlorite and development of S_{2a} transposed foliation in thrust zone. Chlorite schist of the Suki Group along the JBT. Locality - north of Janki Chatti, Yamuna Valley, (D₂₇/884). Crossed X55.

Figure 4.42 - Same thin section as in figure 4.41. Dragging of S_{2a} transposed foliation along S₃ foliation and rotation of chlorite flakes. New incipient chlorite growth along S₃. Crossed X55.

Figure 4.43 - Porphyroblastic plagioclase II syn- to late D₂ deformation along S₂ foliation containing biotite inclusions. Porphyroblastic migmatite of the Suki Group. Locality - Suki (D₂₇/598). Crossed X55.

Figure 4.44 - Subhedral, fresh sodic plagioclase II being replaced by K-feldspar II showing reaction along margins. Porphyroblastic migmatite of the Suki Group. Locality - Suki (D₂₇/600). Crossed 55.

Figure 4.45 - Myrmecitic intergrowth at contact with K-feldspar II with finger like quartz stringers in plagioclase II. Lepidoblastic biotite along S₂ foliation. Porphyroblastic migmatite of the Suki Group. Locality near Suki (D₂₇/597). Crossed X110.

quartz (Fig. 4.38). Most of fibrolite textures are characteristic of the prograde regional metamorphism and represent highest metamorphic zone at Jhala Bridge. Rutile, zircon, apatite and tourmaline are the accessory minerals.

(iv) Pargasite-ferrogedrite-muscovite gneiss: A narrow band (4-5m in width) of pargasite-ferrogedrite-muscovite gneiss occurs just east of Jhala bridge and is underlain by quartz-muscovite-sillimanite gneiss; garnet-kyanite schist overlies the former. This gneiss is greyish green to brownish green, medium to coarse grained having poorly developed thin alternating bands of amphibole and quartz feldspar along gneissosity. Small veinlets of pegmatite are commonly associated with gneiss. Quartz, pargasite, ferrogedrite, muscovite, plagioclase are the main constituents with minor amount of biotite and K-feldspar. Sphene, rutile, apatite, zircon, ilmenite and tourmaline are the accessory minerals.

X-ray diffractogram peaks of sample No. D_{27/615} indicate main amphibole to be pargasite of subhedral character having fairly good pleochroism from colourless to greenish yellow colour. It is characterized by an extinction angle of CAZ -28° . Pargasite commonly shows the development of intergrowth twinning. It usually breaks into a fine grained mixture of fibrous talc and iron oxide when in contact with quartz or plagioclase (Fig. 4.39) and defines well developed foliation, S₂. At times, pargasite contains fibrous to flaky patches of ferrogedrite showing poor pleochroism. Some of these patches show optical

zoning, the central portion having parallel extinction in contrast to margins where CAZ equals 11° . Poikiloblastic ferrogedrite plates contain partially enclosed prisms and basal sections of pargasite (Fig. 4.40).

Quartz is mainly porphyroblastic as well as xenoblastic in character with straight to curved margins. Strained varieties are rarely seen in porphyroblasts. Quartz also occurs along fractures and cleavages of amphiboles especially in ferrogedrite. It shows replacement textures with amphibole indicating its growth after amphibole. Randomly oriented fractures in quartz suggest its brittle deformation during D_4 stage. Plagioclase (An_{11-14}) is closely associated with quartz and is slightly elongated along S_2 and sericitized along twin planes. It shows corroded margins with amphiboles and, at times, contain small inclusions of quartz indicating its post-amphibole and pre-quartz paragenesis. Quartz and plagioclase are randomly fractured and contain inclusions of rutile and sphene. Muscovite occupies intergranular spaces of quartz and also occurs within plagioclase. At times, muscovite flakes cut across quartz and feldspar, thus indicating its post-tectonic growth. Talc occurs within and along margins of amphibole as fine grained pockets or acicular grains formed mainly due to the breakdown of ferrogedrite in quartz rich environment during D_2 deformation and M_2 metamorphism (Fig. 4.39).

Pargasite and ferrogedrite are closely associated with kyanite schist and sillimanite gneiss along a narrow zone. It

is inferred that, pargasite and orthopyroxene were present in the original basic rock in which orthopyroxene later on changed to ferrogedrite in P-T conditions of slightly lower temperature and comparatively higher pressure (Hietanen, 1959) during D_2 deformation. Ferrogedrite then reacted with pargasite and became monoclinic amphibole. Finally, these amphiboles were affected by migmatitic material (later phase acidic igneous activity) in silica rich environment (Deer et al., 1963) during the late phase of D_2 deformation and broke down to talc

4.3.2 Rocks showing cataclastic and retrograde metamorphism:

(i) Mylonitic graphite schist: The mylonitic graphite schist occurs as a thin lenticular band along the JBT and shows prominent development of mylonitic foliation, S_{2a} . The schist is dark grey or brownish grey, medium grained and shows variability in competence. On the surface of the rock, slickensides are profusely developed. Mica flakes and elongated quartz grains impart foliation to the schist, whereas graphite streaks define the lineation. Quartz, muscovite, biotite, plagioclase, K-feldspar and graphite are the main mineral constituents in the schist. Tourmaline, apatite, rutile and clinozoisite are the accessory minerals.

Quartz occurs mainly as porphyroblast and shows strong undulose extinction. Some of the quartz grains exhibit granoblastic texture with straight to curved boundaries. At times, the unstrained quartz grains are characterized by triple

junction, indicating a post-tectonic growth after D_3 deformation. Muscovite and biotite occur in small proportion and, at places, mica flakes show kink bending and breaking as a result of D_3 deformation. Feldspar grains show crushing, fracturing, development of boudins and pressure shadows. Plagioclase grains are sericitized and saussaritized. The graphite scales are mainly confined along the fractures and foliation plane.

(ii) Quartz-chlorite schist: A narrow patch of quartz-chlorite schist has been recorded along the JBT in the Yamuna Valley. The schist is dark grey, fine to medium grained, compact and well foliated. It is mainly composed of quartz, chlorite and biotite with smaller amount of ilmenite, magnetite, apatite and tourmaline. The rock shows development of mylonitic foliation, S_{2a} , and transposition of earlier foliation.

Chlorite exhibits streaky or scaly habit and is inter-layered with biotite flakes along the foliation. The earliest discernible structure in this schist is a folded foliation marked by quartz, biotite and chlorite and occurs as a relict foliation, S_2 , in the rock (Fig. 4.41). Tightly appressed folds affect this foliation and seem to be related to the most prominent transposed foliation, S_{2a} , in the thrust zone (Fig. 4.41). Chlorite mainly occurs as pseudomorph after biotite and is interleaved with the latter. The close association of ilmenite and magnetite grains in chlorite flakes, indicate that chlorite has been produced due to the retrogression of biotite. Later bending and breaking of chloritized biotite flakes along

EXPLANATION OF PHOTOMICROGRAPHS:

FIGURES 4.40 to 4.45

Figure 4.40 - Intergrowth of pargasite and lepidoblastic ferrogedrite. Pargasite-ferrogedrite muscovite gneiss of the Suki Group. Locality - Jhala (D₂₇/615). Crossed X55.

Figure 4.41 - Localized isoclinal folding of S₂ foliation having chlorite and development of S_{2a} transposed foliation in thrust zone. Chlorite schist of the Suki Group along the JBT. Locality - north of Janki Chatti, Yamuna Valley, (D₂₇/884). Crossed X55.

Figure 4.42 - Same thin section as in figure 4.41. Dragging of S_{2a} transposed foliation along S₃ foliation and rotation of chlorite flakes. New incipient chlorite growth along S₃. Crossed X55.

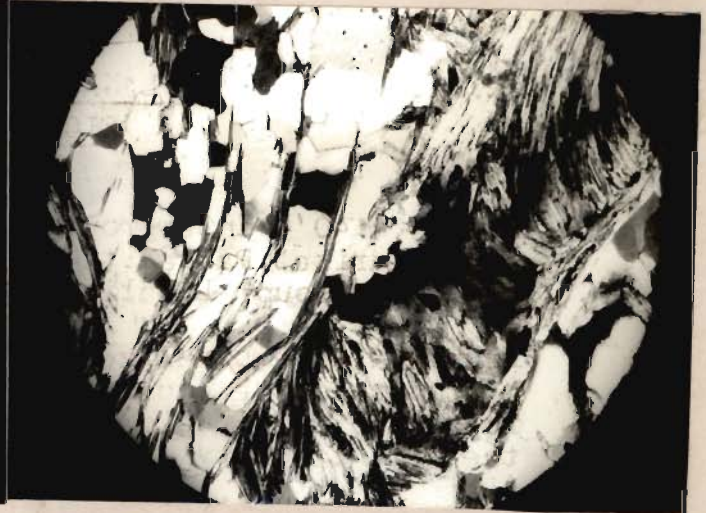
Figure 4.43 - Porphyroblastic plagioclase II syn- to late D₂ deformation along S₂ foliation containing biotite inclusions. Porphyroblastic migmatite of the Suki Group. Locality - Suki (D₂₇/598). Crossed X55.

Figure 4.44 - Subhedral, fresh sodic plagioclase II being replaced by K-feldspar II showing reaction along margins. Porphyroblastic migmatite of the Suki Group. Locality - Suki (D₂₇/600). Crossed 55.

Figure 4.45 - Myrmecitic intergrowth at contact with K-feldspar II with finger like quartz stringers in plagioclase II. Lepidoblastic biotite along S₂ foliation. Porphyroblastic migmate of the Suki Group. Locality near Suki (D₂₇/597). Crossed X110.



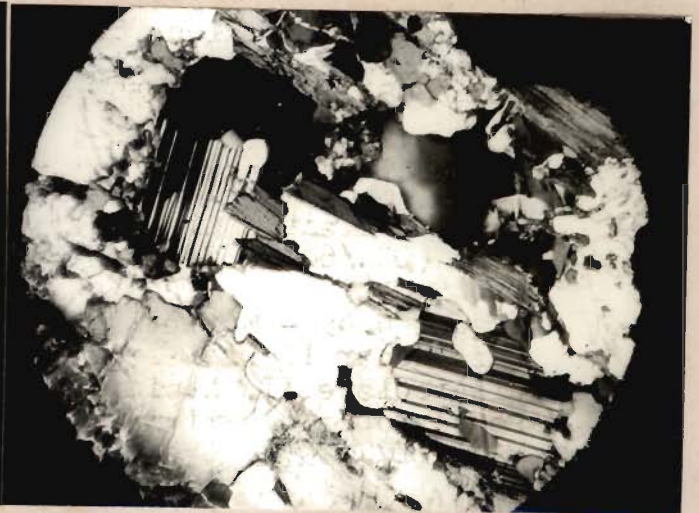
4.40



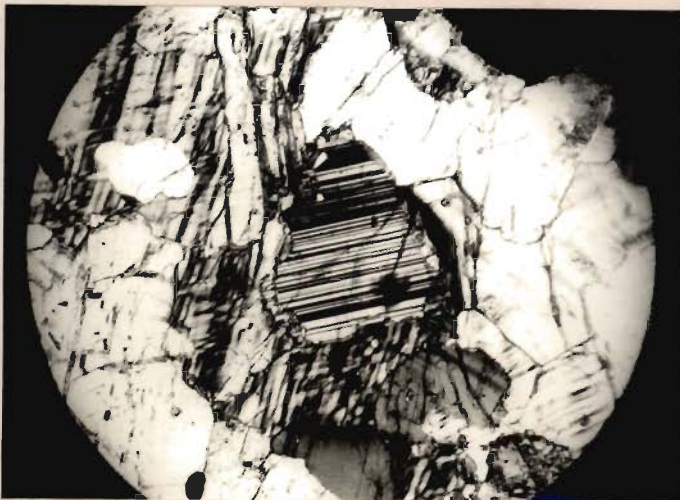
4.41



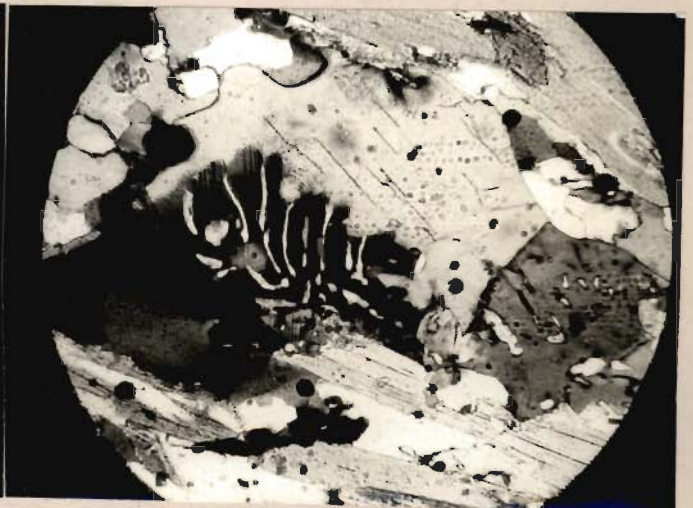
4.42



4.43



4.44



4.45

crenulation foliation, S_3 , clearly indicate its post- S_{2a} development unrelated to the transposition of earlier foliation in the thrust zone (Fig. 4.42).

Quartz occupies the intergranular spaces between chloritized biotite flakes and shows straight to curved margins meeting at triple junction. Most quartz grains are elongate and bounded by chlorite flakes which impart preferred orientation to quartz (Fig. 4.42). The grains show straight to very mild undulose extinction, and helicitic texture with chlorite flakes as inclusions indicating main growth and recrystallization of quartz even after the D_3 deformation.

4.3.3 Igneous derivatives:

(i) Pegmatite: Greyish white to light grey, medium to coarse grained pegmatite contains small books of muscovite and biotite. The other mineral constituents are plagioclase, microcline, perthite, quartz, tourmaline with smaller amount of apatite and zircon.

Plagioclase ranges in composition from albite to oligoclase which is sometimes sericitized along twins and fractures. At times, the twin lamellae are deformed and associated fractures are filled up by quartz. Varying amount of microcline is marked of perthitic and myrmekitic intergrowths. Its grains protrude either into the plagioclase or show intergrowth with the latter indicating a simultaneous crystallization of two minerals for certain period of time. At times, microcline grains

are fractured which are filled in by quartz which has grown after the formation of feldspar.

Muscovite and biotite occur as large flakes and least strained. These occupy quartz-feldspar boundaries and also protrude into them, indicating a last phase crystallization of mica.

Sch~~or~~l~~ite~~ is buff coloured and is closely associated with quartz-feldspar portion as streaks, probably reflecting the flow direction of the anatectic melt associated with the pneumatolytic activity in the area.

(ii) Amphibolite: Thin bands of amphibolite are associated with the Suki Group only in the Yamuna Valley section, whereas no exposure of the amphibolite has been recorded in the Bhagirathi Valley. The rock is dark green, fine to medium grained, compact and shows variation in the development of foliation. Hornblende prisms show kinking due to D_3 deformation. At places, amphibolite exhibits banded appearance due to alternate layers of actinolitic hornblende and quartz or quartz-feldspar. Amphibolite consists of hornblende, quartz, chlorite, biotite, sphene, clinozoisite or epidote, ilmenite and apatite. The preferred orientation of amphibole prisms impart nematoblastic foliation to the rock. Their microscopic characters resemble to a great extent with the amphibolites belonging to the Garhwal and the Bhatwari Groups.

Actinolitic hornblende form the dominant constituents of the rock. Rarely, porphyroblastic green hornblende is

wrapped by actinolitic hornblende along the foliation, S_2 . Hornblende contains inclusion of quartz and opaques along the fractures and margins. At times, the actinolitic hornblende shows the development of biotite or chlorite along the fractures, cleavages and margins. Some of the actinolitic hornblende retrogrades into clinozoisite or epidote.

Quartz is mainly post-tectonic in origin, as it is unstrained having with straight to curved margins. It occupies the intergranular spaces between actinolitic hornblende prisms suggesting that it could be possibly forming a part of the material introduced during migmatization. Plagioclase is mainly occurring as a part of the matrix and is closely associated with quartz. Fine grained plagioclase grains are sericitized and makes their identification difficult. However, there are a few fresh grains of albite which appears to have recrystallized in the late phase. Smaller amount of biotite has formed at the contact of quartz-feldspar with amphibole and seems to be the reaction product of these minerals.

Subhedral grains of sphene are closely associated with ilmenite, which occurs at the margins or in intergranular spaces between hornblende. Ilmenite rarely shows alteration to leucoxene. At places, ilmenite is rimmed around sphene indicating that sphene could have been formed due to the reaction of ilmenite with lime (Ca molecule), liberated during the production of hornblende from the original pyroxene (Wideman, 1934).

(iii) Porphyroblastic migmatite: The porphyroblastic migmatite represents the highest degree of migmatization in the area and is well exposed around Suki and Yamnotri. It is light to dark grey, medium to coarse grained, compact and foliated. Feldspar and quartz porphyroblasts of varying dimensions have grown due to the infiltration of anatectic melt along the foliation planes. The porphyroblastic migmatite could be further classified into foliated, banded and augen varieties depending upon the megascopic characters of the neosome and paleosome.

Under the microscope, the rock exhibits porphyroblastic texture with distinct foliation. Quartz, plagioclase, microcline, biotite and muscovite are the main constituents with lesser amount of apatite, zircon, tourmaline (schrolite), sphene, rutile, garnet and kyanite.

Quartz occurs both as fine grained mass and as porphyroblasts. At times, quartz porphyroblasts are randomly fractured and show undulose extinction. Minute grains of quartz also occurs as inclusion in feldspar and mica. Quartz grains show sutured, curved and straight margins indicating their syn- to post-tectonic growth. It also forms myrmikitic or graphic growth with feldspar.

Oligoclase or albite occurs as porphyroblasts and contains euhedral grains of apatite, sphene, zircon tourmaline and biotite. Some of oligoclase or albite porphyroblasts are strained and slightly sericitized, but most of the grains are fresh. In general, porphyroblastic growth is synkinematic

along the foliation, S_2 , (Fig. 4.43) and represent second phase of migmatization of the Central Crystallines (chronology of migmatization with reference to the Bhatwari Group).

Microcline (potassic feldspar) forms the dominant constituent in most of the thin sections and occurs mainly as porphyroblasts. In general, it protrudes or encloses the plagioclase suggesting that it has crystallized after the formation of plagioclase (Fig. 4.44). However, certain microcline grains show intergrowth with plagioclase probably suggesting their simultaneous growth. The above behaviour of plagioclase and microcline suggest that the microcline started crystallizing when the plagioclase growth was just ending. At places, potash feldspar reveals myrmekitic intergrowth with sodic plagioclase at contacts (Fig. 4.45). Microcline porphyroblasts contains inclusions of apatite, tourmaline, zircon and biotite. Some of the microcline grains are fractured and the fractures are filled up with quartz and biotite of late stage. Some of the microcline grains show perthitic in character. It is therefore evident that the migmatites from the Suki Group reveal an earlier sodic phase followed by a potassic phase of migmatization which corresponds to the migmatization II of the Bhatwari Group, while there is no evidence of the migmatization I in the Suki migmatites.

Biotite I is yellowish brown and defines the most prominent foliation, S_2 . It also occurs as inclusions within the feldspar suggesting that biotite I has formed earlier to feldspar (Fig. 4.42). Biotite I is being replaced by quartz

and also contains inclusions of latter along the intergranular spaces. Biotite II is reddish brown and occurs inclined to S_2 -foliation. Some of the biotite grains contain inclusions of apatite, zircon, rutile and epidote. Muscovite occurs in smaller amount and show similar character as biotite. Biotite and muscovite flakes are often interlayered.

4.4 STUDIES OF FELDSPAR

Feldspar rich portions were separated from 12 samples of augen and porphyroblastic migmatites belonging to the Bhatwari and Suki Groups and were reduced to -100 to +120 mesh size by diamond and then agate mortars. After scanning through binocular microscope it was found that crushed fraction contains 10-15% impurities of quartz, biotite, tourmaline, iron oxide etc. which were removed by Frantz-Isodynamic magnetic separator by adjusting a forward slope of 15° and side tilt of 25° (Hutchison, 1974). Iron oxides and biotite were removed by applying a current of 0.2 amp and 0.4 amp respectively, while tourmaline required a current of 0.6 amp. The feldspar fraction was obtained at 0.8 amp and 12 amp current when a purity of 93 - 95% was obtained. The purified feldspar samples were further reduced to +170 mesh and an angular standard (AR, NaCl) of about 15% of the sample (200 mg) was added to check the shift correction. After thoroughly mixing with pastle agate mortar, these fractions were subjected to X-ray diffraction under the following specifications.

$2\theta \text{ CuK}\alpha = 13^\circ \text{ to } 40^\circ \text{ (upto } 43^\circ \text{ in few samples)}$

Scanning speed = $1/2^\circ/\text{minute}$

Chart speed = 0.5 cm/minute

Rate meter = 1000 C.P.S.

Time Constant = 2 sec.

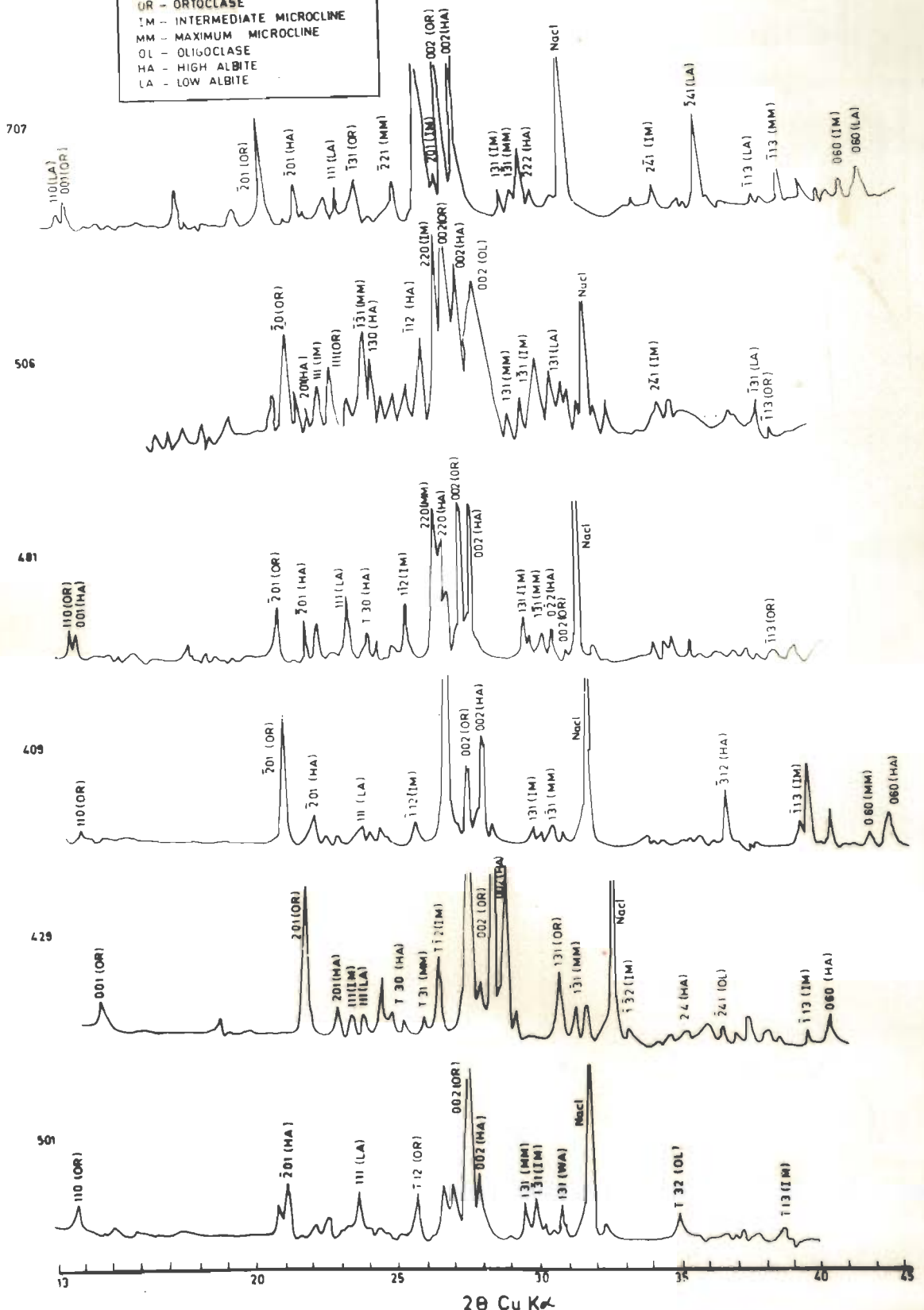
The study was carried out to know the composition of feldspars and their structural state, as emphasized by Goldsmith and Leaves (1954), Orville (1967), Wright and Stewart (1968) and Barth (1969).

The X-ray diffractograms of the Bhatwari Group migmatite (Fig. 4.46) reveal that the composition of K-feldspar varies from orthoclase (OR) to intermediate microcline (IM) with some reflection peaks of maximum microcline (MM). The plagioclase is mainly characterized by high albite (HA) with a few peaks of low albite (LA). Single reflection peak of oligoclase (OL) is present in sample nos. 429, 501, and 506.

On the other hand, the X-ray diffractograms of the Suki Group migmatite (Fig. 4.47) show that the composition of K-feldspar ranges from intermediate to maximum microcline (IM to MM). Orthoclase (OR) has been recorded only in sample no. 592. Plagioclase ranges in composition from high albite (HA) to oligoclase (OL) with a few reflection peaks of low albite (LA). The variability in the composition of K-feldspar indicates that it has suffered polymorphic transformations, which could have taken place comparatively at high temperature (Mehnert, 1968). The presence of (002) and (111) reflection peaks in

SYMBOLS

OR - ORTOCLASE
 IM - INTERMEDIATE MICROCLINE
 MM - MAXIMUM MICROCLINE
 OL - OLIGOCLASE
 HA - HIGH ALBITE
 LA - LOW ALBITE



2θ Cu Kα

FIG-446-X-RAY DIFFRACTOGRAM OF FELDSPAR SEPARATED FROM THE BHATWARI GROUP MIGMATITE

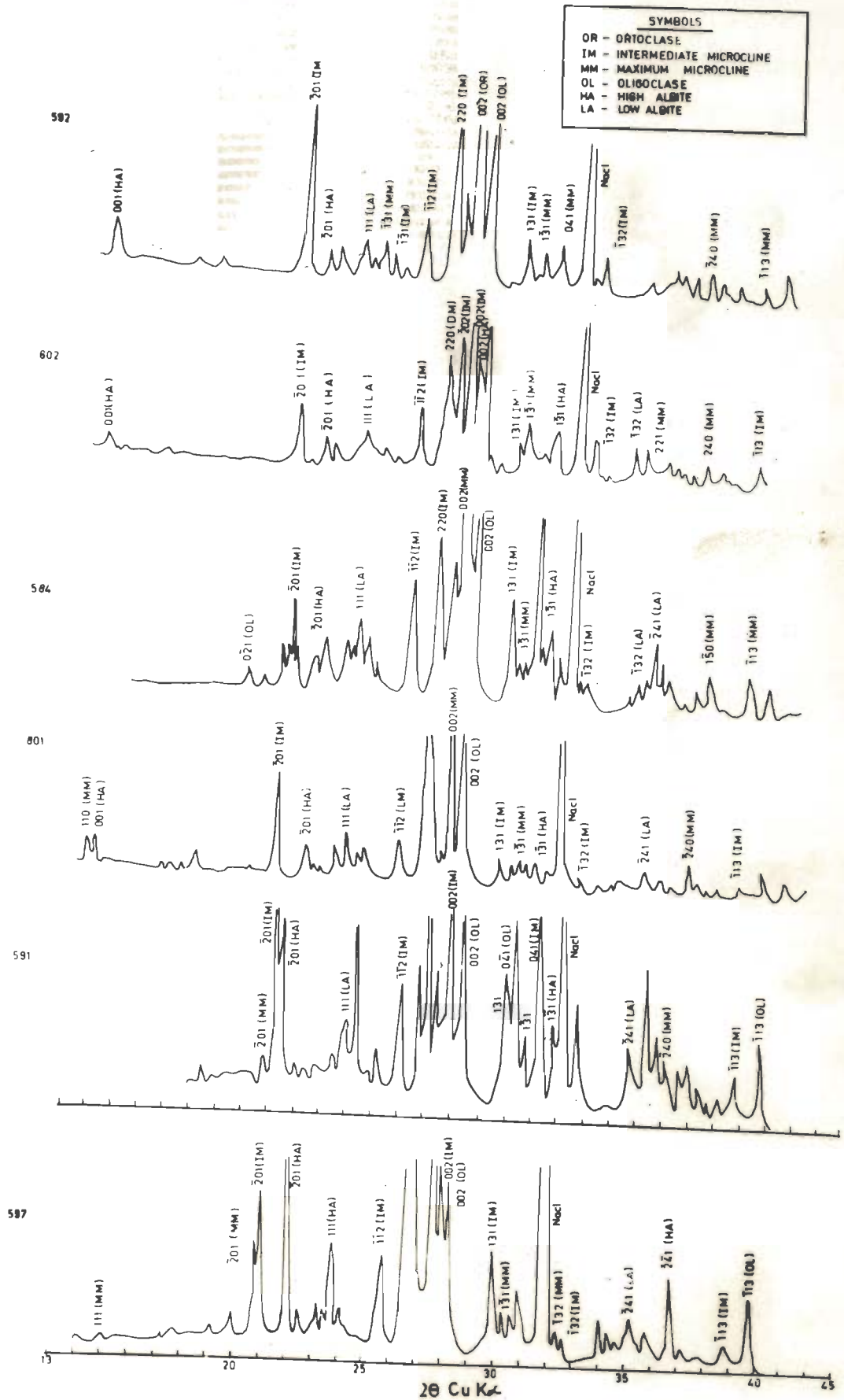


FIG. 4.47-X-RAY DIFFRACTOGRAM OF FELDSPAR SEPARATED FROM THE SUKI GROUP MIGMATITE

albite (HA and LA), besides other diagnostic reflections in the diffractograms (Fig. 4.47) confirm the perthitic nature of the K-feldspar.

4.4.1 Triclinicity:

Goldsmith and Leaves (1954) found that monoclinic K-feldspar shows single reflection peak (131), whereas in triclinic feldspar it resolves into two reflection peaks (131, $1\bar{3}1$). On the basis of $2\theta(131)$ and $2\theta(1\bar{3}1)$, he proposed a scale for the computation of triclinicity (Δ) in K-feldspar, which can be expressed as

$$\Delta = 12.5 (d_{131} - d_{1\bar{3}1})$$

The triclinicity tends to be one in fully ordered K-feldspar (maximum microcline) and Δ tends zero in fully disordered feldspar (orthoclase).

Some of the authors have tried to correlate triclinicity with the petrogenesis of granitic rocks (Dietrich, 1962; Nilssen and Smithson, 1965; Bedi and Prasad, 1978). Taking this into consideration, $2\theta(131)$ and $2\theta(1\bar{3}1)$ reflections were carefully noticed in the diffractograms and triclinicity was computed for the K-feldspar (Table 4.3). The triclinicity (Δ) value in the Bhatwari Group migmatite varies from 0.400 to 0.675 and in case of the Suki Group migmatite from 0.463 to 0.662. Since comparatively large deviation in the value of Δ has been recorded only in a few samples (No.707, 501 of the Bhatwari Group migmatite and No. 567 of the Suki Group

migmatite), therefore it can be generalized that the entire area was probably in the same temperature regime at some time in its orogenic history. Comparatively low values of triclinicity in the K-feldspar of migmatites of the Bhatwari and Suki Groups could be due to comparatively rapid cooling of the anatectic melt (Chapter VI)

TABLE 43 : TRICLINICITY IN K-FELDSPAR SEPARATED FROM MIGMATITES

BHATWARI GROUP

Sample No./ d-value	707	506	481	409	429	501
d_{131}	2.995	3.002	2.997	3.018	3.001	2.991
$d_{\bar{1}\bar{3}\bar{1}}$	2.960	2.957	2.951	2.964	2.958	2.959
Δ	0.438	0.563	0.575	0.675	0.537	0.400

SUKI GROUP

Sample No./ d-value	592	602	584	801	591	597
d_{131}	3.005	2.998	3.001	2.999	2.988	2.997
$d_{\bar{1}\bar{3}\bar{1}}$	2.959	2.945	2.945	2.953	2.947	2.960
Δ	0.575	0.662	0.575	0.575	0.513	0.463

$$\text{Triclinicity}(\Delta) = 12.5 (d_{131} - d_{\bar{1}\bar{3}\bar{1}})$$

CHAPTER V
GEOCHEMISTRY OF AMPHIBOLITE

The problem of distinguishing ortho from para amphibolites in a regionally metamorphosed terrain is of great interest to petrologists, because these play an important role in understanding the tectonic history of the area. Geological setting, field characters, megascopic and petrographic characters of amphibolites from the Central Crystallines of the present area have been detailed earlier in Chapters 2 and 4. In the present chapter, geochemistry of amphibolites and related rocks has been described with an aim to decipher their progenitor, depth and source of magma and a petrogenetic model because little information is presently available for the widespread amphibolites associated with the Central Crystallines.

5.1 ANALYTICAL TECHNIQUES

5.1.1 Major Elements

The major elements were determined following rapid analysis scheme of Shapiro (1975) for silicate rocks with suitable modifications to suit the available laboratory facilities. Estimation of various elements was done by using a series of synthetic standards of different concentrations of A.R. Grade chemicals. The values of Na_2O and K_2O were determined with the help of flame photometer. Silica, alumina, total iron, manganese, titanium and phosphorous were determined calori-

metrically, SiO_2 was estimated by molybdenum blue method and alumina by using alizarian red-S complex. Total iron ($\text{FeO} + \text{Fe}_2\text{O}_3$) was estimated as ferriin complex using ortho-phenanthroline. The estimation of manganese was done by oxidising it to permanganate by ammonia persulphate with silver nitrate as catalyst. P_2O_5 was determined by molybdovanadophosphoric acid complex. TiO_2 was estimated by Tiron complex.

Ferrous iron (FeO) was determined by titration with a standard dichromate solution using sodium diphenylamine sulphonate as indicator. CaO and MgO were estimated titrimetrically by EDTA using screened calcein and O-cresolphthalin indicators. The amount of H_2O in the rock samples was estimated by using sodium tungstate of reagent grades. From the various geochemical plots and geochemical parameters, magmatic nature of progenitor of amphibolite and the composition of parental magma has been established in this work.

5.1.2 Trace Elements

The trace elements can be incorporated or excluded in the structure of different minerals with greater selectivity than the major elements. The abundance and distribution of transition elements (Cr , Co , Ni , Cu , Zn) usually provide information regarding the nature and proportions of the ferromagnesian mineral phases crystallizing out of basic magma. Since, transition elements readily enter early in ferromagnesian mineral phases, they are usually called compatible elements

(Cox et al., 1979).

The distribution of trace elements in the lattices of principal mineral phases is controlled by ionic radii and charge. The incompatible trace elements (K, Ba, Sr, Pb, P etc.) have either too large or too small radii as compared to major elements and, therefore, these are concentrated in the residual liquid (Cox et al., 1979). The behaviour and abundance of incompatible elements are significant in study of magmatic processes because their ratios with very low mineral/melt distribution coefficient (K_d) remain approximately constant during fractional crystallization. The incompatible elements are characterized by K_d value < 1 , whereas, in case of compatible elements K_d is > 1 (Cox et al., 1979).

The estimation of trace elements was made with the help of atomic absorption spectrophotometer (Model IL 751, AA/AE, 1978). The concentration of Co, Ni, Sb, Bi, Mo, Cd, Pb, Zn, Cu, Sr and Li was determined by absorption mode and Ba by emission mode.

5.2 RESULTS

Twelve samples of amphibolites and one sample of meta-andesite of the Bhatwari Group were chemically analyzed for their major oxides and trace elements (Tables 5.1, 5.2). On the basis of major oxides, Niggli values (Table 5.3), cation percentage (Table 5.4) and other relevant geochemical parameters have ^{been} computed (Table 5.5).

TABLE 5.1 CHEMICAL ANALYSIS OF AMPHIBOLITES AND META-ANDESITE

Sample No./ Oxide	525	508	457	543	417	517	411	474	436	567	456	541	756
SiO ₂	54.50	51.70	46.62	47.50	48.05	49.55	51.50	52.60	49.50	51.50	49.55	60.5	52.20
Al ₂ O ₃	13.34	13.35	16.40	16.18	14.11	15.23	13.42	15.55	14.45	14.82	14.24	14.53	12.40
Fe ₂ O ₃	1.38	1.80	1.62	0.78	1.57	1.11	1.51	1.58	1.48	1.10	0.84	0.85	0.85
FeO	8.05	7.73	8.41	11.76	7.16	7.91	9.30	8.43	10.34	9.25	10.05	7.15	10.62
MnO	0.16	0.17	0.18	0.17	0.12	0.17	0.16	0.14	0.18	0.15	0.20	0.27	0.16
MgO	7.25	7.16	8.75	7.16	8.67	9.70	8.76	7.56	8.45	8.39	9.18	4.12	8.28
CaO	10.09	11.43	11.91	9.85	11.56	10.20	10.58	8.29	10.70	9.50	11.12	7.25	7.45
Na ₂ O	1.52	2.12	2.44	2.54	3.37	2.02	1.65	2.15	1.01	1.68	1.86	1.52	2.02
K ₂ O	1.91	1.96	2.26	2.25	2.48	2.15	1.00	2.40	1.12	1.13	1.37	2.26	3.05
TiO ₂	0.45	1.40	0.85	1.02	1.33	0.60	0.82	0.73	1.07	1.37	0.94	0.94	1.84
P ₂ O ₅	0.27	0.23	0.25	0.28	0.37	0.35	0.26	0.35	0.24	0.26	0.28	0.28	0.27
H ₂ O	1.15	1.02	0.82	0.85	0.76	1.20	1.04	0.65	0.87	1.05	0.73	0.95	1.16

525 to 567 - amphibolite
 541 - migmatized amphibolite
 756 - meta andesite

(Analysis : The author)

TABLE 5.2 TRACE AND MINOR ELEMENTS IN AMPHIBOLITES AND METAANDESITE (CONCENTRATION IN PPM)

Sample No./ element	525	508	457	543	417	517	411	577	436	567	456	541	756
Sb	215	180	185	175	215	200	185	145	175	110	315	170	205
Bi	295	260	370	235	325	170	165	170	200	240	245	170	250
Co	94	93	92	92	93	91	93	88	92	93	91	89	96
Ni	167	121	132	119	204	113	134	179	99	121	135	137	123
Cd	8	5	6	5	9	7	7	6	6	7	6	7	9
Pb	152	105	110	130	250	165	120	125	200	135	120	105	130
Zn	256	327	183	231	224	525	281	300	367	255	245	156	298
Cu	615	870	850	930	805	440	475	910	205	475	520	315	
Sr	860	985	735	950	635	640	695	915	750	500	975	360	955
Ba	1190	1310	1395	1150	1300	1080	496	775	555	490	680	1450	1450
Li	104	128	138	232	295	161	203	370	168	276	292	130	274
Cr	118	140	89	99	111	132	130	108	133	103	101	88	83

(Analyst : The author)

TABLE 5.3 NIGGLI VALUES OF AMPHIBOLITES AND METAANDESITE

Sample No./ Niggli parameter	525	508	457	543	417	517	411	577	456	557	436	541	756
Si	136.23	122.86	97.81	105.08	105.08	106.93	118.23	127.49	112.08	113.00	106.43	239.71	119.83
al	19.64	18.70	20.27	21.08	18.18	19.36	18.14	22.19	19.27	23.17	18.02	31.81	17.30
fm	46.76	44.32	44.98	46.97	44.15	47.58	50.72	47.54	50.95	53.89	49.15	36.47	52.08
c	22.91	29.12	26.76	23.34	27.07	25.88	26.00	21.51	25.95	23.51	25.58	20.90	18.89
alk	6.69	7.86	7.98	8.62	10.60	7.18	5.13	8.76	3.83	5.42	5.75	10.83	11.72
k	0.46	0.38	0.39	0.37	0.33	0.41	0.28	0.42	0.42	0.31	0.33	0.49	0.60
mg	0.58	0.57	0.61	0.50	0.64	0.66	0.59	0.57	0.56	0.57	0.60	0.32	0.56
ti	0.85	2.51	1.34	1.70	2.19	0.97	1.42	1.33	1.82	2.38	1.52	2.63	3.28
p	0.29	0.23	0.22	0.26	0.34	0.32	0.25	0.36	0.23	0.25	0.25	0.44	0.27
qz	9.47	-8.58	-33.89	-29.4	-37.32	-21.79	-2.29	-7.55	-3.24	-2.68	-16.5	96.39	-27.05

TABLE 5.4 CATION PERCENT AMPHIBOLITES AND META-ANDESITES

	525	508	457	543	417	517	411	577	436	567	456	541	756
Si	51.56	50.63	42.91	44.33	44.38	45.92	48.51	48.93	47.10	49.30	46.02	58.87	57.47
Al	14.85	15.38	17.76	17.77	15.33	16.60	14.87	17.01	16.17	16.69	15.62	15.60	13.67
Fe ³⁺	0.98	1.32	1.12	0.55	1.09	0.77	1.07	1.10	1.06	0.79	0.53	5.82	0.60
Fe ²⁺	6.35	6.31	6.45	9.14	5.51	6.11	7.30	6.53	8.20	7.38	7.81	5.44	8.30
Mn	0.13	0.14	0.138	0.13	0.09	0.13	0.13	0.11	0.31	0.12	0.15	0.05	0.13
Mg	10.29	10.52	12.08	10.02	12.01	13.48	12.38	10.55	12.06	12.06	12.84	2.91	11.64
Ca	10.23	11.99	11.75	9.85	11.44	10.13	10.68	8.26	10.91	9.74	11.11	5.14	7.48
Na	2.78	4.02	4.35	4.59	6.02	3.63	3.01	3.87	1.86	3.11	3.35	2.68	3.67
K	2.30	2.45	2.66	2.68	2.93	2.54	1.20	2.85	1.36	1.38	1.62	2.63	5.56
Ti	0.32	1.03	1.59	0.72	0.92	0.48	0.58	0.51	0.77	0.98	0.65	0.65	1.29
P	0.22	0.22	0.19	0.22	0.29	0.27	0.28	0.27	0.19	0.21	0.22	0.21	0.21

TABLE 5.5 SPECIAL PARAMETERS OF THE BHATWARI AMPHIBOLITE

	525	508	457	543	417	517	411	577	436	567	456	541	756
Sugimura Index(θ)	38.47	31.95	28.09	28.25	20.65	32.12	38.21	34.05	40.15	38.86	34.58	+1.52	18.72
Larsen Index	-1.03	-3.18	-6.87	-2.42	-5.73	-5.76	-5.69	+0.35	-5.91	-3.99	-6.99	+8.66	+0.85
Discriminating function (X)	+1.58	+4.04	+3.64	+6.42	+2.98	+1.63	+1.95	+0.50	+3.22	+3.51	+4.22	+0.24	+4.48
$\text{Fe}_2\text{O}_3/\text{FeO}$	0.17	0.23	0.19	0.067	0.22	0.14	0.16	0.19	0.14	0.12	0.09	0.19	0.08
Mg. No.	58.25	57.79	61.30	50.71	64.37	66.03	59.45	57.85	56.45	59.26	60.32	48.3	44.29
Oxidation ratio	13.18	17.29	14.78	5.64	16.50	11.21	12.84	14.45	11.44	9.68	7.0	9.67	6.69
Ba/Sr	1.38	1.33	1.90	1.21	2.05	1.69	0.71	0.85	0.74	0.98	0.70	1.51	1.52
Sr/Ba	0.72	0.75	0.53	0.83	0.49	0.59	1.40	1.18	1.35	1.02	1.43	0.66	0.66
K/Sr	26.74	24.87	36.19	28.21	46.14	39.69	17.27	31.15	18.13	27.60	16.61	28.64	38.42
K/Ba	19.32	18.70	19.07	23.30	22.54	23.52	24.19	36.97	34.50	20.18	23.82	18.96	21.03
Ca/Sr	118.95	121.73	159.86	103.68	180.16	158.28	153.67	90.27	145.47	194.80	113.95	76.98	78.64

5.2.1 Magmatic Nature of Progenitor:

The magmatic nature of the progenitor of these amphibolites has been deciphered mainly on the basis of chemical plots using Niggli values, discriminatⁿ function 'X' of major oxides (Shaw and Kudo, 1965) and Orville's model (1969). All the inferences drawn from various chemical plots are based on the presumption that these amphibolites have been least effected by the secondary processes. This presumption is not out of place in view of the discussion which follows:

The Niggli mg-c plot (Fig. 5.1) clearly depicts the position of various pelite-limestone mixtures and igneous rocks. All the amphibolites from the Bhatwari Group occupy the position of middle differentiate of Karroo dolerite trend (igneous trend in fig. 5.4), as given by Leake (1964). The above plot suffers from a draw back of having overlapping, because both para- and ortho-amphibolites are mineralogically identical (mainly comprising hornblende and plagioclase, a characteristic of basaltic magma). The plot of Niggli c against (al-alk) is more significant, because it shows the field of igneous rocks and all possible combinations of different sedimentary rocks, which can result into para-amphibolites (Fig. 5.2). In this, central part is quite inconclusive for distinction between ortho- and para-amphibolites of similar composition. However, the 'ortho' or 'para' nature of the amphibolites can be best elucidated within this field by means of different trends of sedimentary and igneous rocks. It is clear that all the points

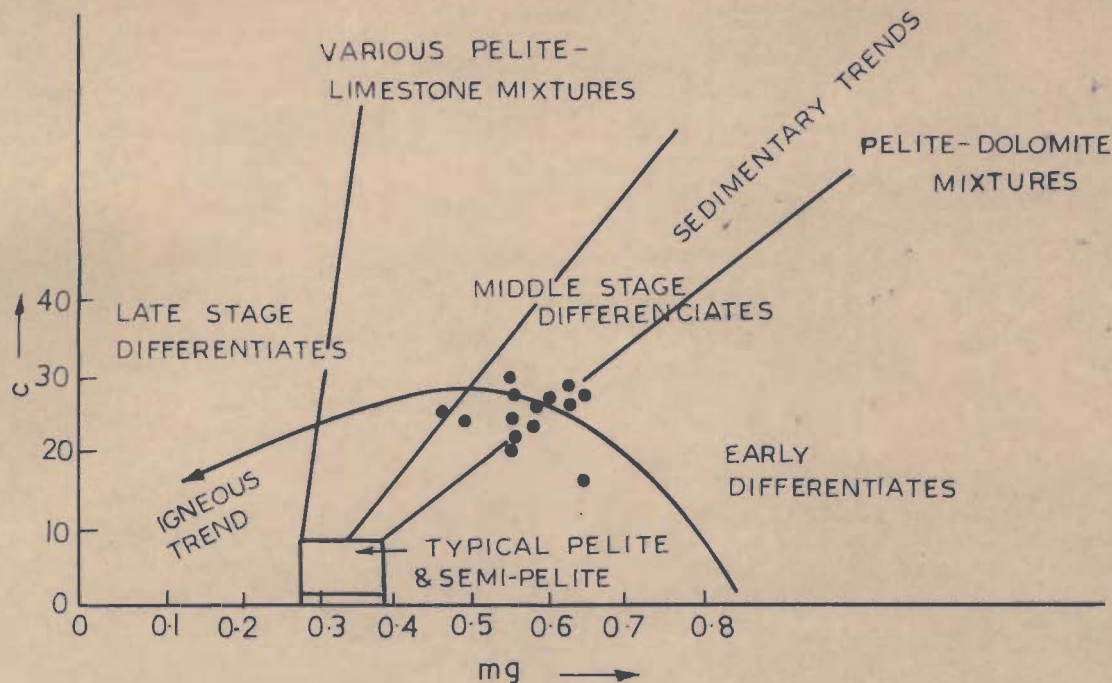


FIG. 5-1-NIGGLI mg VERSUS c PLOT FOR BHATWARI AMPHIBOLITE. TREND LINE OF KARROO DEOLERITES (IGNEOUS TREND), AFTER LEAKE (1964).

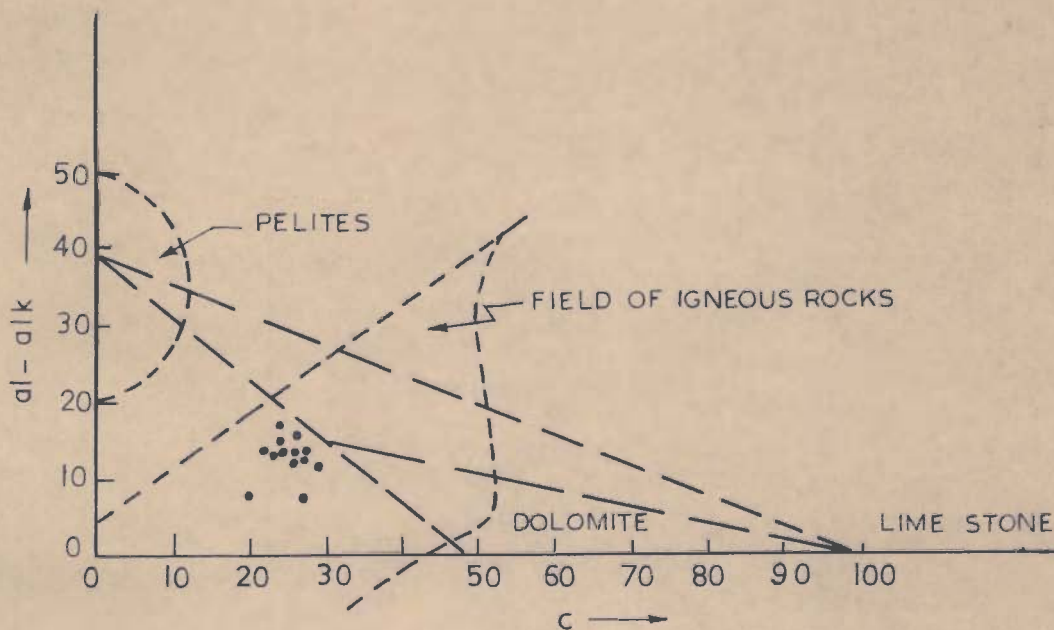


FIG. 5-2-NIGGLI c VERSUS (al - alk) PLOT FOR BHATWARI AMPHIBOLITE. DIFFERENT COMPOSITIONAL FIELDS ARE AFTER KAMP (1964).

representing these amphibolites fall well within the field of igneous rocks.

A triangular plot of the Niggli values c , (al-alk) and mg indicates that the Niggli values of amphibolites from the studied area fall near the igneous trend given for Karroo-dolerites (Leake, 1964). Some points show scatter, which might be due to the later effects of non-magmatic processes (Fig. 5.3).

Shaw and Kudo (1965) have used discriminant function 'X', computed on the basis of major oxides percentages ($X = 7.07 \log \text{TiO}_2 + 1.91 \log \text{Al}_2\text{O}_3 - 3.29 \log \text{Fe}_2\text{O}_3 + 8.48 \log \text{FeO} + 2.97 \log \text{MnO} + 4.81 \log \text{MgO} + 7.80 \log \text{CaO} + 3.92 \log \text{P}_2\text{O}_5 + 0.15 \log \text{CO}_2 - 15.08$), for distinguishing ortho- and para-amphibolites. Although they are of the opinion that the discriminant function may not be applicable to amphibolites of other areas of different ages, results obtained for amphibolites of the Bhagirathi Valley show a remarkable distinction between ortho- and para-amphibolites. Most of the samples have positive values from 0.24 to 6.42, hence these amphibolites are probably derivatives of igneous rocks.

Orville (1969) proposed a model in the form of ACF diagram, which demarcates the approximate positions of basic igneous rocks and carbonate rocks. The ACF plot for these amphibolites fall well within the field of basic igneous rocks, except the migmatized amphibolite which lie just near the outer-margin (Fig. 5.4)

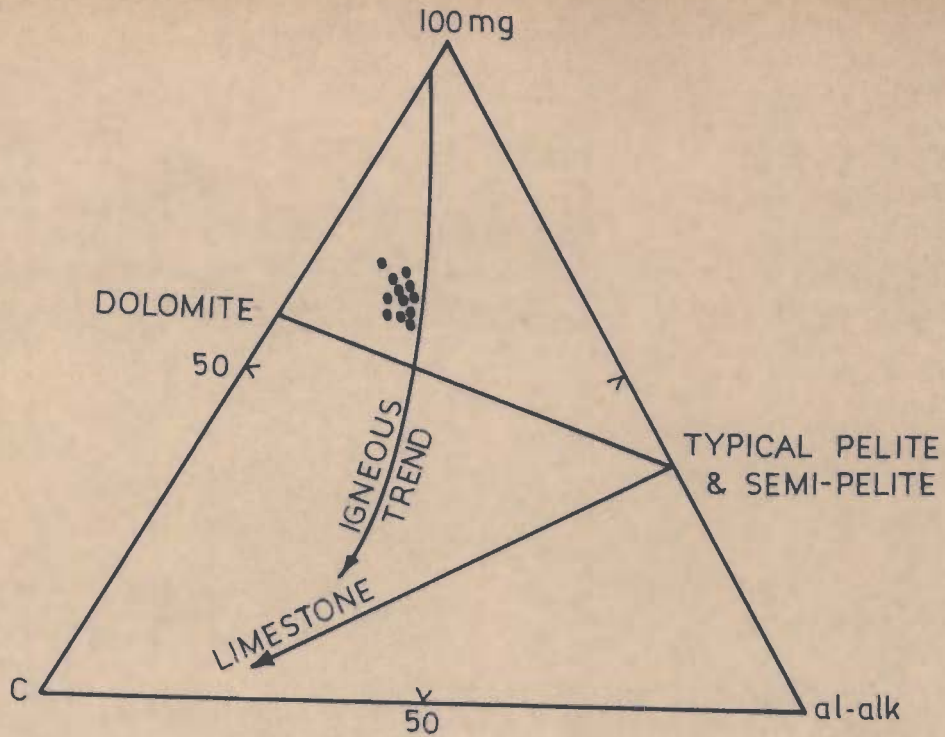


FIG. 5.3 - NIGGI VALUES, mg-c-(al-alk), VARIATION DIAGRAM (AFTER LEAKE, 1964) FOR THE AMPHIBOLITES OF THE AREA

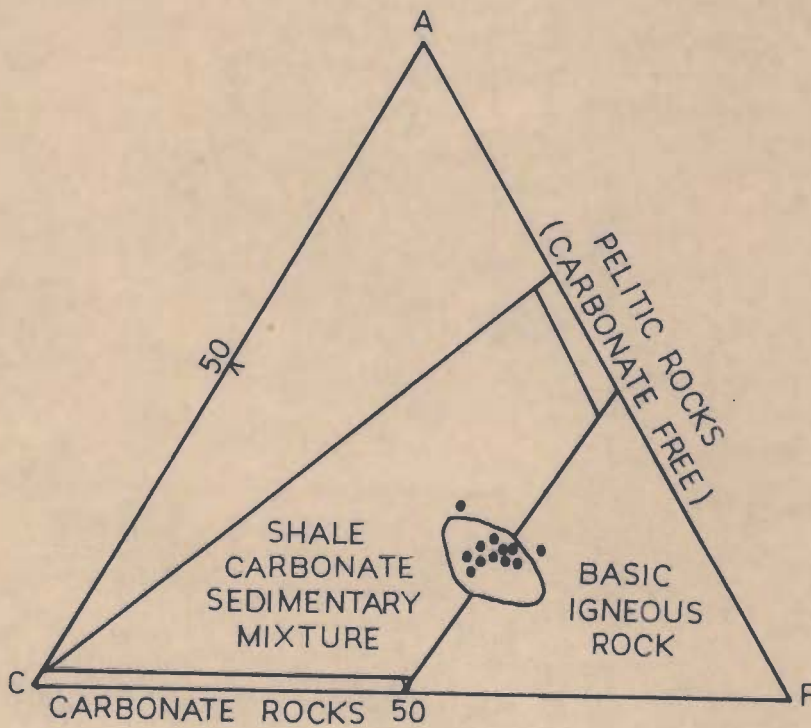


FIG. 5.4-ACF PLOT SHOWING COMPOSITION FIELD OF BASIC IGNEOUS ROCKS AND OTHER SEDIMENTARY MIXTURES (AFTER ORVILLE, 1969) POSITION OF THE BHATWARI AMPHIBOLITES IS SHOWN BY SOLID CIRCLES

Several diagrams have been used for plotting data such as Si vs. (al + fm) - (c + alk) and $(\text{FeO} + \text{Fe}_2\text{O}_3)/(\text{FeO} + \text{Fe}_2\text{O}_3 + \text{MgO})$ (after Prasad et al., 1980). These diagrams are not shown here because these broadly confirm the findings that the amphibolites of the area are derivatives of basic igneous rocks.

5.2.2 Composition of Progenitor

The modified Larsen index, $(1/3 \text{ Si} + \text{K}) - (\text{Ca} + \text{Mg})$ for these amphibolites shows variation from -6.99 to +0.35 (Table 5.5). Larsen index is comparatively higher in migmatized amphibolite (+8.66). Carmichael (1964) has studied the volcanics of Iceland and classified them on the basis of this index as given below:

Larsen index	Composition
- 4.0	Olivine tholeiites
- 4 to 0	Tholeiites
1 to 9	Basaltic andesites and ice-landites
12 to 14	Rhyolites

The values of Larsen index in the present case (except sample no. 541) reveal that the parental magma was tholeiitic in character. Sample no. 541 shows a bulk composition of andesite and is affected by migmatization thereby showing large deviation.

A plot between cation percentages against Larsen index was attempted (not shown here). Although the variation trends clearly depict magmatic source of these rocks and indicates a nearly continuous differentiation of the parental basaltic magma, the points were scattered bearing testimony to the metamorphic and metasomatic changes.

Niggli mg vs. k, p, ti and alk plot exhibits good resemblance with Karroo dolerites (Leake 1964). The clustering habit of k, p, ti and alk within a small range of mg values (0.5 to 0.65) is a characteristic feature in the plot (Fig. 5.5). The steep to vertical slope in every case reflects a nearly progressive fractionation of the parental magma of basaltic affinity.

A persual of Niggli values reveals a slight general decrease in alk, c, mg values and increase in fm values with the increase of Si (Table 5.2). However, it has been noticed that alk, c and al show sympathetic behaviour, whereas fm exhibits antipathic behaviour. The migmatized amphibolite shows increase in al and alk values and decrease in fm and c with the increase in Si. The parental source of these amphibolites can be identified from the values of alk between 3.83 to 10.60, which is usually given for basaltic rocks. The alk values, given in literature for typical spilites, range between 12.50-16.00 (Eskola, 1937) or between 9.15-13.50 (Ehris, 1964), while Vuagnant (1949) considered it to be 16.50. The alk values for keratophyres are considerably higher. Since alk values for most of the

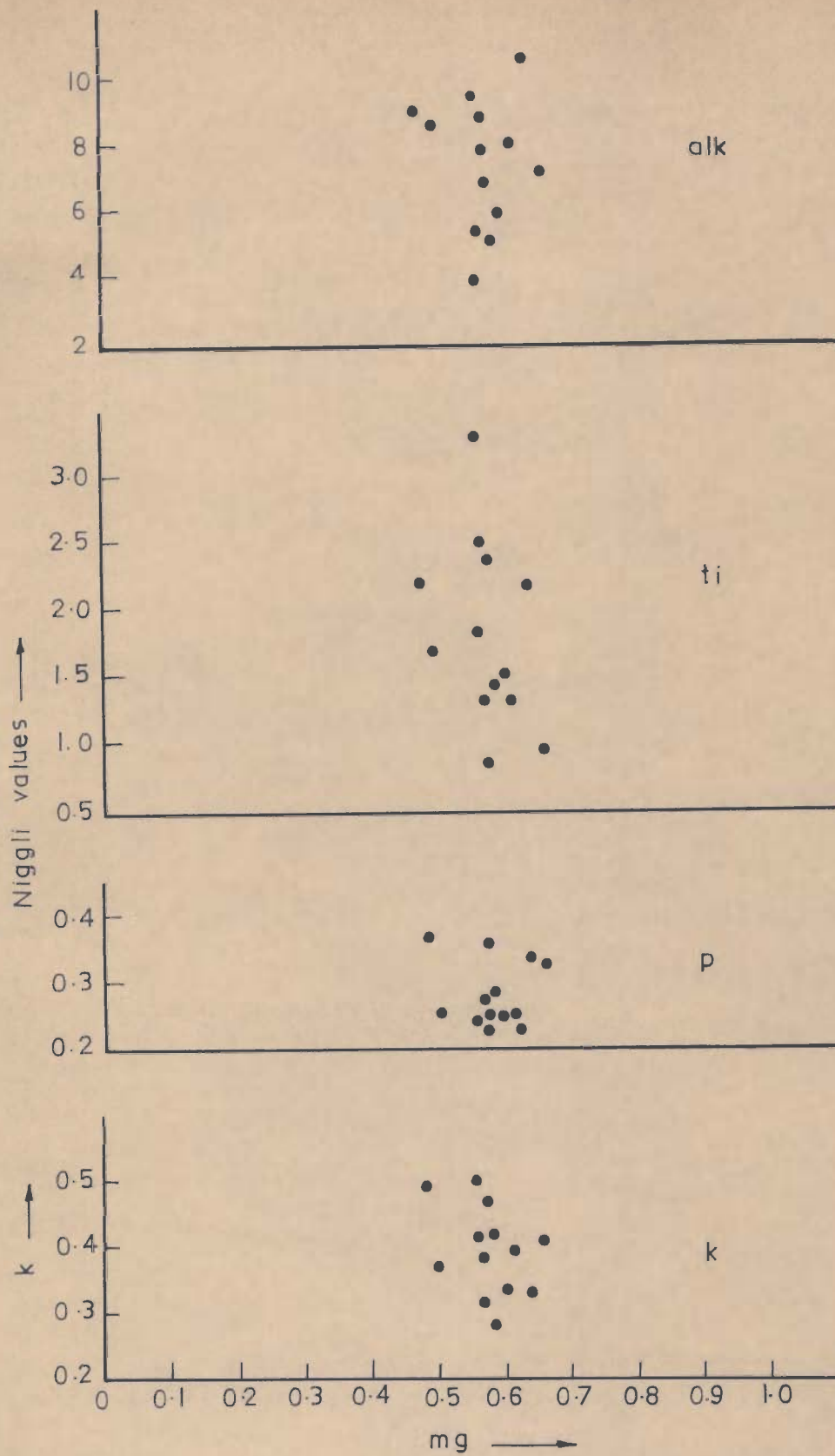


FIG. 5-5 - NIGGLI mg VERSUS k, p, ti AND alk PLOT FOR THE BHATWARI AMPHIBOLITE

amphibolites from this area are < 9.0 , these rocks do not have any affinity with spilitic or keratophyre group.

SiO_2 vs. $\text{Na}_2\text{O} + \text{K}_2\text{O}$ plot brings out the salient subalkaline to alkaline character of parental basaltic magma (Fig. 5.6). The magmatic behaviour of the amphibolites is further substantiated by SiO_2 vs. $\text{TiO}_2/\text{P}_2\text{O}_5$ plot, which shows a definite trend from slightly acidic to basic composition of original rocks (Fig. 5,7). Most of the samples fall in the hawailite field whereas slightly acidic ones occupy the mugearite and trachyte fields.

The tholeiitic to alkalic character of the progenitor of the metabasites is also evident from CaO vs. MgO and CaO vs. Al_2O_3 plots (Figs. 5.8, 5.9). In both the diagrams, majority of the data fall well within the field of tholeiites (continental and oceanic) given by Flyod (1976) or metatholeiites (Viljoen and Viljoen, 1969). However, three samples occupy the field continental alkali basalt. Since these metavolcanics contain higher amount of K_2O , these are mainly continental tholeiites rather than oceanic tholeiites. The scatter in CaO content and behaviour of CaO against MgO indicate that CaO content has been affected by later processes and may not be the direct consequence of magmatic processes.

Kuno et al. (1957) gave the following values of $\text{Fe}_2\text{O}_3/\text{FeO}$ ratio characterising the original nature of basaltic rock series giving rise to amphibolites.

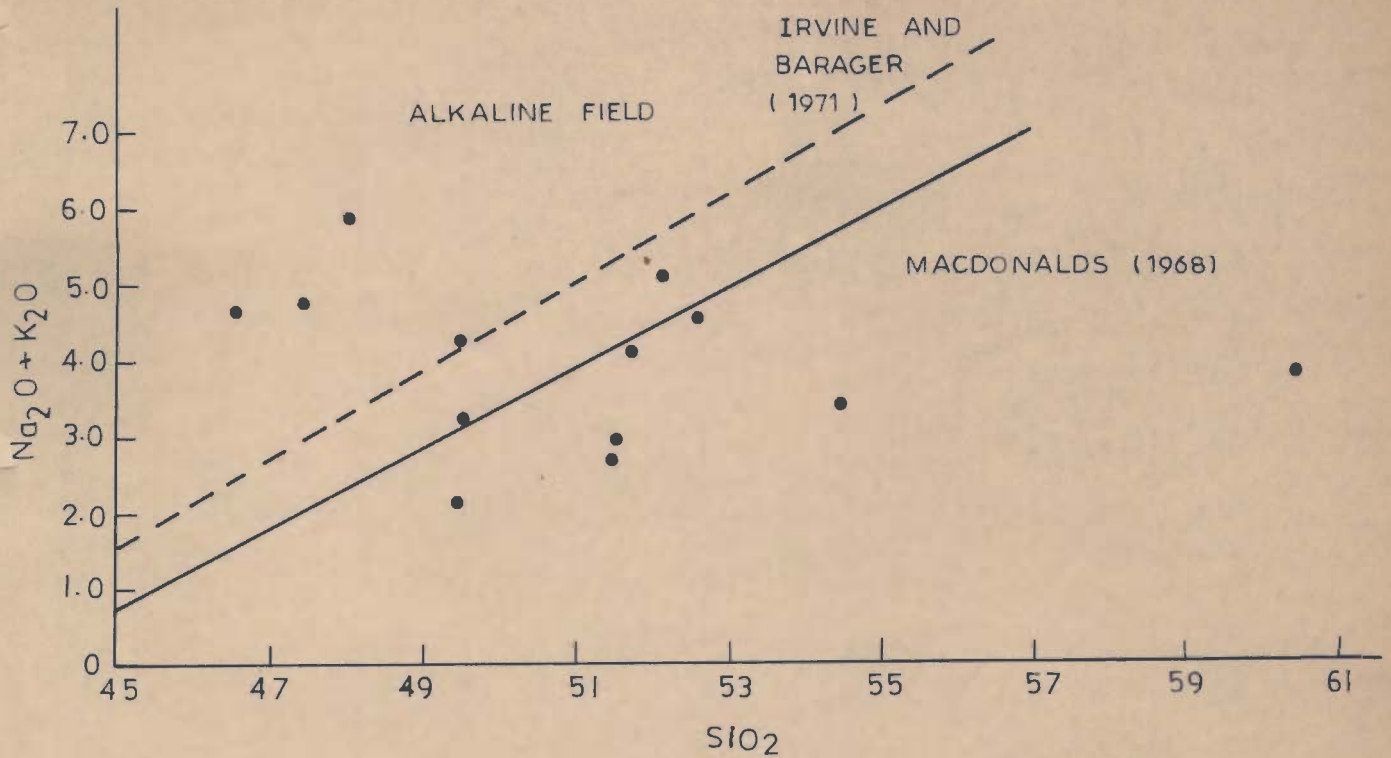


FIG. 5.6 - SiO_2 VERSUS TOTAL ALKALI PLOT FOR THE AMPHIBOLITE OF AREA. THE SEPARATION LINES BETWEEN ALKALINE AND SUB-ALKALINE FIELDS SHOWN AFTER MACDONALDS (1968) AND IRVINE AND BARAGER (1971).

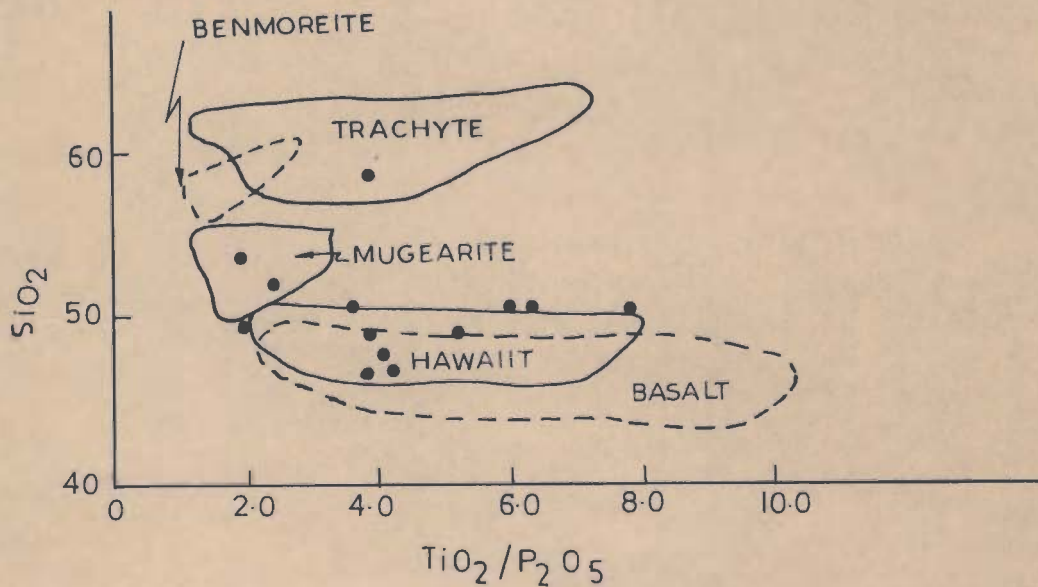
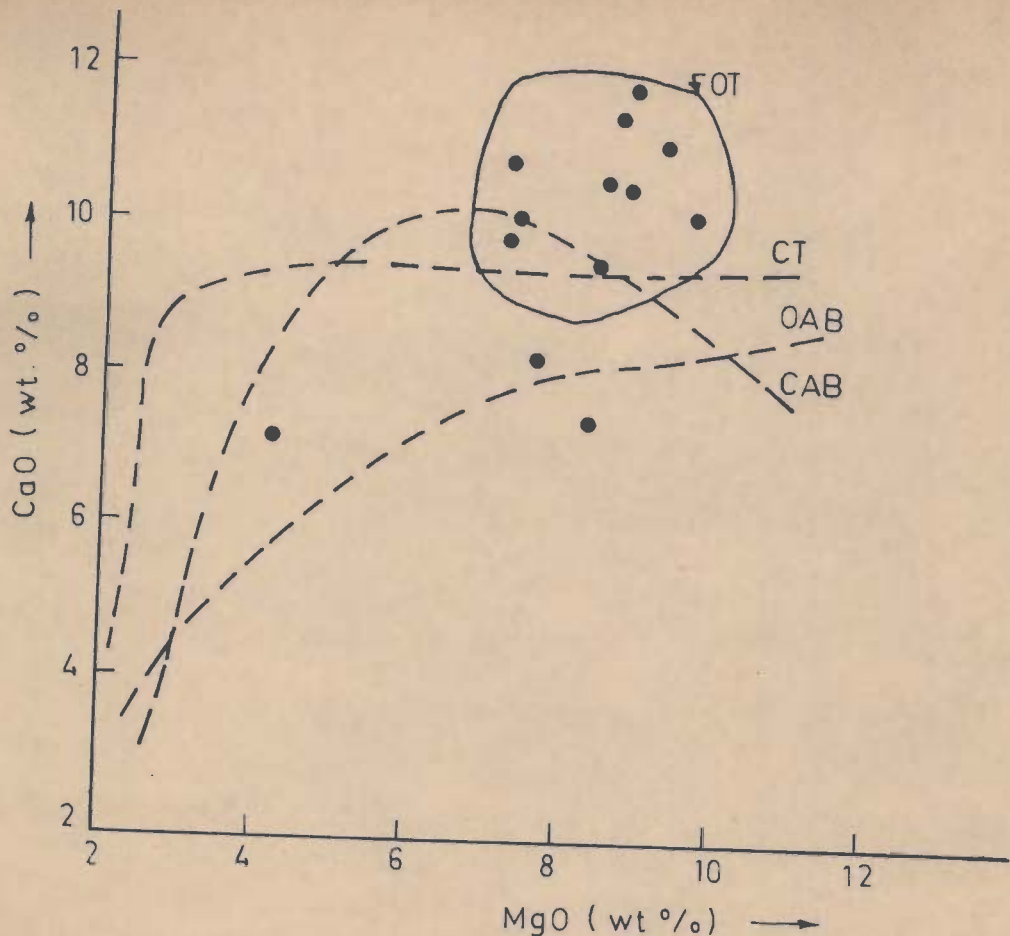
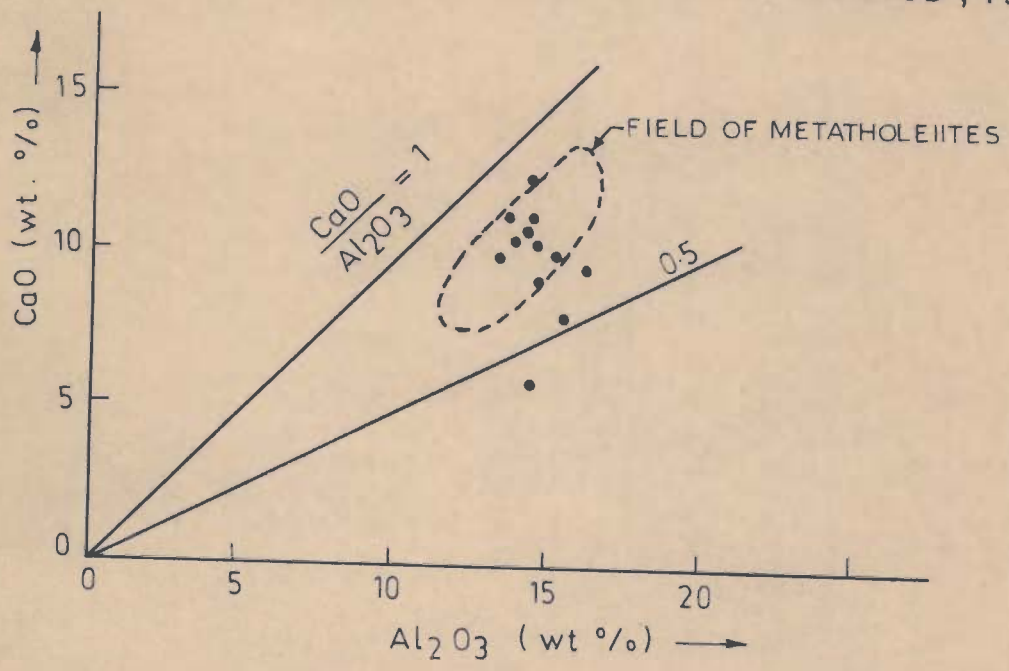


FIG. 5.7 - $\text{TiO}_2 / \text{P}_2\text{O}_5$ VERSUS SiO_2 FOR THE AMPHIBOLITE OF THE BHATWARI AREA. VARIOUS IGNEOUS COMPOSITIONAL FIELDS ARE AFTER FLYOD (1976).



5.8 - MgO VERSUS CaO PLOT FOR THE AMPHIBOLITES OF THE BHATWARI AREA. OT, CT, OAB AND CAB REPRESENT THE FIELDS OF OCEANIC THOLEIITES, CONTINENTAL THOLEIITES, OCEAN ALKALI BASALT AND CONTINENTAL ALKALI BASALT (AFTER FLYOD, 1976).



5.9 - Al₂O₃ VERSUS CaO DIAGRAM FOR THE AMPHIBOLITE OF THE AREA (AFTER VILJOEAN AND VILJOEAN, 1969).

Tholeiitic series	=	0.28
Alkali rock series	=	0.47
Nepheline basalt and basanites	=	0.56

$\text{Fe}_2\text{O}_3/\text{FeO}$ ratio in these amphibolites ranges from 0.07 to 0.23 (average 0.15), thereby reflecting the tholeiitic nature of the source rock.

From the AFM diagram, tholeiitic to calc-alkaline nature of parental magma has been concluded for amphibolites of the area (Fig. 5.10). A consideration of the K-Na-Ca triangular plot further strengthens the observations made above (Fig. 5.11) since most of the points fall on sodic side of the median line (Na:K=1:1), which is the average of all igneous rocks (Green and Poldervaart, 1958). In this diagram, all the points fall outside the field of spilites and show a positive correlation with Karroo dolerites, thereby suggesting that the parental rocks have doleritic affinity.

Tholeiitic nature of the magma source is also evidenced from a plot between Ni vs. P_2O_5 where all the points fall in the field of tholeiitic greenstone (Fig. 5.12).

Geochemically, Co behaves similar to Ni, though it usually has lesser abundance than Ni e.g., these amphibolites contain 88.96 ppm Co and 99-204ppm Ni with Ni/Co ratios varying from 1.08 to 2.19. Ni/Co vs. Ni plot, as proposed by Ringwood (1975), shows that all the amphibolites occupy a field

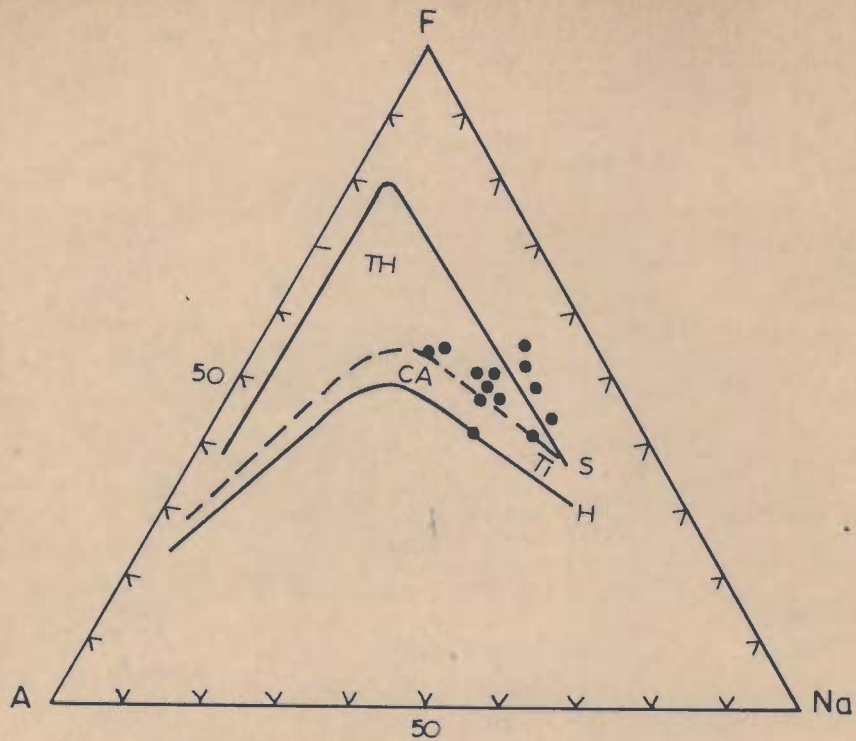


FIG. 5-10-AFM ($\text{Na}_2\text{O} + \text{K}_2\text{O} - \text{FeO} + \text{Fe}_2\text{O}_3 - \text{MgO}$) DIAGRAM FOR THE AMPHIBOLITE OF THE AREA, SHOWING THE TRENDS OF SKAERGAARD INTRUSION (S) AND HAWAIIAN ALKALI SERIES (H), AFTER Mac DONALD et al. , 1964. T-T' IS A LINE SEPARATING THOLEIITES (TH) FROM CALC-ALKALI (CA), AFTER IRVINE AND BARAGER (1971).

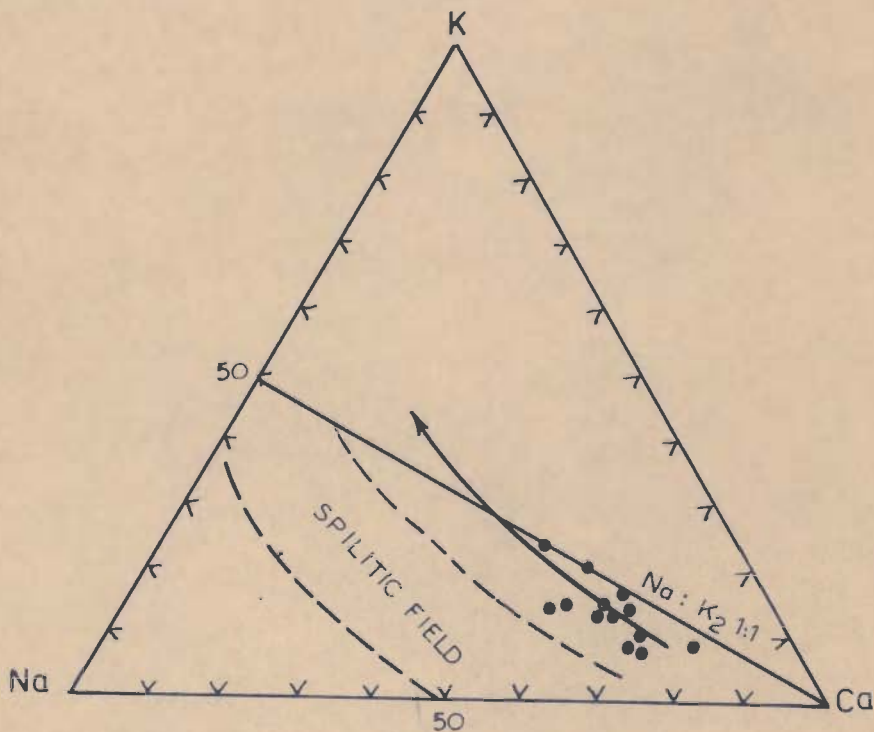


FIG. 5-11-K-Na-Ca PLOT FOR THE BHATWARI AMPHIBOLITE. ARROW POINTS OUT THE TREND OF KARROO DOLERITE.

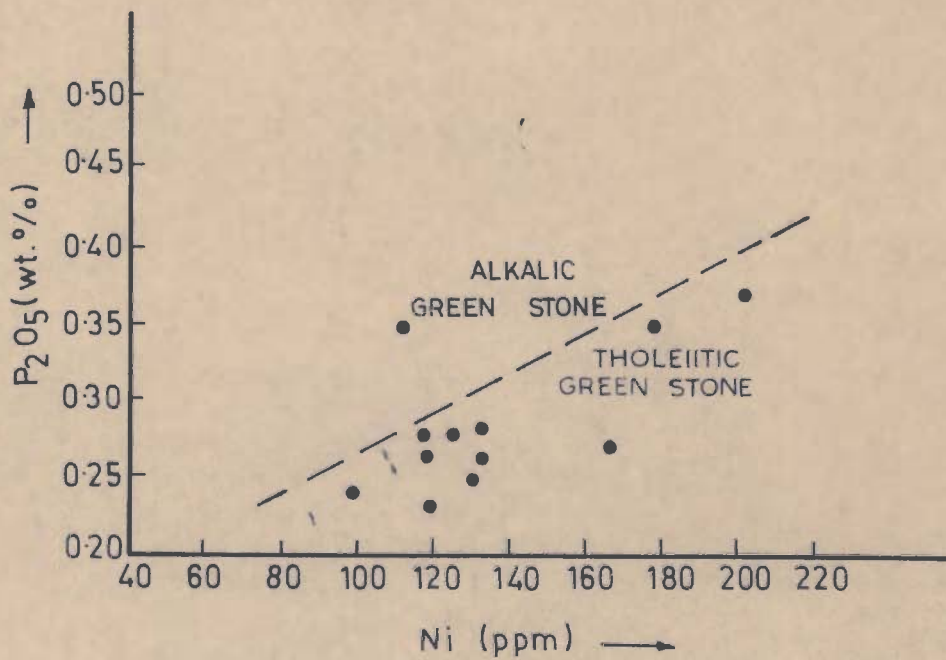


FIG.5-12-Ni VERSUS P₂O₅ PLOT FOR THE BHATWARI AMPHIBOLITE (AFTER FLYOD,1976)

which is superimposed by terrestrial tholeiites and low Ti Mare basalt (Fig. 5.13).

Confirmation regarding the composition of magma source has also been made by Cr. vs. Ni plot where considerable clustering of points occurs in the field of tholeiitic basalts (Fig. 5.14). Turkian (1963) opined that Cr/Ni ratio does not markedly change during fractional crystallization, which is dominantly responsible for the diverse composition of basalts.

The concentrations of K, Ba, and Sr in these amphibolites are considerably higher than those in oceanic tholeiites, island arc and submarine volcanics (Condie et al., 1969) thereby excluding the possibility of the latter three sources (Table 5.3). The ratios K/Ba (18.96 to 36.77), K/Sr (16.61 to 46.14), Sr/Ba (0.49 to 1.43) and Ca/Sr (76.98 to 194.88) from amphibolites of the Bhatwari Group show good resemblance with Precambrian continental tholeiites and alkali basalts (Wyoming diabase) of Chile region (cf, Condie et al., 1969). Further, K/Ba and Sr/Ba ratios also exhibit close resemblance with enriched alkali tholeiites (EAT) and high alkali andesites (HAA) of the Archean greenstone belts (Condie, 1976).

Elemental ratios such as K/Sr, K/Ba, Ba/Sr and Ca/Sr of these amphibolites have been plotted as a function of K concentration indicating a differentiation index (Figs. 5.15 a-d). According to Condie et al. (1969), such diagrams are useful in illustrating fractionation of elements with respect to each other during magmatic evolution. Figures 5.15 a-c reveal

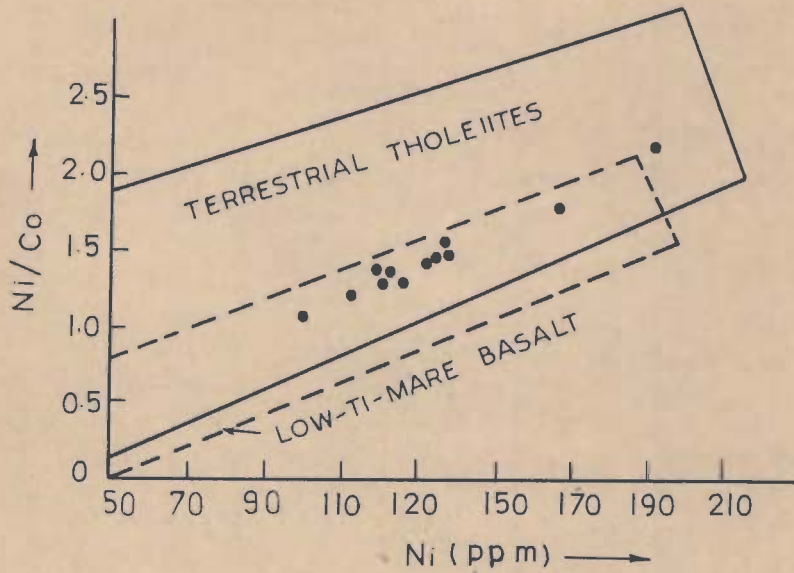


FIG. 5-13-Ni VERSUS Ni/Co PLOT OF THE BHATWARI AMPHIBOLITE IS COMPARED WITH THE CORRESPONDING FIELDS OF LOW-Ti MARE BASALT AND TERRESTRIAL THOLEIITES (FROM DELANO AND RING WOOD, 1978)

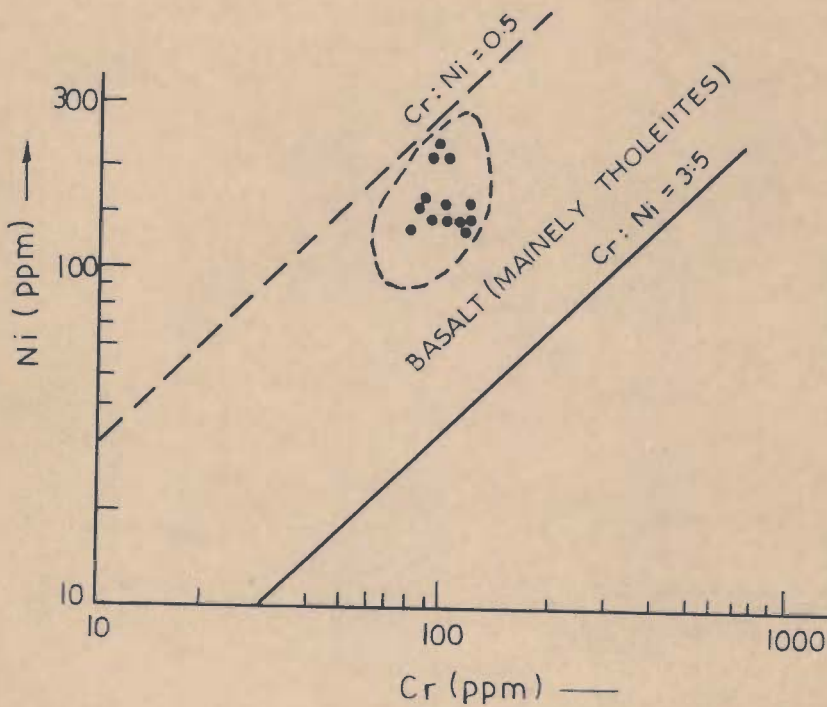


FIG. 5-14-Cr VERSUS Ni PLOT FOR THE AMPHIBOLITE FIELD OF BASALT IS MARKED ON THE BASIS OF Cr/Ni RATIO (TUREKIAN, 1963)

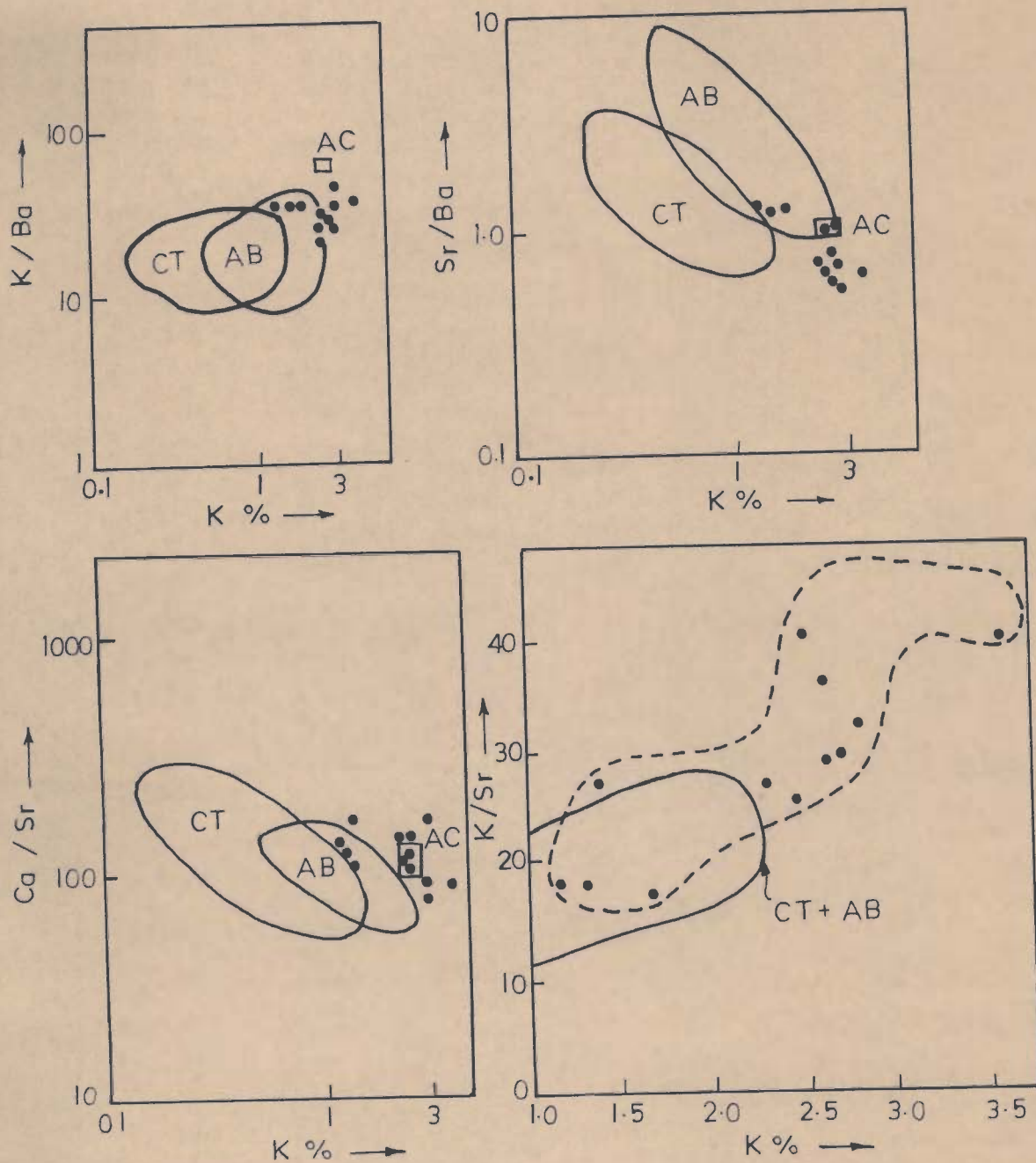


FIG. 5-15-K (CATION PERCENT) VERSUS K/Ba, Ca/Sr, Sr/Ba AND K/Sr PLOTES (a, b, c, d RESPECTIVELY) FOR THE AMPHIBOLITE OF THE BHATWARI AREA. CT, AB AND AC REPRESENT THE POSITION OF CONTINENTAL THOLEIITES, ALKALI BASALT AND AVERAGE CRUST (AFTER CONDIE, et. al. 1969).

that amphibolites from this area have attained the composition of alkali basalt to average continental crust. No significant conclusion was made from Fig. 5.15 d, because K/Sr ratio shows large dispersion. Since these metabasites have suffered migmatization to a certain extent, an enrichment of K content is obvious. Taking this factor into account, the parental magma could be considered as continental tholeiite (as is evidenced from major oxides), which has attained the composition of alkali basalt to average continental crust due to the enrichment of K contents.

K/Ba ratio remains nearly constant with the increase in K content (Fig. 5.15 a) indicating a control of Ba content by K concentration in these rocks. Similarly, Ca/Sr ratio shows small dispersion with the enrichment in K contents, revealing that the concentration of Sr has been mainly governed by Ca and no significant contribution has been made by K. This argument is further supported by K vs. Sr/Ba and K vs. K/Sr ratio plots (Fig. 5.15 b, d) in which Sr/Ba ratio decreases and K/Sr ratio increases with K concentration.

5.2.3 Intrusive or Extrusive Nature of the Progenitor

In order to assess whether the progenitor of amphibolites in this area represents an intrusive or extrusive character, oxidation ratio ($\text{mole } 2\text{Fe}_2\text{O}_3 \times 100 / 2\text{Fe}_2\text{O}_3 + \text{FeO}$) has been used by several workers (Eugster, 1959; Chinner, 1960). They have concluded that the oxidation ratio of the intrusive amphibolites is significantly higher than that of the extrusive amphibolites.

Accordingly, higher degrees of metamorphism do not produce appreciable changes in oxidation state of the involved rocks.

The oxidation ratio in amphibolites, associated with the Bhatwari Group, ranges from 5.64 to 17.29 with an average of 11.57 and can be comparable with the intrusive and extrusive basic rocks of other areas as given below:

Intrusive basic rocks and amphibolites	Fe ₂ O ₃	FeO	Oxidation Ratio	Extrusive basic rocks and amphibolites	FeO	Fe ₂ O ₃	Oxidation Ratio
Palisades dolerite (Walker, 1969)	1.6	8.7	14.2	Karoo basic intrusive (Walker, 1969)	3.4	8.6	26.11
Karoo basic intrusive (Walker and Poldervarrt, 1949)	1.2	9.3	11.0	200 amphibolites (Poldervarrt, 1955)	2.7	7.9	23.6
Chaur massive amphibolites (Chadha, 1977)	1.88	10.90	13.35	Chaur schistose amphibolites (Chadha, 1977)	3.50	8.15	27.70
Bhatwari amphibolites (author)	1.27	8.86	11.57	-	-	-	-

5.2.4 Depth of Source Magma

Sugimura Index: The index $(\text{SiO}_2 - \text{Na}_2\text{O} + \text{K}_2\text{O} / \text{Al}_2\text{O}_3)$ of volcanic rocks was proposed by Sugimura (1968). For oceanic tholeiites, 'θ' value is > 36, whereas its value is < 30 for alkalic basalt. When 'θ' value is < 36, it generally represents continental

tholeiites. In the present case, ' θ ' value ranges from 18.72 to 41.52 (average 32.73, Table 5.4), thereby indicating a continental tholeiitic to alkalic character of these metabasic. θ value of < 36 indicates that the magma was poor in SiO_2 and rich in K contents. Most of the continental tholeiites ($\theta < 36.00$) occur on the continental crust with a crustal thickness more than 30km. The higher is the value of this index, lower is depth of magma generation. From the index values of 32 for the Wyoming diabase dikes, an Early Precambrian crustal thickness of about 40 to 50 km has been estimated by Condie et al. (1969). Since the average ' θ ' index value in the present case is equivalent to Wyoming diabase (32.73), therefore ~~crustal thickness~~ crustal thickness in this area was probably between 40 to 50km. This argument can be supported by the higher contents of K_2O in the amphibolites.

5.2.5 Nature of Source Magma

In recent years, Mg number (Mol. prop. $100 \text{MgO}/\text{MgO} + \text{FeO}$) has been widely used for identifying the original composition (primitive, parental, and/or derivative) of the basaltic magma (Green, 1970, Kuno et al., 1957; Blanchard et al., 1976; Nesbitt and Sun, 1976 and Ringwood, 1979). The primitive magma is characterised by high Mg number. The Mg number in these amphibolites varies from 44.29 to 66.03 (average 57.26), suggesting that these rocks have been derived from a parental magma which

was tholeiite to alkalic Olivine basalt in composition. The Mg number values are characterized by three gaps between Mg number 44.5 and 48.5, 51 and 56 and between 61.5 and 64.3 (Fig. 5.16). These gaps in Mg number can be explained by (a) discontinuous fractionation of the parental magma and (b) secondary changes that resulted during metamorphic and metasomatic events.

Further observations regarding the nature of source magma have been made from distribution of trace elements concentration plots against Mg number in the amphibolites of the area (Fig. 5.16). In the above diagram, region occupied by Mg number 57.6-61.4 seems to be a significant area for the distribution of trace elements, Li, Ba, Sb, Bi and Pb show increase in their concentration, whereas Zn, Sr, Ni and Cr show decrease in their concentration on either side of this spot. The above behaviour of trace elements against Mg number suggests that they might have been accommodated in different ferromagnesian mineral phases during fractional crystallization. This conclusion is compatible with the fact that chalcophile elements show close resemblance with Mg^{2+} and Fe^{2+} in magma (Shipulin, 1975). No significant variation is noticed in case of Cu, except in meta-andesite (sample No.756), which contains 2655ppm Cu. Such a high content of Cu in meta-andesite is either due to sulphide contamination or migration of this element into the host rock (since the rock contains sulphide mineralization). Similarly, no appreciable change has been recorded in the

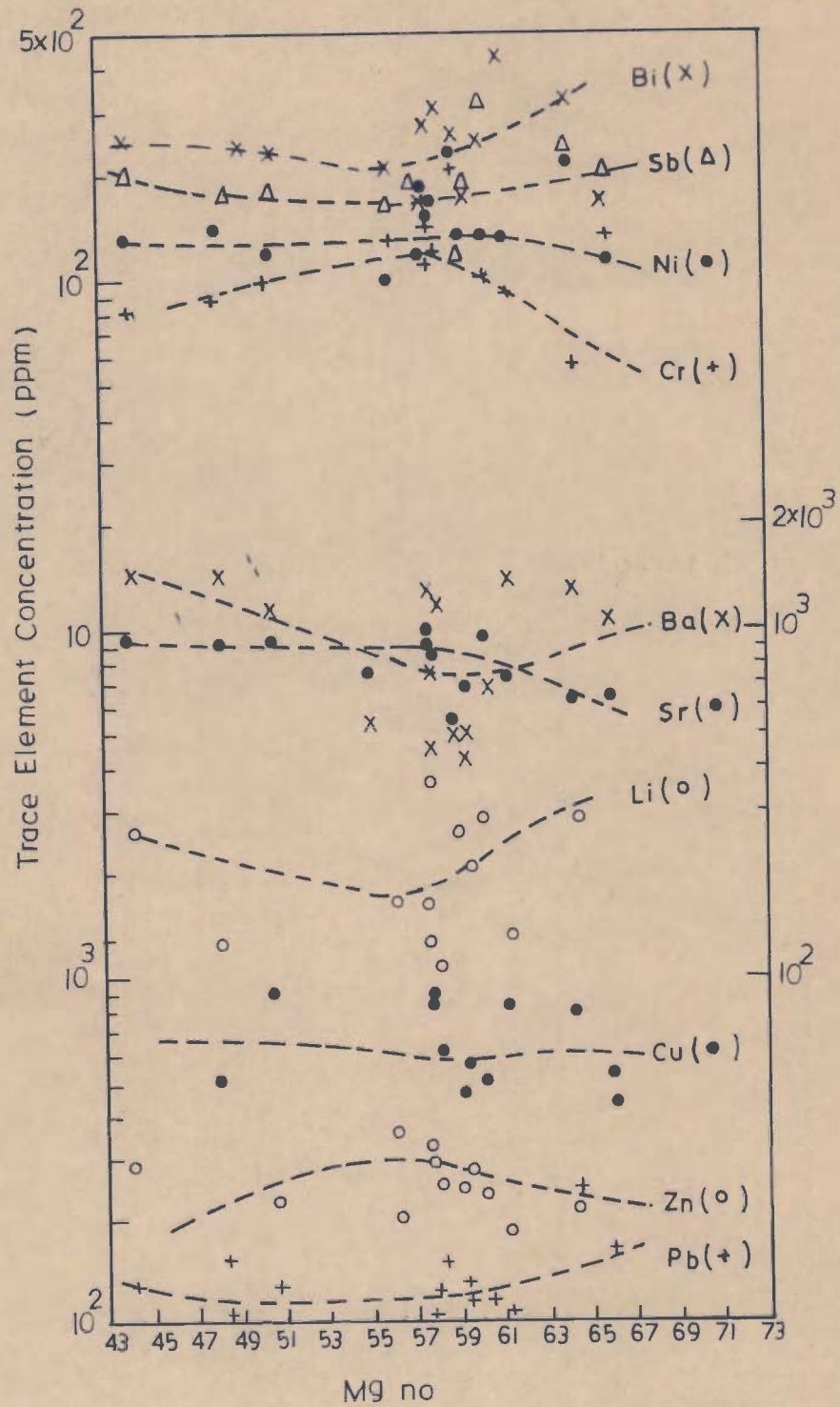


FIG. 5-16 - Mg NUMBER VS Pb, Zn, Cu, Li, Sr, Ba, Cr, Ni, Sb AND Bi PLOT FOR AMPHIBOLITES AND META-ANDESITE. SYMBOLS ADJACENT TO A TREND LINE REFER TO THE ELEMENTS ON THE RIGHT HAND MARGIN

concentration of CO (88-94ppm) and Cd (5-9ppm).

A comparison between Pb concentration and Sb/Bi ratio reveals that between 110 to 140ppm, Pb content, there is almost continuous increase in the Sb/Bi ratios (from 0.45 to 1.3). This may be due to nearly continuous fractional crystallization of the basic magma on the analogy of lower Sb/Bi ratio in galena at higher temperatures (Malakhov, 1968 in Vaughan, 1976).

Ni^{2+} and Cr^{3+} are readily accommodated in ferromagnesian minerals (pyroxene or olivine), because their ionic radii and charge are similar to Mg^{2+} , Ni^{2+} 0.72Å, Cr^{3+} 0.69Å, Mg^{2+} 0.65Å. Both Cr and Ni relatively poor concentration in these amphibolites. Cr content varies from 83-140ppm and Ni content in majority of the samples, ranges from 99-137ppm (except in three samples where Ni content varies from 167-204ppm). According to Ringwood (1979), the primary magma should have higher concentration of Ni (300ppm) and Cr (400ppm) and higher value of Mg number (65 to 75). Since in the present case, Cr and Ni show poor concentration and relatively low Mg number (average 57.26), composition of these rocks is far off from the primary liquid but closer to parental magma.

According to Rayleigh, fractionation model, the concentration of Ni and Cr can be reduced to half, when about 7 to 10% of olivine may have crystallized from the melt (Cox et al., 1979). These data indicate that the parental magma of these amphibolites was relatively poor in olivine.

Mg number has also been widely used to monitor the effects of olivine fractionation in igneous rocks due to

constant (0.30 - 0.36) value of distribution coefficient (Kd). Plotting on the crystallization and composition models (plots between $100 \text{ Al}/(\text{Mg} + \text{Fe}^{2+})$ vs. $100 \text{ Mg}/(\text{Mg} + \text{Fe}^{2+})$, as proposed by Irvine (1979), indicate that in certain samples of the amphibolites from the present area, about 40 to 50% solidification of the magma has taken place (Fig. 5.17 a,b). However, a significant number of samples fall in a region with little (10-15%) or no solidification. The above inference can be further justified on the basis of composition model in which all the samples fall either in the zone of PX-01 suspensions or PX-P1-01 accumulates indicating a low degree of fractionation of the magma. The higher concentration of K, Ba and Sr in these amphibolites could be due to partial crystallization of magma during emplacement.

5.2.6 Time of Emplacement

The distribution of Cr and Ni in the Indian basalts of different ages indicate a low Cr/Ni ratios (0.15-0.37) for the Precambrian basalts in comparison to the younger basalts (0.35 to 0.88) of Paleozoic to Mesozoic age (Ghosh and Trofimov, 1970). The Cr/Ni ratios in amphibolites from the Bhatwari Group ranges from 0.54 to 1.34 (average 0.84), ^{probably} indicating a Paleozoic-Mesozoic period for the basic activity in the area. Further support to this argument comes from Ni/Co ratios. Condie et al. (1969) showed that Ni/Co ratio for the Archean volcanic rocks is higher (2.6 to 2.8) and lower in the case of

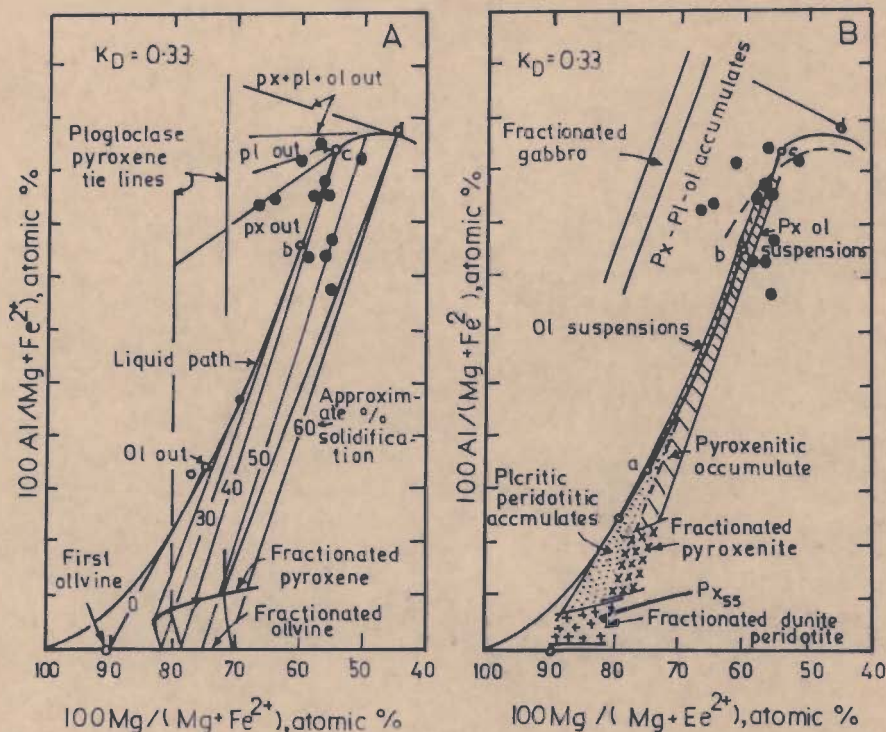


FIG. 5-17 - PLOTS OF BHATWARI AMPHIBOLITES ON IRVINE DIAGRAMS (1979)

A. CRYSTALLIZATION MODEL ON A PLOT OF $100 \text{ Al} / (\text{Mg} + \text{Fe}^{2+})$ VS $100 \text{ Mg} / (\text{Mg} + \text{Fe}^{2+})$, BASED ON THE LIQUIDUS FRACTIONATION CURVES FOR A LIQUID THAT FRACTIONATES ACCORDING TO THE CRYSTALLIZATION ORDER: OLIVINE; CLINOPYROXENE; PLAGIOCLASE.

B. INFERRED COMPOSITION FIELDS FOR THE DIFFERENT KINDS OF ROCKS THAT MIGHT BE PRODUCED BY ACCUMULATING THE FRACTIONATED MINERALS IN THE MODEL IN A WITH DIFFERENT PROPORTIONS OF CONTEMPORARY LIQUID.

modern volcanic rocks (e.g. modern andesites are having Ni/Co ratio - 0.75). The average Ni/Co ratio in the present case is 1.49 thus suggesting progenitor of these amphibolites probably belongs to Paleozoic - Mesozoic period. This conclusion should be considered inconclusive for want of geochronological data.

5.3 PETROGENETIC MODEL

From the earlier discussions, the following inferences have been drawn for geochemical characters of amphibolites of the Bhatwari Group.

- (i) The various geochemical plots such as Niggli c-mg, c-(al-alk), c-(al-alk)-mg, ACF diagram and discriminant function 'X' clearly indicate the magmatic origin of these amphibolites occupying the position of middle differentiate in Karroo dolerite trend.
- (ii) Continental tholeiitic dolerite to alkali basalt composition of the magma is evident from modified Larsen Index (-6.99 to +0.35), chemical plots such as SiO_2 vs. total alkali, CaO vs. MgO, CaO vs. Al_2O_5 , AFM and $\text{Fe}_2\text{O}_3/\text{FeO}$ ratio (average 0.15), and trace elements data.
- (iii) The oxidation ratio (average 11.57) of these amphibolites indicates an intrusive character of the parental magma.
- (iv) Sugimura Index of these amphibolites (average 32.73), when compared with the available data on Wyoming diabase dikes indicates an intrusion in the Bhatwari group at a depth of 40-50km. Almost similar crustal thickness have also been obtained from the available seismological data (Banerjee, personal communication, 1982).

- (v) Comparitively low value of Mg number (57.76 to 61.4), Cr content (83-140ppm) and Ni content (99-137ppm) also confirms the parental nature of the source magma (Ringwood, 1979).
- (vi) Magnesium-iron fractionation model (Irvine, 1979) indicates a low degree of fractionation of the parental magma (15% solidification in majority of the samples) which could be responsible for the enrichment of K, Ba and Sr content in the amphibolites.
- (vii) When Cr/Ni ratio (average 0.84) and Ni/Co ratio (average 1.49) of these amphibolites were compared with available data on Indian basalts (Ghosh and Trofimov, 1970) and also with Archean and Modern volcanic rocks (Condie et al., 1969) it has been inferred that progenitor of these amphibolites belongs to Paleozoic-Mesozoic period.

Ganser^s (1964) was of the opinion that the amphibolites, metadolerites etc. associated with the Lesser Himalayan thrust sheets and Main Central Thrust are submarine to ophiolitic in character. Further he suggested that they may be Precambrian to Early Cambrian in age and controlling the location of the Himalayan thrusts. Taron (1976) assigned an Early Paleozoic to Mid-Paleozoic age to the volcanic rocks and their metamorphic derivative associated with Pithoragarh-Rudraprayag Inner Deoban Sedimentary Belt of the Garhwal Lesser Himalaya and Shali structural belt of Himachal Pradesh. Das (1968) opined that the

metamorphosed basic rocks of Dwarahat-Chaukhutia area to be of Paleozoic in age. Jain (1972) assigned an Upper Cretaceous age to the metabasic associated with the Garhwal Group in Uttarkashi area, being emplaced along the dislocation zones.

On the basis of geological evidences, Agarwal and Kumar (1973) assigned Precambrian to Ordovician age to the metabasics occurring in the Uttarkashi area. Pande and Prasad (1977) also considered most of the basic magmatic rocks of the Himalaya to be of Paleozoic-Mesozoic period. Jain and Thakur (1978) considered Aor volcanics of Arunachal Himalaya to be of Late Precambrian to Lower Paleozoic in age. Sinha Roy and Furnes (1978) studied the basic volcanic rocks associated with the Lower Gondwana sequence in the Sikkim Himalaya and assigned Upper Paleozoic age to these rocks. On the basis of alkalic (potassic) character and high contents of 'incompatible' trace elements in the volcanic rocks, they inferred that the basic magma could have generated at greater depth and probably related to initial stage of continental rifting.

In the amphibolites of the Bhatwari Group from the Bhagirathi and Yamuna Valleys, field and textural studies indicate absence of the first phase of deformation and migmatization. They show concordant relationship with most prominent foliation (S_2) of the country rocks and have been affected by second phase of deformation and migmatization. The above behaviour of these amphibolites in the Bhatwari Group reveals that they could have been emplaced along the foliation planes (S_2).

synkinematically during the 2nd phase of deformation and migmatization.

From the earlier discussions, it has been concluded that the Bhatwari amphibolites are derivatives of continental tholeiitic dolerite. Further, on the basis of different petrogenetic models, an attempt has been made to explain the relatively strong enrichment of K, Ba and Sr.


If the uppermost mantle contain 10% hornblende peridotite with 5-10% melt, it can give rise to tholeiitic basalt and not alkali basalt. However, contamination of these melts with 0.2 to 0.5% of phlogopite can produce both tholeiitic and alkali basalts with relatively higher concentration of K, Ba and Sr (Griffen and Murthy, 1969).

There are two types of hornblende which are seen in some thin sections (D27/411 and D27/407). One is the normal green variety and the other a brown variety. No textural evidences have been recorded for the existence of primary hornblende and biotite. The green hornblende and biotite present in the rock show nematoblastic and lepidoblastic schistosity respectively and hence are clearly of metamorphic origin. Brown hornblende, although rarely present does not show clear metamorphic texture and could be representing the primary hornblende on the basis of the fact that brown hornblende generally richer in Na_2O , K_2O , TiO_2 , Al_2O_3 and poorer in SiO_2 (Deer, 1937 cited in Heinrich, 1965).

Strong enrichment of Ba in particular is limited to a range of few percent fractional melting. In order to produce liquids with 200-400ppm Ba and 300-700ppm Sr, mantle Ba and Sr contents of 10-20ppm and 30-60ppm respectively required (Gast, 1968). From the above study it can be said that the basaltic magma from which these amphibolites have been derived was rich in Ba (50-60ppm) and Sr (40-70ppm) and had undergone least fractional melting (5-10%).

It is also probable that the primary magma could have formed in the upper mantle but the fractionate got contaminated during their upward journey by the crustal rocks and thereby were enriched in K, Ba and Sr contents.

To summarise, the amphibolites of the Bhatwari Group except cummingtonite-biotite schist have intruded into the rocks along S_2 foliations during the Late Mesozoic period as doleritic sills at the depth of 40-50km. The source magma was tholeiitic to alkali basalt type.



CHAPTER - VI

PETROCHEMISTRY OF MIGMATITE

As mentioned in Chapter II, the Bhatwari Group is characterised by streaky migmatite derived from amphibolite and augen migmatite (and its variations) which are derived from metasediments. In the Bhatwari Group, metamorphism belongs to the garnet grade, except near the MCT, where retrograde metamorphism is intense. On the other hand, the migmatite of the Suki Group is characterised by porphyroblastic and banded characters and by the presence of concordant pegmatite veins. The country rocks in the Suki Group show metamorphism varying from garnet to sillimanite grade, although the migmatization is confined upto kyanite grade only. Considering the genesis of the Himalayan migmatites being controversial, an attempt has been made to analyse these chemically and to interpret the genesis of migmatites from the field, petrographic and geochemical data.

6.

6.1 GEOCHEMISTRY

6.1.1 Techniques

19 representative samples of different varieties of migmatites and country rocks belonging to the Bhatwari and Suki Groups were chemically analysed for their major oxides and trace elements for deciphering geochemical changes during migmatization after methods described in Chapter 5.

TABLE 6.1 CHEMICAL ANALYSIS OF MIGMATITES AND THEIR COUNTRY ROCKS (BHATWARI GROUP)

Sample No./ Oxide	506	451	409	460	415	416	429	439	477	441	481	830	834
SiO ₂	64.35	70.50	67.50	67.52	69.50	68.25	66.35	65.50	69.15	58.35	68.75	69.62	66.45
Al ₂ O ₃	15.94	14.29	15.29	14.87	13.94	15.37	14.65	15.29	14.46	15.02	14.67	13.82	15.93
Fe ₂ O ₃	1.17	0.62	0.73	0.74	1.61	1.39	1.17	1.37	1.85	1.54	1.69	0.55	1.19
FeO	1.74	1.44	2.33	2.90	2.42	3.02	2.54	2.26	1.92	2.40	2.42	4.12	4.32
MnO	0.50	0.04	0.12	0.07	0.08	0.15	0.05	0.11	0.14	0.08	0.03	0.07	0.07
MgO	2.61	3.02	2.93	2.83	3.43	3.24	3.65	2.62	2.52	2.71	2.25	3.15	2.42
CaO	2.71	2.57	2.40	2.29	2.42	2.69	2.93	2.97	2.97	2.0	2.71	2.71	2.99
Na ₂ O	2.69	2.16	3.19	3.73	1.12	1.42	2.75	2.85	2.36	2.29	2.52	1.62	0.84
K ₂ O	6.17	3.21	3.75	4.15	2.86	2.81	4.25	5.04	4.07	4.45	3.99	3.80	3.65
TiO ₂	0.42	0.63	0.32	0.34	0.44	0.91	0.83	0.63	0.17	0.35	0.20	0.48	0.30
P ₂ O ₅	0.28	0.16	0.35	0.32	0.26	0.37	0.38	0.33	0.28	0.23	0.37	0.31	0.27
H ₂ O ⁺	1.02	0.78	0.98	0.63	0.82	0.45	0.75	0.92	0.23	0.47	0.51	1.10	1.15

506, 451, 409, 460,)
 429, 439, 477, 441,)
 481

(Analyst : The author.)

- Augen Migmatite and its varieties

415

- Quartz-Mica Schist

416, 830, 834

- Garnetiferous Mica Schist

TABLE 6.1 CHEMICAL ANALYSIS (SUKI GROUP)

Sample No./ Oxide	494	597	591	592	602	589
SiO ₂	69.55	64.85	64.5	63.58	62.60	68.25
Al ₂ O ₃	14.11	14.70	14.70	15.89	16.28	15.47
Fe ₂ O ₃	0.85	1.46	0.91	1.81	1.85	0.69
FeO	3.08	1.76	2.89	3.04	2.92	2.15
MnO	0.16	0.08	0.06	0.04	0.20	0.03
MgO	1.92	3.14	2.58	3.92	3.53	2.42
CaO	2.42	2.85	2.71	1.71	2.57	1.99
Na ₂ O	1.75	3.78	3.56	3.35	3.15	2.72
K ₂ O	3.87	5.65	5.45	5.77	5.10	4.85
TiO ₂	0.66	0.27	0.37	0.43	0.73	0.82
P ₂ O ₅	0.29	0.28	0.27	0.30	0.35	0.28
H ₂ O ⁺	0.85	0.79	0.69	0.73	0.72	0.52

494 - Kyanite Schist
 597, 591, 592 } Porphyroblastic Migmatite
 602, 584 }

(Analyst : The Author)

TABLE 6.2 CATION PERCENT (MIGMATITES AND THEIR COUNTRY ROCKS) (BHATWARI GROUP)

	506	451	409	460	415	416	429	439	477	441	481	830	834
Si	60.53	67.02	63.55	62.63	67.22	65.19	62.05	61.62	65.02	64.47	64.84	66.46	63.99
Al	17.64	15.98	16.88	16.23	15.86	17.27	16.12	16.92	15.99	16.67	16.28	15.53	18.05
Fe ³⁺	0.82	0.44	0.51	0.52	1.17	1.00	0.82	0.96	1.30	1.09	1.19	0.39	0.86
Fe ²⁺	1.37	1.14	1.91	2.24	1.95	2.16	1.98	1.77	1.51	1.88	1.90	3.28	3.48
Mn	0.39	0.03	0.10	0.06	0.06	0.12	0.04	0.09	0.11	0.06	0.02	0.06	0.57
Mg	3.69	4.31	4.13	3.94	4.98	4.64	5.12	3.70	3.55	3.84	3.19	4.52	3.50
Ca	2.71	2.62	2.42	2.28	2.52	2.75	2.93	2.99	2.99	2.02	2.74	2.77	3.08
Na	4.90	3.98	5.79	6.70	2.10	2.62	4.98	5.19	4.29	4.18	4.60	2.99	1.56
K	7.41	3.89	4.49	4.91	3.16	3.38	5.07	6.05	4.88	5.36	4.80	3.41	4.48
Ti	0.30	0.45	0.23	0.24	0.32	0.65	0.58	0.45	0.22	0.25	0.14	0.34	0.21
P	0.22	0.13	0.28	0.25	0.21	0.17	0.30	0.27	0.22	0.18	0.29	0.25	0.22

TABLE 6.2 CATION PERCENT (MIGMATITES AND THEIR COUNTRY ROCKS) SUKI GROUP

	494	597	591	592	602	584
Si	66.85	60.35	60.07	59.09	58.38	63.88
Al	15.96	16.08	17.33	16.72	17.86	17.03
Fe ³⁺	0.51	0.98	0.64	1.26	1.29	0.48
Fe ²⁺	2.47	1.36	2.24	2.35	2.27	1.68
Mn	0.13	0.06	0.05	0.03	0.16	0.02
Mg	2.77	4.38	3.60	5.47	4.94	3.40
Ca	2.49	2.84	2.71	1.70	2.54	1.99
Na	3.26	6.81	6.42	6.03	5.69	4.94
K	4.75	6.71	6.48	6.85	6.07	5.79
Ti	0.48	0.19	0.26	0.28	0.51	0.58
P	0.24	0.22	0.21	0.22	0.26	0.22

TABLE 6.3 NIGGLI VALUES OF MIGMATITES AND THEIR COUNTRY ROCKS (BHATWARI GROUP)

Sample No./ Niggli parameter	506	451	409	460	415	416	429	439	477	441	481	830	834
Si	252.55	327.69	280.87	273.04	313.97	288.86	260.64	261.17	294.82	293.14	296.28	302.59	271.84
al	36.85	39.12	37.49	35.42	37.09	38.82	33.20	35.91	36.32	37.95	37.24	35.38	38.39
fm	26.09	28.84	28.99	9.35	38.01	36.08	33.33	27.58	29.29	31.83	28.76	37.42	35.61
c	11.39	12.79	10.70	9.92	11.76	12.19	12.33	12.68	13.56	9.19	12.51	12.61	13.10
alk	25.67	19.24	22.82	25.32	13.14	13.41	21.13	23.82	20.82	21.69	21.50	14.58	12.90
k	0.60	0.49	0.44	0.42	0.63	0.57	0.51	0.54	0.53	0.56	0.51	0.53	0.74
mg	0.58	0.73	0.63	0.58	0.61	0.57	0.64	0.56	0.55	0.56	0.50	0.55	0.41
ti	1.24	2.20	1.01	1.03	1.50	2.90	2.45	1.89	0.55	1.18	0.65	1.57	0.92
p	0.46	0.32	0.62	0.55	0.50	0.48	0.63	0.56	0.50	0.42	0.68	0.57	0.41
qz	49.87	150.73	93.58	71.76	161.41	135.22	76.12	65.89	111.54	106.38	110.28	144.27	120.54

TABLE 6.3 NIGGLI VALUES OF MIGMATITES AND THEIR COUNTRY ROCKS (SUKI GROUP)

Sample No./ Niggli parameter	494	597	591	592	602	584
Si	326.84	247.06	246.73	230.86	224.33	294.84
al	39.06	32.99	33.65	32.70	34.36	39.37
fm	29.19	27.70	26.76	35.50	33.18	26.68
c	12.18	11.63	11.10	6.65	9.86	9.21
alk	19.57	27.68	26.49	25.14	22.59	24.74
k	0.59	0.50	0.50	0.53	0.52	0.54
mg	0.46	0.64	0.55	0.60	0.57	0.58
ti	2.33	0.77	1.04	1.18	1.97	2.67
p	0.58	0.45	0.44	0.46	0.50	0.51
qz	148.63	36.34	40.77	30.10	33.97	95.88

6.1.2 Results

Table 6.1 presents the chemical data of major oxides of the migmatites from the Bhatwari and Suki Groups, while computed cation percentage (Barth, 1962) and Niggli values are given in Tables 6.2 and 6.3 respectively.

ACF diagram as proposed by Winkler (1976), reveals that country rocks of the Bhatwari and Suki Groups have attained the composition of graywacke during migmatization (Fig. 6.1). This is further supported by Al-Si-Fe (cation percent) diagram (Cf., Moore and Dennen, 1970) in which majority of the migmatite samples occupy the top position and the country rocks the bottom position of graywacke field or near subgraywacke field (Fig. 6.2). Cation percentage plot also reveals a decrease in Si content and slight increase in Al and Fe contents have taken place during migmatization (Fig. 6.2).

A triangular plot of Si-(Na + K)-(Mg + Fe), as proposed in this work, suggests depletion in Si content and enrichment in alkali content during migmatization (Fig. 6.3). The position of the country rocks and migmatites fall distinctly in two nearby fields. A slight fall in (Mg + Fe) content during migmatization is also worth mentioning. The addition of alkalis during migmatization is also supported by a plot between Na_2O vs. K_2O (Fig. 6.4), as suggested by Mehnert (1968). From this diagram, it is clear that the addition of K_2O in the country rocks of the Suki Group is comparatively more marked as compared to that in the Bhatwari Group rocks. The concentration of

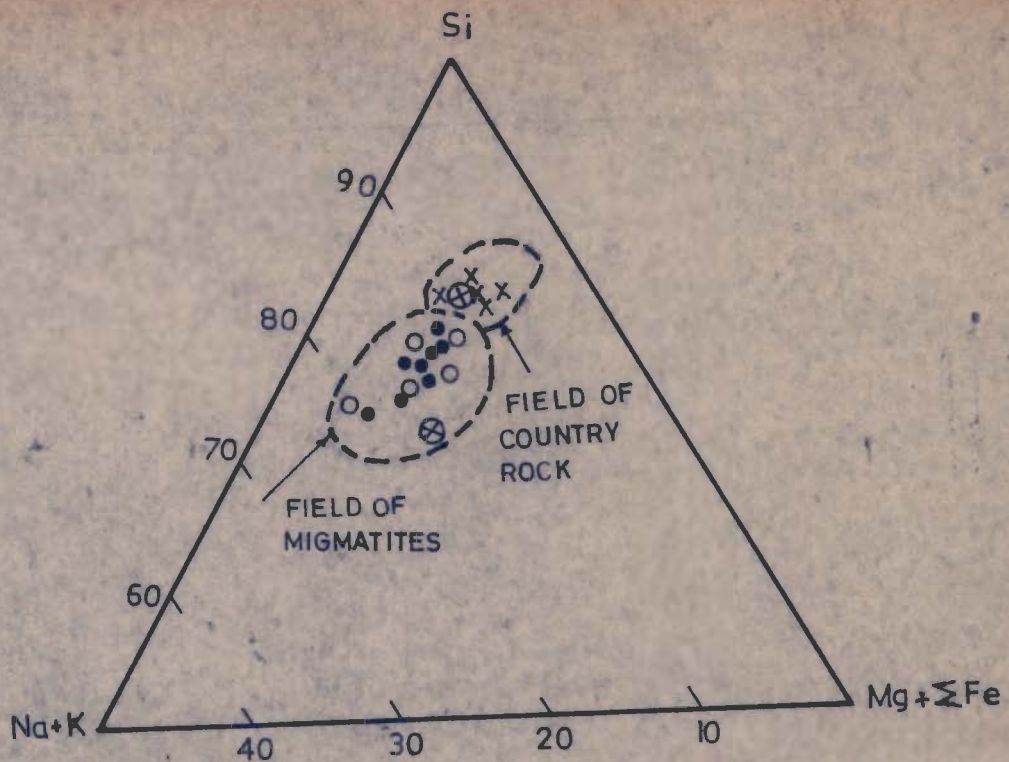


FIG. 6.3 - Si-(Na + K) - Mg + Σ Fe DIAGRAM OF MIGMATITES AND THEIR COUNTRY ROCKS (after author)

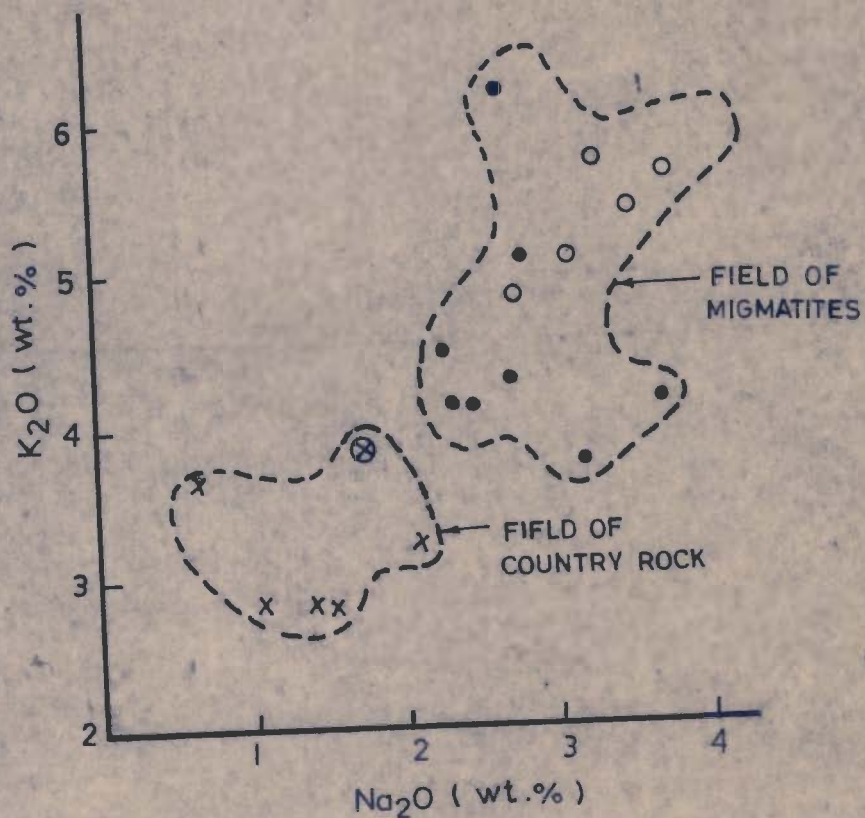


FIG. 6.4 - DISTRIBUTION PATTERN OF K_2O AGAINST Na_2O IN MIGMATITES AND THEIR COUNTRY ROCKS (after Mehnert, 1968)

Na_2O in both the groups is more or less the same. The scattering behaviour of K_2O against Na_2O may be considered as the effect of anatexis (Kay, 1976; Iden, 1981). The high alkali content in the migmatite is commonly recorded in the modern calc-alkaline rocks of continental margin environments (Jakes and White, 1972). Mehnert (1968) is also of the opinion that high alkali contents in migmatite could be the result of anatexis.

SiO_2 vs. major oxide percentage plots indicate that an increase in Al_2O_3 , Na_2O and K_2O contents have taken place with the decrease in SiO_2 while CaO , MgO , Fe_2O_3 and FeO have been least affected during migmatization (Fig. 6.5). The behaviour of FeO and Fe_2O_3 is, generally antipathetic, although it shows a sympathetic tendency near the MCT and Jhala. Nearly sympathetic behaviour of K_2O , Na_2O and Al_2O_3 reveals enrichment in alkali during migmatization.

A plot between approximate distance (i.e., sample localities) vs. oxide percentages for the Bhatwari and Suki Groups indicate that a general decrease in K_2O , Na_2O and Al_2O_3 and comparable increase in SiO_2 and FeO have taken place in the Bhatwari Group from south (near the MCT) towards north (near the JBT) (Fig. 6.6). The above behaviour of major oxides suggests that the intensity of migmatization was comparatively higher on southern side. No significant changes in MgO , CaO , Fe_2O_3 and P_2O_5 have been noticed in this group. On the other hand Na_2O , K_2O , Al_2O_3 , Fe_2O_3 , MgO and CaO show increase towards Suki, but beyond this locality their values decrease in the Suki Group.

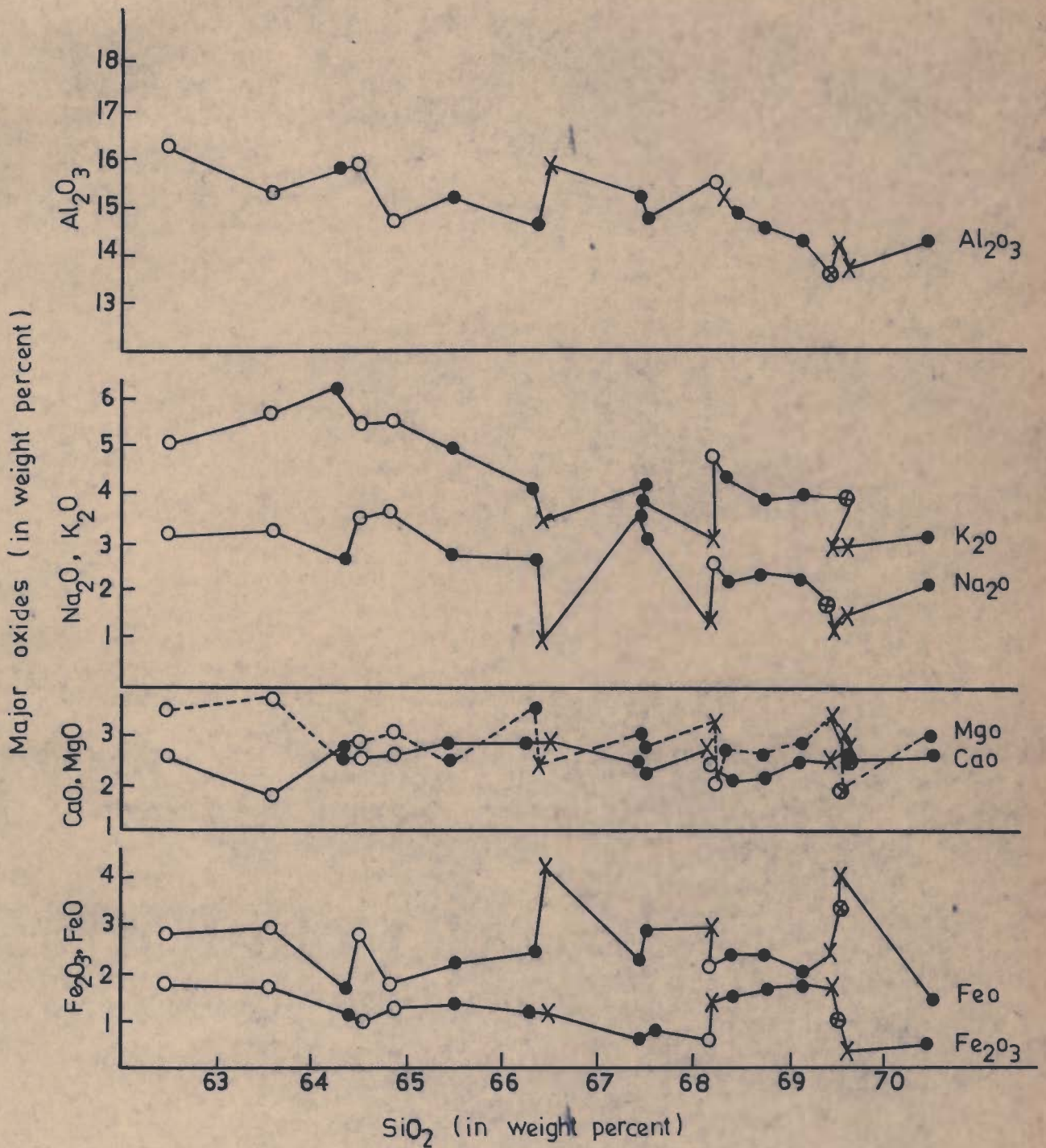


FIG.6.5 - SiO₂ VERSUS MAJOR OXIDES VARIATION DIAGRAM

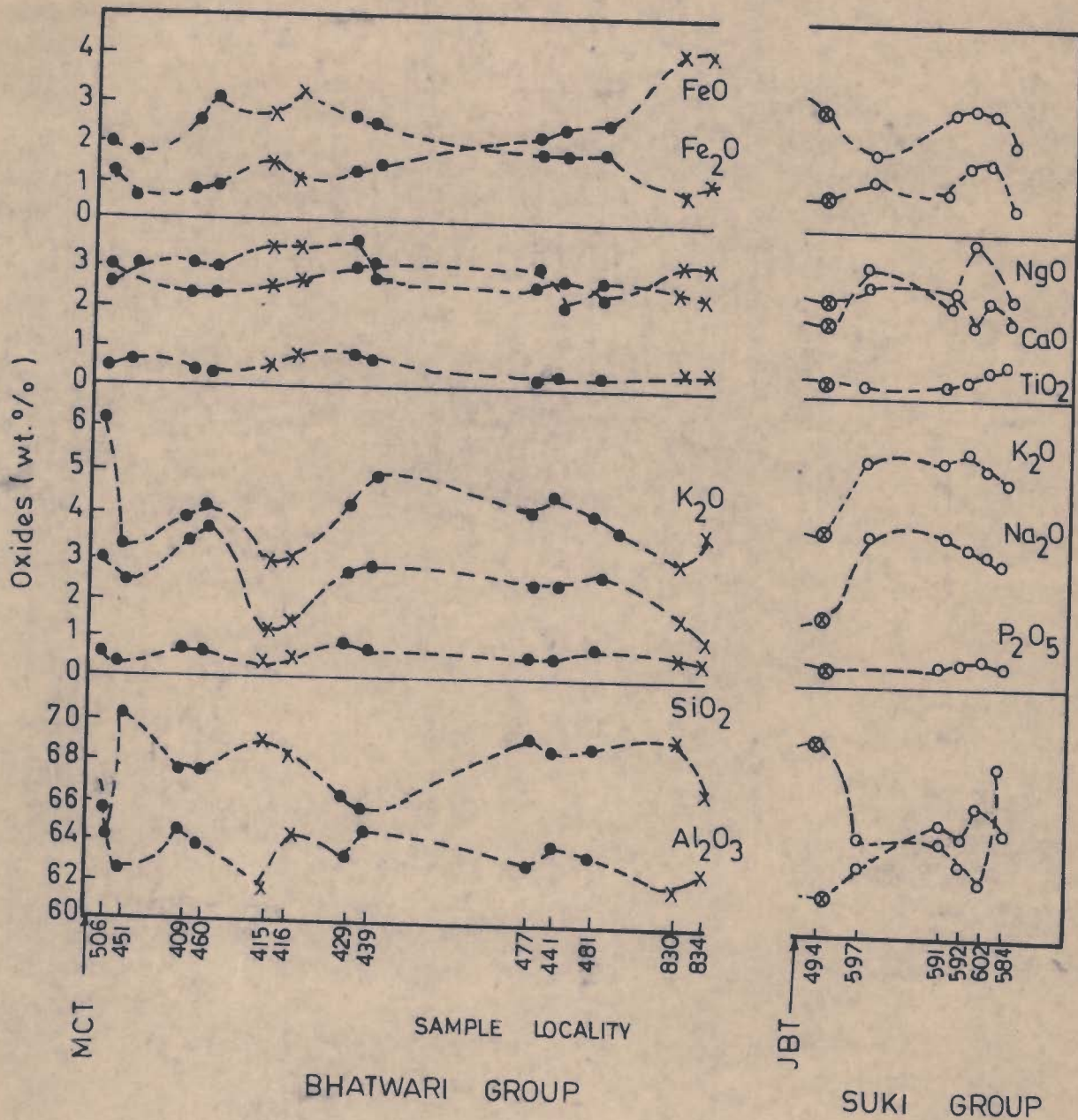


FIG. 6-6 - VARIATION OF OXIDES IN SPACE NORTHWARDS FROM MCT OR JBT

SiO_2 content shows depletion towards Suki. The above behaviours of alkali and SiO_2 suggest that the intensity of migmatization was maximum near Suki and has decreased further northwards. No significant change in FeO , TiO_2 and P_2O_5 has been recorded in the Suki Group.

Niggli values of migmatites also lead to conclusions which are not at variance with those discussed above. Niggli Si vs. c, alk, fm and al plot suggests that slight decrease in al, fm and large increase in alk have taken place during migmatization, but no significant change has been noticed in the c value (Fig. 6.7). It is worth mentioning that al and fm show antipathic behaviour in porphyroblastic migmatites, occurring at Suki and nearly sympathetic trend in other varieties. Antipathetic behaviour is also observed between alk and fm in all the varieties, except in augen and porphyroblastic migmatites where a sympathetic pattern is seen. A positive correlation between c and alk is noticed in all the varieties, except the porphyroblastic migmatite where c and alk exhibit a negative correlation.

In order to get an idea about the perfection in migmatization, $\text{CaO-K}_2\text{O-Na}_2\text{O}$ contents were plotted in a diagram, as proposed by Harpum (1963) for different varieties of granitic rocks (Fig. 6.8). The plot indicates that original rocks have attained the composition of adamellite to potassic granite due to migmatization. It is interesting to note that the migmatite samples belonging to the Suki Group fall near the

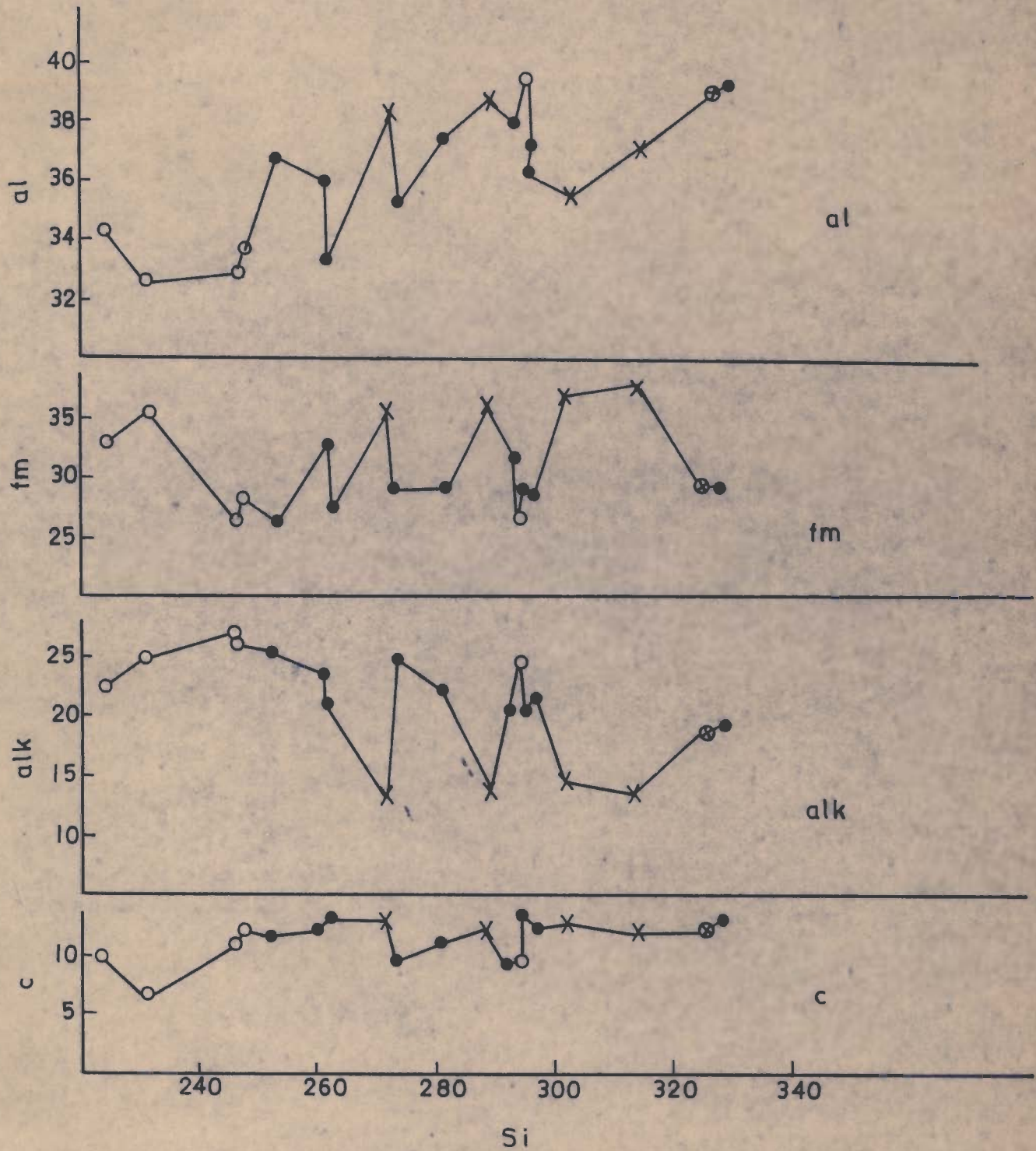


FIG. 67-VARIATION DIAGRAM BETWEEN NIGGLI Si VERSUS c , alk , fm & al

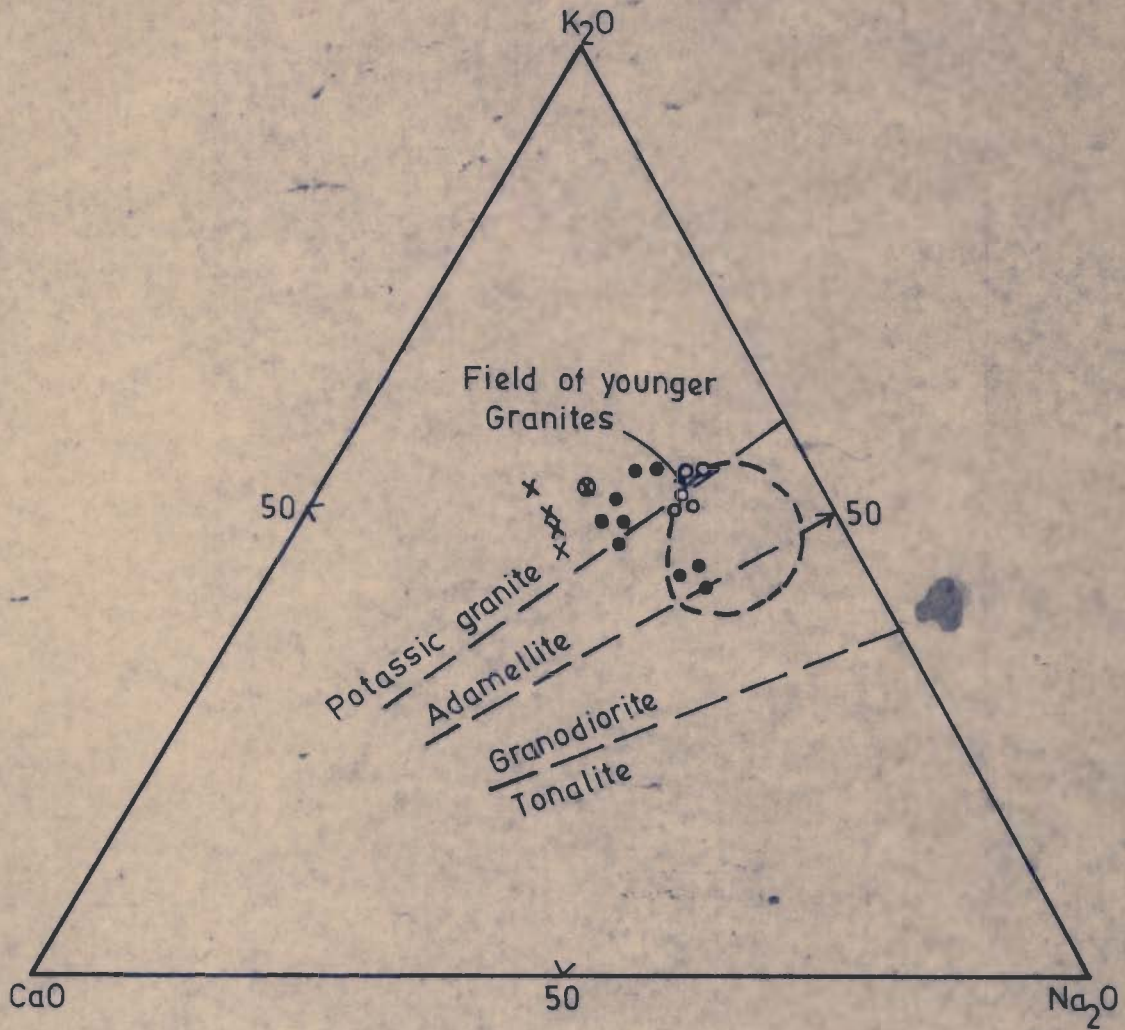


FIG. 6-8 - TRIANGULAR PLOT BETWEEN $K_2O:CaO:Na_2O$ FOR MIGMATITES OF THE AREA. LINES SEPARATING VARIETIES OF GRANITE ARE FROM HARPUM (1963)

field of younger granites. This feature indicates that migmatization in the Suki Group could have taken place in late stage probably during the Himalayan Orogeny in comparison to the migmatization of the Bhatwari Group. However, three samples belonging to the Bhatwari Group also occupy the field of younger granite. This may be due to the fact that the Bhatwari Group has suffered migmatization twice; (i) once much prior to the Himalayan Orogeny probably during Precambrian around 1900-2300m.y. (See Chapter 8) and the other along with the Suki Group during Cenozoic. Potassic granite to adamellite composition has been attained by the rocks due to addition of alkali and depletion of CaO.

Chemical data was also studied on the basis of methods adopted by Kleeman (1965) and Kapila et al. (1980). As the interpretations from these diagrams are in conformity with those discussed here, a further discussion was not thought essential and desirable.

6.2 TRACE ELEMENTS DISTRIBUTION

Distribution of trace elements in migmatites is of great significance in understanding their petrogenesis (White, 1966; Hedge, 1972; Druary, 1972; Hanson, 1978; Sighinolfi and Gorgoni, 1978). Therefore, these rocks have been analysed for their trace elements, such as Pb, Zn, Cu, Li, Sr, Ba, Co, Ni, Sb, Bi and Cd and concentration of these elements in ppm have been shown in Table 6.4.

TABLE 6.4 TRACE AND MINOR ELEMENTS IN MIGMATITES AND THEIR COUNTRY ROCKS
(CONCENTRATION IN ppm) BHATWARI GROUP

Sample No./ Element	506	451	409	460	415	416	429	439	477	441	481	830	834
Sb	235	185	85	320	130	140	200	140	210	150	200	135	165
Bi	210	165	245	220	205	300	215	210	160	235	175	290	290
Co	86	87	86	84	76	65	88	87	87	86	90	83	73
Ni	81	64	92	54	97	92	75	124	68	104	83	101	88
Cd	6	5	8	9	7	6	5	7	5	5	7	6	7
Pb	135	116	90	100	80	65	140	115	90	92	115	85	115
Zn	261	278	117	207	176	301	151	144	126	292	111	169	306
Cu	475	120	935	560	580	210	495	710	795	530	585	255	690
Sr	460	440	340	440	310	345	285	275	455	360	335	365	350
Ba	1250	950	1350	835	700	650	775	1400	450	465	410	845	950
Li	159	552	645	603	224	158	405	648	498	558	369	487	570

(Analyst : The author)

TABLE 6.4 TRACE AND MINOR ELEMENTS IN MIGMATITES AND THEIR COUNTRY ROCKS
(CONCENTRATION IN ppm) (SUKI GROUP)

Sample No./ Element	494	597	591	592	602	584
Sb	75	145	200	150	215	225
Bi	450	175	205	150	295	170
Co	87	88	87	85	87	85
Ni	117	84	86	77	135	63
Cd	5	5	5	6	8	8
Pb	95	105	101	105	115	105
Zn	231	192	179	101	306	231
Cu	155	925	490	330	225	655
Sr	320	285	330	260	415	285
Ba	995	1075	935	950	1305	1105
Li	419	328	345	801	1167	1130

(Analyst: The author)

On the basis of a comparative study of the trace elements major oxides and modal components of migmatites and non-migmatized rocks from the Bhagirathi Valley (Tables 6.1, 6.4, 6.5)

the following broad conclusions have been made:

Pb, Zn and Cu: The lead content ranges from 65 to 140ppm showing slight enrichment during migmatization. Relatively poor concentration of Pb may be due to its incompatible nature during partial melting (Snowden and Snowden, 1981). Lead may have gone into the structure of apatite by replacing Ca^{2+} , as evidenced from the positive correlation of Pb with P_2O_5 although some amount of Pb might have also been substituted from K^+ in the structure of K-feldspar or biotite. It has been found that Pb^{2+} preferentially enters into K-feldspar rather than plagioclase by a factor of about 2.4 (Doe and Tilling, 1967; Leeman, 1979).

Zinc shows a general increase in its concentration from 101-306ppm with an increased intensity of migmatization. This may probably be a reflection of the introduction of leucocratic material from internal source. Both Pb and Zn exhibit sympathetic behaviour. Zinc shows positive correlation with FeO, TiO_2 and MgO indicating that it has been diadochically substituted in the structure of ilmenite, biotite and/or tourmaline (Wedepohl, 1972). A negative correlation between Zn and Cu could be related to the poor concentration of Zn in plagioclase and apatite (Rankama and Sahama, 1950).

Copper shows relatively higher concentration in most of the migmatites and ranges from 120-935ppm. Such a large disper-

TABLE 6,5 MODAL ANALYSIS OF MIGMATITES OF THE BHAGIRATHI VALLEY (VOLUME %)

Sample No. Mineral Component	466	481	529	540	597	591	592	602	584
Quartz	34.50	41.54	45.30	43.11	43.76	33.52	33.85	28.31	46.50
Plagioclase	30.50	34.80	24.43	33.02	24.52	35.47	34.60	35.29	30.35
K-feldspar (including perthite)	11.90	4.25	3.63	4.21	16.98	14.15	10.14	21.33	6.80
Biotite	11.50	9.98	16.28	7.70	8.60	7.85	14.35	10.48	10.35
Cordierite	-	-	-	-	-	0.31	0.85	0.45	-
Muscovite	8.50	4.25	5.52	6.67	2.25	1.25	1.75	0.75	1.35
Chlorite	-	0.17	0.67	0.31	-	-	-	-	-
Garnet	-	-	0.81	0.46	-	2.55	0.25	0.45	0.45
Kyanite	-	-	-	-	-	0.65	-	0.20	-
Accessories (apatite, zircon, tour- maline, iron oxide etc.)	3.10	4.01	3.36	4.52	3.89	4.25	4.21	2.76	4.20

466 to 540 - Augen migmatite

597 to 584 - Porphyroblastic migmatite

TABLE 6.5 MODAL ANALYSIS OF MIGMATITES OF THE BHAGIRATHI VALLEY (VOLUME %)

Sample No. Mineral Component	501	506	451	409	460	513	514	429	439	441 *	454
Quartz	36.54	33.60	40.38	35.20	31.50	40.50	38.50	30.00	34.75	46.87	50.70
Plagioclase	21.86	15.44	22.19	25.80	42.50	29.40	30.45	11.50	40.35	22.02	14.83
K-feldspar (including perthite)	15.03 11.50	25.92 25.92	17.62 17.62	20.30	14.50	10.35	6.65	10.50	8.20	5.23	12.58
Biotite	11.50	15.95	11.34	10.70	7.50	4.15	7.35	12.50	11.60	10.64	8.21
Muscovite	9.30	6.57	4.24	3.50	1.50	12.20	12.45	2.50	2.25	11.69	10.94
Chlorite	0.50	0.23	0.73	0.25	0.40	0.80	-	1.00	0.60	0.35	0.61
Accessaries (apatite, zircon, tour- maline and iron oxides etc.)	5.22	2.29	3.50	4.25	2.10	2.60	4.60	2.00	2.35	3.20	2.13

501 to 454 - Augen migmatite (and its variance)

*Position of sample No. 540

TABLE 6.5 MODAL ANALYSIS OF NON-MIGMATIZED ROCKS OF THE BHAGIRATHI VALLEY (VOLUME %)

Sample No./ Mineral Component	415	416	477	469	830	834	494	571	average schist
Quartz	59.80	46.80	46.69	54.50	52.65	50.45	49.35	51.70	51.49
Plagioclase	11.70	3.25	12.87	6.50	2.45	2.50	13.85	13.45	8.32
K-feldspar (including perthite)	2.50	0.75	3.41	4.20	-	-	3.58	2.71	2.14
Biotite	14.50	8.50	18.25	8.50	10.60	4.60	15.10	15.23	11.91
Muscovite	6.60	21.80	13.37	23.20	14.25	25.30	8.60	7.94	15.13
Chlorite	2.50	2.50	1.22	-	5.40	2.15	-	0.28	-
Hornblende	-	10.20	-	-	-	-	-	-	-
Garnet	-	3.60	0.89	-	10.60	11.35	0.95	0.26	-
Kyanite	-	-	-	-	-	-	6.16	3.73	-
Accessories (apatite, zircon, tour- maline, iron oxides etc.)	2.40	2.60	3.30	3.10	4.05	3.65	2.41	4.70	3.28
	415, 477, 469		- Quartz mica schist						
	416, 830, 834		- Garnetiferous mica schist						
	494, 571		- Kyanite schist						

sion in Cu content may be due to the addition of Cu from an external source. Since these rocks are devoid of sulphide mineralization and Cu shows an antipathetic behaviour with Zn, it is not likely to accompany the later hydrothermal pneumatolytic activity. It might have been added, therefore, by migmatizing fluid on a local scale.

Copper can replace Fe^{2+} and Mg^{2+} in mineral structure in the absence of an appropriate supply of sulphur (Ramdohr, 1940; Carobbi and Pieruccini, 1947). In the present case, Cu shows sympathetic behaviour with CaO , FeO , TiO_2 , P_2O_5 and nearly antipathetic behaviour with MgO , probably suggesting that Cu is accommodated in the structure of ilmenite and apatite.

Li, Sr and Ba: Lithium content ranges from 158-1167ppm. Such a large dispersion in its concentration has definitely resulted due to heterogeneity caused by the addition of leucocratic material and not due to metamorphism. Lithium content remains unchanged during metamorphism as has been reported by several workers (Kamp, 1970; Sighinolfi, 1971; Wedepohl, 1972). It has been reported in quartz (Dennen, 1967) but a negative correlation with SiO_2 in the present case does not support this possibility. It shows close distribution pattern with MgO and FeO , revealing that it could have been substituted for Mg^{2+} and Fe^{2+} into the structure of tourmaline and biotite. A high concentration of Li in biotite from granitic rocks has been reported by Vorontrov and Lin (1969) and Baratov (1975).

Strontium content ranges from 260-490ppm and shows a regular increase from foliated to porphyroblastic migmatites. These migmatites are characterised by high K/Sr ratio, which ranges from 100-200. The variability in the concentration of Sr in these rocks may be explained due to the effects of anatexis (McCarthy, 1976; Kays, 1976). Sr shows nearly positive distribution pattern with CaO and a negative pattern with K_2O indicating that their concentration is mainly controlled by plagioclase.

Ba shows large variability in its concentration and ranges from 410-1450ppm. The possible effects of anatexis and the distribution of Ba are poorly known but the argument used above for Sr may be applicable for Ba (McCarthy, 1979; Kay, 1976). Barium shows close resemblance with Li content, whereas Sr indicates negative correlation in a few samples. This may either be due to original composition of the rocks or due to variability in the intensity of migmatization. Ba shows nearly a positive correlation with K (Fig. 6.9), indicating that Ba content to a greater extent might have been diadochically substituted in the structure of K-feldspar and/or biotite with the replacement of K^+ . A negative correlation with CaO indicates that Ba is poorly concentrated in plagioclase.

The migmatites occurring on the northern side of the Bhatwari Group (Agra migmatite) occupy a different position, as evident from comparatively higher value of K/Ba (100) ratios. In the remaining portions, migmatites show a large dispersion

in K/Ba ratios ranging from 30 to 70. The Agra migmatites can be again separated from the Bhatwari (exposed on the southern side) and the Suki migmatites on the basis of Ba vs. Sr plot (Fig. 6.9). The Agra migmatites are characterised by Ba/Sr ratio between 1 and 2 whereas Ba/Sr ratio in the remaining migmatites ranges from 2-5. Different behaviour of the Agra migmatites could be due to poor intensity of migmatization (as evident from field, microscopic and major oxides data) or due to variability in the composition of original rock (paleosome).

Co and Ni: Co content remains almost constant during migmatization and ranges from 84-90ppm, whereas Ni content shows variation from 54-137ppm.

Cobalt and nickel might have been diadochically substituted in the mineral structures of ilmenite and tourmaline by replacing Mg^{2+} and Fe^{2+} , because these elements show positive distribution with MgO, FeO, and TiO_2 (Wedepohl, 1972). Co vs. Ni plot reveals that many samples are characterised by Co/Ni ratio >1 , whereas in a few samples Co/Ni ratio varies from 0.7 to 1.0. It seems possible that migmatites of this area, being evolved by anatexis of crustal material might have Co/Ni ratio >1 , have similar analogy as has been propounded for hydrothermal deposits (Bralia et al., 1979; see also Chapter 7).

Sb and Bi: Antimony and bismuth range from 75-320 and 150-450ppm respectively. Sb preferentially enters the structure of ilmenite with the replacement of Fe^{2+} (Wedepohl, 1972). In the present case, a negative correlation has been observed between TiO_2

Strontium content ranges from 260-490ppm and shows a regular increase from foliated to porphyroblastic migmatites. These migmatites are characterised by high K/Sr ratio, which ranges from 100-200. The variability in the concentration of Sr in these rocks may be explained due to the effects of anatexis (McCarthy, 1976; Kays, 1976). Sr shows nearly positive distribution pattern with CaO and a negative pattern with K_2O indicating that their concentration is mainly controlled by plagioclase.

Ba shows large variability in its concentration and ranges from 410-1450ppm. The possible effects of anatexis and the distribution of Ba are poorly known but the argument used above for Sr may be applicable for Ba (McCarthy, 1979; Kay, 1976). Barium shows close resemblance with Li content, whereas Sr indicates negative correlation in a few samples. This may either be due to original composition of the rocks or due to variability in the intensity of migmatization. Ba shows nearly a positive correlation with K (Fig. 6.9), indicating that Ba content to a greater extent might have been diadochically substituted in the structure of K-feldspar and/or biotite with the replacement of K^+ . A negative correlation with CaO indicates that Ba is poorly concentrated in plagioclase.

The migmatites occurring on the northern side of the Bhatwari Group (Agra migmatite) occupy a different position, as evident from comparatively higher value of K/Ba (100) ratios. In the remaining portions, migmatites show a large dispersion

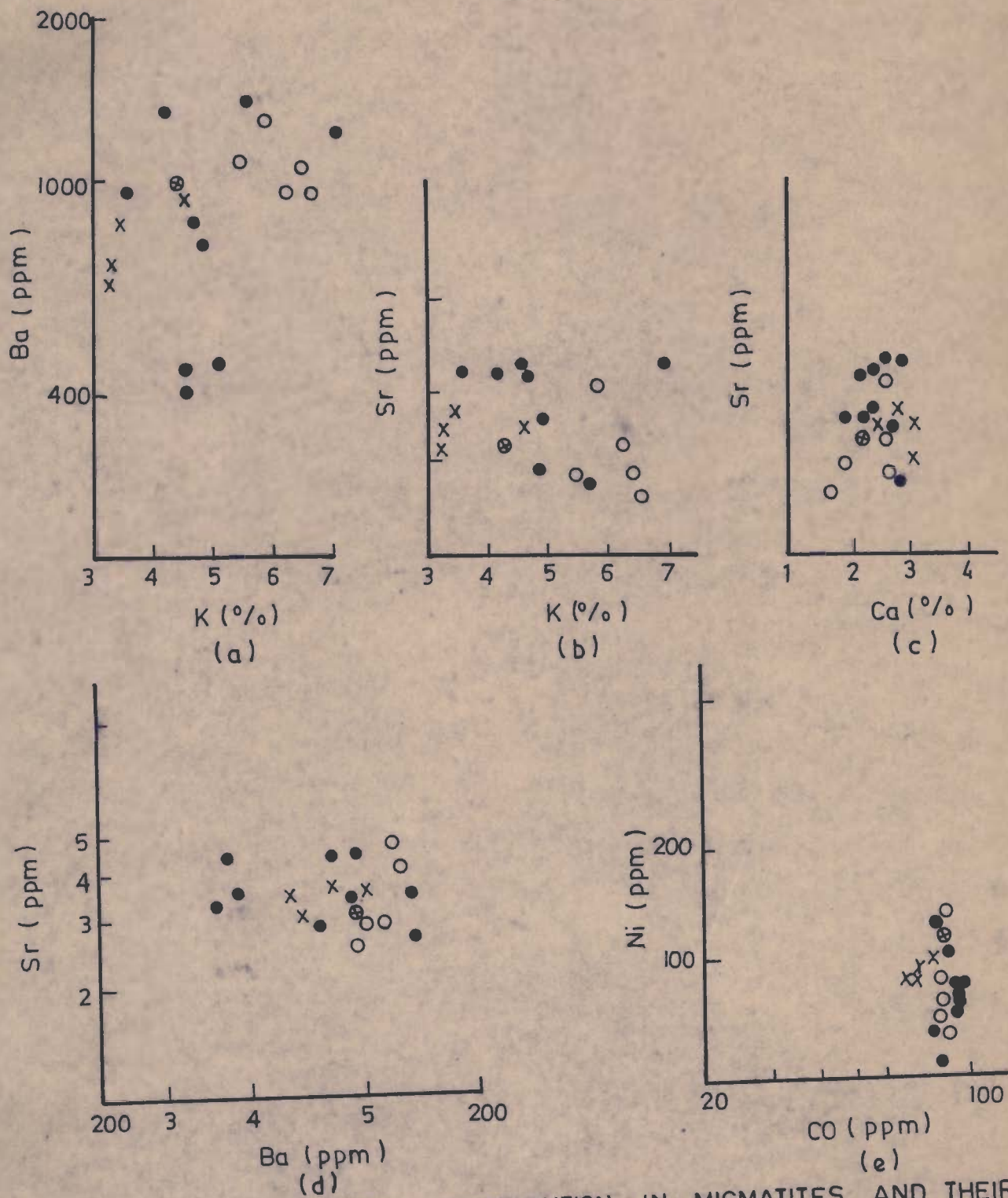


FIG. 6-9 - TRACE ELEMENTS DISTRIBUTION IN MIGMATITES AND THEIR COUNTRY ROCKS

(a) K VS Ba, (b) K VS Sr, (c) Ca VS Sr, (d) Ba VS Sr, (e) Co VS Ni

in K/Ba ratios ranging from 30 to 70. The Agra migmatites can be again separated from the Bhatwari (exposed on the southern side) and the Suki migmatites on the basis of Ba vs. Sr plot (Fig. 6.9). The Agra migmatites are characterised by Ba/Sr ratio between 1 and 2 whereas Ba/Sr ratio in the remaining migmatites ranges from 2-5. Different behaviour of the Agra migmatites could be due to poor intensity of migmatization (as evident from field, microscopic and major oxides data) or due to variability in the composition of original rock (paleosome).

Co and Ni: Co content remains almost constant during migmatization and ranges from 84-90ppm, whereas Ni content shows variation from 54-137ppm.

Cobalt and nickel might have been diadochically substituted in the mineral structures of ilmenite and tourmaline by replacing Mg^{2+} and Fe^{2+} , because these elements show positive distribution with MgO , FeO , and TiO_2 (Wedepohl, 1972). Co vs. Ni plot reveals that many samples are characterised by Co/Ni ratio >1 , whereas in a few samples Co/Ni ratio varies from 0.7 to 1.0. It seems possible that migmatites of this area, being evolved by anatexis of crustal material might have Co/Ni ratio >1 , have similar analogy as has been propounded for hydrothermal deposits (Bralia et al., 1979; see also Chapter 7).

Sb and Bi: Antimony and bismuth range from 75-320 and 150-450ppm respectively. Sb preferentially enters the structure of ilmenite with the replacement of Fe^{2+} (Wedepohl, 1972). In the present case, a negative correlation has been observed between TiO_2

and Sb, thus lending little support to this possibility. Antimony shows a sympathetic behaviour with FeO, MgO and P₂O₅, reflecting that it could have gone into the structure of tourmaline with the replacement of Fe²⁺ and Mg²⁺ and/or in apatite with the replacement of Ca²⁺. A positive correlation of Bi distribution with P₂O₅ indicates that this element has probably been concentrated in the structure of apatite by replacing Ca²⁺.

The Sb/Bi ratios have been utilized as a geothermometer in sulphide deposits (Malakhov, 1968 in Vaughan, 1976). The Sb/Bi ratio in sedimentary deposits is $\gg 6$, whereas igneous deposits are characterised by Sb/Bi ratio $\ll 1$, Sb/Bi ratio is close to 1.0 in these migmatites, therefore it can be inferred that these rocks could have been formed due to anatexis. On the basis of arguments presented above, it would be worth investigating the applicability of Co/Ni and Sb/Bi ratio for the genesis of migmatite.

6.3 GENESIS OF MIGMATITE

The genesis of migmatites of Himalayas has been a matter of controversy because of the heterogeneous nature and complex structure of these rocks. The origin of Himalayan migmatites has been explained on the basis of commonly accepted ideas of injection hypothesis, metasomatism, metamorphic differentiation or anatexis (cf., Hyndman, 1972; White, 1966; Page, 1968).

Migmatites are commonly associated with orogenic belts due to steeper geothermal gradient prevalent in such belts (Mehnert, 1968). The association of migmatites with medium

to high grade metamorphites is a very common feature in the Himalaya as reported by Heim and Gansser (1939), Gansser, (1964), Jhingran et al. (1976), Thakur (1977) and GSI (1976). However, migmatites are also associated with low grade metamorphites in certain localities (Kashyap, 1972). From the literature survey, a brief account on the origin of Himalayan migmatites has been discussed here.

Misch (1949) thoroughly investigated the granitic rocks and associated metamorphites of the Nanga Parbat region and suggested a synkinematic granitization on a batholithic scale. The granitization phenomena begin at the kyanite zone which have led to the formation of banded, augen and prophyroblastic migmatites due to lit-par-lit replacement.

The migmatite bands (75-110m in width), associated with the green schist facies rocks in the Ramgarh (Nanital) area, seem to have been formed due to alkali metasomatism in which soda phase was followed by potash phase (Kashyap, 1972).

Wakholo and Dhar (1972) identified a zone of permeation associated with kyanite and sillimanite schists of Kishtwar (Kashmir) area. The breakdown of muscovite into K-feldspar and other evidences led them to conclude that these migmatites have been produced due to the process of anatexis and mobilization.

For the migmatites associated with Jutogh metasediments of Narkanda (Simla) area Viridi (1976) suggested a alkali metasomatism in two stages - soda metasomatism followed by

potash metasomatism with mineral assemblages revealing migmatization taking place under P-T conditions of middle amphibolite facies.

In the Almora Crystallines of the Simla-Dudatoli-Almora Thrust Sheet, Agarwal et al. (1972) worked out the petrogenesis of granitic rocks occurring as sheet-like bodies in which the study of field, textural and optical characters of feldspar led them to conclude that these bodies have been formed due to the introduction of granitic material along the foliation planes. Within some sequence of south Almora region Desai (1973) proposed alkali metasomatic origin for migmatites. While Karnath and Shah (1977) opined intrusion of the semi-consolidated anatectic melt in the form of sheets at great depth into the metasediments in Almora and Kapleshwar and granitization of adjacent rocks. According to them, emplacement of granitic rocks and local granitization took place prior to the nappe movement. Kapila et al. (1980) proposed a lit-par-lit replacement origin for the migmatites associated with metamorphites of Mukteswar (Nainital) area. Further, they concluded that the granitic melt was formed due to the reactivation of basement during the Himalayan Orogeny and ruled out the possibility of in situ anatexis due to absence of breakdown of muscovite to K-feldspar and sillimanite. For the granitic gneisses of Dwarahat, Das (1979) concluded that these rocks have been formed due to the reactivation and mobilization of granitic mass with the metamorphic mineral assemblages revealing P-T

conditions of about 550-600°C at about 4 Kb PH_2O which are insufficient to produce in situ anatexis.

Gupta (1978, 1979) studied the rocks of Badrinath-Mana pass area of the Central Crystallines and suggested anatectic origin for granitic rocks associated with metamorphites under upper amphibolite facies on the basis of the following evidences: (i) presence of sillimanite-cordierite-K-feldspar-almandine assemblage, (ii) association of tourmaline and mobilizates with paleosome, suggesting a pneumatolitic activity in the area and (iii) association of pegmatite with Badrinath complex indicative of an advanced stage of anatexis.

On the basis of petrological data, Gupta and Dave (1979) proposed an anatectic-cum-lit-par-lit replacement origin for the migmatites of the Central Crystallines of the Bhagirathi Valley. However, none of the earlier workers have recognised two separate stages of migmatization in the Central Crystallines, which is generally considered as monolithic thick pile of meta-sediments and migmatites.

6.3.1 Migmatites from the present area

As has been already described, the Central Crystallines from the Bhagirathi and Yamuna Valleys are comprised of two distinct litho-tectonic groups, namely the Bhatwari Group and the Suki Group; the former revealing an earlier phase of metamorphism (M_1), deformation (D_1) and first phase of migmatization than the Suki Group. The genesis of migmatites has, therefore, to be viewed from this angle. Whereas petrological

and structural criteria make it possible to decipher two distinct phases of migmatization in the Bhatwari Group geochemical criteria are not convincing enough to differentiate between the two groups. The various criteria associated with migmatites of the Bhatwari and Suki Groups have been discussed together but, wherever differences are noticed, they are highlighted in ensuing text.

Field Criteria: (a) The presence of ptygmatic, phlebitic, stromatic, ophalmitic and schlieren and rarely nebulitic structures (Mehnert, 1968). The ophalmitic and schlieren structures are commonly recorded in the Bhatwari and Suki migmatites. The remaining structures are associated with schistose and streaky migmatites and are uncommon in the area.

In ptygmatic structure, the leucosome (granitic or aplitic or pegmatitic portion) shows conformity with the paleosome with irregular outlines. At places, leucosome encloses biotite or hornblende forming a part of paleosome. Phlebitic (veins) structure is seen in mica schist and amphibolite, which are traversed by granitic material resulting into irregular occurrences of biotite or hornblende. The granitic veins are broadly concordant with the foliation. At times, neosome of this structure contains segregation of biotite and/or amphibole.

Stromatic structure is recorded in schist and gneiss (paleosome) of both the groups. The neosome shows gradational (rarely sharp) contact with the paleosome. The field observations

suggest that this structure has formed due to (i) the enrichment of granitic or aplitic or pegmatitic material along the foliation planes, (ii) lensoidal nature of porphyroblasts (feldspar or quartz), (iii) selective segregation of various mineral components, during metamorphism. This feature is only recorded at one locality (Malla) in the Bhatwari Group.

Further, it has been noticed that the leucocratic bands contain segregations of biotite (rarely garnet) in the Bhatwari Group and biotite, garnet and kyanite in the Suki Group.

Ophthalmitic structure is the most common feature in both the Bhatwari and Suki Groups. With the increased intensity of migmatization, stromatic structure grades into ophthalmitic (augen). The augen or porphyroblasts are rectangular or squarish, subrounded and rarely elliptical in shape and are bordered by schistose portion. Feldspar (rarely quartz) augen or porphyroblasts show broad parallelism with the foliation. Feldspar augen seldom show rotation, which is seen only in the Bhatwari Group. The studded nature of augen or porphyroblasts with crude foliation suggest that they have grown due to lit-par-lit replacement (Kapila et al., 1978). However, near the tectonic zones, some of them might have formed due to subsequent deformations particularly in the Bhatwari Group.

Schlieren structure is commonly associated with ophthalmitic migmatites and shows darker streaks of mainly biotite in neosome having tapering ends with irregular to sharp margins. In certain localities, biotite or hornblende schlieren are also recorded

in the stromatic and streaky migmatites. Nebulitic structure is occasionally seen in granitoid migmatite in which paleosomes can only be recognised by faint coloured variations. Rarely, one can find diktyonitic structure along the tectonic zones. This structure has been formed due to filling in of shear planes by late phase aplitic or pegmatitic material.

- b) Concordant attitude of structural elements such as foliation, lineation and minor folds in migmatites with the country rock remnants are indicative of synkinematic migmatization (Kizaki and Hayashi, 1979). This argument can be further supported by the alignment of feldspar augen or porphyroblasts parallel to the main foliation showing lit-par-lit replacement
- c) The gradational contact between neosome and paleosome, lack of thermal aureole or chilled margins at the junction of neosome with paleosome does support the forceful injection in the area (Dietrich, 1960; Hyndman, 1972). However, the migmatite of the Bhatwari Group at Sayana Chatti in the Yamuna Valley shows sharp contacts with the country rocks without metamorphic cell or chilled margins, which could be the result of lit-par-lit injection (Buddington, 1958; Reesor, 1965).
- d) The coarsening of quartzo-feldspar portion from non-migmatized or least migmatized to augen or porphyroblastic migmatized indicative of lit-par-lit replacement (Misch, 1949; Ramberg 1952; Kapila et al., 1980).

- e) There are no direct evidences of anatexis in rocks of the Bhatwari Group, because these have been metamorphosed only upto garnet grade. The chemical data do indicate an anatexis origin for the migmatizing fluids. Migmatization is related to a distinct source which is also indicated by migmatite bands in amphibolite. The neosome bands have been formed due to replacement and reaction as is evidenced by remnants of amphibole in them and formation of biotite along the margins and cleavages of amphibole. Absence of structures indicative of forceful injection during emplacement of migmatizing fluids favours the idea of lit-par-lit replacement (Misch, 1949).

The rocks of the Suki group, which grade upto sillimanite-bearing assemblage, do provide evidences of anatexis. Near Jhala, for example, lenses and veins of leucosome are found in the garnet-kyanite (rarely sillimanite) schist (restites). The neosome activity increases in the same locality, especially where migmatizing fluids could soak the country rocks, as is evident by the growth of K-feldspar and plagioclase along with quartz, which ultimately give rise to porphyroblastic migmatite.

- f) Large dimension of migmatite bands in comparison to the remnants of country rocks rule out the possibility of their formation by metamorphic differentiation (Hyndaman, 1972).
- g) According to Dietrich (1960), Mehnert (1968), Winkler (1976, 1979), association of concordant aplite and pegmatite bodies with schist and gneiss undergone medium to high

grade metamorphism in a migmatized terrain is an indicative of anatexis. This argument applies well to the Suki migmatite. Linear arrangement of tourmaline in aplite and pegmatite veins is suggestive of the flow direction of migmatizing fluids.

- h) Association of biotite selvages with leucosome in migmatized schist, gneiss and amphibolite of both the groups suggest that the migmatizing fluids could be of anatectic origin (Hughes, 1970).

Microscopic Criteria: Metasomatic origin of migmatite occurring in the Bhatwari and Suki Groups is well documented by the following textural and mineralogical evidences.

- (a) Perfect transformation of quartz-mica schist and garnetiferous mica schist to augen or granitoid migmatite through foliated and banded migmatites showing gradual increase in feldspar content and depletion in quartz content. In the Suki Group, kyanite schist or sillimanite gneiss gradually passes to porphyroblastic migmatite through stromatic (banded) migmatite in a narrow zone, which is indicative of lit-per-lit replacement (Desai, 1973).
- (b) On the basis of textural evidences, (Chapter 4), it has been shown that the sequence of formation of feldspar is as follows:

K-feldspar II - Mainly microperthitic; microcline twins visible in patches and contains inclusions of rounded

quartz, subrounded to subhedral plagioclase I and/or subhedral plagioclase II; also shows intergrowth with Plagioclase II.

Plagioclase II - Clear and occurs as inclusion in K-feldspar II or as rims around Plagioclase I, especially when in contact with K-feldspar II.

Plagioclase I - Highly sericitised and deformed showing patchy inclusions of K-feldspar I or occurs as inclusion in later feldspar.

K-feldspar I - Occurs as separate grains or as inclusions in Plagioclase I; twinning uncommon.

From the nature of K-feldspar II and its relation with plagioclase II, it is apparent that the crystallization of both the minerals was simultaneous for some time. However, K-feldspar II continued to grow later. The occurrence of inclusions of plagioclase I and quartz in K-feldspar II porphyroblasts suggests a time gap between the formation of feldspar and crystallization in two phases. This is supported by the following additional evidences (Chapter 4):

- (i) Plagioclase I showing parallelism with S_1 foliation which has been subsequently isoclinally folded by the F_2 folds having S_2 axial plane foliation marked by muscovite-biotite-lepidoblasts. It is not rare to get plagioclase I surrounded by K-feldspar II porphyroblast in conformity with biotite and muscovite.

- (ii) Plagioclase II has grown along S_2 foliation which is a distinctly later structural event as axial plane foliation of F_2 folds. The structural history of the migmatites have been discussed elsewhere (Chapters 3 and 4).

On the basis of above evidences, it has been suggested that the Bhatwari Group has undergone two stages of migmatization:

- (1) First phase is characterized by potash metasomatism followed by soda metasomatism;
- (2) Second phase is characterized by soda metasomatism followed by K-metasomatism.

It may be worthwhile to emphasize that feldspar of the second phase, is not prominent in the Bhatwari Group migmatites wherever present, except in the granitoid migmatite of the Yamuna Valley. The replacement of plagioclase I and II by K-feldspar II has led to the formation of patchy, stringer and film perthites. Further, it has been noticed that, wherever myrmekitic intergrowth took place, the feldspar is perthitic in character indicating that the phenomena of myrmekitization is related to the formation of perthite (Kashyap, 1972).

The K-feldspar II porphyroblasts, at times, contain obscure carlsbad twinning and show indistinct, patchy and complete cross-hatching. Complete cross-hatched twinning is seen at Suki. This feature has been observed by some workers in certain parts of the Lesser Himalaya and Archean terrains where it has been suggested that microcline perthite has been

formed by inversion of an earlier high temperature polymorphic (orthoclase) due to tectonic upliftment (Chaudhari and Narayan Rao, 1966; Agarwal et al., 1972). The predominance of orthoclase-perthite is an indicative of P-T conditions of amphibolite facies, because orthoclase-microcline transformation takes place at that stage (Marmo, 1958). The presence of orthoclase and intermediate microcline in the Bhatwari Group migmatites and intermediate to maximum microcline in the Suki Group migmatite as evidenced from X-ray reflection peaks supports this argument (Chapter 4).

Formation of discontinuous rims of albite around sericitized plagioclase I and K-feldspar II in migmatite could be explained due to reactions between the former and the latter, as evident from textural relations. For the Almora granite gneiss, Desai (1973) suggested a late sodic phase metasomatism, probably connected to the pegmatitic activity with orthoclase originating at depth, while the rims of albite growing after the gneiss was uplifted to low structural level. Misra and Sharma (1966) and Mehta (1977) thought post kinematic potassic solutions affecting the pre-existing solid rocks and developing albite rims along the contact of plagioclase by a process of decalcification of latter in the Devidhura gneiss and from Kulu respectively (also, Merh and Vaghi, 1965). Hanmer (1982) suggested that both plagioclase (An_{29}) and K-feldspar are transformed to albite with increasing strain and emphasized that the transformation to albite is due to interaction of

metamorphic and structural processes at the grain scale.

In the Suki Group, however, K-feldspar II occurs as subhedral crystals in intragranular spaces as well as marginal replacement of plagioclase. It appears, therefore, that there was some melting involved in the Suki Group and that the anatexis took place comparatively closer to these rocks. Inclusions of quartz or plagioclase II along with those of biotite are also seen in these K-feldspar II (essentially microcline-microperthite), thus indicating its paragenesis.

(c) The presence of almandine-kyanite-cordierite-sillimanite assemblage in the migmatite zone of the Suki Group is a characteristic feature of anatectic migmatite (Hensen and Green, 1971; ^{both cited in Winkler, 1976} Currie, 1971) and Kizaki and Hayashi, 1979). Evidences of breakdown of muscovite into sillimanite have been noticed indicating the possibility of insitu anatexis.

(d) Plagioclase (I and II) and K-feldspar generally occur as subhedral grains. The plagioclases show complex twinning, zoning and fading of twin lamellae. The above behaviour of feldspar in both the groups indicate its crystallization from a melt (Hibbard, 1965; Aswarth, 1976).

Mineralogical criteria: From the previous discussions, it has clear that these migmatites have been formed mainly due to the process of lit-par-lit replacement. A look at the modal analysis of migmatites (Tables 6.5, 6.6,; Fig.6.10) enables us to study the mineralogical changes taking place during the process of migmatization of the average country schistose rock.

TABLE 6.6 MODAL ANALYSIS FOR MIGMATITES AND THEIR COUNTRY ROCKS
OF THE YAMUNA VALLEY(VOL %)

Sample No/ Mineral Component	697	705	707	733	711	699	744	848	853	763
Quartz	41.06	35.89	22.47	34.19	48.75	39.52	35.39	35.27	30.24	44.91
Plagioclase	15.89	18.55	26.19	21.20	6.56	13.86	28.61	22.04	31.19	10.20
K-feldspar (including perthite)	8.49	28.12	27.12	17.05	1.51	16.29	21.16	27.15	12.08	1.65
Biotite	20.85	4.29	12.23	13.60	25.32	21.29	5.38	6.18	10.77	15.35
Muscovite	10.81	10.38	8.93	10.87	13.45	6.37	4.19	7.12	11.56	19.03
Hornblende	-	-	-	-	-	-	-	-	-	-
Garnet	-	-	-	-	-	-	-	-	-	5.36
Kyanite	-	-	-	-	-	-	-	-	-	-
Chlorite	0.45	0.23	1.61	0.49	1.63	0.34	1.45	0.21	0.26	0.16
Accessaries (apatite, tourmaline, ilmenite, rutile,etc.)	2.45	2.54	5.45	3.94	2.78	2.33	3.82	2.03	3.90	2.22

711 - Quartz mica schist
763 - Garnetiferous mica schist
697, 705, 707, 733) - Augen migmatite (and its variance)
699, 744, 848, 853)

TABLE 6.6 MODAL ANALYSIS FOR MIGMATITES AND THEIR COUNTRY ROCKS OF THE YAMJNA VALLEY (VOL %)

Sample No./ Mineral Component	882	768	877	864	791	806	892	896	805	Average schist
Quartz	40.24	40.41	51.45	40.01	46.48	45.31	34.00	38.34	38.18	47.38
Plagioclase	24.26	24.00	12.85	28.41	6.61	4.22	29.62	26.54	32.73	8.05
K-feldspar (including perthite)	10.35	16.68	3.48	9.03	4.31	2.61	8.64	8.40	9.0	2.72
Biotite	11.58	9.13	16.20	13.63	20.46	30.00	13.73	11.04	10.51	20.47
Muscovite	10.10	8.08	8.50	4.43	6.56	11.60	19.20	10.67	7.20	10.63
Hornblende	-	-	-	-	5.88	-	-	-	-	ND
Garnet	-	-	1.70	-	11.63	3.36	1.55	2.45	-	ND
Kyanite	-	-	3.31	-	-	-	1.29	-	-	ND
Chlorite	0.22	-	-	0.49	6.46	-	-	-	-	ND
Accessories (apatite, tourmaline, rutile, etc.)	3.27	1.70	2.51	3.94	3.67	2.86	2.06	2.56	2.38	ND

791 - Garnetiferous mica schist
 807 - Kyanite schist
 892, 768, 864) -
 806, 892, 896 } Porphyroblastic Migmatite
 805 }

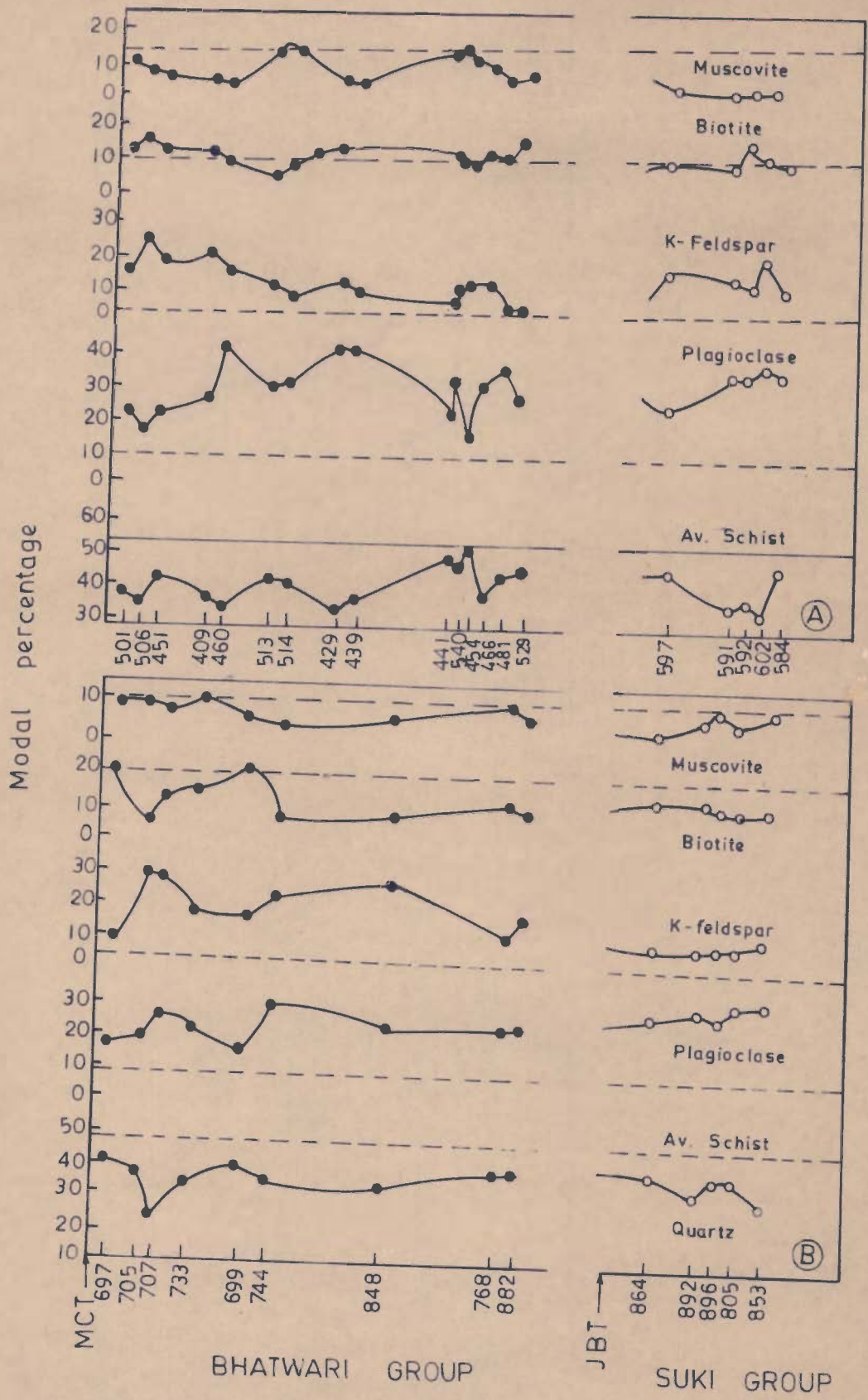


FIG.6-10 - MINERALOGICAL VARIATION IN SPACE NORTHWARDS FROM MCT OR JBT
 A - BHAGIRATHI VALLEY
 B - YAMUNA VALLEY

(a) It would be seen that a significant increase in K-feldspar and plagioclase content and decrease in quartz content are conspicuous. In the Bhatwari Group, enrichment in feldspar and depletion in quartz contents are more prominent in the basal part towards the MCT. This feature suggests that the intensity of migmatization decreases from south to north indicating that the 'zone of anatexis' in the Bhatwari Group was towards south (near the MCT). On the other hand, intensity of migmatization in the Suki Group increases towards the north, suggesting a second anatectic zone on the northern side of the Suki Group. Thus, it can be inferred that there were two anatectic zones in the area during the all pervasive second phase of migmatization.

(b) Biotite decreases northwards along the Yamuna Valley, whereas no appreciable change in its content has been recorded along the Bhagirathi Valley.

(c) A decrease in muscovite content is prominent along the Bhagirathi Valley.

The variation in both the micas may be explained by variation either in the nature of paleosome or in the intensity of migmatization. No clear evidences in favour of one or the other are available.

Chemical evidences: The geochemical consideration of major oxides reveals an addition of Na_2O , K_2O and Al_2O_3 during migmatization of garnet and kyanite bearing rocks, with the depletion of SiO_2 . Slight increase in CaO , MgO and Fe_2O_3 and decrease in FeO contents have also taken place. TiO_2 , P_2O_5 and MnO do not

show appreciable changes. A significant increase in alkalis with decrease in SiO₂ content has taken place in rocks undergone maximum migmatization, thus indicating an addition of alkalis and alumina at the expense of silica. This is exactly what would happen if feldspar grows from quartz. Niggli values also support this argument. In the process of migmatization, a large decrease in Si and an increase in alk values have taken place. No significant change in the al, fm and c values has been noticed.

A high concentration of trace elements such as Ba, Li, Sr and Cu also could be an indication of anatectic source. Co/Ni ratio (>1) and Sb/Bi ratio (<1) in these migmatites indicate that the area has suffered hydrothermal activity. A slight increase in Pb and Zn contents with the degree of migmatization also support the above statement.

Further confirmation regarding the metasomatic transformation of metasediments can be made from the standard cell data, computed on the basis of 160 (O, OH), adopting Barth's (1962) (Table 6.7) for the country rocks and migmatites of the Bhatwari and Suki groups. The gain and loss have been computed for the two groups separately in relation to I_I and I_{II} equations on the basis of following formulas and presented in Table 6.7.

Bhatwari Group

- I. Country rock: Quartz mica schist and garnet mica schist
(average of sample no. 415, 416) K_{3.25} Na_{2.21} Ca_{2.46}
Mg_{4.47} Fe_{3.05} Al_{15.42} Ti_{0.46} Si_{61.87} P_{0.20} (O, OH) 160

TABLE 6.7 STANDARD CELL OF MIGMATITES AND THEIR COUNTRY ROCKS ON THE BASIS OF 160 (O, OH) (BHATWARI GROUP)

	506	451	409	460	415	416	429	439	477	441	481	830	ε34
Si	57.83	61.48	59.40	59.73	62.00	61.73	58.96	58.43	61.09	60.47	60.64	60.63	59.62
Al	16.87	14.69	15.86	15.49	14.65	16.40	15.02	16.08	15.05	15.65	15.25	13.59	16.26
Fe ³⁺	0.79	0.41	0.49	0.49	1.08	0.94	0.78	0.92	1.23	1.02	1.22	0.31	0.75
Fe ²⁺	1.31	1.05	1.71	2.15	1.80	2.28	1.89	1.69	1.42	1.77	1.79	3.08	3.20
Mn	0.38	0.03	0.09	0.05	0.06	0.11	0.04	0.09	0.11	0.06	0.02	0.05	0.05
Mg	3.50	3.92	3.84	3.73	4.56	4.37	4.84	3.48	3.32	3.58	2.96	4.18	3.25
Ca	2.61	2.40	2.26	2.17	2.32	2.61	2.79	2.84	2.81	1.90	2.56	2.61	2.71
Na	4.68	3.66	5.44	6.40	1.94	2.49	4.74	4.93	4.04	3.92	4.36	3.13	1.08
K	7.07	3.57	4.21	4.69	3.26	3.24	4.83	5.73	4.58	5.02	4.49	4.18	3.25
Ti	0.29	0.41	0.21	0.23	0.29	0.62	0.56	0.42	0.11	0.23	0.13	0.31	0.16
P	0.22	0.12	0.26	0.24	0.19	0.21	0.29	0.25	0.21	0.17	0.28	0.20	0.10

TABLE 6.7 (Contd) : STANDARD CELL OF MIGMATITES AND THEIR COUNTRY ROCKS
ON THE BASIS OF 160(O, OH) (SUKI GROUP)

	494	597	591	592	602	584
Si	61.22	58.42	58.15	57.44	56.55	60.10
Al	14.63	15.62	16.81	16.28	17.33	16.05
Fe ³⁺	0.56	0.95	0.62	1.23	1.26	0.40
Fe ²⁺	2.27	1.33	2.18	2.95	2.20	1.50
Mn	0.14	0.06	0.05	0.03	0.15	0.22
Mg	2.52	4.22	3.47	5.28	4.75	3.18
Ca	2.28	2.75	2.62	1.65	2.48	1.88
Na	2.98	6.61	6.22	5.86	6.29	4.64
K	4.35	6.50	6.27	6.65	5.87	5.45
Ti	0.44	0.18	0.24	0.29	0.50	0.54
P	0.21	0.22	0.29	0.11	0.25	0.21

TABLE 6.7 GAIN AND LOSS IN STANDARD CELLS DURING MIGMATIZATION

	Bhatwari Group		Suki Group	
	Gain	Loss	Gain	Loss
Si	-	3.13	-	3.58
Al	0.45	3.4	1.88	-
Fe ³	-	0.29	0.46	-
Fe ²	-	0.28	-	0.07
Mn	0.06	-	-	-
Mg	-	0.58	1.91	-
Ca	0.14	-	0.10	-
Na	2.98	-	3.26	-
K	2.33	-	1.97	0.14
Ti	-	0.08	-	-
P	0.05	-	0.02	-
	6.01	4.36	9.6	3.79

II. Augen migmatite: (average of sample no. 439, 506, 429, 460)

$K_{5.58} Na_{5.19} Ca_{2.60} Mg_{3.89} Fe_{2.50} Al_{15.87} Ti_{0.38} Si_{58.74}$
 $P_{0.25} (O, OH) 160$

Suki Group

I. Kyanite schist (sample no. 494) $K_{4.35} Na_{2.98} Ca_{2.28} Mg_{2.52}$
 $Fe_{2.83} Al_{14.63} Ti_{0.44} Si_{61.22} P_{0.21} (O, OH) 160.$

II. Porphyroblastic migmatite: (average of sample no. 591, 592,
 597, 602) $K_{6.32} Na_{6.24} Ca_{2.38} Mg_{4.43} Fe_{3.18} Al_{26.51} Ti_{0.30}$
 $Si_{57.64} P_{0.23} (O, OH) 160$

Gain and loss calculations do not support isochemical transformation of the country rocks into augen and porphyroblastic migmatites and reveal an extensive loss in Si and gain in Na and K. during migmatization. The above conditions do not support the metamorphic differentiation as an important process for the genesis of migmatite associated with the Bhatwari and Suki Group of rocks.

6.4 P-T CONDITIONS

As evident from the earlier discussions, the Bhatwari Group is metamorphosed upto garnet grade and the Suki Group upto sillimanite grade. The mineral assemblages of the Bhatwari Group migmatites and their country rocks (quartz + K-feldspar + albite + biotite + muscovite + almandine ± hornblende ± chloritoid) reveal that the P-T conditions were insufficient to produce insitu anatexis, although the available field, textural

and chemical evidences do support the origin of the Bhatwari Group migmatite by lit-par-lit replacement. Comparatively low value of triclinicity (Δ) in feldspar (Table 4.2) and presence of microcline patches in K-feldspar developed at high temperature (Rao and Raju, 1977) is indicative of polymorphic transformation. Further, the Bhatwari Group is characterised by normal metamorphic sequence. Therefore, it can be said that the P-T conditions were probably sufficient to produce anatectic melt at deeper level or it could have been formed due to the remobilization of the basement.

On the other hand, the Suki Group of migmatite and its country rocks are characterised by the following mineral assemblages:

- a) Quartz + albite (or oligoclase) + biotite + muscovite + K-feldspar + almandine.
- b) Quartz + oligoclase (or albite) + biotite + muscovite + K-feldspar + almandine + kyanite + cordierite.
- c) Quartz + muscovite + oligoclase + sillimanite.

On matching the Al_2SiO_5 -bearing assemblages of the country rocks and the anatectic portion exposed around Jhala with reaction curves given by Storre and Karotke (1971), Merrill et al. (1970) and Tuttle and Bowen (1958), it is inferred that the anatexis has taken place at a temperature of 650 to 680°C and at a pressure of 6.0 to 7Kb. Almost similar results were obtained from P-T diagram, proposed by Hensen and Green (1971) and Currie (1971), ^{cited in Winkler, 1976} for coexisting Crd + Alm + Sil + Qz at various $FeO/(MgO + FeO)$ ratios of the bulk

composition. In the Suki Group, $\text{FeO}/(\text{MgO} + \text{FeO})$ ratio varies from 0.37 to 0.62 (Fig. 6.11), Rocks of the Suki Group fall close to the anatexis minima which is defined by a temperature of 640 to 670°C and a pressure of 6 to 7Kb. (Fig. 6.11).

Normative mineral plots (O-Ab-Or and An-Ab-Or, Table 6.8, Fig. 6.12) suggest depletion in An and enrichment in Ab and Or contents during the formation of migmatites. These plots were matched with experimental P-T diagrams as proposed by Winkler (1976). It was found that in Ab-Or diagram at 5Kb ($P_{\text{H}_2\text{O}} = 5\text{Kb}$), all the points occupy the position between 670° to 700°C isotherms, whereas at 7Kb ($P_{\text{H}_2\text{O}} = 7\text{Kb}$) these points fall between 655-685°C isotherms. On comparing these data with An-Ab-Or plot ($P_{\text{H}_2\text{O}} = 5\text{Kb}$), it was noticed that all the points fall in a region occupied by 670-700°C isotherms, whereas at $P_{\text{H}_2\text{O}} = 7\text{Kb}$, isotherms value between 655-670°C.

TABLE 6.8 NORMATIVE MINERALS OF MIGMATITES AND THEIR COUNTRY ROCKS OF THE AREA (BHATWARI GROUP)

Sample No./ Normative mineral	506	451	409	460	415	416	429	439	471	441	481	830	835
Q	14.82	35.51	25.45	19.51	41.43	37.94	22.56	19.08	29.76	29.20	29.56	35.36	32.68
Or	36.70	18.90	22.24	24.46	16.68	16.62	25.02	30.02	23.91	26.13	23.35	16.57	21.57
Ab	22.53	18.34	26.72	31.96	9.43	12.00	23.06	24.10	19.91	19.29	21.48	15.14	7.07
An	13.34	11.87	9.65	9.29	10.29	11.59	11.95	12.51	12.79	8.67	10.93	11.43	13.09
C	0.31	2.89	2.48	0.78	5.31	6.34	1.22	0.51	1.53	3.24	2.19	3.76	5.15
Hy	8.51	8.63	8.95	11.34	9.17	11.26	11.61	8.98	8.28	9.34	9.31	14.18	12.59
Di	-	-	-	-	-	-	-	-	-	-	-	-	-
Mt	1.62	0.91	1.16	1.07	2.32	2.02	1.63	1.86	2.78	2.32	2.46	0.79	1.62
Il	0.76	1.20	0.61	0.65	0.84	1.73	1.52	1.06	0.32	0.61	0.38	0.91	0.58
Ap	0.62	0.31	0.78	0.79	0.56	0.59	0.84	0.72	0.62	0.49	0.81	0.68	0.59

TABLE 6.8 NORMATIVE MINERALS OF MIGMATITES AND THEIR COUNTRY ROCKS OF THE AREA (SUKI GROUP)

Sample No/ Element	494	597	591	592	602	584
Q	35.53	11.46	12.49	11.93	13.69	25.38
Or	22.80	33.36	32.25	33.92	27.80	28.91
Ab	14.67	31.96	29.87	28.30	26.20	23.06
An	10.12	6.39	11.40	6.48	13.73	8.34
C	2.66	-	-	1.19	1.08	2.65
Hy	5.02	6.42	9.97	13.31	12.04	8.65
Di	-	6.18	0.69	-	-	-
Mt	1.16	2.09	1.32	2.55	2.32	0.93
Il	1.22	0.46	0.70	0.82	1.52	1.52
Ap	0.62	0.62	0.59	0.62	0.72	0.56

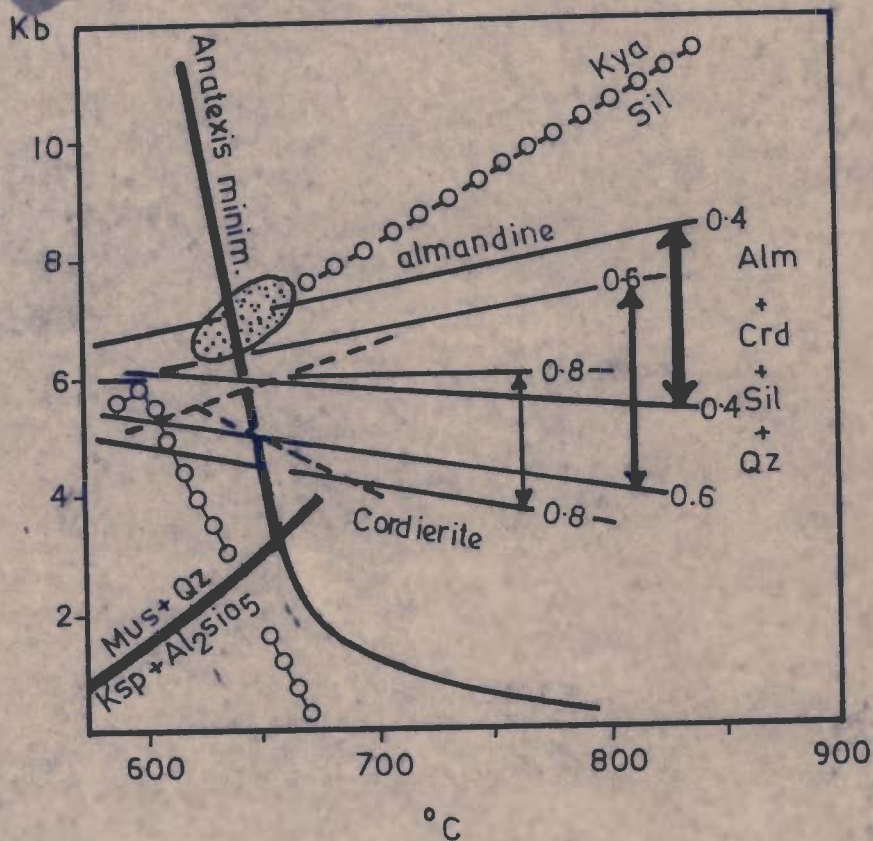


FIG. 6.11 - P-T DIAGRAM OF COEXISTING $\text{Crd} + \text{Alm} + \text{Sil} + \text{Qz}$ FOR VARIOUS $\text{FeO}/(\text{MgO} + \text{FeO})$ RATIOS OF THE BULK COMPOSITION SHOWING ALSO THE REACTIONS DEFINING THE BOUNDARY BETWEEN MEDIUM-GRADE AND HIGH-GRADE METAMORPHISM AND THE APPROXIMATE PHASE BOUNDARIES-KYANITE/SILLIMANITE AND ANDALUSITE/SILLIMANITE. POSITION OF THE SUKI GROUP ANATECTIC ZONE IS SHOWN BY ENCLOSEUR.

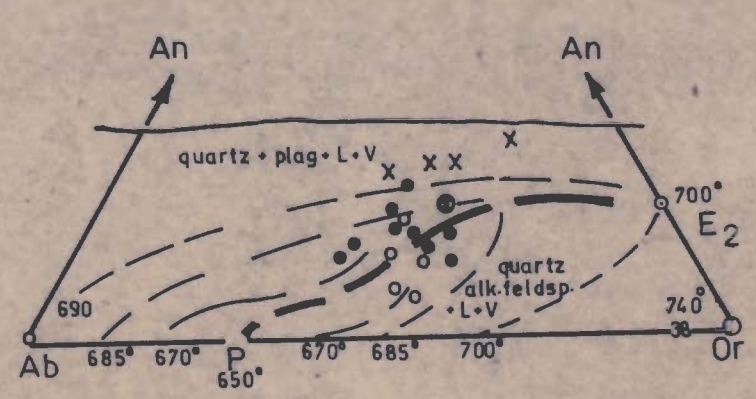
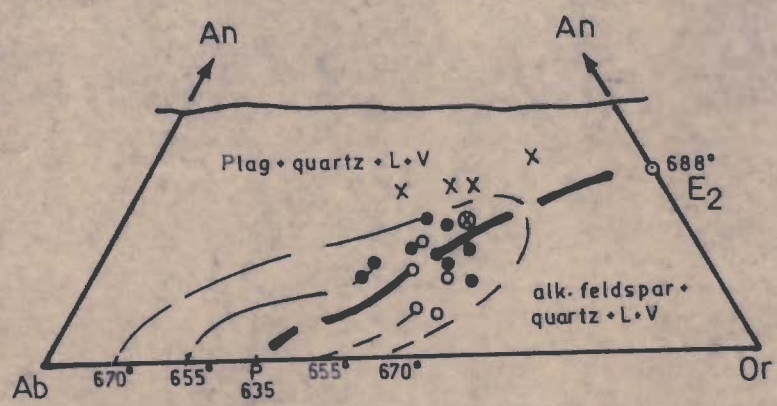
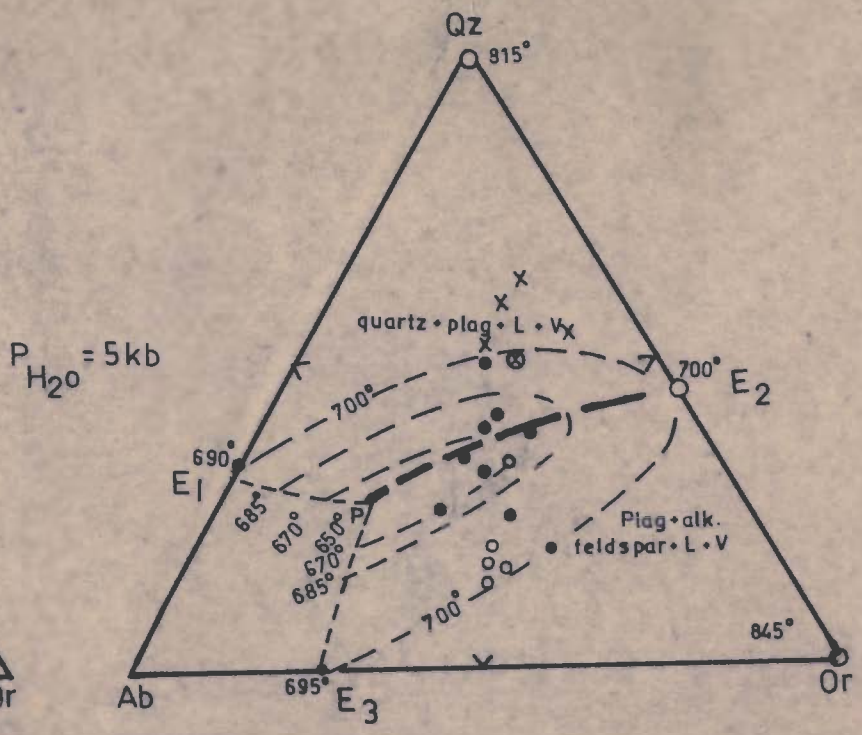
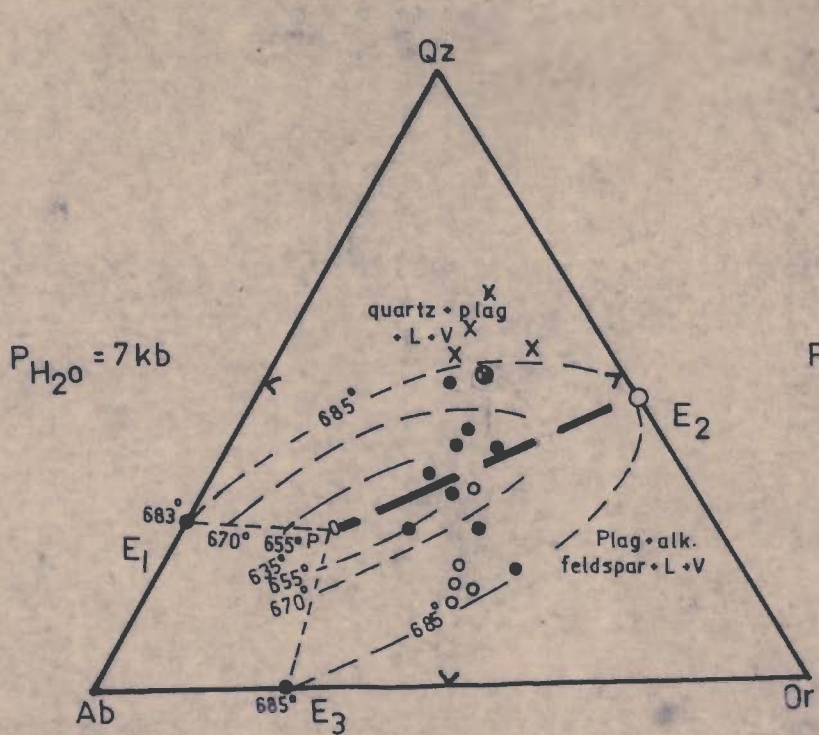


FIG.6.12-PROJECTIONS OF COTECTIC LINE P-E2 AND ISOTHERMS THAT ARE LOCATED ON THE THREE COTECTIC SURFACES OF THE SYSTEM Qz-Ab-Or-An-H₂O. DATA VALID FOR 5 kb and 7 kb WATER PRESSURE (MODIFIED AFTER WINKLER, 1976)

CHAPTER - VII

SULPHIDE MINERALIZATION

Fluid inclusions are thermodynamically isolated microgeochemical system entrapped in various minerals during their growth. Each inclusion entrapped and isolated in one of the zones of a growing crystal records the state of mineral forming media at the moment of entrapment. In the present work, they have been utilized to evaluate temperature of formation of quartz associated with sulphide mineralization. Three occurrences of sulphide mineralization have been encountered at Janki Chatti, Banas and Pindki areas within the Janki Chatti Formation and the Bhatwari Group (Fig. 2.1). The mineralization is related to quartz and quartz-calcite veins.

Geothermometric studies have been carried out using decrepitation techniques. Homogenization method envisages that mineral forming media are entrapped in a homogeneous state by growing host mineral. On cooling, entrapped material becomes heterogeneous with the appearance of gaseous, liquid or solid phases. On heating these inclusions, the phase boundaries within the inclusion disappear. The temperature of disappearance of phase boundaries is taken as minimum temperature of entrapment of inclusions (filling temperature), which in turn, is the minimum temperature of formation of the mineral (Roedder, 1979).

When inclusions are heated to temperatures above their temperature of homogenization, a rapid build up of pressure inside the inclusion cavity results in the rupture of the inclusion producing cracking sounds. Decrepitation method is based on recording of these cracking sounds. Temperature at which mass scale explosion of inclusion begins is termed as temperature of decrepitation and is taken as minimum temperature of entrapment of inclusions and hence also as the minimum temperature of formation of host mineral. Decrepitation study has been carried out on decrepitemeter (temperature interval 0 to 450°C), fabricated in the department (Jaireth, 1981). Before taking up fluid inclusion analysis, sulphides along with associated quartz and calcite from the discussed localities were studied using ore microscope with an aim to understand ore paragenesis. Trace element geochemistry of sulphides was taken up to decipher environment of formation of sulphides.

7.1 MINERALIZATION AT JANKI CHATTI

About 1.4 km north of Janki Chatti, pyrite bearing quartz and quartz-calcite veins occur within calc-schist forming a part of the Janki Chatti Formation of the Garhwal Group. The veins are aligned parallel to the schistosity of the host rocks (dips 30-35° NE). Veins are marked by pinch and swell structure with thickness varying between 0.5 to 4.5 cm.

Pyrite is the main sulphide constituting about 95% by volume of sulphides and occurs as large (a few mm) idiomorphic grains disseminated irregularly in quartz and calcite matrix of veins. A few (two to three) smaller grains of pyrrhotite are also present. Quartz is the main gangue mineral associated with calcite and muscovite in the decreasing order of abundance. Paragenetic sequence of mineral formation is quartz-muscovite-pyrite-pyrrhotite-calcite.

7.2 MINERALIZATION AT BANAS

Mineralization has also been recorded on the left bank of the Yamuna River near Banas where quartz and quartz-calcite veins bearing chalcopyrite and pyrite mineralization is associated with meta-andesite, which have undergone retrograde changes along NW-SE trending fault. Veins show pinching and swelling with maximum thickness of a single vein reaching a few centimeters, Veins are, in general, concordant with the host rock dipping $35-40^{\circ}$.

At the contacts of veins, meta-andesite and biotite schist have been chloritized. Some quartz veins have also been observed in adjoining chlorite schist, but these are, in general, devoid of sulphide mineralization.

Pyrite is the dominant sulphide followed by chalcopyrite. Pyrrhotite and sphalerite are very scanty. Pyrite forms large idiomorphic grains with chalcopyrite developing as irregular stringer and patches inside pyrite or independent of it.

Pyrrhotite occurs as small irregular grains and veinlets in pyrite. Chalcopyrite at places, contains exsolved grains of sphalerite. Covellite is present as alteration product of chalcopyrite forming small veinlets. Quartz is the dominant gangue followed by calcite. Biotite and apatite are present in small amounts. Sequence of mineral formation is quartz-biotite-pyrite-pyrrhotite-chalcopyrite-sphalerite-calcite.

7.3 MINERALIZATION AT PINDKI

About 1 km SW of Pindki village, quartz veins bearing chalcopyrite and galena occur within highly jointed and sheared sub-augen migmatites. Malachite staining is conspicuous on the surface. Vein is concordant with the host rock dipping $25-30^{\circ}$

NE. The vein is comparatively thicker than other localities mentioned before and varies in thickness between 0.6 to 1.4 m.

Chalcopyrite and galena are the main sulphides, followed by extremely small amounts of pyrite and sphalerite. Both chalcopyrite and galena occur as irregular dissemination in quartz. Galena, at places, shows signs of deformation with slight bending of cleavage planes. Sphalerite gives starlet exsolutions in chalcopyrite. At places, chalcopyrite has been replaced by secondary covellite.

Quartz is the dominant gangue followed by muscovite in small amounts. General sequence of mineral formation is quartz-muscovite-chalcopyrite-sphalerite-galena-covellite.

Figures 7.1 to 7.6 show intersecting textural relations between ore and gangue minerals. Paragenetic sequence, derived on the basis textural relations at the above localities, is simple (Fig. 7.7).

EXPLANATION OF FIGURES FROM 7.1 to 7.6

Figure 7.1 - Pyrrhotite (Po) surrounded by pyrite grains (Py) in quartz-sulphide vein. Locality - Janki Chatti. Scale - 1cm = 25 microns.

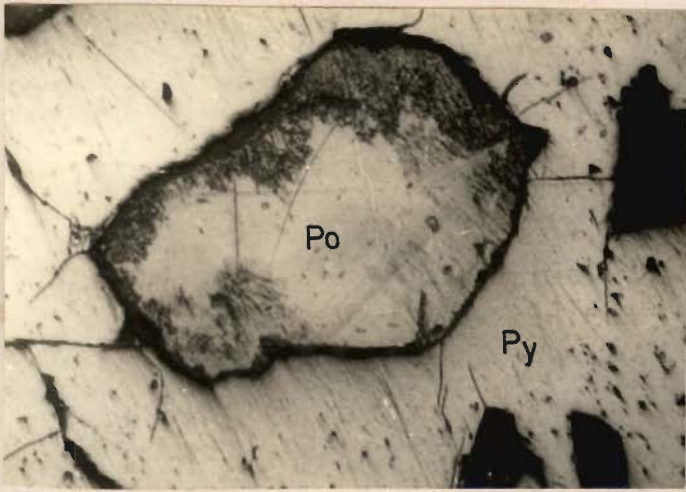
Figure 7.2 - Calcite (Cal) replacing pyrite (Py) along margins and cracks in quartz-calcite-sulphide vein. Locality - Janki Chatti, Scale - 1cm = 25 microns.

Figure 7.3 - Chalcopyrite (Cpy) replacing pyrite (Py). Sphalrite (Sp) occurs as exsolution starlet within chalcopyrite in quartz-sulphide veins. Locality - Banas. Scale 1cm = 25 microns.

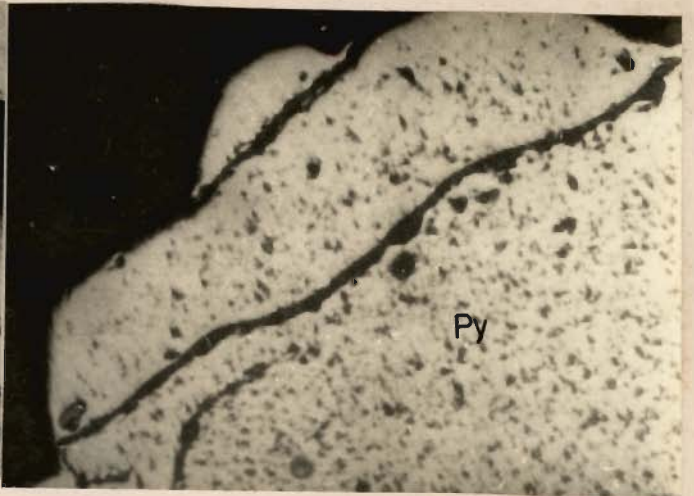
Figure 7.4 - Chalcopyrite (Cpy) and galena (Gl) occurring in a deformed quartz vein. Covellite (Cvl) occurring as secondary product. Locality - Pindki. Scale 1cm = 25 microns.

Figure 7.5 - Exsolved sphalerite (Sp) in chalcopyrite (Cpy) from quartz vein. Locality - Pindki. Scale 1cm = 25 microns.

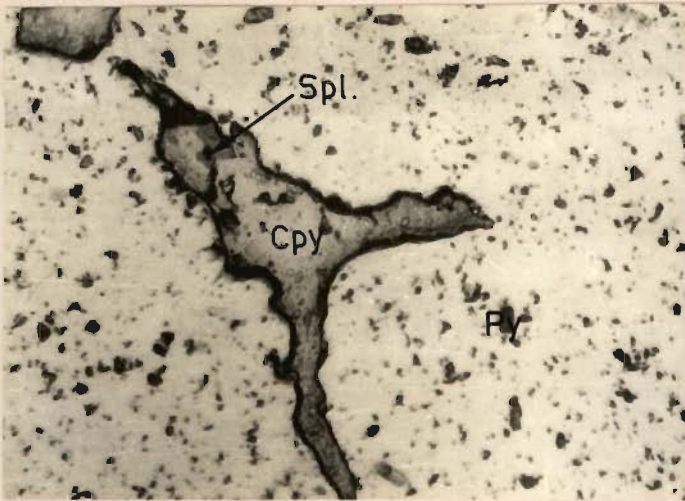
Figure 7.6 - Galena showing bending of cleavage planes and triangular pits. Locality - Pindki. Scale 1 cm = 12.5 microns.



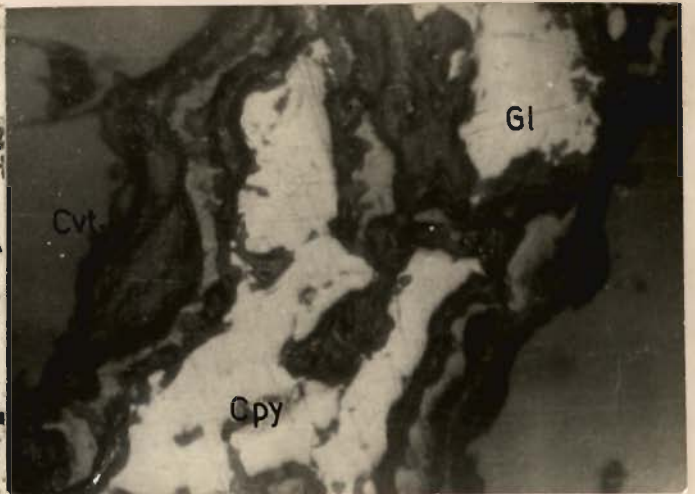
7.1



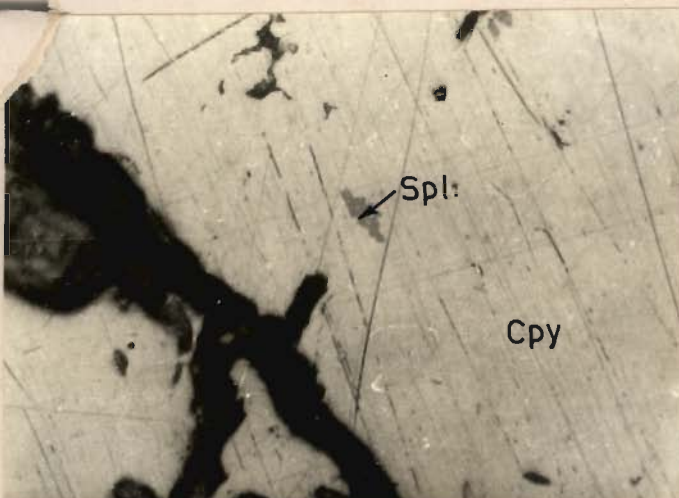
7.2



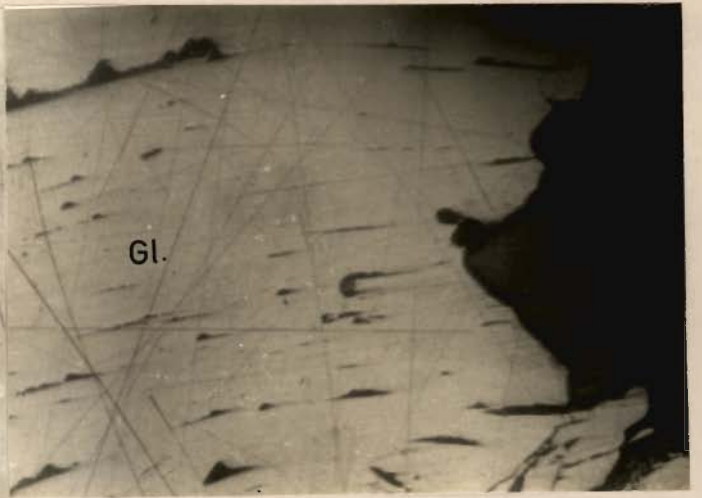
7.3



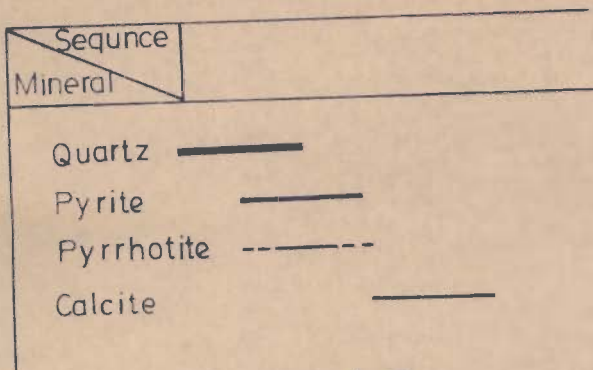
7.4



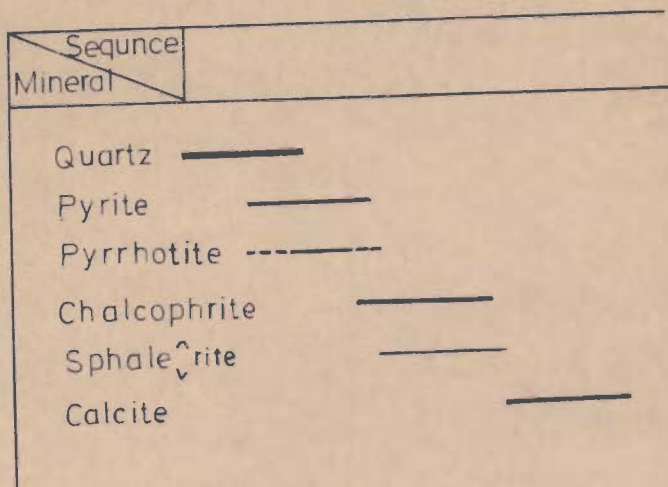
7.5



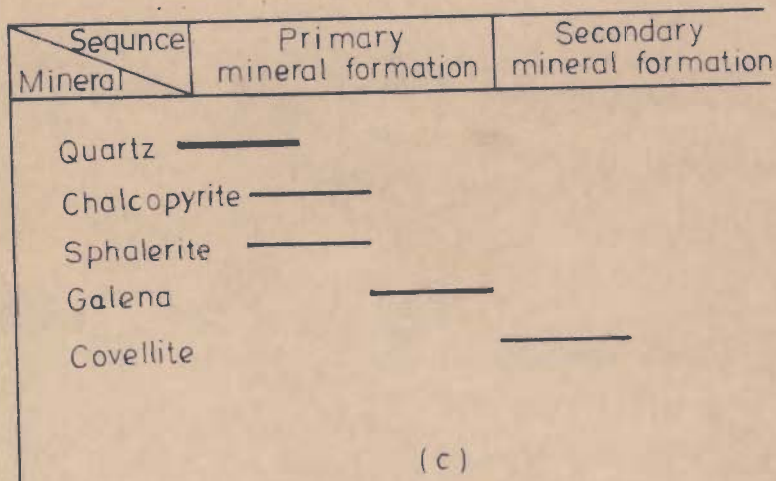
7.6



(a)



(b)



(c)

FIG. 7.7 - PARAGENETIC SEQUENCE IN QUARTZ SULPHIDE (-CALCITE) VEINS FROM JANKI CHATTI (a), BANAS (b), AND PINDKI (c)

7.4 GEOCHEMISTRY AND TRACE ELEMENTS

7.4.1 Techniques

Ten sulphide bearing samples from Janki Chatti, Banas and Pindki were first reduced to a mesh size of -100 to +120 by using diamond mortar and agate mortar. The above fractions were checked through binocular microscope and it was found that gangue and sulphide opaques show minimum interlocking. These fractions were repeatedly treated with bromoform (sp. gr. = 2.89), to get concentrated sulphide fractions. Out of ten dried samples, eight were analysed for major and trace constituents to know the bulk composition of sulphides. A portion of all the samples was used for the separation of sulphide mineral species (galena, chalcopyrite and pyrite).

The separation was effected by scanning samples under a binocular microscope and a purity of 95 to 97% was gained. The bulks were analysed at the laboratory of Hindustan Zinc Limited (Table 7.1). 200 mg from 14 samples of pyrite, chalcopyrite and galena fractions were digested by adding concentrated HCl (2-4 ml), HNO_3 (5-8ml) and HClO_4 (2-3 ml) with slow heating in a glass beaker (covered with lid) till the samples were totally digested. When no solid remained, it was diluted to 100 ml and stored in plastic bottles. The standard solutions were prepared as given in 'SP 2900' and 'IL 751' manuals. Finally, various trace elements were determined with the help of Atomic Absorption Spectrophotometer (AAS). The analytical data on the trace elements of sulphide minerals is given in Table 7.2.

TABLE 7.1 : BULK CHEMICAL COMPOSITION OF SULPHIDES
(percent by weight)

Sample No.	Pb	Zn	Fe	Cu	Cd	Ni
<u>JANKI CHATTI</u>						
801	0.0052	0.094	42.4	0.048	0.0009	0.0158
787	0.0054	0.120	43.0	0.340	0.006	0.0178
<u>BANAS</u>						
754	0.0040	0.600	26.2	3.19	0.0016	0.0450
750	0.0080	1.180	30.2	6.30	0.0026	0.1160
<u>PINDKI</u>						
857	12.6	0.460	9.0	7.40	0.0009	0.0023
863	66.2	0.098	4.4	3.48	0.0022	0.0008
865	78.4	0.096	0.6	0.46	0.0010	0.0010
861	77.8	0.210	1.3	0.98	0.0013	0.0005

(Analyst : Rakesh Babuguna)

TABLE 7.2 : TRACE ELEMENTS IN PYRITE, CHALCOPYRITE AND GALENA

Sample No.	Locality	Composition in ppm											
		Mn	Co	Ni	Cd	Sb	Bi	Zn	Pb	Cu	Mo	Co/Ni	Sb/Bi
<u>TRACE ELEMENTS IN PYRITE</u>													
778	Janki Chatti	70	295	264	18	10	145	987	97	683	25	1.12	0.07
801	Janki Chatti	50	337	307	10	20	110	995	59	627	10	1.10	0.18
787	Janki Chatti	40	314	295	13	15	210	1139	84	227	20	1.06	0.07
754	Banas	25	2454	1979	28	20	75	1174	87	N.D.	15	1.24	0.27
750	Banas	50	2296	2023	26	18	80	399	86	N.D.	30	1.14	0.23
<u>TRACE ELEMENTS IN CHALCOPYRITE</u>													
754	Banas	55	1278	1047	66	30	80	3559	175	N.D.	25	1.22	0.38
750	Banas	45	1326	1056	62	25	100	3864	85	N.D.	10	1.26	0.25
857	Pindki	15	123	50	21	20	355	2424	3696	N.D.	20	2.46	0.06
863	Pindki	10	170	139	25	40	655	3179	5516	N.D.	20	1.25	0.06
<u>TRACE ELEMENT IN GALENA</u>													
857	Pindki	15	84	27	26	85	2375	2039	N.D.	N.D.	80	3.11	0.04
863	Pindki	25	64	33	18	105	2115	879	N.D.	N.D.	75	1.94	0.05
865	Pindki	20	210	138	17	95	2215	489	N.D.	N.D.	95	1.52	0.04
860	Pindki	30	60	33	18	145	2265	209	N.D.	N.D.	70	1.82	0.06
861	Pindki	30	67	30	20	100	2335	325	N.D.	N.D.	85	2.23	0.04

(Analyst : The author)

7.4.2 Results

Upon comparing the bulk chemical composition (Table 7.1) with the chemical data of sulphide minerals (Table 7.2), no clear concentration ratios are available. Although an approximate correlation can be made, for example, Ni concentration ratio in pyrite (Ni concentration in pyrite/Ni concentration in bulk) varies from 1.65 to 4.39. On comparing with Cu content of the bulk, it was noticed that Ni concentration ratio decreases with the increase in Cu content. The concentration ratio in chalcopyrite varies from 0.90 to 2.35, except in sample No. D₂₇/863 where its value goes upto 17.37. Galena also shows large variability in their concentration ratio (1.17 to 13.8). From the limited number of analysed samples, it was not possible to draw any conclusion.

Trace elements have been effectively used as indicators of environment of formation of major phases. In cases where suitable pairs of major phases are present, partitioning of some trace elements is also used as geothermometers (Bethke and Barton, 1971). The absence of suitable pairs limits the use of trace elements in the present case, nevertheless, a few important conclusions can still be made. Pyrite, chalcopyrite and galena are characterised by their typical trace and minor elements (Table 7.2). Co/Ni ratio in pyrite has long been used as geochemical indicator of environment of formation of pyrite. According to Bralía et al. (1979) sedimentary pyrite is characterized by generally low values of Co/Ni ratio ($\text{Co/Ni} < 1$, average 0.63) and igneous hydrothermal vein pyrite is marked by high Co/Ni ratio (ratio > 1 , average 1.17).

Pyrite in Banas area is richer in both Co and Ni than the pyrite at Janki Chatti with Co/Ni ratios at both places more than one (Table 7.2). Average Co/Ni ratio of Banas pyrite is higher than in Janki Chatti pyrite. Plot of Co/Ni ratio on a Co-Ni concentration diagram taken from Braliala et al. (1979) shows that the pyrite from these localities fall in the field occupied by various vein type, igneous hydrothermal deposits (Fig. 7.3).

Similarly, Sb/Bi ratio in galena can also be used as geochemical indicator. Both Sb and Bi show preference for lead, but a relative enrichment of galena by any one of the two is important (Malakhov, 1968 in Vaughan, 1976). It has been shown that a low Sb/Bi ratio (<0.06) indicates galena to be formed at higher temperature, whereas high Sb/Bi ratio (6.0-13.0) is indicator of relatively lower temperatures characterising sedimentary environment.

Galena of Pindki area analysed for Sb and Bi shows that it is enriched by these elements in comparison to the coexisting chalcopyrite. Sb/Bi ratio in galena varies between 0.043 to 0.064 averaging around 0.046 (Table 7.2). Hence, both Co/Ni ratio in pyrite of Banas and Janki Chatti and Sb/Bi ratio in galena of Pindki indicate relatively high temperature igneous hydrothermal mode of formation.

7.6 FLUID INCLUSION STUDIES

More than 15 polished plates and thin sections of quartz from the three localities were studied under usual polarized light microscope in order to classify them according to physical

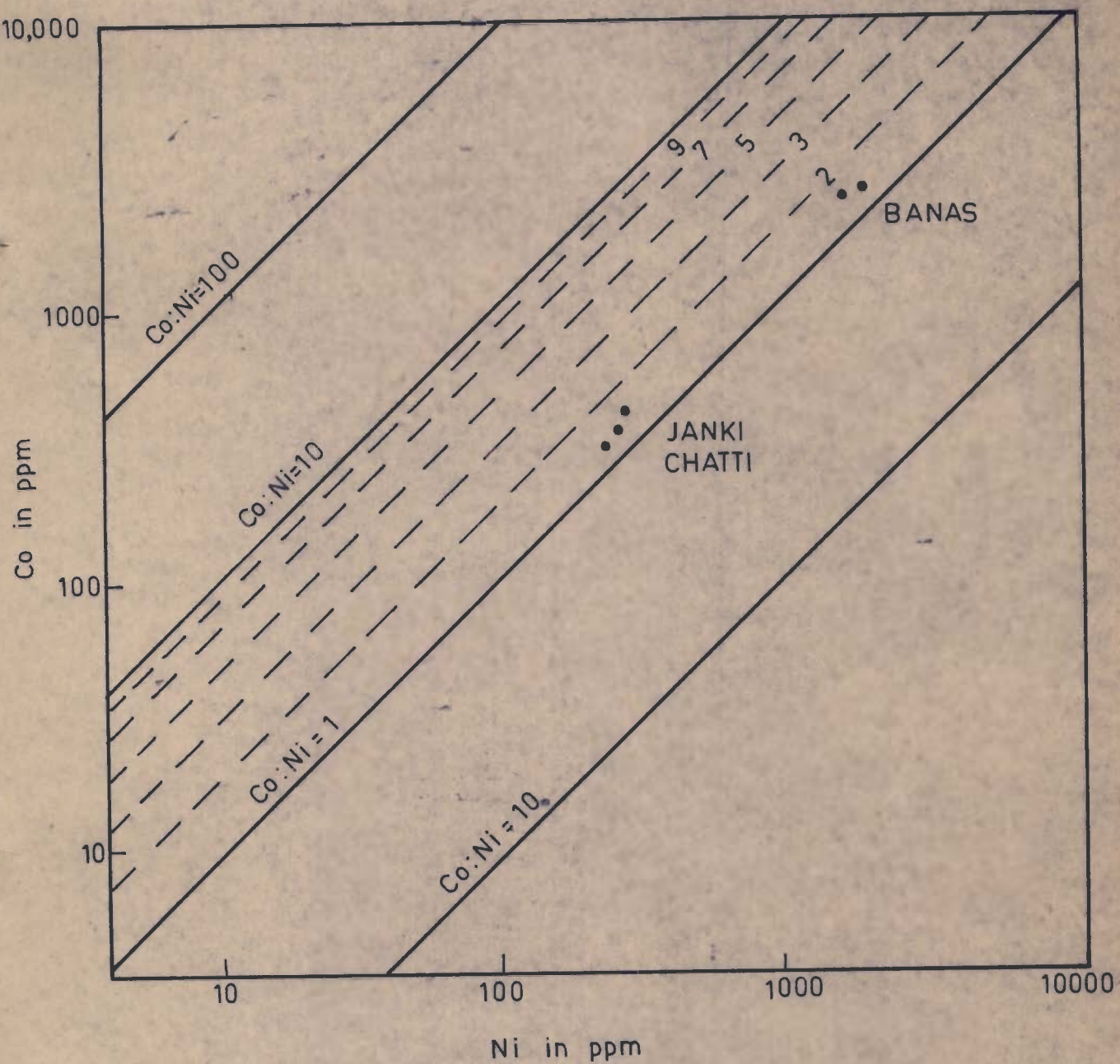


FIG. 7-8 - Co - Ni CONCENTRATION DIAGRAM FOR THE PYRITES OF JANKI CHATTI AND BANAS (AFTER BRALIA ET AL., 1979)

state of entrapped material and also according to their relative time of entrapment. Table 7.3 shows various types of inclusions present in quartz of the three localities. Figures 7.9 to 7.14 and d illustrate various types of gas-liquid inclusions present in quartz of veins from the discussed localities. The terminology used to describe the genetic types of fluid inclusions is based on Roedder (1979).

Quartz of Janki Chatti area contains three types of inclusions which differ in phase composition of entrapped material at room temperature, whereas quartz from Pindki veins contains only one predominantly liquid inclusions with very small gas bubble at room temperature. Quartz from Banas area is characteristically different from the other two as it reveals polyphase inclusions containing immiscible liquid CO_2 at room temperature. Quartz from Janki Chatti area is marked by coexisting syngenetically entrapped inclusion showing varied gas percentage at room temperature i.e., coexistence of primary and/or pseudo-secondary gas-liquid inclusion (gas = 20-45%) and liquid-gaseous inclusions (gas = 70-75%). This indicates that mineral forming media was in a heterogenous boiling state where gaseous and liquid solution coexisted leading to entrapment of inclusions in the varied amount of gas-liquid ratio at the time of formation of Janki Chatti quartz.

A general feature of inclusions in quartz from various localities is the absence of polyphase inclusion containing solid phases showing formation of quartz and associated sulphides from low salinity aqueous solution.

TABLE 7.3 : TYPES OF FLUID INCLUSIONS IN QUARTZ

Locality	Types of inclusion		
1. Janki Chatti	Predominantly-liquid (g < 5%), secondary	Gas-liquid inclusion (g=20-45%), Primary, psuedo secondary	Liquid-gaseous (g=70-75%) Primary, psuedo- secondary.
2. Banas	Predominantly-liquid (g < 5%), secondary	Gas-liquid polyphase inclusion containing liquid CO ₂ (g+LCO ₂ = 20%) Primary, psuedo second- ary	-
3. Pindki	Predominantly liquid (g < 5%) primary, psuedo-secondary	-	-

g = gas ; % of gas measured at room temperature

L = liquid

7.6 DECREPITATION STUDIES

One cubic centimeter of pure fraction of quartz from three localities was heated in a decrepitor upto 600°C at the rate of about $15\text{-}20^{\circ}\text{C}/\text{minute}$. Cracking sounds produced due to explosion of inclusions were recorded with the help of a condenser microphone through an amplifier and counted through a mechanical counter. Figure 7.15 shows decrepitorographs on the basis of results of decrepitation. Decrepitorographs of all the three quartz show a high temperature peak beyond 540°C which probably corresponds to the transformation of low temperature α -quartz into high temperature β -quartz. Other peaks are caused by breaking of inclusions.

In case of Janki Chatti quartz, temperature of decrepitation of predominant liquid inclusions (gas $<5\%$) is 180°C whereas gas-liquid (gas = $20\text{-}45\%$) and liquid-gaseous (gas = $70\text{-}75\%$) inclusions decrepitate from $300\text{-}320^{\circ}\text{C}$. Large broad peak is caused by presence of inclusions with varied gas-liquid ratios.

For Banas quartz, gas-liquid polyphase inclusions containing liquid CO_2 begin decrepitating at 340°C . Broad peak in this case is caused by presence of CO_2 in the inclusions. Such inclusions are known to decrepitate after appreciable overheating. Predominantly liquid inclusion (gas $<5\%$) were comparatively very scanty and hence have not appeared on the decrepitorographs.

7.7 DISCUSSION AND CONCLUSIONS

A detailed fluid inclusion analysis should include, in addition to optical microscopy and decrepitation of inclusion, such studies as homogenization on heating and freezing, thermo-

EXPLANATION OF FIGURES FROM 7.9 TO 7.14

Figure 7.9 - 7.14 - Fluid inclusions in quartz from quartz-sulphide veins. Estimates of gas percentage by volume at room temperature and locality is specified below. Scale - 1 cm = 12.5 microns.

Figure 7.9 - Gas - 30-35%. Janki Chatti

Figure 7.10- Gas - 20-25%. Janki Chatti

Figure 7.11- Gas - 40-45%. Janki Chatti

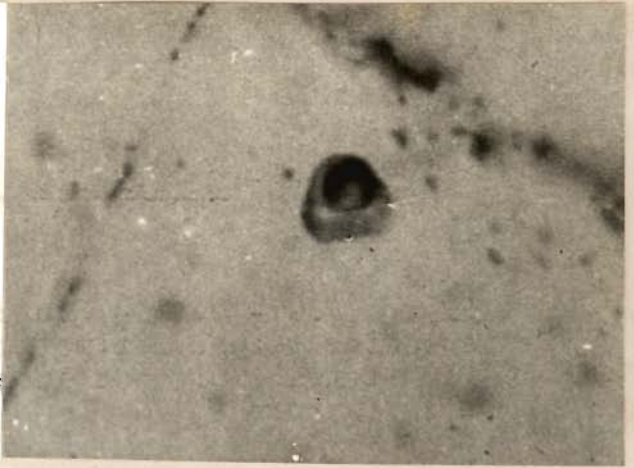
Figure 7.12- Gas - 15-20%. Janki Chatti

Figure 7.13- Gas - 14-18%. Janki Chatti

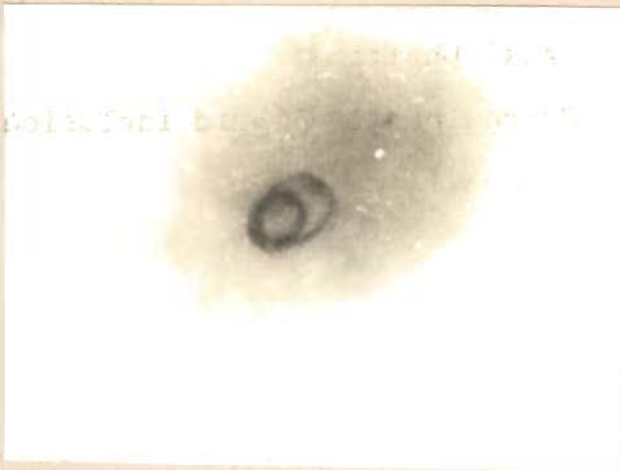
Figure 7.14- Gas - 5-10%. Predominantly liquid inclusion. Pindk.



7.9



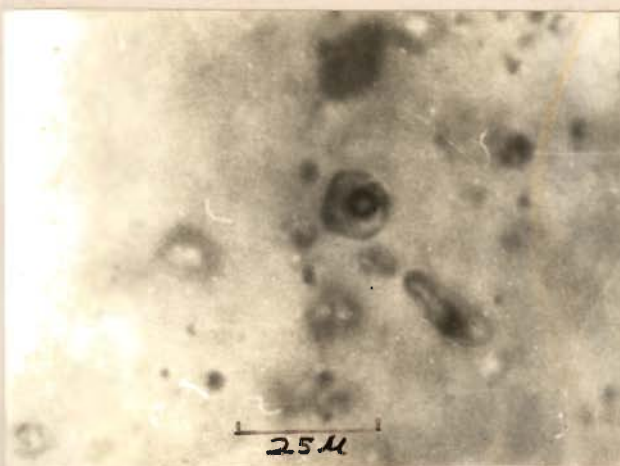
7.10



7.11



7.12



7.13



7.14

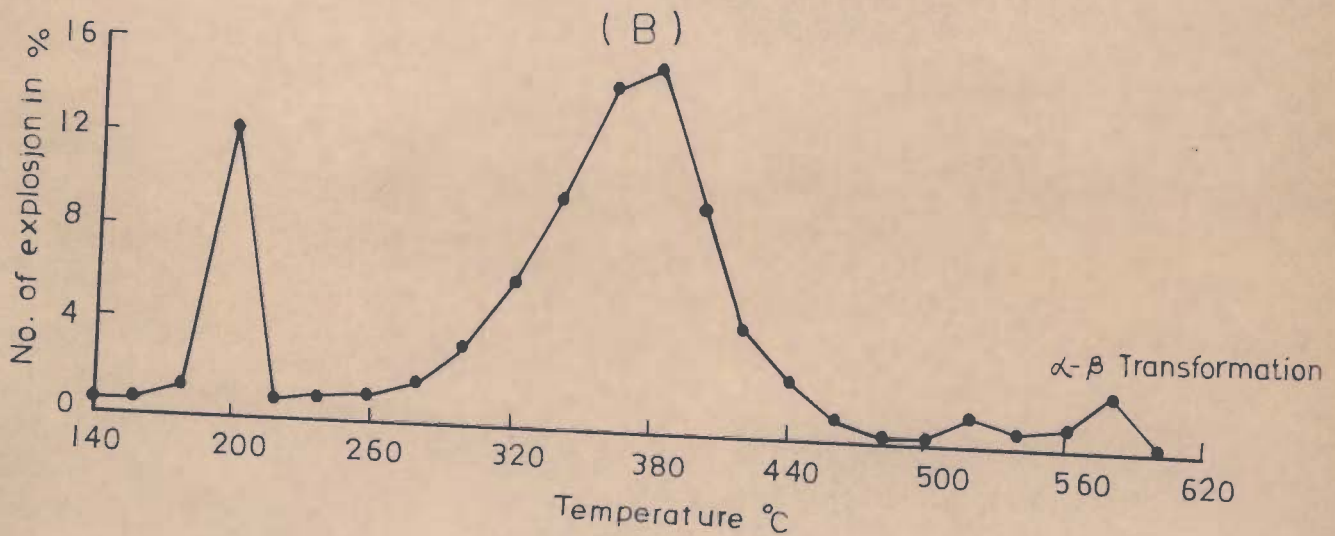
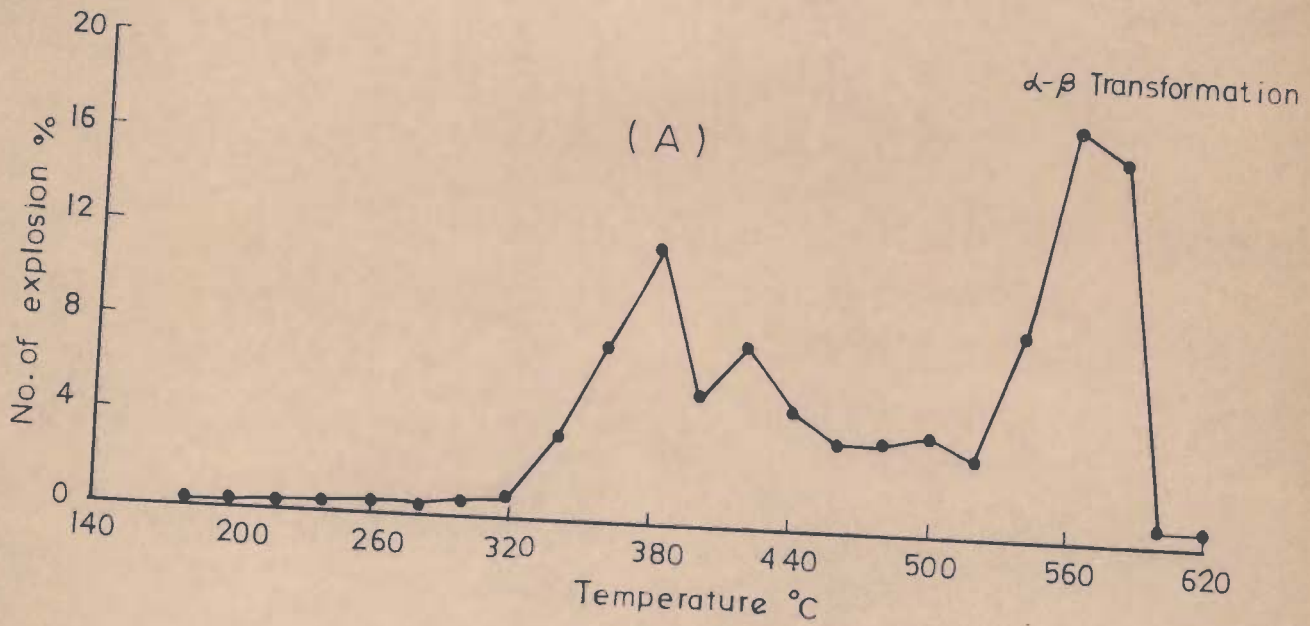


FIG. 7-15- DECREPITOGRAPHS OF QUARTZ FROM QUARTZ - CALCITE - SULPHIDE VEINS

A - QUARTZ FROM BANAS

B - QUARTZ FROM JANKI CHATTI

vaccum analysis and leachate analysis. In the present study, only decrepitation has been used. In spite of these limitations, a few important conclusions can still be made.

- a) Quartz from the three localities have been formed from hot aqueous hydrothermal solutions. Though homogenization experiments are not complete, it is very well clear that all inclusions show low amount of gas that would invariably homogenize on heating into a liquid phase thereby indicating liquid state for the mineral forming media.
- b) In case of Janki Chatti quartz, coexistence of gas-liquid and liquid-gaseous inclusions show entrapment from boiling hydrothermal solutions. Most probably, Janki Chatti quartz veins are formed at relatively shallower depths in comparison to other two quartz in which vapour pressure of solutions exceeded hydrostatic pressure causing boiling.
- c) Quartz from all the three localities was formed from solutions of low salinity because solid phases (daughter minerals) are absent in inclusions of all quartz. Low salinity of mineral forming solutions may be one of the reasons of relatively poorer, uneconomic concentration of sulphides in veins.
- d) Quartz from Janki Chatti and Banas is formed at relatively higher temperature (at about 300-320 to 340°C) as compared to Pindki quartz, as indicated by temperatures of decrepitation. For more precise temperature, homogenization experiments are essential. Usually such temperatures, as determined above, are minimum temperatures because corrections due to pressure

acting at the time of entrapment are to be applied. In the present case, however, these temperatures can be taken as correct temperatures because (i) in case of Janki Chatti, entrapment was from boiling solution i.e., external pressure was lower than vapour pressure, hence requiring no correction (Roedder, 1979); (ii) hydrothermal veins are usually formed at pressures below 500 atm. (Barnes, 1979) for which correction to temperature is less than $+15^{\circ}\text{C}$.

e) Calcite associated as fluid inclusion could not be studied using decrepitation techniques, because calcite gives so called anomalous decrepitation due to breakage along cleavage planes. Optical microscopy shows that calcite contains primary, predominantly liquid, inclusions (gas = 5%) which are similar to secondary and/or pseudo-secondary predominantly liquid inclusions in quartz from Janki Chatti and Banas. Calcite has thus, clearly formed later and superimposed on earlier formed quartz. As is evident from the decrepito-graphs (Fig. 7.15), predominantly liquid inclusions begin decrepitating at 180°C , which may therefore, be taken as temperature of formation of calcite.

f) Paragenetic sequence of mineral formation indicates that sulphides have been formed after quartz and before calcite, hence it can be concluded that sulphides must have been crystallised between $320-340^{\circ}\text{C}$ to $160-180^{\circ}\text{C}$ at Janki Chatti and Banas respectively.

g) Co/Ni ratio in pyrite of Janki Chatti and Banas also indicates a relatively high temperature environment. In addition, chalcopyrite in Banas area contains exsolved sphalerite indicating a temperature of more than 350°C .

CHAPTER VIII

RADIOMETRIC DATING

As has been indicated in the previous chapters, the present section of the Central Crystallines reveals a polyphase deformational and metamorphic history. It was envisaged that radiometric dating of gneissic samples might reveal absolute age of formation of minerals, cooling rates and the rate of uplift in the region by the fission-track methods. (Nagpaul, 1981). A review of Rb/Sr whole rock isochron ages from the NW-Himalaya is also incorporated for better understanding of the tectonic units and their mineral ages which have direct bearing to the tectonics of the region. Table 8.1 summarises the available Rb/Sr whole rock isochron ages from the NW-Himalaya.

8.1 Rb/Sr AGES IN GARHWAL-KUMAON HIMALAYA

8.1.1 Kumaon (Central Himalaya)

The Central Crystalline Group in the Kumaon Himalaya is comprised of nearly 15-20km thick northeasterly dipping pile of pelites, semipelites, gneiss, amphibolite, calc-silicates and ~~ps~~mmites in the almandine-amphibolite facies. It is thrust southward over the sediments of the Inner Lesser Himalaya along the Main Central Thrust (Heim and Gans^ser, 1939) and is conformably overlain by the fossiliferous Cambrian to Cretaceous sediments of the Tethys Himalaya.

TABLE 8.1 : RB/SR WHOLE ROCK ISOCHRON AGES FROM GRANITE/GNEISS FROM THE METAMORPHIC SEQUENCES OF THE NW-HIMALAYA

Metamorphic sequence	Name of granite/gneiss	Area	Author	Age (10^6 yr)
Salkhala Group	Mandi Granite (4 samples isochron)	Himachal Pradesh	Jager et al. (1971)	500 ± 100 (518)
Central Gneiss	Granite gneiss (3 samples isochron)	Mandi, Jaspa, Goda Gosh-aini	Frank et al., (1977)	443 ± 12
	Mandi Granite (3 sample isochron)	H.P.	Mehta (1977)	545 ± 12 (564)
	Mandi leucogranite (3 sample isochron)	H.P.	Mehta (1977)	311 ± 6 (322)
	Dalhousie Granite (2 sample isochron)	H.P.	Bhanot et al., (1974)	456 ± 50 (472)
	Dalhousie Granite Pegmatite	H.P.	Bhanot et al., (1975)	350 ± 50 (362)
	Metabasic xenoliths in Mandi Granite (3 samples isochron)	H.P.	Mehta (1976)	640 ± 20 (663)
	Gneiss (1 sample)	Rohtang, H.P.	Bhanot et al. (1975)	$612 \pm 100^{***}$
	Migmatite gneiss (4 sample isochron)	Kulu	Mehta (1977)	500 ± 8 (518)
	Gneiss (5 sample isochron)	Manali-Rohtang	Mehta (1977)	581 ± 9 (601)
	Migmatite as intrusive granite (7 sample isochron)	Rohtang, Jaspa, Hanuman, Tibba, Bandal	Frank et al. (1977)	495 ± 16
	Foliated granite	Sarangi, Runga Thach. NE of Manikaran	Bhanot et al. (1979)	467 ± 45

TABLE 8.1 contd.

Simla-Duda- toli-Almora Belt	Ranikhet gneiss (5 sample isochron)	Ranikhet, Kumaon	Pandey et al. (1981)	485 ± 55
	Masi gneiss (6 sample isochron)	Masi, Kumaon	Pandey et al., (1981)	370 ± 115
	Almora gneiss	Almora, Kumaon	Pandey et al. (1981)	370 ± 60
Jutogh gneiss	Nirath-Baragaon gneiss (3 sample isochron)	Sutlej valley, Rampur, H.P.	Bhanot et al. (1978)	1430 ± 150
	Central Crystallines (9 sample isochron)	Bhillangana valley, H.P.	Raju et al. (1981)	1276 ± 12 1139 ± 46
	Bairnath Crystall- ines (5 sample isochron)	Kasauni, Almora Dist, Kumaon	Bhanot et al. (1980)	1307 ± 79
	Ramgarh migmatites (1 sample isochron)	Ramgarh, Nainital District, Kumaon	Bhanot et al. (1980)	1170 ± 120 (1121)
	Basement Tectonic Slice	Dhakuri-Gneiss, Central Crystall- ines (3 sample isochron)	Pindar, valley Kumaon	Bhanot et al. (1980)
Munsiari Gneiss, Central Crystallines (3 sample isochron)		Goriganga Valley, Kumaon	Bhanot et al. (1980)	1890 ± 155
Chaili gneiss, Central Crystallines (4 sample isochron)		Bhillangana Valley, Garhwal	Raju et al. (1981)	2121 ± 60*
Askot Crystallines Lesser Himalayan Klippe (5 sample isochron)		Ranganga Valley, Kumaon	Bhanot et al. (1980)	1983 ± 77
Basement (Autochthon)		Bandal granite gneiss (4 sample isochron)	Bandal, Sainj (Tirthan and Sainj valleys H.P.)	Frank et al. (1977)

Table 8.1 Contd.

Bandal granite gneiss (3 sample isochron)	Bandal, Sainj	Bhanot et al. (1976)	1220 ± 100 (1263)
Uranite in Manikaran Quartzite	NE flank of the Rampur window	Narayan Das et al. (1979)	1220 and 700**

-
1. Ages in brackets represent recalculated values with new values for the decay constant for the beta decay of ^{86}Pb (1.42×10^{-11} /year) instead of older values of 1.47×10^{-11} /year after (Bhanot et al., 1980) and being multiplied by a factor of 1.0352 (Bhanot et al., 1979).

* Values for decay constant not mentioned

** U-Pb dates

*** Indicates upper age limits because of a single whole-rock sample

Radiometric Rb/Sr dating of this enormously thick pile of the Central Crystalline Group from the basal part near Munsiri along the Gori Ganga yield a two point isochron age of 1830 ± 200 m.y. for the gneisses (Bhanot et al. 1977), while a later age determination on third sample provides an isochron age of 1890 ± 155 m.y. with an initial $^{87}\text{Sr}/^{86}\text{Sr}$ ratio of 0.725 ± 0.01 (Bhanot et al., 1980). Interestingly, a three-point isochron from the Dhakuri gneiss between Pindar and Sarju Rivers (the Dhakuri Formation Misra and Bhattacharya, 1976) indicates an age of 2326 ± 193 m.y. having initial $^{87}\text{Sr}/^{86}\text{Sr}$ ratio of 0.696 ± 0.054 (Bhanot et al., 1980), thereby indicating a period of gneissification in the Central Himalayan region as old as 2300m.y.

8.1.2 Bhillangana Valley (Central Himalaya)

Lying to the next adjoining valley in east close to the present area of investigations from where the fission track dates are being described, the Bhillangana nappe (Tewari et al. 1971) is thrust over the low grade pelites exposed in the Ghutu Window. However, Valdiya (1978, 1980) considers the lower part of the sequence belonging to the Debguru porphyroids of the Chail-Barkot (Bhatwari-Ramgarh) Nappes in the lower part, followed by the Munsiri unit thrust southward over the Ramgarh Nappe along the Munsiri Thrust and finally by the Vaikrita Thrust, being the tectonic contact between the Lesser Himalaya and the Central Himalaya.

Rb/Sr isochron whole rock age of 3 samples of mylonitized granite gneiss from the outermost part near the Main Central Thrust from Brijranigad have yielded an isochron of 1276 ± 12 m.y., while 9 bore hole samples from the Ingedinala give an isochron age of 1139 ± 46 m.y. with initial $^{87}\text{Sr}/^{86}\text{Sr}$ ratio of 0.82 and 1.10 respectively (Bhattacharya et al., 1981). According to them, these frontal mylonitised granite gneiss is a paragneiss formed due to granitization, profuse K-metasomatism and greisenization of metasediments, thus indicating ages of the metasomatism and metamorphic events in this area.

On the other hand, 4 granite gneiss samples about 10km NE from the previous localities of the Main Central Thrust, located in higher tectonic levels yield an isochron age of 2121 ± 60 m.y. with initial $^{87}\text{Sr}/^{86}\text{Sr}$ ratio of 0.710 ± 0.020 . (Raju et al., 1981). This age has been interpreted as the age of the granite emplacement.

8.1.3 Askot and Baijnath Crystallines

Heim and Gansser (1939) observed two detached crystalline masses in the Kumaon Himalaya between the Main Central Thrust and the North Almora Thrust and consider them as remnants of an extensive crystalline thrust sheet/nappe (also, Valdiya, 1962; Thakur, 1980). These crystalline klippe are comprised of nearly identical rocks, namely an association of granite-gneiss, garnet mica schist, amphibolite and quartzite bands and have identical structural and deformation and metamorphic history (Thakur, 1980; Bhanot et al., 1977; Sarkar and Shrish, 1976).

Rb/Sr radiometric dates from 2 samples of granite-gneiss of the Askot Crystallines along the Thal-Didihat road indicate an age of about 1960 ± 100 m.y. with an initial $^{87}\text{Sr}/^{86}\text{Sr}$ ratio of about 0.72 (Bhanot et al., 1977), while 3 more samples from this area analysed later on now provide a five-point whole rock isochron age of 1983 ± 77 m.y. with an initial $^{87}\text{Sr}/^{86}\text{Sr} = 0.727 \pm 0.007$ (Bhanot et al., 1980). On the other hand, the Gwaldam granite from the Baijnath crystallines in the area of Binaik Pass and from Dangoli provide a five-point isochron age of 1307 ± 79 m.y. with initial $^{87}\text{Sr}/^{86}\text{Sr} = 0.793 \pm 0.017$ (Bhanot et al., 1980). This granite-gneiss has a high initial ratio indicating an anatectic origin and affected by later metamorphic events, while an age of 1300 m.y. indicates the time of homogenization of Sr isotopes during later events (Bhanot et al., 1980).

8.1.4 Kiodal Gneiss, Ramgarh (Lesser Himalaya)

Furthermore, the gneissic rocks of the Ramgarh area, termed as quartz porphyry of Precambrian age by Heim and Gansser (1939) or migmatites of Tertiary age (Pandey, 1956; Kashyap, 1972) have yielded an apparent Rb/Sr age of 1170 ± 120 m.y. (1211 m.y.) from a single sample from Koidal (Bhanot et al., 1980).

8.1.5 Simla-Dudatoli-Almora Belt (Lesser Himalaya)

Recent mapping in parts of Srinagar-Pauri-Dudatoli region has indicated westward extension of the Almora 'nappe' (Heim and Gansser, 1939) into the low grade metapelitic sequence of the Kumaon Supergroup (Kumar et al., 1974) which has been extended along the Bhagirathi-Yamuna valleys as a continuous belt called as the Simla-Dudatoli-Almora Thrust Sheet (Jain, 1981).

No radiometric Rb/Sr data were available uptill now except the recent brief report by Pandey et al. (1981) from gneiss and granite of this belt. They found Rb/Sr whole rock isochron for the Ranikhet gneiss as 485 ± 55 m.y. and for the Masi gneiss and Almora gneiss to be 370 ± 115 m.y. and 370 ± 60 m.y. These data compare very well with those obtained from the Salkhala Group of western Himachal Pradesh and seem to confirm eastward extension of this thrust sheet in Kumaon.

8.2 Rb/Sr AGES IN HIMACHAL PRADESH

8.2.1 Mandi-Dalhousie Granite

A concordant, NW-SE trending batholithic granitic intrusive is emplaced into the Salkhala metasediments in the region of Dalhousie, Dhauladhar Range, Mandi, Pandoh, Baghi, Karsog and has been previously referred to as the Dhauladhar Granite, Dalhousie Granite, Mandi Granite, or Karsog Granite (McMohan, 1881, 1885; West, 1934; Fuchs and Gupta, 1971; Bhatia and Kanwar, 1971, 1972, 1976; Thakur, 1973). Srikantia and Bhargava (1974) have traced the Salkhala Group metasediments of western Himachal Pradesh and Kashmir further eastward and have concluded that the previously classified Chails or Jutogh and others in this part of Himachal Pradesh are overthrust Salkhala Group which has formed the floor of the Late Palaeozoic - Mesozoic sediments in the Kashmir Valley and in Chamba.

First ever Rb/Sr radiometric age from a Himalayan rock suit of the Mandi Granite was 500 ± 100 m.y. by Jäger et al. (1971), which was later on corrected to be 518m.y. by Bhanot

et al. (1980) by considering new values for the beta-decay of ^{87}Rb constant (1.42×10^{-11} year) instead of 1.47×10^{-11} years. This age has been subsequently confirmed by Mehta (1977), when he obtained a 545 ± 12 (564) m.y. isochron for the Mandi Granite, while a leucogranite phase within the main body yielded 311 ± 6 m.y. (322m.y.).

Likewise, Bhanot et al. (1974) obtained a 456 ± 50 m.y. (472m.y.) age for the granite near Dalhousie, while a pegmatite phase within the Dalhousie granite has yielded a much younger age of 350 ± 50 m.y. (362m.y.), thereby indicating at least two ages of emplacement of this granite intrusive body i.e., an older main granite intrusion around 500m.y, followed by a later phase of leucogranite intrusion at about 320m.y. and a related pegmatitic phase around that period (Table 8.1).

Mineral ages from the Dalhousie Granite and Chor Granite indicate Early Tertiary metamorphism yielding 61 ± 10 m.y. and 50 ± 10 m.y. respectively (Bhanot et al., 1975) while, those from the Mandi granite biotite yield an age ranging from 20.5 ± 0.8 m.y. to 31.4 ± 2.9 m.y. (Table 8.2).

The Dalhousie Granite has been considered as a part of the Central Gneiss (Stolizka, 1866; McMohan, 1882; Middlemiss, 1876) and was thought to be a part of the geanticlinal barrier or the Himalayan ridge separating the Tethyan basin from the southern unfossiliferous basin. Various ages of the intrusion of the Dalhousie Granite has been postulated: (i) at the close of Eocene period (McMohan, 1882), (ii) during Triassic

TABLE 8.2 : Rb/Sr RADIOMETRIC MINERAL AGES FROM THE GRANITE/
GNEISS OF THE NW-HIMALAYA

Rock Type	Area	Author	Age(10^6 yr.)
<u>A. BIOTITE AGES</u>			
Mandi Granite	H.P.	Jager et al. (1971)	2.05 \pm 0.8
			24.0 \pm 2.4
			31.4 \pm 2.9
		Mehta (1977)	18.6 \pm 0.5
			19.3 \pm 0.5
Dalhousie Granite	H.P.	Bhanot et al. (1975)	61 \pm 10
Chor Granite	Simla hills	Jager et al. (1971)	50 \pm 10
<u>B. MUSCOVITE AGES</u>			
Mandi Granite	H.P.	Mehta (1977)	322 \pm 10
			368 \pm 85
Gneiss from Salkhala Group	Kulu Manali	Mehta (1977)	24.2 \pm 1
			24.8 \pm 1
			28.2 \pm 1
			20.5 \pm 1
	Rohtang	Frank et al. (1977)	29.0 \pm 4
			37.4 \pm 3.7
	Sarangi and Runga Thack NE of Mani- karan H.P.	Bhanot et al. (1979)	88

(Middlemiss, 1896); (iii) intrusion of Central Gneiss sometime between the Cambrian and Carboniferous (Auden, 1933); (iv) during the F_1 folds along weak axial planes paralleling the main thrust plane in post-Late Eocene imprinting a contact metamorphism over the regional metamorphism during the Himalayan Orogeny (Bhatia and Kanwar, 1971; Kanwar and Bhatia, 1977); (v) during Late Precambrian-Early Palaeozoic (500-600m.y.) synkinematically to the high grade metamorphism and migmatization (Mehta, 1975, 1977, 1978).

8.2.2 Nirath-Baragaon Gneiss

Bhargava et al. (1972) considered the gneissic rocks of this area along the Sutlej valley belonging to the allochthonous Jutogh Formation, being thrust southward along the folded Jutogh Thrust. Pandey and Viridi (1970), however, assigned these gneisses and underlying carbonaceous schist and phyllites to the Chail Formation. A revised scheme of classification of metasediments in the Sutlej valley by Srikantia and Bhargava (1974) and Bhargava (1980) indicated ^{that} these belong to the eastern extension of the Salkhala Formation of the NW-Himalaya.

A six point isochron of these gneissic rocks belonging to the Jutogh Formation indicate an age of 1430 ± 150 m.y. with initial $^{87}\text{Sr}/^{86}\text{Sr}$ ratio to be 0.746 (Bhanot et al., 1978). This has been interpreted as the gneissification of still older rock material belonging to these metasediments. Viridi (1976) opined this mylonitic gneiss to representing a granitic to granodioritic intrusion emplaced in these metamorphics after the first phase of major recumbent folds.

8.2.3 Bandal Granite and Manikaran Quartzite (Rampur Window)

The Bandal gneissic complex occurring underneath the Manikaran Quartzite is exposed into a NW-SE trending Rampur Window being thrust over by the crystallines of the Salkhala Group (Srikantia, 1965; Sharma, 1977; Frank et al. 1977; Bhargava and Chopra 1981). Frank et al. (1977) report a four-point Rb/Sr whole rock isochron of the Bandal granite as 1840 ± 70 m.y. from samples collected from Bandal (Tirthan River) and near Sainj (Sainj Khand). On the other hand, Bhanot et al. (1976) reported a three point Rb/Sr isochron age of 1220 ± 100 m.y. age of the Bandal Granite from samples collected from nearly the same area. It is interesting to note that these values coincide with U-Pb dating of six uraniumite samples from the overlying Manikaran Quartzite, where two distinct episode of Precambrian uranium mineralization at 1200 m.y. and 700 m.y. have been worked out (Narayan Das et al., 1979).

Frank et al. (1977) pointed out an absence of a true basement with a pronounced unconformity, though sharp contact between the Rampur Group and gneissic complex indicate the latter being an old basement of 1850 m.y. age which on later remobilization intruded into the Rampur Group around 1200 m.y. and mineralised around the same time (Sharma, 1977; Bhargava and Chopra, 1981).

8.2.4 Kulu-Manali-Rohtang-Jaspa Region (Salkhala/Central Gneiss)

A concerted efforts by a number of investigators in this part of Himachal Pradesh have yielded very useful Rb/Sr whole rock isochron data and mineral ages which have been, nevertheless,

interpreted differently (Bhanot et al., 1975; Mehta, 1976, 1977, 1978, 1980; Powell and Conaghan, 1973, 1978; Frank et al. 1977). Bhanot et al. (1975) measured whole rock Rb/Sr age of one gneiss sample from Rohtang Pass as 612 ± 100 m.y. Mehta's (1976, 1977) elaborate 4 point Rb/Sr isochron of the migmatite gneiss of Kulu area yielded an age of 500 ± 8 m.y., while a 5 point isochron from Central gneisses of Manali-Rohtang Pass area gave an age of 581 ± 9 m.y.

Data from Frank et al. (1977) reveal that migmatites as intrusive granites from Rohtang Pass, Jaspas in S-Lahul Valley and Hanuman Tibba fall on a Rb/Sr whole rock isochron of 495 ± 16 m.y. An older age (500-600m.y.) for these granite gneisses has also been agreed upon by Powell and Conaghan (1978) from their unpublished data (Crawford and Powell, unpublished data).

Further support to Early Palaeozoic magmatitic activity (467 ± 45 m.y.) in the Salkhala Group/Central Gneiss has been received by recent Rb/Sr whole rock isochron (4 samples) ages from Sarangi and Runga Thack area, located NE of Manikaran, H.P. (Bhanot et al. 1979). Biotite separated from these granite-gneiss reveal very young 8.8m.y. age.

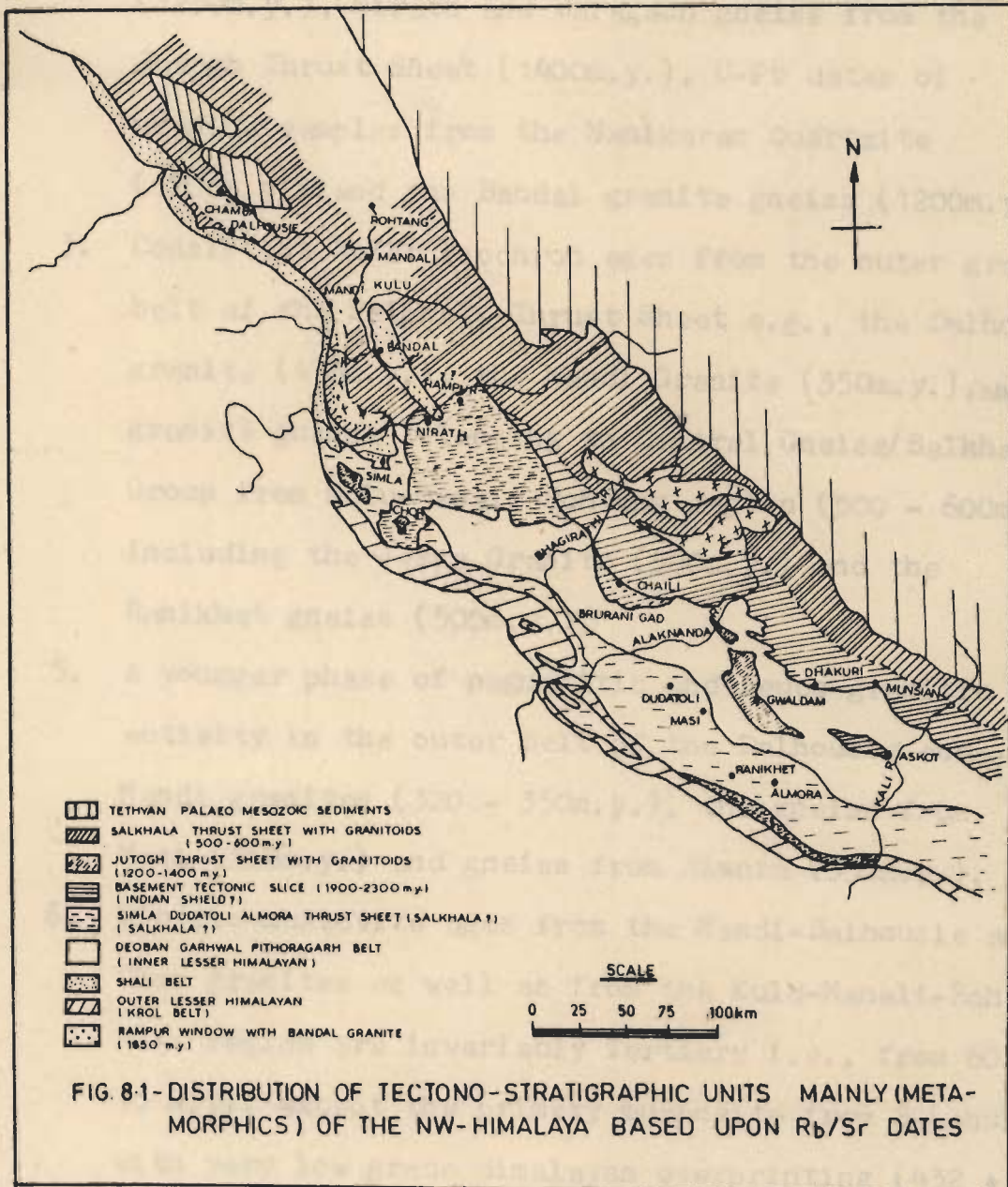
In this region, the Central Crystalline Zone was recognized as a major tectonic element separating the fossiliferous Cambrian to Eocene marine sediments of the Tibetan zone from the unfossiliferous pre-Tertiary rocks to the south (McMahon, 1879; Lydekker, 1883; Hayden, 1904). Recent investigations in this part of the Central Himalaya have indicated that the almandine-amphibolite facies metamorphics have been migmatized and belong

either to the Jutogh or Chail Formation or Salkhala (Bhargava et al. 1972; Srikantia and Sharma, 1976; Sharma, 1977; Mehta, 1977; Srikantia and Bhargava, 1974; Bhargava and Chopra, 1981) forming the floor for (a) Upper Palaeozoic-Mesozoic Manjir, Salooni and Kalhel sequence in Chamba; (b) The Tandi Group in Lahaul and (c) Phanerozoic sequence in the Lahaul-Spiti (Bhargava, 1981).

8.3 GEOLOGICAL INTERPRETATION OF Rb/Sr WHOLE ROCK AGES FROM THE NW-HIMALAYA

Figure 8.1 represents the main tectonic units of the NW-Himalaya and localities of the available Rb/Sr whole rock ages. These may be classified into the following groups, as it has been very categorically observed that Rb/Sr whole rock isochron ages of the granite and gneiss are mostly much older than the mineral ages from the same very samples, which are mostly Cenozoic (Jaeger, et al. 1971; Powell and Conaghan, 1978, 1980; Frank et al. 1973, 1977; Mehta 1976, 1977, 1978, 1980; Bhanot et al. 1980).

1. Rb/Sr isochron of the Dhakuri Gneiss as 2300m.y at the base of the Central Crystalline Group in the Pindar Valley, the Chaili gneiss in the Bhilangana Valley as 2150m.y, the Munsuari gneiss (1900m.y.). Askot gneiss (1950m.y.) and Bandal granite gneiss (1850m.y.) associated with the Manikaran Quartzite in the Rampur Window.



2. Rb/Sr isochron ages of the Gwaldam gneiss (130m.y.), gneiss from basal parts of the Bhillangana Valley (1250m.y.), Nirath and Baragaon gneiss from the Jutogh Thrust Sheet (1400m.y.), U-Pb dates of uranite samples from the Manikaran Quartzite (1200m.y.) and the Bandal granite gneiss (1200m.y.).
3. Consistent Rb/Sr isochron ages from the outer granite belt of the Salkhala Thrust Sheet e.g., the Dalhousie granite (475m.y.), the Mandi Granite (550m.y.), and the granite gneiss belonging to Central Gneiss/Salkhala Group from Kulu-Manali-Rohtang region (500 - 600m.y.) including the Jaspa Granite (500m.y.) and the Ranikhet gneiss (500m.y.).
5. A younger phase of pegmatitic and leuco-granitic activity in the outer belt of the Dalhousie and Mandi granites (320 - 350m.y.), the gneiss from Masi (350m.y.) and gneiss from Almora (350m.y.).
6. Biotite-muscovite ages from the Mandi-Dalhousie and Chor granites as well as from the Kulu-Manali-Rohtang Pass region are invariably Tertiary i.e., from 60 to 10 m.y., except the primary muscovite from S-Lahul with very low grade Himalayan overprinting (432 ± 12 m.y.; Frank et al., 1977).

Though controversies still persist in the Himalayan Orogen regarding the existence of pre-Himalayan gneiss and granite (see Powell and Conaghan, 1978; Mehta, 1978), Rb/Sr isochron

ages as old as 2300m.y. in the Central Himalaya, pre-Himalayan deformation and metamorphism in certain parts of the crystallines and low grade metamorphics (present work; Thakur, 1980; Schwan, 1980, Ghose, et al. 1974; Sinha Roy, 1973) clearly demonstrate the involvement of much older fabric in the Cenozoic Himalayan Belt. It can be visualised that the Precambrian Indian Shield elements in the northern parts viz. the Bundelkhand granite gneiss, the Banded Gneissic Complex, the Aravalli are probably involved in the Central Himalayan tectonics and are presently occurring as tectonic slivers in the basal parts of the Central Crystalline Group which is thrust over the Precambrian sedimentary cover. These slivers occur as presently exposed as Munsiri-Dhakuri-Chaili-Bhatwari gneiss (1900-2300m.y.) and has been provisionally termed as the Himalayan Basement Slice.

Early Precambrian basement is thrust over another frontal thrust sheet having root zone in certain sections of the Central Himalaya. The outer crystalline thrust sheet which contains younger gneissic elements (1200-1400m.y.) has been called the Jutogh Thrust Sheet. The pear-shaped type locality of this thrust sheet extends to Chor Mountains and has been traced continuously to the Sutlej valley in the Rampur area where the Nirath-Baragaon gneiss yield an isochron of 1400m.y. Considering the Rb/Sr dates of this gneiss, it is likely to belong to the Jutogh Thrust Sheet, as has been previously postulated by Bhargava (1972) and may not be a part of the Salkhala Thrust Sheet. Other outcrop of this thrust sheet are the basal crystalline sequence in the Bhillangana valley and the

Baijnath Crystallines, while the Askot Crystalline belongs to the Himalayan Basement Slice. The Kiodal gneiss of the Ramgarh Nappe radiometrically belongs to the Jutogh Thrust Sheet and not to the Chail nappe as has been postulated by Valdiya (1978). This thrust sheet has a much better frontal development in Himachal Pradesh and overrides the Simla-Dudatoli-Almora Thrust Sheet.

The Paleozoic-Mesozoic fossiliferous Tethyan sequence of Kashmir, Chamba-Bhadarwah and Spiti regions are underlain by the Salkhala Group metamorphics, which have been synkinematically intruded by the Dalhousie-Mandi-Kursang granites in the frontal parts. These granites yield an age of around 500-600m.y., which is also a persistent isochron of granite gneisses from the Kulu-Manali-Jaspa region. It is likely that the Salkhala Thrust Sheet is predominantly made up of granite gneisses of 500-600m.y. thereby warranting a separate tectonic status than the Central Crystallines of Kumaon and the Jutogh metamorphics of Himachal Pradesh.

Highest tectonic levels in the Central Crystallines of Lahul-Garhwal and Kumaon are conformably overlain by the Late Precambrian Batal-Haimanta-Martoli argillites and then by the Palaeozoic-Mesozoic Tethyan sequences (Heim and Gansser, 1939; Hayden, 1908; Thakur, 1980; Valdiya and Gupta, 1972; Shah and Sinha, 1974). Immediately underlying this sequence and the radiometrically dated horizons in basal parts of the Central Crystallines incorporates sections about 10-20km thick

crystalline rocks whose ages have not been radiometrically determined in Himachal Pradesh, Garhwal and Kumaon. Logically, it would be fruitful to presume that this sequence would belong to a time span between 1000-600m.y. and therefore might be the eastward extension of the Salkhala Group in Himachal Garhwal and Kumaon. Till more radiometric dates are available, we presume this to be 1000-600m.y. old sequence, intruded by late Tertiary tourmaline granite and truncating the basal older gneisses of Bhatwari Group whose detailed deformational and metamorphic history establishes atleast one older phase of deformation, metamorphism and migmatization. The older Himalayan Basement Slice seems to be cut off in the Himachal Pradesh where Jutogh Thrust Sheet is overriding the Salkhala Thrust Sheet. Figure 8.2 sketchamically illustrates these relations.

8.4 FISSION TRACK DATING

Fission track dating technique was first applied by Price and Walker (1963) for the determination of uranium concentration and absolute age of rocks and minerals. This method was later on elaborated by Fleiseher and Price (1964). Fission track dates of coexisting and cogenetic minerals like garnet, muscovite, biotite, zircon, apatite etc. have been found useful in many geological problems e.g., cooling and uplift rates of an area (Nagpaul et al. 1973; Nagpaul and Lal, 1971; Lal and Nagpaul, 1973; Sharma et al. 1978, 1980; Saini, et al. 1978, 1979; Nagpaul, 1981; Saini, 1982). It has been commonly observed that fission track ages are generally much younger

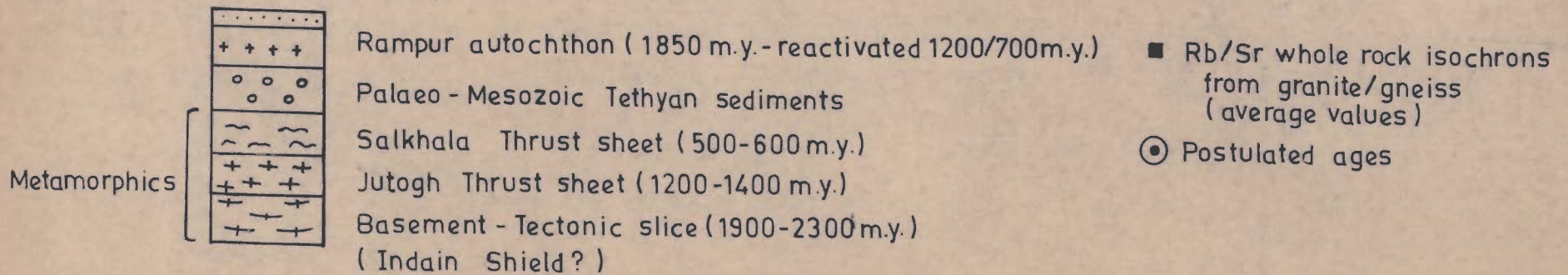
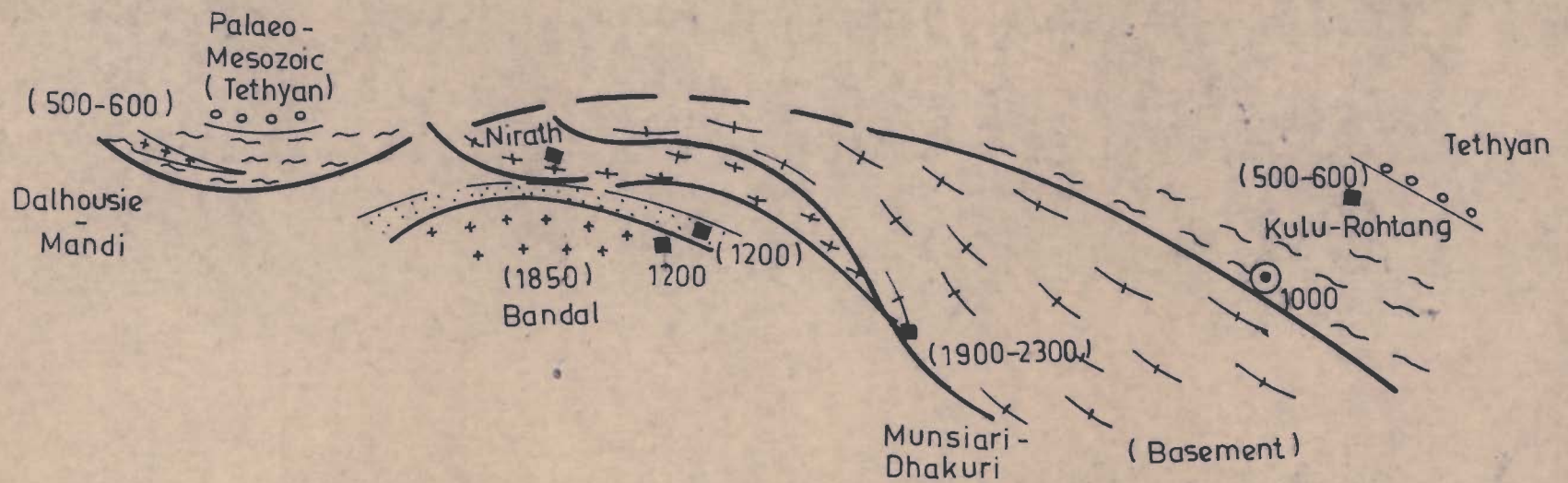


FIG. 8-2. SCHEMATIC INTERPRETATION AND EXTENSION OF CRYSTALLINE THRUST SHEETS ON THE BASIS OF Rb/Sr WHOLE ROCK ISOCHRON AGES.

than those by other radioactive methods. Even the coexisting and cogenetic minerals differ in fission track ages, while apatite shows variation in ages in a batholith depending upon the rate of cooling and uplift (Sharma, et al. 1978). Since no data on the radiometric age of the Central Crystallines along the Bhagirathi and Yamuna valley was available, it was planned to undertake this work with the Department of Physics, Kurukshetra University for better understanding of the deformational and tectonic history of the metamorphics.

8.4.1 Experimental Procedure

The fission track phenomena produce a radiation damage in the lattice structure of minerals. The fission tracks can be enlarged by etching with suitable chemical reagents and studied under optical microscope. The etchant attacks the damaged lattices and produce fossil tracks of micron size. In the present study, 13 apatite, 10 garnet and 3 zircon fractions were separated from 26 rock samples belonging to the Central Crystallines of the Bhagirathi Valley. The minerals separation was done with the help of isodynamic separator (Hutchison, 1974) and checked through optical microscope. The minerals grains were mounted and polished on thin sections. These grains were sent to Bhabha Atomic Research Centre (BARC) for thermal neutron irradiation and were etched by their respective etchant. Etched fission track density was recorded through optical microscope. The fission track ages were determined from the formula which can be derived from the following equations (Nagpaul, 1981).

$$\rho_s = \frac{\lambda_F n^{238} (\exp \lambda_D T - 1)}{\lambda_D} \dots\dots\dots 1$$

$$\rho_i = n^{235} \phi \sigma F \dots\dots\dots 2$$

From equations (1) and (2) we get

$$T = \frac{1}{\lambda_D} \ln \left(1 + \frac{\rho_s \lambda_D}{\rho_i \lambda_F} \phi \sigma I \right) \dots\dots\dots 3$$

where ρ_s = fossil track density, ρ_i = induced track density, λ_D = total decay constant of uranium, λ_F = spontaneous decay constant of uranium, n^{238} = number of U^{238} atoms/cm³ of the mineral, n^{235} = number of U^{235} atoms/cm³ of the mineral, F = a constant depending upon the etchable range of fission tracks, etching efficiency and geometry etc., ϕ = thermal neutron dose, σ = thermal neutron cross-section for fission of U^{235} , and I = isotopic abundance ratio of uranium.

The values of various constant used are as follows:

$$I = 7.25 \times 10^{-3}$$

$$\lambda_D = 1.55 \times 10^{-10} \text{ yr}^{-1}$$

$$\sigma = 580 \times 10^{-24} \text{ cm}^2$$

$$\lambda_F = (7.03 \pm 0.11) \times 10^{-17} \text{ yr}^{-1}$$

After putting the values of these constants in equation 3, we obtain a simplified age equation which can be expressed as

$$T = 6.45 \times 10^3 \left[1 + 9.31 \times 10^{-8} \frac{\rho_s}{\rho_i} \phi \right]$$

8.4.2 Results and Discussions

Tables 8.3, 8.4 summarises the fission track data on three minerals, namely zircon, garnet and apatite from the gneissic rocks of the Central Crystallines of the Bhagirathi Valley. It may be mentioned here that fission track dates of zircon and garnet are the oldest so far found in the Himalaya ^(Kiran, personal communication) hence have not been taken into serious discussion till more data is available.

Radiometric data from these sections are totally lacking by other Rb/Sr, K/Ar or U-Pb methods. As has been elaborated in the previous section, available Rb/Sr whole rock isochron ages from the adjoining regions indicate that the Bhatwari Group metamorphics represent a basement tectonic slice (1900-2300m.y.) involved in the Himalayan deformation and metamorphism, thereby showing Cenozoic mineral ages as is indicated from other metamorphic sequences from the Lesser and Central Himalaya. All the Rb/Sr whole rock ages point towards Pre-Himalayan dates suggesting involvement of a Early PreCambrian basement and widespread magmatic activity atleast twice during the geological history of the Himalaya viz., during 1200-1400m.y. and 500-600m.y. besides that associated with the Himalayan Orogeny. Mineral ages from the Himalayan Orogen are mostly Cenozoic except a few Early Palaeozoic mineral ages indicating resetting of blocking temperatures of the metamorphic minerals. The fission track mineral ages indicate the following:

TABLE 8.3 : FISSION TRACK AGE DATA OF THE BHATWARI GROUP

Sample number	Thermal neutron dose (ϕ)	Fossil track density (ρ_s)	Induced track density (ρ_i)	Age in m.y.
<u>Garnet</u>				
517	1.19×10^{17}	2.9×10^3	1.31×10^5	161.6
512	1.19×10^{17}	3.48×10^3	1.70×10^5	145.9
463	1.19×10^{17}	7.35×10^3	3.68×10^5	140.3
831	1.19×10^{17}	3.29×10^3	1.63×10^5	143.3
491	1.19×10^{17}	*	*	143.4
<u>Zircon</u>				
453	1.12×10^{15}	0.89×10^5	0.65×10^5	91.4
<u>Apatite</u>				
814	2.21×10^{15}	1.36×10^4	4.01×10^5	4.4
543	1.22×10^{15}	6.52×10^3	1.93×10^5	4.1
411	1.22×10^{15}	1.97×10^4	1.57×10^5	5.1
831	2.21×10^{15}	6.57×10^3	3.74×10^5	5.3
527	2.21×10^{15}	1.97×10^4	1.04×10^5	2.6

* Data not available

TABLE 8.4 : FISSION TRACK AGE DATA OF THE SUKI GROUP

Sample number	Thermal neutron dose (Φ)	Fossil track density (ρ_s)	Induced track density (ρ_i)	Age in m.y.
<u>Garnet</u>				
27. 837	1.19×10^{17}	3.01×10^3	1.39×10^5	152.4
609	1.19×10^{17}	3.35×10^3	1.51×10^5	158.3
595	1.19×10^{17}	3.02×10^3	1.33×10^5	159.2
571	1.19×10^{17}	3.47×10^3	1.64×10^5	151.2
572	1.19×10^{17}	3.50×10^3	1.67×10^5	148.5
<u>Zircon</u>				
571	1.12×10^{15}	0.96×10^5	0.71×10^5	90.4
595	1.12×10^{15}	1.01×10^5	0.70×10^5	96.3
<u>Apatite</u>				
586	2.21×10^{15}	1.93×10^4	10.30×10^5	90.4
591	2.21×10^{15}	*	*	3.1
618	2.21×10^{15}	1.56×10^4	4.72×10^5	4.5
632	1.22×10^{15}	6.69×10^3	1.63×10^5	5.6
571	1.22×10^{15}	7.92×10^3	1.56×10^5	5.9
572	1.22×10^{15}	6.28×10^3	1.61×10^5	4.8
597	2.21×10^{15}	2.43×10^4	9.86×10^5	3.2
633	*	*	*	5.8

* Data not available

TABLE 8.5 : COOLING AND UPLIFT RATES OF THE CENTRAL CRYSTALLINES
ALONG THE BHAGIRATHI VALLEY BASED UPON FISSION TRACK
AGES IN APATITES

Sample No.	Apatite Ages (m.y.)	Elevation in meters	Total uplift (mm/year)	Cooling rates °C/m.y.
D586	2.4	2780	2.825	35.41
D591	3.1	2760	2.180	27.41
D618	4.5	2720	1.49	18.80
D814	4.4	1670	1.288	19.31
D543	4.1	1810	1.417	20.73
D632	5.6	2720	1.200	15.17
D571	5.9	2240	1.057	14.40
D411	5.1	1560	1.090	16.66
D572	4.8	2640	1.383	17.70
D597	3.2	2210	1.940	26.56
D831	5.3	1820	1.098	16.03
D633	5.8	2620	1.141	14.65
D527	2.6	1640	2.169	32.69
Average	4.37	2245	1.56	21.22

TABLE 8.6 : COOLING AND UPLIFT RATES FROM DIFFERENT PARTS OF THE HIMALAYA

S.No.	Locality/ Region	Method	Author	Age span	Uplift rate (mm/year)	Cooling rate (°C/m.)
1.	Outer Himala- ya	Geodetic Survey	Narain (1975)	Past 75 years	0.8	-
2.	Mandi	Fission track	Sharma et al. (1978)	32-16m. y. 16-8m. y.	-	2.0-3.0
3.	Kinnaur	Fission track	Saini et al. (1979)	200-46m. y. 31-20m. y. 20-11m. y. 15-7m. y.	0.03 0.08 0.15 0.08	1 2 4 25 (sub- sequent to thrusting)
4.	Kulu-Rohtang	Rb/Sr mineral ages	Mehta (1979)	25-10m. y.	0.8	21
5.	Kulu	Rb/Sr mineral ages	Frank et al. (1977)	-	-	Rapid cooling in vicinity of thrust zones
6.	Bhagirathi Valley	Fission track	Present work (Table 8.5)	4.3m. y. to present	1.56	21.22

Garnet: The ages of ten samples are less than 150m.y. This is the limiting case, because exact dates could not be determined due to low U concentration in the mineral. The closing temperature of garnet is 300°C (and the data does not reveal any distinction of ages of syn- or post-tectonic garnets as was initially guessed.

Zircon: The fission track zircon ages of three samples are 90, 91 and 96m.y. These samples are from different levels of the crystallines with no age difference. The closing temperature of zircon is 250°C which nearly is close to garnet fission track clock. The zircon ages should be treated as cooling ages because of its closing temperature value.

Apatite: The age of thirteen apatites varies from 2.5 to 6m.y. The difference in ages is not sufficiently large to correlate spatial distribution of ages with geological structure. This is normally expected because the closing temperature of apatite is related only to recent tectonic movements. Garnet and zircon fission track ages are rather old since the zircon age of 93m.y. from the U.P. Central Himalaya are the oldest dates so far, the oldest being 70m.y. from Nause, H.P. from the Lesser Himalaya (Kiran, personal communication). Till more data on garnet and zircon ages are available from this section and adjoining region, it is difficult to interpret these more conclusively except the geothermal gradient in the U.P. Central Himalaya causing progressive regional metamorphism during the Himalaya Orogeny were probably initiated since 150m.y.

Considering an effective blocking temperature of 110°C for apatite and a geothermal gradient in the Central Crystallines to be 30°C, a depth of 3-4km for this terrain is feasible during the past 3-6m.y. Assuming no heating subsequent to the achievement of blocking temperatures of apatite since 6m.y., it is then possible to calculate the cooling rate and rate of uplift.

Closing temperature for apatite = 110°C

Present average temperature = 25°C

Temperature difference = 85°C

Cooling rate = $\frac{\text{Temperature difference}}{\text{Age}}$

Rate of uplift = $\frac{\text{Total uplift}}{\text{Age}}$

Table 8.5 represents the data upon the cooling rate and rate of uplift in the present area. A summary of the investigations and interpretation has been presented below indicating that the Central Himalaya is uplifted at a much faster rate than the Lesser Himalaya and is also envisaged in its very immature topography (Table 8.6).

8.4.3 COOLING AND UPLIFT RATES

Rb/Sr, K-Ar and fission track ages on the coexisting minerals in the Himalayan crystallines from certain sections are now available to warrant a comparative analysis of cooling and uplift rates of the Himalaya (Bhanot et al. 1980; Frank, et al. 1977; Jäger et al. 1971; Mehta, 1976, 1977, 1981; Saini et al. 1977, 1979). Cooling rates in the Himalayan regions have been worked out in the Kulu, Mandi, Kinnaur region of

Himachal Pradesh and the present traverse section across the Central Crystallines along the Bhagirathi valley (Tables 8.5, 8.6).

Mandi: Saini et al. (1977) measured fission track ages of apatite from the Mandi Granite along the Pandoh-Baghi tunnel and reported a range from 7 to 27m.y. Metamorphic mineral ages from the Mandi Granite using other methods range from 24 ± 2.4 to 31.4 ± 2.9 m.y. on biotites (Jager^{White}, 1972), while that from the Dalhousie Granite is 61 ± 10 m.y. (Bhanot et al. 1975). Along the Pandoh-Baghi Tunnel, Saini et al. (1977, 1978) calculated cooling rates of each sample to vary from 2.7 to 8.2°C/m.y. with an average of 4.7 C/m.y.

Kulu-Rohtang Area: Though the fission track data in this region is lacking for calculating the rate of cooling, Rb/Sr and K-Ar radiometric dating by Mehta (1976, 1977, 1981), Mehta and Rex (1977) and Frank et al. (1977) clearly demonstrate rapid cooling rates in central parts of the Salkhala Thrust Sheet, as has been worked on the previous section. Mehta (1980) ascribes two main phases of rates of cooling on the basis of Rb/Sr radiometric ages of coexisting muscovite and biotite from Kulu region. He calculates a very slow rate of cooling of about 4°C/m.y. from 50m.y. to 25m.y. and more so between 40 to 25m.y. and an enhanced rate of cooling of 21°C/m.y. during the 25-10m.y. period. Frank et al. (1977) also envisage a rapid cooling by overthrusting in the cooling ages of biotites from 21m.y. at the front of the crystalline nappe to a value of 16 ± 2 m.y. of the Larji Window; the 21m.y. data at the front of nappe giving maximum age for thrusting.

Kinnaur Region: Lying to the eastern parts of the crystalline sequence in Himachal Pradesh along the Sutlej valley, the Kinnaur region has yielded a cooling rate of $1^{\circ}\text{C}/\text{m.y.}$; $2^{\circ}\text{C}/\text{m.y.}$ and $4^{\circ}\text{C}/\text{m.y.}$ for the periods between 200-46m.y.; 31-20m.y. and 21-11m.y. respectively (Saini et al. 1979). Between 15-7m.y. it is suggested that rate of cooling is much rapid to about $25^{\circ}\text{C}/\text{m.y.}$

Uplift Rates: Saini et al. (1978) calculated the rate of uplift of the Mandi Granite between 27 and 7m.y. to be 0.06mm/year and a rate of 0.05mm/year in the past 8m.y. (Sharma et al. 1978).

For the Rohtang and Kulu regions, Mehta (1981) using the Rb/Sr mineral ages of muscovite and biotites from granite gneiss gave a rate uplift as 0.80mm/year during the past 25-7m.y. Still in the interior of the crystalline belt, Saini et al. (1979) suggested uplift rates of 0.04mm/year, 0.08mm/year and 0.15mm/year for the period 200-46m.y., 31-20m.y. and 21-11m.y. respectively for the Kinnaur region.

8.4.4 Cooling and Uplift Rates from the Bhagirathi Valley: Fission track data of apatite from the Central Crystallines of the Bhagirathi valley indicate that the gneiss exposed on the surface attained thermal stability for apatite around 110°C at rather consistent ages between 2.4 to 5.8m.y. (mean Apatite age -4.37m.y.). Considering the present average temperature to be 25°C in the region, a cooling rate of $21^{\circ}\text{C}/\text{m.y.}$ is obtained during the past 4m.y. for the Central Crystallines of the Bhagirathi valley, which is interestingly less than the

cooling rate of $25^{\circ}\text{C}/\text{m.y.}$ during 15-7m.y. for the Kinnaur region (Saini et al. 1979) and $21^{\circ}\text{C}/\text{Ma}$ during 25-10m.y. for the Rohtang region (Mehta, 1980). Presuming a uniform spatial cooling rates in the Central Crystallines, a consistent cooling rate of $21^{\circ}\text{C}/\text{Ma}$ is obtained for the axial zone of the Himalaya during the past 25m.y., though a fall in cooling rates from $25^{\circ}\text{C}/\text{m.y.}$ to $21^{\circ}\text{C}/\text{m.y.}$ may also be suggested since 7m.y. This contrasts well with very low cooling rates for the outer Himalayan region where it averages $4.7^{\circ}\text{C}/\text{m.y.}$ in the Mandi region.

Taking a uniform geothermal gradient of $30^{\circ}\text{C}/\text{km}$ and an average elevation of sampling site to be 2.2km above MSL (Mean Sea Level) a depth of 6.2km is envisaged at about 4m.y. when apatite grains attained track stability. An average rate of uplift of $1.56\text{mm}/\text{year}$ is indicated for this section of the Central Crystallines during the past 4m.y. On the contrary, Saini et al. (1976) calculated $0.8\text{mm}/\text{year}$ the rate of uplift for Kinnaur during 15-7m.y., while $0.8\text{mm}/\text{year}$ uplift is also postulated for the Rohtang region during 25-10m.y. A gradual increase in the rate of uplift is indicated from the available fission track data of Kinnaur and the Bhagirathi valley from $0.04\text{mm}/\text{year}$ during 200-46m.y. to $0.80\text{mm}/\text{year}$ during 31-20m.y. to $0.15\text{mm}/\text{year}$ during 21-11m.y. and to $1.36\text{mm}/\text{year}$ since 4m.y. It is in contrast with the slow rate of uplift along the frontal belt of Mandi, where the rate is $0.06\text{mm}/\text{year}$ during 27-7m.y. and $0.05\text{mm}/\text{year}$ in the past 8m.y. (Sharma, et al., 1978). It is therefore likely that various tectonic units in the Himalaya have undergone diff-

erent rates of uplift, the outermost revealing the slowest uplift hence it is rather difficult to generalise the uniform rate of uplift for the Himalaya till more data are available. Different rates of uplift are available from the following diversified data:

- a) 0.8-0.9mm/year rise of Pir Panjal Range during the past 2m.y. from the present elevation of the Karewa sediments.
- b) 1.55mm/year in Nepal from the K-Ar ages being the rate of erosion and uplift (Krummenacher, 1971).
- c) 0.8mm/year as the revised rate of uplift in Nepal (Bassett et al., 1978).
- d) 0.8mm/year as current rate of uplift from geodatic surveys (Narain, 1975).
- e) 0.22mm/year as the rate of erosion in the Himalaya over the past 40m.y. and 0.62mm/year in the western and 1.0mm/year in the eastern Himalaya as present rate of erosion (Menard, 1962).
- f) 9mm/year movement (not uplift) across the Nahan Thrust in U.P.Himalaya by strain meter surveys (Sinvhal et al., 1973).

CHAPTER IX

DISCUSSION AND CONCLUSIONS

Geological set up, petrography and structure of the rock formations exposed in the investigated parts of the Bhagirathi and the Yamuna Valleys have already been described in the earlier chapters. Petrology and geochemistry of amphibolite and migmatite have been described in Chapters IV, V and VI and genetic interpretations have been drawn therein. A regional survey of radioactive dates obtained in various parts of Himalaya was presented with a view to offer possible correlation of the Bhatwari and Suki Groups with various metamorphic (= crystalline) rocks of the Lesser and Central Himalaya in order to underline the importance of this type of studies in solving the problems of regional tectonics. It would be rather naïve to suppose that the metamorphic rocks of the Yamuna or Bhagirathi Valleys are isolated ones. These are as much a part of the Himalayan tectonic framework as any other, lying from northwest to southeast extension of this complex orogenic belt.

A wealth of data is now available on the Himalaya, including on its tectonics, metamorphism and structure. Attempts to correlate different 'belts' of Kashmir, Simla, Kumaun, Nepal, Sikkim and Arunachal have been made and many generalised maps are available by different workers. An attempt has been made here to discuss some of these basic problems of the Central Himalayan deformation, metamorphism

and tectonics in the wider framework of the Plate Tectonics and to evolve a working hypothetical model.

9.1 THE MAIN CENTRAL THRUST (MCT)

A basic difference between the investigations made in Nepal Himalaya and north-western Himalaya (Kumaun to Kashmir) is the use of the term - Main Central Thrust (MCT). In Nepal, French workers regard it as a boundary between the Tibetan slab and the Midland Formations (Pecher, 1976; Le Fort, 1981). Valdiya (1980) regards 'Tibetan Slab' corresponding to the Vaikrita Formation and the Upper Midland and Lower Midland Formations corresponding to the Muasiari and the Bhatwari Formation respectively. In a recent publication, Thakur (1980) has evidently agreed with Gansser (1964) in referring that thrust as the MCT which separates the metamorphics from the Krol-Berinag Nappes or Chail Nappe of the Inner Lesser Himalaya. In the Garhwal-Kumaun Himalaya, therefore, the MCT has conventionally being referred to as what Valdiya (1980) would call as the Bhatwari-Ramgarh Thrust. In this work, the MCT has been used in the convention followed by Heim and Gansser (1939) and Gansser (1964), because the evidences enumerated in the previous chapters do not justify its changed status being no more the tectonic boundary between the Lesser and Central Himalayas. In fact, concept of the MCT being the tectonic demarcating surface between the two regimes itself needs drastic rethinking due to involvement of the Lesser Himalayan elements in the Central Himalaya, not only in the MCT zone but much

farther north due to imbrication in certain cross-sections.

9.2 DEFORMATION AND METAMORPHISM

Table 9.1 summarizes the history of metamorphic structural episodes in the Central Himalaya as discussed earlier in this work. It is envisaged that the sediments, now representing the Bhatwari Group are the earliest group of rocks deposited on a basement whose identity is no more preserved. Sediments were largely graywacke, type, as is evident from the chemical composition (Chapter 6, Figs. 6.1 and 6.2). During certain pre-Himalayan period, rather pre-Mesozoic, these were metamorphosed upto garnet grade and were migmatized as evidenced by remanants of plagioclase containing inclusions of largely altered K-feldspar. If Rb/Sr whole rock isochron ages from the adjoining valleys are any indications of this syntectonic migmatization during the earliest decipherable D_1 deformation, the Bhatwari Group migmatite was probably evolved during 1900-2300 m.y. and represent the oldest rocks dated upto now in the Himalaya. The amphibolite of the Bhatwari Group represent the basic igneous activity in this group prior to migmatization.

The existence of the pre-Himalayan metamorphism and deformation as described in this work (Chapters 3 and 4) is a matter of controversy. Gansser (1964), Fuchs (1967), Sinha Roy (1973, 1974, 1976), Saxena (1971), Ghose *et al.*, (1974), Mehta (1977), Karanth and Shah (1977), Pande and Prasad (1971), Acharyya (1978), Schwan (1980), Jain *et al.* (1980) and Jain (1981) found evidences in different parts of the Himalaya

TABLE 9.1 SUMMARY OF DEFORMATION AND METAMORPHIC CHARACTERS OF THE CENTRAL HIMALAYA ALONG BHAGIRATHI AND YAMUNA VALLEYS

DEFORMATION	STRUCTURAL FEATURES			METAMORPHISM	REMARKS
	Folds	Foliation	Lineation		
(DEPOSITION OF THE BHATWARI GROUP OVER AN UNKNOWN BASEMENT)					
D ₁	F ₁ : Reclined isoclinal to very tight folds plunging NE/SW	S ₁ : Axial plane foliation dipping NE	L ₁ : Mineral lineation plunging NE/SW	M ₁ : Regional metamorphism upto garnet grade; syntectonic garnet-I; retrograde metamorphism (scanty evidences)	Anatexis leading to migmatization of the Bhatwari Group; K-followed by Na-metasomatism; anatectic zone towards south; basic igneous activity
(DEPOSITION OF THE SUKI AND GARHWAL GROUPS WITH BASIC IGNEOUS ACTIVITY MAINLY IN THE LATTER)					
D ₂	F ₂ : Recumbent, tight to isoclinal folds plunging NW/SE and developed upon S ₁ foliation (in the Bhatwari Group) and upon S ₀ lithological layering in the Garhwal and Suki Groups	S ₂ : Axial plane foliation to F ₂ and coplanar to S ₁ foliation ¹ (in the Bhatwari Group)	L ₂ : Mineral lineation plunging NW/SE	M ₂ : Regional metamorphism upto sillimanite grade in the Suki Group; quartz I, biotite I, muscovite I, amphibole, kyanite-sillimanite and garnet II growths Earliest Himalayan metamorphism 48 my (middle Eocene)	Anatexis leading to migmatization of the Suki Group; Na-followed by K-metasomatism in both Suki and Bhatwari Groups. Anatectic zone towards north, near Jhala; basic igneous activity mainly in the Bhatwari Group.

D_{2a}

- S_{2a}: Mylonitic foliation and transposition of earlier planar structures in thrust zones

- Major thrusting from deeper levels in late D₂ deformation phase: development of schuppen structure with imbricated Lesser Himalayan sediments within the Central Himalaya; andesite sill

D₃

F₃: Upright to overturned folds on S₁/S₂ foliation; crenulation plunging NW/SE; major Himalayan longitudinal macroscopic folds

S₃: Crenulation foliation

L₃: Lineation due to crenulation folds on S₁/S₂ foliation

M₃: Meta- Possible southward morphism; translation along rotation and thrusts and growth of development of quartz II, faults biotite II, muscovite II, garnet III; chloritization of higher grade minerals

D₄

F₄: Upright, open cross-folds plunging NE/SW; development of culmination and depression

- Development of joints, slickensides; tranverse to oblique faults and lineaments

of pre-Himalayan deformation and metamorphism. Thakur (1977 1980) is also of the view that there may be a pre-Himalayan fabric in the Central Crystallines of the Kumaon Himalaya which has probably evolved during the Caledonian Orogeny. On the other hand, Merh and Vashi (1965), Naha and Ray (1970, 1971, 1972), Mukhopadhyay and Gangopadhyay (1971), Powell and Conaghan (1973), Frank et al. (1973, 1977) Le Forte (1975) and others deny any pre-Himalayan episode. Lal et al. (1981), although largely agree to the view that M_1 metamorphism is related to the earlier phase of the Himalayan Orogeny (Late Cretaceous to Early Tertiary), also subscribe to the view that

"The earlier metamorphism preceeding M_1 may have been of low grade (green schist faces) in the Eastern Himalaya (may also be of amphibolite or granulite facies in other areas of Himalaya as Precambrian metamorphites of different ages are involved during this episode".

Pending further age data, the author believes that the Bhatwari Group has suffered a pre-Himalayan episode. Does the Bhatwari Group represent a geanticline (Wadia, 1957) or a crystalline axis (Pande and Saxena, 1968; Saxena, 1971)? It would be interesting to quote Le-Forte (1975):

"In fact, two major basins existed, separated by a ridge that provided the material for detritic deposition on both sides (north of Lesser Himalayas and south of Higher Himalayas), Possibly the ridge came into existence in the Late Precambrian-Early Paleozoic or Siluro-Devonian times, and was accompanied by volcanic activity".

Table 9.2 compares the deformational and metamorphic episodes from the Bhatwari and the Suki Group of the Central Crystallines with some known elaborate schemes from the Himalaya. It seems plausible that superimposed deformations in identical stress field have largely obliterated older events, which are still preserved in isolated regions, as is the case with the Bhatwari Group.

9.3 INVERTED METAMORPHISM

Detailed petrographic and structural characters of the Central Himalayan metamorphics from the Bhagirathi and Yamuna Valleys have demonstrated that the Bhatwari Group which had already undergone a phase of deformation, regional metamorphism and migmatization underwent a polyphase Himalayan metamorphism and migmatization. The Suki and the Garhwal Groups have suffered the well known Himalayan deformations (D_2 to D_4 of this work) and metamorphism with the difference that there are no signs of migmatization in the Garhwal Group. It seems to author, that the Bhatwari Group represents the oldest basement forming a micro-continent over which the Garhwal Group would have been deposited on its southern side and the Suki Group on its northern side. In the present juxtaposition, the Garhwal Group underlies the Bhatwari Group along the MCT and the Suki Group overlies the Bhatwari Group along the JBT. The intensity of the Himalayan phase shows garnet grade in the Bhatwari Group, but beyond the JBT it rapidly progresses from garnet to sillimanite grade in the Suki Group. Chapters 2 and 4 present the distinctive

TABLE 9.2 DEFORMATION AND METAMORPHIC EPISODES IN THE HIMALAYA - A COMPARISON

NAHA & RAY, 1972	POWELL & CONAGHAN, 1973	THAKUR, 1980	SCHWAN, 1980	PRESENT WORK
Simla Klippe	Central Gneiss, Rethang Pass, H.P.	Central Crystallines, Kumaon	Eastern and NW-Himalaya	
THREE DEFORMATIONS F ₁ -F ₃	THREE DEFORMATIONS- D ₁ -D ₃	FOUR DEFORMATIONS - D ₁ -D ₄	FIVE DEFORMATIONS-D ₁ - D ₅	FOUR DEFORMATIONS-D ₁ - D ₄
			Pre-Himalayan/ Pre-Permian	Precambrian
		Metamorphic banding - a pre-F ₁ fabric and pre-Himalayan	D ₁ -B ₁ -Fabric-F ₁ /S ₁ /L ₁ NE plunging overturned/recumbent folds, mineral lineation	D ₁ -F ₁ /S ₁ /L ₁ reclined isoclinal to very tight folds plunging NE or SW having axial plane foliation - S ₂ and B-mineral lineation
			D ₂ -B ₂ Fabric-F ₂ /S ₂ /L ₂ same as above; WNW/ESE vergence	M ₁ - Regional metamorphism and anatexis leading to migmatites
			Associated metamorphism	(Only in the Bhatwari Group)
			Precambrian and/or Paleozoic Orogenies (Aravalli/Coledonian)	

Table 9.2 Contd.

<p>F₁-S₂/L₁ isoclinal recumbent/ reclined folds, shallow E/W plunge; S₂ axial plane fol- iation as earliest structures on bedding surface (S₁)</p>	<p>D₁-F₁/S₁/L₁ intra- folial folds, isoclines WN plunging S₁ axial plane folia- tion; earliest structures Post-Middle Jurassic deformation.</p>	<p>D₁-F₁/L₁ isoclinal/ reclined folds plunging NW and NE, axial plane schistosity; mineral lineation</p>	<p>D₃-B₃ Fabric- F₃/S₃/T₃/L₃ folds with WNW trends, SSW, vergence</p>	<p>D₂-F₂/S₂/L₂- recumbent, tight to isoclinal folds plunging NW or SE; coplanar to F₁; axial plane foliation, S₂, B-mineral line- ation plunging NW or SE.</p>
<p>M₁-Progressive regional met- amorphism of the Jutoghs during F₁</p>	<p>Synkinematic metamorphism</p>	<p>M₁-Synkine- matic met- amorphism</p>		<p>M₂-Regional metamorphism with sillimanite grade in Suki Group; anatexis leading to migma- tization</p>
<p>Break in met- amorphism T₁ Jutogh Thrust - Cataclasis myl- onitization Post-F₁ thrust- ing</p>		<p>M₂-Acme of met- amorphism, por- phyroblastic growth of minerals</p>		<p>D_{2a}-Major thrusting and mylonitic fol- iation S_{2a}</p>
<p>F₂-Upright, tight to isoclinal folds in north; S₃ axial plane cren- ulation cleavage. Coaxial to F₁; strong slippage along S₃</p>	<p>D₂-F₂/S₂/L₂- open to very tight folds, weak axial sur- face crenulation cleavage and renulation lineation</p>	<p>D₂-F₂-asymmet- ric folds of open style, overturned; crenulation schistosity along F₂ axial surfaces</p>	<p>D₄-B₄ Fabric- F₄/S₄/T₄/L₄ WNW trends; folding major nappes</p>	

M₂-metamorphism across the Jutogh Thrust.

Asymmetry of F₂ folds represent strong overthrusting from NE

Intrusion of leucocratic unfoliated granites

D₃-F₃/S₃L₃- Upright³ to overturned folds; foliation, S₃ along axial surface; crenulation lineation

M₃-metamorphism

F₃-Conjugate to chevron folds N-S axial planes; axes trend N; folding F₁ and F₂ Thrusting T₁ precede F₃ and coeval to F₂ movements

E₃-F₃/L₃- Regional broad antiforms and synforms All Himalayan deformation Earliest deformation and metamorphism D and is post-Middle Jurassic

E₃-F₃-Broad open folds and warps transverse to regional trend plunging NE/SW: culmination and depressions

M₃-Retrogressive-phases of metamorphism

D₄-Kink bands, fractures and joints of two to three sets.

D₅-B₅ Fabric F₅ cross-folds NE trends folds no vergence

D₄-F₄-upright open cross-folds plunging NE/SW; culmination and depressions; joints; faults

D₂ to D₄ and M₂, M₃ related to Himalayan Orogeny

characters of the Bhatwari and Suki Groups. At Jhala, the sillimanite gneiss is exposed with pods of anatectic melts. Further northeast of Jhala, the metamorphism decreases from sillimanite grade to as low as biotite grade (not described in this thesis).

Such "reversal" of metamorphic grade, followed by "normal" metamorphism has been recorded by many workers in the Himalaya and other orogenic belts (Auden, 1935; Ghosh, 1956; Gansser, 1964; Powell and Conaghan, 1973; Frank et al. 1973, 1977; Pecher, 1977; Thakur, 1977, 1981; St-Onge, 1980; Banerji et al. 1980). Inverted sequence of metamorphism was noticed as early as 1907 by Loczy in the Eastern Himalaya. Since, then, three interpretations have been put forward.

(i) That it is due to large scale recumbent folding subsequent to regional metamorphism. No evidences of this are available around Jhala.

(ii) Diminishing effects of retrogression away from thrust contact has changed the high grade rocks to lower grades. This idea is not tenable as all evidences point to a progressive metamorphism in this region.

(iii) Higher thermal levels in the region due to variation in thermal gradient or nearness to the granitic pluton.

The last idea is not only modern but is also relevant in the present context. Similar ideas have been invoked by Bird and Toksoz (1975) and Toksoz and Bird (1977).

It is envisaged that, in the movement towards north of the Bhatwari microcontinent, the sediments deposited over it

obducted southwards near Jhala with hot lithosphere coming up and creating a thermal rise along the narrow zone near Jhala giving rise to the divergent/inverted metamorphic grades. Large scale anatexis took place resulting into porphyroblastic granitoid gneiss (Bhaironghati Gneiss - not described in this work). The Jhala region was only a narrow region very close to anatectic depths. This idea broadly coincides with the Zagros phase, described by Toksoz and Bird, except that the zone near Jhala is too narrow to show all the accompanying phenomena. The main thrust zone is not, however, at Jhala, but at the JBT. The sillimanite gneiss at Jhala, showing a very complex contorted pattern and occurrence of zoned pargasite-ferrogedrite bearing rock (which could be a metamorphosed ultrabasic (Bhaskar Rao - personal communication), have given rise to the idea proposed above. It may not be out of place to mention that Dave and Jain (personal communication) have seen sillimanite gneiss grading to porphyroblastic granitoid gneiss in other sections of the Central Himalaya. Had the region near Jhala not been topographically much lower than that of Suki, the importance of this feature could not have been recorded.

9.4 PLATE TECTONICS AND EVOLUTION OF THE CENTRAL HIMALAYA

9.4.1 Type of Geotectonic Elements:

Let us review some of the recent literature on the Himalayan Orogeny in view of the Plate Tectonics. Gansser (1980) has opined that ophiolitic melanges together with

crystalline slices along the 5000 km long Peri-Indian Suture Zone indicates that the ocean basins were highly complicated, with island arcs and continental fragments. Mitchel (1981) has explained the obduction of the Indus ophiolite southwards due to the Cretaceous collision of the Greater India with an island arc, probably separated from Tibet by a marginal basin. Several zones of ophiolites have been recognized by workers in Tibet region and have been used to explain several geological and tectonic features (Gansser, 1979; Veevers et al. 1975; Powell and Conaghan, 1975; Shackleton, 1981). The earlier concepts of a Precambrian Tibetan slab underlying the Tethys Paleozoic sequence is, according to Shackleton (1981), untenable.

It seems, therefore, that many ideas have been used by workers with different ends in view. New data coming for Tibetan and Chinese areas are gradually sorting out problems of regional scale such as, the southernmost limit of the continent lying north of the Tethys (Neotethys Gupta, et al., 1982). Involvement of a pre-Mesozoic elements in the Himalayan framework have been recognized by many workers.

Some workers (Valdiya, 1976; Dickins and Shah, 1980; Sinha Roy and Furnes, 1980; Chandra, 1978) consider that the rocks corresponding to those of present Peninsular India were involved in the Himalaya. Opinions differ, however, over the time of metamorphism and preservation of structures. It seems strange that, when most of the radioactive dates on metamorphic belts are Precambrian and were continental in nature, they did not suffer similar metamorphic and tectonic history as

their counterparts in the Indian Peninsula. If the Greater Indian continent could traverse as far north as Kun Lun-Astin Tagh belt (Veevers et al. 1975; Gansser, 1980) in 75 - 100 my why it could as well have developed metamorphic belts as seen in the Peninsular India. A Central Crystalline Axis may be a partial answer (Saxena, 1971). Ideas of microcontinents (Sinha Roy, 1976, 1978a, 1978b) or island arcs (Gansser, 1980; Mitchell, 1981) or intra-continental subduction zones (Bird, 1978) have been proposed with a view to explain several thrusts in the Himalaya south of Tibet, just as they have been proposed for the region lying in China. A detailed chronological study along with geochemistry and structure of individual sections would only be able to provide the right answer to such questions.

3.4.2. Timing and place of collision

There is no agreement as to when and where the first collision took place. Gupta et al. (1982) have grouped the available models into three categories following Klootwiik (1981).

- (i) Models considering the extension of the Greater India very far north in China and regard the Indus-Zangbo Suture Zone as a temporary narrow opening where ocean-type crust developed. Another version, followed by Stocklin (1977) and Boulin and Bouyz (1977), considers that southern Asia existed as a separate zone of amalgamated fragments which broke off Gondwanaland in about Triassic times and

coalesced with southern Angaraland by the early Jurassic prior to their capture by northward drifting Arabia and the Indian subcontinent during the late Cretaceous to Paleogene.

- (ii) Models of an enlarged Indian subcontinental block and underthrusting beneath the Tibetan Plateau along the leading edge of the north-moving Indian plate. The greatest exponents of this idea consider that first opening of the Gondwanaland started 150 my. ago (Athavale et al., 1971; Veevers et al., 1975, 1980). However, Veevers et al. (1971) had considered the major movement to be associated with Late Cretaceous-Cenozoic drift. Mitchell (1981) has considered Late Permian to early Triassic age for collision of the Burmese block with Malaya-Chiang Rai-Nukiang zone, but an Early Eocene collision of India and Asia. Bordet et al. (1971) consider an early Cretaceous collision of the Greater India with an island arc, probably separated from Tibet by a marginal basin while Curry et al. (1980) think collision of India with South Asia along the Indus-Tsangpo in early Eocene. Shackleton (1981) has reported pre-Mesozoic deformation in the Kangdese tectonic unit, which could be even Precambrian or Variscan and, if Precambrian, could be an island arc related to the Indian Plate on the basis of paleomagnetic and paleontological evidences.

Alternatively, if this unit is Variscan, then it became a part of the Asian plate before the Mesozoic. First evidences of crustal shortening in Kangdese zone indicates a Cretaceous age, but he thinks that the locus of maximum deformation migrated southward to the Zangbo ophiolite belt in Eocene and then to the High Himalaya and the MCT in Oligocene and along the M.B.F. during Miocene. He considers that the deformation south of the suture represent a series of north-dipping crustal shear zones resulting from collision. The Indus-Zangbo suture zone represent, therefore, the northernmost boundary of the Indian Plate. Shackleton (1981), therefore, does not agree with a very large extent of 'Greater Indian Plate' and is more in agreement with Gansser (1974) in this respect.

(iii) Models envisaging not more than 55 my. old collision between rigid crustal plates (Gupta et al. 1982; Molnar and Tapponnier (1975). Such models are supported by Toksoz and Bird (1977) in the true continent-continent collision style, unlike several others who have supposed island arcs or continental fragments. The problems in such models are with respect to the underthrusting of one continental block below the other due to the problem of density or buoyancy. Powell and Conaghan (1975) have correctly

pointed out that "the problem can be sidestepped by ignoring the mantle part of the lithosphere but this begs the question as to what happens to this part of the lithosphere or whether does it exist".

9.5 PRESENT MODEL

Sinha Roy (1978) applied the concept of microcontinent to the Himalayan tectonics whose thermal mechanism is not yet clear, although it seeks to explain the geological features of India and Tibet. It seems to the author that this model, partly modified with ideas of Shackelton (1981), may be able to offer a plausible explanation to surface geology of the Himalayan-Tibet region. A crude attempt towards this has been made by the author by way of a series of simplified cartoon (Fig. 9.1). Caution must, however, be exercised as the author has studied only the area under investigation, as reported in this work and at the best, could be regarded as thoughts emerging after literature survey. What is learned out of this and the evidences emerging out from the Bhagirathi-Yamuna Valleys may be summarized as follows:

- (i) The Himalayan Orogeny is not a simple subduction phenomenon.
- (ii) Continental blocks have not gone too far northwards below another continental block, although some amount of underthrusting of continental crust cannot be totally disallowed (Bird *et al.*, 1975).

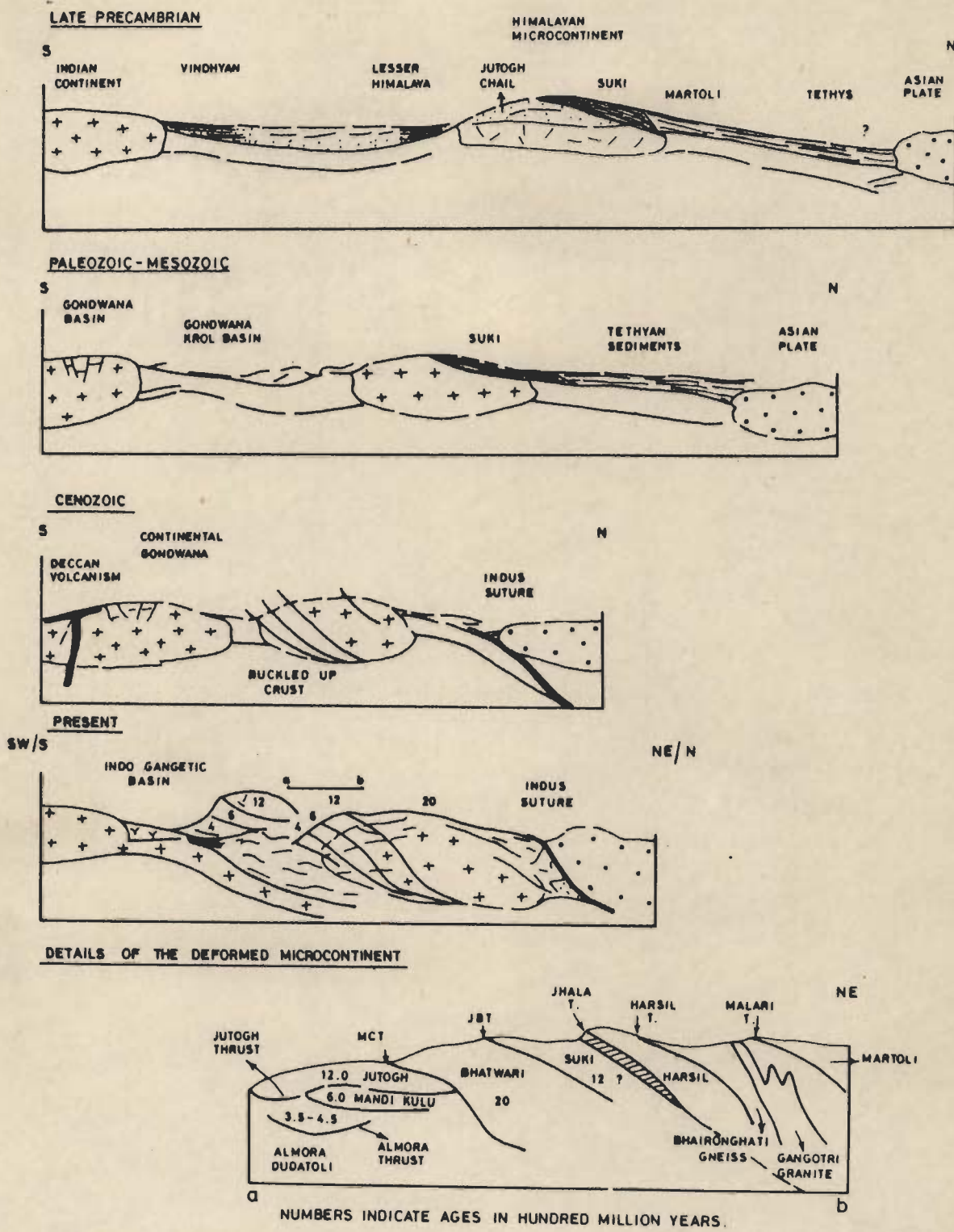


FIG. 9-1- CARTOONS SHOWING EVOLUTION OF THE NW-HIMALAYAN METAMORPHIC BELTS

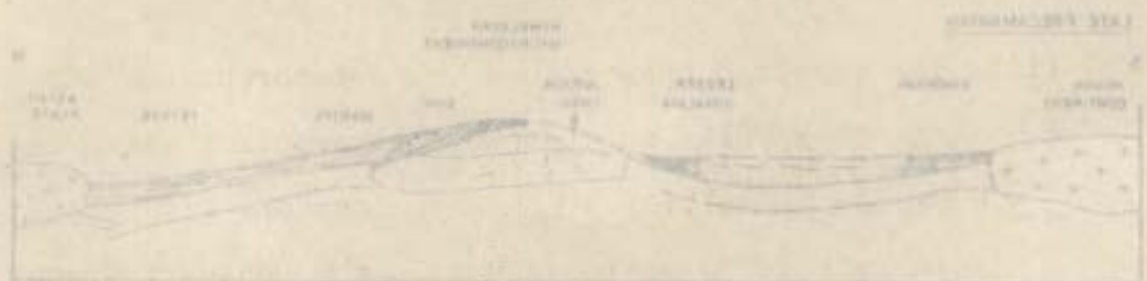


FIG. 1. CARBONS SHOWING EVOLUTION OF THE NW-HIMALAYAN HETEROCENTRIC BELTS

- (iii) The involved basement may be metamorphosed. But it undergoes a subsequent metamorphism during the period of collision and hence one may get polymetamorphosed formations such as the Bhatwari Group, thrusting up the once metamorphosed formations.
- (iv) The younger formations can ride over the older ones along the narrow zones of obduction giving rise to thermal domes leading to "normal" metamorphism on one side and "inverted" metamorphic sequences on the other; the zone of high grade metamorphic rocks thus occupying a tight or isoclinal thermal anticline such as around Jhala and elsewhere within the Central Himalaya of Garhwal and Kumaon, Many kilometers away from the MCT. This contrasts is more evident in comparison to the MCT zone in the Nepal Himalaya.
- (v) The Himalayan region might be consisting of one or more microcontinents or there may be intracontinental subduction before the two Tethyan sediments are involved.
- (vi) The subduction of the southern continent or of microcontinents and the Indian plate could be explained on the basis of several models.
- (vii) In different sections, topographically different levels might now be exposed giving rise to differences in metamorphism or appearance of

granite or anatectic zones. The importance of this conclusion has already been explained regarding observations at Jhala.

(viii) The late stage deformation (D_4) may bring one block relatively upwards than the other and changing the continuity of exposed geological details.

(1) Late Precambrian - It is envisaged that a Himalayan micro-continent occupied space between the Indian Plate and the southern margin of the Asian Plate and had undergone D_1 phase of deformation, M_1 progressive metamorphism and first phase of migmatization a result of which the gneisses, variously named as the Chaili gneiss along the Bhillangana Valley, the Dhakuri gneiss along the Pindar Valley and the Munsiri gneiss in Kumaon, were formed during 1900-2300 my. This microcontinent was probably overlain by Jutogh-Chail-Siki-Garhwal Group metasediments of 1200-1400 my. on both sides, while the Great Vindhyan Basin developed on northern margins of the Indian Continent, having Late Precambrian - early Paleozoic sediments of the Lesser Himalaya (Jain et al. 1980).

(2) Paleozoic-Mesozoic - Deformation of southern margin of the Himalayan microcontinent is evident during a early Paleozoic episode when the Salkhala Group sediments had undergone extensive migmatization during 500-600 my. Large track of the Lesser Himalaya was uplifted to constitute provenance for the southerly developing Gondwana-Krol Basin during Late Paleozoic-Mesozoic with extensive fragmentation of the Gondwana basins

and widespread Panjal volcanism in South, while an almost continuous sedimentation took place in the Tethyan Basin on northern margin of the Himalayan microcontinent.

(3) Late Mesozoic-Cenozoic - During the initial phases of the Himalayan Orogeny, the Indian Plate with the Himalayan microcontinent and the Tethyan sediments along its northern boundary collided with the Asian Plate along the Indus Suture Zone and had undergone fragmentation in its central part. As a result, extensive shortening and deformation of the microcontinent caused isoclinal folding, and progressive regional metamorphism during the D_2 deformation phase (in fact the first during the Himalayan Orogeny). Further crustal shortening initiated largescale translation of the thrust sheets from deeper crustal levels of about 20 km southward (D_{2a} deformation). This was probably achieved after the Tethyan Basin totally closed down as a result of subduction along the Indus Suture. Continuous deformation of the thrust sheets has caused the imbrication and tectonic slicing of the microcontinent as a result of which the Himalayan Basement Sliding (the Bhatwari Group) and the Suki Group are imbricated with the Lesser Himalayan elements. The present disposition of the thrust sheets probably constituting the Precambrian Himalayan microcontinent are shown in the last sketchmatic diagram where a tectono-stratigraphic inversion may be seen at different tectonic levels.

(4) Late Cenozoic-Holocene - The whole pile of the Central Himalayan metasediments along with the Lesser Himalaya sediments

were thrust southward over the foreland along the Main Boundary Fault at much shallower levels causing considerable resistance to the overthrust sheets. As a result, these thrust sheets were slightly metamorphosed in deeper levels in the Central Himalaya and deformed during the D_3 phase which has mainly caused macroscopic folding of the tectonostratigraphic units. Rapid cooling and uplift of the Central Himalayan pile resulted in faster vertical movements and considerable immature topography. NW-SE compression during the present northerly movement of the Indian Plate causes NE-SW trending open folds (D_4 deformation) and large-scale strike-slip movements which have produced two important lineaments.

R E F E R E N C E S

- Acharyya, S.K., 1978, Mobile belts of the Burma-Malaya and the Himalaya and their implications of Gondwana and Cathaysia/Laurasia continent configurations: In : Nutalaya, P., (Ed.), 3rd Regional Conf. Geol. & Min. Resources SE Asia, Asian Inst. Technology, Bangkok, p.121-127.
- Acharya, S.K., 1979, Pre-Tertiary fabric and metamorphism in Eastern Himalaya: In Verma, P.K., (Ed.), Metamorphic Rock Sequences of the Eastern Himalaya, K.P. Bagchi & Co., Calcutta, p.67-82.
- Acharyya, S.K., 1980, Stratigraphy and tectonics of Arunachal Lesser Himalaya : In Valdiya, K.S. and Bhatia, S.B. (Eds.), Stratigraphy and Correlations of Lesser Himalayan Formations, Hindustan Publishing Corporation (India), Delhi, p.231-241.
- Agrawal, L., Pande, A.R., and Powar, K.B., 1972, Petrogenesis of granitic rocks of Almora crystalline mass: Him.Geol., V.2, p.145-167.
- Agarwal, N.C. and Kumar, G., 1973, Geology of the Upper Bhagirathi and Yamuna Valleys, Uttarkashi District, Kumaon Himalaya: Him.Geol., V.3, p.1-23.
- Agarwal, N.C., and Kumar, G., 1980, The Garhwal Group - a critical reappraisal of its lithostratigraphy correlation and age: In Valdiya, K.S., and Bhatia, S.B., (Eds.), Stratigraphy and Correlations of Lesser Himalayan Formations, Hindustan Publishing Corporation (India), Delhi, p.52-78.
- Andrieux, J., Brunel, M., and Hamet, J., 1976, Metamorphism, granitization and relations with the Main Central Thrust Nepal : $^{87}\text{Rb}/^{87}\text{Sr}$ age determinations and discussion : Colloq. Int. CNRS, No.268, Ecologie et Geologie de Himalaya, Sci. de la Terre, Paris, p.31-40.
- Ashworth, J.R., 1976, Petrogenesis of migmatites in the Huntly-Portsoy area, north-east Scotland : Min. Mag., V.40, p.661-682.
- Athavale, R.N., Verma, R.K., Bhalla, M.S. and Pullaiah, G., 1970, Drift of the Indian sub-continent since Pre-Cambrian times : In Runcorn S.K., (Ed.), Paleogeophysics : London, Academic Press, p.291-305.
- Auden, J.B., 1933, On the age of certain Himalayan Granites : Rec. Geol. Surv. India, v.66, p.461-471.
- Auden, J.B., 1935, Traverses in the Himalaya : Rec. Geol. Surv. Ind. V.69, p.123-167.

- Auden, J.B., 1937, Structure of the Himalaya in Garhwal :
Rec. Geol. Surv. India, V.71, p.407-433.
- Auden, J.B., 1939, General Report of G.S.I. for 1937 : Rec.
Geol. Surv. India, V.73, p.99-101.
- Auden, J.B., 1949, General Report of G.S.I. for 1939 : Rec.
Geol. Surv. India. V.78, p.74-78.
- Augustithis, S.S., 1973, Atlas of the textural patterns of
granites, gneisses and associated rock types : Elsevier
Scientific Publishing Company, Amsterdam, 378 p.
- Banerji, P.K., Guha, P.K. and Dhiman, L.C., 1980, Inverted
metamorphism in the Sikkim-Darjeeling Himalaya, India :
Jour. Geol. Soc. India, V.21, No.7, p.330-342.
- Baratov, V.V., Mogorovskie and Melinichenko, A.K., 1975, The
geochemistry of lead and zinc in granitoids exemplified
by the Gissar Pluton in southern Tien Shan : In Tugarinov,
A.I., (Ed.), Recent contributions to Geochemistry and
Analytical Chemistry, John Wiley and Sons, New York, p.393-399.
- Barnes, H.L., (Ed.), 1979 Geochemistry of hydrothermal ore deposits:
John Wiley and Sons, Inc., 768 p.
- Barth, T.F.W., 1962, Theoretical Petrology : John Wiley and
Sons, Inc. New York, 416 p.
- Bedi, R.S. and Prasad, A.K., 1976, Study of the "outerband"
of the Dalhousie granite Chaori Khas, Chamba area,
Himachal Pradesh : Him. Geol., V.6, p.389-402.
- Bedi, R.S. and Prasad, A.K., 1980, X-ray studies of potassium
feldspars of granitic rocks Dhauladhar Batholith Chaori
Khas-Chamba area, Himachal Pradesh, India : Publication of
the Centre of Advanced Study in Geology, Chandigarh, No.12.
- Bedi, R.S. and Prasad, A.K., 1981, Metamorphism in the aureole
zone and associated metasediments of Dhauladhar batholith,
Chaori Khas (H.P.) : In Saklani, P.S., (Ed.), Metamorphic
Tectonities of the Himalaya, p.63-88.
- Berthe, D. Chaukroune, P. and Jegouzo, P., 1979, Orthogneiss,
mylonite and non-coaxial deformation of granites : the
example of the South American Shear Zone : Jour. Struct.
Geol., V.1, p.31-42.
- Bethke, P.M. and Barton, P.B., 1971, Distribution of some
minor elements between co-existing sulphide minerals :
Econ. Geol., V.67, p.140-163.

- Bhanot, V.B., Pandey, B.K., Singh, V.P., and Thakur, V.C., 1977, Rb-Sr whole-rock age of the granitic-gneiss from Askote area, Eastern Kumaun and its implication on tectonic interpretation of the area : *Him. Geol.*, V.7, p.118-119.
- Bhanot, V.B., Singh, V.P., Kansal, A.K., and Thakur, V.C., 1977, Early Proterozoic Rb-Sr whole-rock age for Central Crystalline Gneiss of Higher Himalaya, Kumaun : *Jour. Geol. Soc. India*, V.18, p.90-91.
- Bhanot, V.B., Kwatra, S.K., Kansal, A.K., and Pandey, B.K., 1978, Rb-Sr whole-rock age for Chail Series of northwestern Himalaya : *Jour. Geol. Soc. India*, V.19, p.224-225.
- Bhanot, V.B., Bhandari, A.K., Singh, V.P. and Kansal, A.K., 1979, Geochronological and geological studies on a granite of Higher Himalaya, Northeast of Manikaran, H.P. : *Jour. Geol. Soc. India*, V.20, p.90-94.
- Bhanot, V.B., Gill, J.S., Arora, R.P., and Bhalla, J.K., 1974, Radiometric dating of the Dalhousie granite. *Curr. Sci*, V.43, p.208.
- Bhanot, V.B., Goel, A.K., Singh, V.P. and Kwatra, S.K., 1975, Rb-Sr radiometric studies for the Dalhousie and Rohtang areas, Himachal Pradesh. *Curr. Sci.*, V.44, p.219-220.
- Bhanot, V.B., Pandey, B.K., Singh, V.P. and Kansal A.K., 1980, Rb-Sr ages for some granitic and gneissic rocks of Kumaun and Himachal Himalaya : In Valdiya K.S. and Bhatia, S.B., (Eds.), *Stratigraphy and Correlations of Lesser Himalayan Formations*, Hindustan Publishing Corporation, (India), Delhi - 110007, p.139-142.
- Bhanot, V.B., Singh, V.P., Kansal, A.K. and Thakur, V.C., 1976, Early Proterozoic Rb-Sr whole rock age for Central Crystalline Gneiss of Higher Himalaya : *Jour. Geol. Soc. India*, V.18, p.90-101.
- Bhargava, O.N., 1972, A reinterpretation of the Krol Belt : *Him. Geol.*, V.2, p.47-81.
- Bhargava, O.N., 1980, Outline of the stratigraphy of Eastern Himachal Pradesh, with special reference to the Jutogh Group : In Valdiya, K.S. and Bhatia, S.B., (Eds.) *Stratigraphy and Correlations of Lesser Himalayan Formations*, Hindustan Publishing Corporation, (India) New Delhi p.117-125
- Bhargava, O.N. and Chopra, S., 1981, Metamorphic facies map of the Himachal Himalaya : A preliminary attempt : *Bull. Ind. Geol. Assoc.*, V.41, No.1, p.45-58.

- Bhargava, O.N., Narain, K. and Dass A.S., 1972, A note on the Rampur Window, District Mahasu, H.P. : Jour. Geol. Soc. India, V.13, No.3, p.277-280.
- Bhatia, G.S. and Kanwar, R.C., 1971, On the age of Dalhousie Granite : Bull. Ind. Geol. Assoc., V.4, p.78-79,
- Bhatia, G.S. Kanwar, R.C., 1973, Mylonitization in outer granite band of Dalhousie, Himachal Pradesh, Him. Geol., V.3, p.103-115.
- Bhatt, B.K., 1972, Preliminary study of the Bhagirathi Basin between Uttarkashi and Gaumukh : Geol. Surv. India, Misc. Publ. No.15, p.1-8.
- Bhattacharya, A.K., Bhatnagar, G.S., Narayan Das, G.R., Gupta, J.N., Chhabria, T and Bhalla, N.S., 1981, Rb-Sr dating and geological interpretation of sheared granite-gneisses of Brijranigad-Ingedinala, Bhilangana Valley, Tehri District, U.P. (Abstract) 12th Him. Geol. Seminar, Dehra Dun.
- Billings, M.P., 1974, Structural Geology : Prentice Hall, New York, 606 p.
- Bird, P., 1978, Initiation of intracontinental subduction in the Himalaya : Jour. Geophy. Res., V.83- No.B10, p.4975-4987.
- Bird, P., Toksoz, M.N. and Sleep, N.H., 1975, Thermal and Mechanical models of continent-continent convergence zones : Jour. Geophy. Res., V.80, No.32, p.4405-4416.
- Bisaria, P.C., 1972, On garnet porphyroblasts of the Jutogh metamorphities : Him. Geol. V.2, p.397-403.
- Blanchard, D.P., Rhodes, J., Duncan, M., Rodger, K., Donaldson, C., Brannon, J., Jacobs, J. and Gibson, E., 1976, The chemistry and petrology of basalts from Leg 37 of the Deep Sea Drilling Project : Jour. Geophy. Res. V.81, p.4232-4246.
- Bordet, P., Colehen, M. and Le Fort, P., 1972, Some features of the Geology of the Annapurna range, Nepal Himalayas : Him. Geol. V.2, p.537-563.
- Bralia, A., Sabatini, G. and Troja, F., 1979, Revaluation of the Co/Ni ratio in pyrite as geochemical tool in ore genesis problems : Evidences from southern Tuscany pyrite deposits : Miner. Deposite, V.14, p.353-374.
- Bouchez, J.L., and Pecher, A., 1981, The Himalayan Main Central Thrust pile and its quartz-rich tectonites in Central Nepal : Tectonophysics, V.78, p.23-50.

*
Chibber, H.L., 1958, Landforms of the Bhagirathi Valley :
Nat. Geogr. Jour. India (Presidential Address).

- Boulin, J. and Bouzy, E., 1977, Introduction a la geologie de l'Hindon Kouch occidental : Mem. h. Ser. Soc. Geol. Fr., V.8, p.87-105.
- Buddington, A.F., 1948, Origin of granitic rocks of the Northwest Adirondcks : In Gilluli, J., (Ed.), Origin of Granite Mem. Geol. Soc. Am., V.28, p.21-43.
- Carmichael, I.S.E., 1964, The petrology of Thingmuli, a Tertiary volcano in Eastern Iceland : Jour. Petrol. V.5, p.435-460.
- Carmichael, I.S.E., Turner, F.J. and Verhoogen, J., 1974, Igneous Petrology : McGraw-Hill Book Company, New York, 739 p.
- Carrobi, G. and Pierruccini, R. e, 1947, Spectrographic analysis of tourmalines from the island of Elba with correlation of color and composition : Am. Mineral., V.32, p.121.
- Chadha, D.K., 1977, Petrology and Geochemistry of amphibolites from north-east of Chaur Peak, Himachal Pradesh, India : In Tiwari, B.S., and Gupta, V.J., Recent Researches in Geology (Vol.3), Hindustan Publishing Corporation, New Delhi, p.252-279.
- Chandra, U., 1978, Seismicity, Earthquake mechanisms and tectonics along the Himalayan mountain range and vicinity : Physics of the Earth and Planetary Interiors, V.16, p.109-131.
- Chaudhary, J.M., and Narayan Rao, M., 1966, Optical studies on the potash felspar of Archean granites and their petrogenetic significances : Quartz. Jour. Geol. Min. Metal. Soc. Ind., V.38(3), p.157-159.
- *
Chinner, G.A., 1960, Pelitic gneisses with varying ferrous/ferric ratios from Glen Glova, Angus, Scotland : Journal of Petrology, V.1, p.178-217.
- Condie, K.C., 1976, Trace-element geochemistry of Archean greenstone belts : Earth Sc. Rev., V.12, p.393-417.
- Condie, K.C., Barsky, C.K. and Mueller, P.A., 1969, Geochemistry of Precambrian diabase dikes from Wyoming : Geochem. Cosmochim. Acta, V.33, p.1371-1388.
- Cox, K.G., Bell, J.D., and Pankhurst, R.J., 1979, The Interpretation of Igneous Rocks : George Allen & Unwin (Publishers) Ltd., London, 450 p.
- Curray J.R., Emmel, F.M., Moore D.G. and Raitt, R.W., 1980, Structure, tectonics and geological history of the Northeastern Indian Ocean : In Nairn, A.E.M. and Stehhl, F.G.(Eds.), The Ocean Basins and Margins, V.G., The Indian Ocean, Plenum Press New York,

- Das, B.K., 1968, A study in metamorphism of the basic rocks of some parts of Kumaon : Publication of the Centre of Advanced study in Geology, Panjab University, Chandigarh No.5, p.79-88.
- Das, B.K., 1978a, Polyphase medium to high pressure regional metamorphism of pelitic rocks around Kishtwar, Jammua and Kashmir State, India : N. Jb. Miner. Abh, V.132, p.173-190.
- Das, B.K., 1978b, Relation between metamorphic crystallization and deformation : An example from lower Himalayan terrain, India : Geol. Rundschau, V.68, p.351-364.
- Das, B.K., 1979, A study in metamorphism of the basic rocks of some parts of Kumaun : Publication of the Centre of Advanced Study in Geology, Panjab University Chandigarh, No.5, p.79-88.
- Das, B.K., 1979, Petrology and structure of the granitic gneisses and the associated mesograd metamorphites of the Dwarahat area, Lower Kumaun : In Saklani, P.S., (Ed.), Structural Geology of the Himalaya, p.41-58.
- Das, B.K. and Pande, I.C., 1963-64, On the occurrence of 'garnet in garnet' in the mica schist of Chaukhutia area, Almora district, U.P. India : Jour. Sci. Res, B.H.U. V.14, p.23-24.
- Dave, V.K.S., Gupta, S.K. and Singh, B.K., 1981, Causes and classification of landslides in the Central Himalayan Regions of Uttarkashi and Chamoli, U.P. : G.S.I. Symp. on 3 Decades of Engineering Geological Investigation in India, Dehra dun, in pres
- Deer, W.A., Howie, R.A. and Zussman, J., 1963, Rock-Forming Minerals : Vol.2, Longmans, Green & Co. Ltd., 379 p.
- Deer, W.A., Howie, R.A. and Zussman, J., 1963, Rock-forming Minerals, Vol.4, Longmans, Green and Co. Ltd., London, 435 p.
- Delano, J.W. and Ringwood, A.E., 1978, Siderophile elements in the lunar highlands : nature of the indigenous component and implications for origin of the Moon : Proc. Ninth Lunar Planet. Sci. Conf.
- Denmen, W.H., 1967, Trace elements in quartz as indicators of provenance : Bull. Geol. Soc. Am. V.75, p.125-130.
- Desai, S.J., 1973, Mode of origin and tectonic setting of gneissic rocks of Siahni Devi area, District Almora, U.P., Hi. Geol. V.3, p.345-356.

*

Fleuty, M.J., 1964, The description of folds : Geol. Assoc. Proc.,
V.75, Pt.4, p.461-489.

- Dickins, J.M. and Shah, S.C., 1980, Permian paleogeography of Peninsular and Himalayan India and the relationship with the Tethyan region : In : Creswell M.N. and Vella. P.(Eds.), Gondwana, Five, A.A.Balkema, Rotterdam, p.79-83.
- Dietrich, R.V., 1960, Banded gneisses : Jour. Petrol. V.I, p.99-120.
- Dietrich, R.V., 1962, K-feldspar structural states as petrogenetic indicators : Norsk. Geol. Tidssk., V.42, II (feldspar Vol.), 394 p.
- Doe, D.R. and Tilling, R.I., 1967, The distribution of lead between coexisting K-feldspar and plagioclase : Am. Mineral, V.52, p.805-816.
- Drury, S.A., 1972, The chemistry of some granitic veins from the Lewisian of Coll and Tiree, Argyllshire, Scotland: Chem. Geol., V.9, p.175-193.
- Ernst, W.G., 1968, Amphiboles : Monography series of theoretical and experimental studies, Vol.1, Springer Verlag, New York, 125 p.
- Eskola, P., 1937, An experimental illustration of the spilitic reaction : Comm. Geol. Finlande. Bull., V.119, p.61-68.
- Eugster, H.P., 1959, Reduction and oxidation in metamorphism: In Researches in Geochemistry, N.Y. Wiley, p.397-426.
- Fabries, J., 1964, Les formations cristallines et métamorphiques du Nord Est de la province de Seville (Espagne). Essai sur le métamorphisme des roches basiques - Sciences de la terre mem No.4.
- Fleischer, R.L. and Price, P.B., 1964, Technique for geological dating of minerals by chemical etching of fission fragments tracks : Cosmochim. Acta., V.28, p.1705-1714.
- *
Floyd, P.A., 1976, Geochemical variation in the Greenstones of S.W. England : Journal of Petrology, V.17, p.523-545.
- Frank, W., Hoinkes, G., Miller, C., Purtscheller, F., Richter W. and Thoni, M., 1973, Relations between metamorphism and orogeny in a typical section of the Indian Himalayas: Tscherm. Mine. Petr. Mitl., V.20, p.303-332.
- Frank, W., Thoni, M., and Purtscheller, F., 1976, Geology and petrography of Kulu-South-Lahul area : Colloqu. Int. CNRS No.268, Ecologie de l'Himalayan Sci. de al Terre, Paris, p.147-171.

- Frank, W., Gansser, A. and Trommsdorff, V. 1977, Geological observations in the Ladakh area (Himalayas), a preliminary report : Schweiz Minral. Petrogr. Mitt., V.57, p.89-113.
- Fuchs, G., 1967, Zum Bau des Himalaya : Oesterr. Akad. Wiss. Math. Naturwiss. KI., Sitzungsber., Abt., V.113, p.1-211.
- Fuchs, G. and Gupta, V.J., 1971, Paleozoic Stratigraphy of Kashmir, Kishtwor and Chamba (Panjab Himalayas) : Verh. Geol., B-A, V.1, p.68-97.
- Gangopadhyay, P.K., 1979, Structural Framework of the Daling Darjeeling-Permian Rocks. In Verma P.K.(Ed.), Metamorphic Rock Sequences of the Eastern Himalaya, K.P. Bagchi & Co. Calcutta, p.23-42.
- Gansser, A., 1964, Geology of the Himalayas : Interscience Publishers, London, 289 p.
- Gansser, A., 1974, The Himalayan Tethys : Mem. XIV Contributi stratigrafic e paleogeografici sul Mesozoica della Tetide, Milano, p.393-411.
- Gansser, A., 1980, The Peri-Indian suture zone : Mem. du. B.R.G.M. No.115, Colloque 5, p.140-148.
- Gansser, A., 1980, The significance of the Himalayan suture zone: Tectonophysics, V.62, p.37-52.
- Gast, P.W., 1968, Trace element fractionation and the origin of tholeiitic and alkaline magma types : Geochim. Cosmochim. Acta., V.32, p.1057-1086.
- Geological Survey of India, 1976, Geology of the Himalaya-appraisal of status and definition of problems, Him. Geol. Seminar, New Delhi, Geol. Surv. Ind., 48 p.
- Ghose, N.C., 1979, Hydrothermal Melting relationship of some high-grade metamorphic rocks of Darjeeling : In Verma, P.K., (Ed.), Metamorphic Rock Sequences of the Eastern Himalaya, K.P. Bagchi and Co., Calcutta, p.139-149.
- Ghose, A., Chakrobarati, B. and Singh, R.K., 1974, Structural and metamorphic history of the Almora Group : Him. Geol. V.4, p.171-194,
- Ghosh, A.M.N., 1956, Recent advances in geology and structure of Eastern Himalaya : Pres. Address. Ind. Sci Congr. Pt. 3, p.85-99.
- Ghosh, N.C. and Trofimov, N.N., 1970, Abundance of nickel and chromium in the basaltic rocks of India : Symposium on applications of geochemistry in Earth Sciences (abstract), Geochem. Soc. India.

- Glen, R.A., 1980, Reorientation of early biotites during schistosity formation in andalusite schists, Mount Frank area, Broken Hill, N.S.W. : *Tectonophysics*, V.68, p.213-232.
- Goldsmith, J.R. and Laves, F., 1954, The microcline-sanidine stability relations : *Geochim. Cosmochim. Acta*, V.5, p.1-19.
- Green, J. and Poldervaart, A., 1958, Petrochemical fields and trends : *Geochim. et. Cosmochim. Acta*, V.13, p.87-122.
- Green, D.H., 1970, A review of experimental evidences on the origin of basaltic and nephelinitic magmas : *Phy. Earth Planet. Inter.*, V.3, p.221-235.
- Gregg, W.J., 1980, The texture of cross-micas in rocks affected by schistosity-parallel displacements : *Jour. Struct. Geol.*, V.2, p.333-340.
- Griesbach, C.L., 1891, Geology of the Central Himalayas : *Mem. Geol. Surv. India*, V.23, p.232.
- Griffin, W.L. and Murthy, V.R., 1969, Distribution of K, Rb, Sr and Ba in some minerals relevant to basalt gneiss : *Geochim. Cosmochim. Acta*, V.33, p.1389-1414.
- Gupta, L.N., 1978, Metamorphism, mobilization and anatexis of the crystalline rocks of Badrinath region, Central Himalaya: *The Indian Mineralogist*, V.19, p.34-41.
- Gupta, L.N., 1979, On the field aspects of the Root-zone of Badrinath and Mana-pass areas, Central Himalaya : In Suklani, P.S., (Ed.), *Structural Geology of the Himalaya*, Today and Tomorrow's Publisher, New Delhi.
- Gupta, H.K., Rao, V.D. and Singh, J., 1982, Continental collision tectonics : Evidence from the Himalaya and the neighbouring regions : *Tectonophysics*, V.81, p.213-238.
- Gupta, S.K. and Dave, V.K.S., 1977, Petrology and metamorphism of the Bhagirathi Valley, Central Crystallines, Distt. Uttarkashi, U.P. : *Him. Geol.* V.9, Part II, p.512-528.
- Gupta, S.K., and Dave, V.K.S. 1982, Geological investigations of the Bhagirathi blockage of August 1978 : In Singhal, B.B.S. (Ed.), *Engineering Geosciences*, Sarita Prakashan, Meerut, p.50-64.
- Hanmer, S.K., 1982, Vein arrays as kinematic indicators in Kinked anisotropic materials : *Jour. Struct. Geol.*, V.4(2), p.151-160.

- *Hutchison, C.S., 1974, Laboratory Handbook of Petrographic Techniques : John Wiley & Sons, New York, 527 p.
- Hammer, S.K., 1982, Microstructure and geochemistry of plagioclase and microcline in naturally deformed granite : Journal of Structural Geology, V.4, p.197-213.
- Hanson, G.N., 1978, The application of trace elements to the petrogenesis of igneous rocks of granitic composition : Earth Planet. Sci. Lett., V.38, p.26-43.
- Harris, R.L., Jr., 1977, Displacement of relict zircons during growth of feldspathic porphyroblasts : Bull. Geol. Soc. Am., V.88, p.1828-1830.
- Harpum, J.R., 1963, Petrographic classification of granitic rocks in Tanganyika by partial chemical analyses : Tanganyika Geol. Survey. Rec., V.10, p.80-88.
- Hayden, H.H., 1904, The geology of Spittitwith parts of Bashahr and Rupshu : Mem. Geol. Surv. India. V.36, 129 p.
- Hedge, C.E., 1972, Source of leucosomes of migmatites in the Front Range, Colorado : Geol. Soc. Am. Mem. 135, p.65-72.
- Heim, A. and Gansser, A., 1939, Central Himalaya, Geological observations of the Swiss Expedition 1936 : Mem. Soc. Helv. Sci. Nat. V.73, 245 p.
- Heinrich, E. Wm., 1965, Microscopic Identification of Minerals: McGraw-Hill Book Company, New York, 414 p.
- Henningsen, D., 1967, Crushing of sedimentary rock samples and its effect on shape and number of heavy minerals: Sedimentology, V.8., p.253-255.
- Hietanen, A., 1959, Kyanite-garnet gedritite near Orofino, Idaho : Am. Min., V.44, p.539.
- Hibbard, M.J., 1965, Origin of some alkali feldspar phenocrysts and their bearing on petrogenesis: Jour. Sci. V.263, p.245-261.
- Hughes, C.J., 1970, The significance of biotite selvages in migmatites. Geol. Mag., V.107, p.21-24.
- Hyndman, D.W., 1972, Petrology of Igneous and Metamorphic Rocks : McGraw-Hill Book Company, New York, 533 p.
- Iden, I.K., 1981, Geochemistry of Precambrian basal gneisses in Lofotenvesteralen, Northern Norway : Precambrian Research, V.14, p.135-166.

*

Irvine, T.N. and Barager, W.R.A., 1971, A guide to the chemical classification of the common volcanic rocks : Can. Jour. Earth Sci., V.8, p.523-548.

- Irvine, T.N., 1979, Rocks whose composition is determined by crystal accumulation and sorting : In Yoder, H.S., Jr., (Ed.), The Evolution of the Igneous Rocks, Princeton University Press, Princeton, New Jersey, p.245-306.
- *
Jager, E., Bhandari, A.K. and Bhanot, V.B., 1971, Rb/Sr age determination on Biotites and whole-rock samples from Mandi and Chor granite (H.P.) India : *Ecologae. Geol. Helv.*, V.64, p.1889-1906.
- Jakes, P. and White, A.J.R., 1972, Major and trace element abundances in volcanic rocks of orogenic areas : *Bull. Geol. Soc. Am.*, V.83, p.29-40.
- Jain, A.K., 1971, Stratigraphy and tectonics of Lesser Himalayan region of Uttarkashi, Garhwal Himalaya : *Him. Geol.*, Vol.1, p.25-58.
- Jain, A.K., 1972, Heavy minerals in Precambrian quartzite of the Lesser Himalaya, Garhwal, India : *Jour. Sed. Petrol.*, V.42, p.940-941.
- Jain, A.K., 1972, Overthrusting and emplacement of basic rocks in Lesser Himalaya, Garhwal U.P. : *Jour. Geol. Soc. India*, V.13, p.226-237.
- Jain, A.K., 1981, Stratigraphy, petrography and paleogeography of the Late Paleozoic diamictulis of the Lesser Himalaya : *Sed. Geol.*, V.30, p.43-78.
- Jain, A.K., Goel, R.K. and Nair, N.G.K., 1980, Implications of Pre-Mesozoic Orogeny in the geological evolution of the Himalaya and Indo-Gangetic Plains : *Tectonophysics*, V.62, p.67-86.
- Jain, A.K., and Thakur, V.C., 1978, Abor volcanics of the Arunachal Himalaya : *Jour. Geol. Soc. India*, V.19, No.8, p.335-349.
- Jain, A.K., Thakur, V.C. and Tandon, S.K., 1974, Stratigraphy and structure of the Siang district, Arunachal (NEFA) Himalaya *Him. Geol.* V.4, p.28-60.
- Jaireth, S.K., Santosh, M and Mohan, P.C., 1981, Fluid inclusion thermometry of quartz from Odara pegmatite, Kerala : *Proc. Ind. Acad. Sci (Earth and Planetary Sciences)*, in press
- Jhingran, A.G., Thakur, V.C. and Tandon, S.K., 1974, Stratigraphy and structure of the Siang dist., Arunachal (NEFA) Himalaya : *Him. Geol.* V.4, p.28-60.

- Kamp, van de P.C., 1970, The green beds of the Scottish Dalradian Series : Geochemistry, origin and metamorphism of mafic sediments : Jour. Geol. v.78, p.281-303.
- Kanwar, R.C. and Bhatia, G.S., 1977, Tectonics of Dalhousie granites : Recent Researches in Geology. V.4, p.159-186,
- Kanwar, R.C. and Bhatia, G.S., 1977, Structural analysis of the rocks of the Dalhousie-Chamba area, Himachal Pradesh, India : Recent Researches in Geology, V.3, p.300-328.
- Kapila, S.P., Jiwan, J.S. and Prasad, A.K., 1980, Petrochemistry of the migmatites of Mukteswar area, Kumaun Himalaya, India : Publication of the Centre of Advanced Study in Geology No.4, p.286-302.
- Karant, R.V. and Shah, An., 1977, An interpretation of the origin and tectonic setting of the granitic rocks of Almora in Kumaun Himalaya : Him. Geol., V.7, p.398-415.
- Kashyap, S.R., 1972, Migmatites of Ramgarh area, Dist. Nainital, U.P. : Him. Geol. V.2, p.271-288.
- Kays, M.A., 1976, Comparative geochemistry of migmatized, interlayered quartzofeldspathic and pelitic gneisses : a contribution from rocks of southern Finland and northeastern Saskatchewan : Precambrian Research, V.3, p.433-462.
- Kizaki, K., and Hayashi, D., 1979, Migmatite tectonics of the Hidaka metamorphic belt, Hokkaido, Japan : Tectonophysics, V.56, p.203-220.
- Kleeman, A.W., 1965, The origin of granitic magma : Jour. Geol. Soc. Aust., V.12, p.35-51.
- Klootwijk, C.T., 1981, Greater India's northern extent and its underthrust of the Tibetan Plateau : Paleomagnetic constraints and implications : In, Delany, F.M. and Gupta, H.K., (Eds.) Zagros-Hindu Kush-Himalaya Geodynamic Evolution. Geodynamics Series, Am. Geophys. Union-Geol. Soc. Am.
- Krishna Rao, J.S.R. and Raju, R.D., 1977, X-ray studies on the structural state, orthoclase content and Al-distribution in tetrahedral of potassium feldspar from southern India : Jour. Geol. Soc. Ind., V.18, p.117-124.
- Krummenacher, D., 1961, Determinations de l'age isotopique des roches de l'Himalaya du Nepal par la methode potassium-argon : Bull. Suisse. Min. Petrogr. V.41, p.273-283.
- Kumar, S., 1975, Mineral growth and deformation in the crystalline schist of Central Himalaya around Rohtang Pass (H.P.), India : Geol. Rundschau, V.64, p.248-259.

*

Mac Donald, G.A., 1968, Composition and origin of Hawaiian lavas,
Mem. Geol. Soc. Am., V.116, p.477-522

- Kumar, G., Prakash, G. and Singh, K.N., 1974, Geology and Deoprayag - Dwarahat area, Garhwa, Chamoli, and Almora, Kumaun Himalaya, Uttar Pradesh : *Him. Geol.*, V.4, p.323-347.
- Kuno, H. Yamasaki, K, Lida, C. and Nagashima, K., 1957, Differentiation in Hawaiian magma : *Jap. Jour. Geol. and Geog.*, V.28, p.129-218.
- Lal, R.K., Mukerji, S. and Ackermant, D., 1981, Deformation and Barrovian metamorphism at Takdah, Darjeeling (Eastern Himalaya) : In Saklani P.S. (Ed.), *Metamorphic Tectonities of the Himalaya*, p.231-278.
- Larsen, E.S., 1938, Some new variation diagrams for groups of igneous rocks : *Jour. Geol.*, V.46, p.505-520.
- Leake, B.E. 1964, The chemical distinction between ortho- and para- amphibolites : *Jour. Petrol.*, V.5, p.238-254,
- Leeman, W.P., 1979, Partitioning of Pb between volcanic glass and coexisting sanidine and plagioclase feldspars : *Geochim. Cosmochim. Acta*, V.43, p.171-175.
- Le Fort, P., 1975, Himalayas, : the collided range, Present Knowledge of the continental arc : *Am. Jour. Sc.*, V.275-A, p.1-44.
- Le Fort, P., 1981, Manaslu leucogranite : a collision signature of the Himalaya, a model for its genesis and emplacement: *Jour. Geophys. Res.*, V.86, No.B11, P.10545-10568.
- Lister, L.A. (Ed.), 1973, Symposium on granites, gneisses and related rocks : *Geol. Soc. of South Africa Special Publication No.3*, 509 p.
- Loczy, L. von., 1907, Beobachtungen in ostlichen Himalaya : *Folds. Kozlem*, V.35, p.1-24.
- Lydekker, R., 1883, The Geology of the Kashmir and Chamba territories and the British district of Khagan, : *Mem. Geol. Surv. India*, V.22, 344 p.
- *
Marmo, V., 1958, Orthoclase and microcline granites : *Am. Jour. Sci.* V.256, p.360-364.
- McCarthy, T.S., 1976, Chemical interrelationships in a low-pressure granulite terrain in Namaqualand, South Africa and their bearing on granite genesis and the composition of the lower crust : *Geochim. Cosmochim. Acta*. V.40, p.1057-1068.
- McCarthy, T.S. and Groves, D.I., 1979, Blue-Tier batholith, Northern Tasmania : *Contrib. Mineral. Petrol.*, V.71, p.193-209.

- McMahon, C.A., 1879, Notes of a tour through Hangrang and Spiti: Rec. Geol. Surv. India, V.12, p.57-69.
- McMahon, C.A., 1881, Note on the section from Dalhousie to Pangivia Sach Pass : Rec. Geol. Surv. India, V.14, p.305-310.
- McMahon, C.A., 1882, The Geology of Dalhousie : Rec. Geol. Surv. India, V.15, p.36-51.
- McMahon, C.A., 1885, Some further notes on the geology of Chamba : Rec. Geol. Surv. India, V.18, p.78-110.
- Mehdi, S.H., Kumar, G and Prakash, G, 1972, Tectonic evolution of eastern Kumaun Himalaya : A new approach : Him. Geol., V.2, p.481-501.
- Mehnert, K.R., 1968, Migmatites and the origin of granitic rocks : Elsevier Publishing Company, Amsterdam, 393 p.
- Mehta, P.K., 1975, Rb-Sr dating of the Kulu-Manali belt, NW Himalayas: Its implications for Himalayan tectogenesis (Abs): WIHG, Sixth Seminar, Dehradun, p.10-11.
- Mehta, P.K., 1976, Structural and metamorphic hisotry of the crystalline rocks of Kulu valley, Himachal Pradesh, in relation to the tectonics of the northwestern Himalaya : Geotettonica Accad. Naz. Lincei, V.21, p.215.
- Mehta, P.K., 1977, Origin of albite rims around feldspars in the migmatitic gneisses of Kulu : In Tiwari, B.S., and Gupta, V.J. (Ed.), Recent Researches in Geology (Vol. 3), Hindustan Publishing Corporation, New Delhi, p.337-341.
- Mehta, P.K., 1978, Rb-Sr Geochronology of the Kulu-Mandi Belt. Its implications for the Himalayan Tectogenesis - A reply: Geol. Rundschau, V.68, p.383-392.
- Mehta, P.K., 1979, Tectonic significance of the young mineral dates and the rates of cooling and uplift in the Himalaya: Tectonophysics, V.62, p.205-217.
- Mehta, P.K., 1980, Tectonic significance of the young mineral dates and the rates of cooling and uplift in the Himalaya : Tectonophysics, V.62, p.205-217.
- Mehta, P.K. and Pande, I.C., 1977, Growth, rotation and degeneration of garnet in the crystalline schists of Kulu, NW Himalaya : Bull. Ind. Geol. Assoc., V.40, p.23-32.
- Mehta, P.K. and Rex, D.C., 1977, K-Ar geochronology of the Kulu-Manali belt, N.W. Himalay, India : N. Jb. Miner. Mh. V.48, p.343-355.

- Mehta, P.P. and Nagpaul, K.K., 1970, Fission track ages of some Indian apatites Ind. Jour. Pure. Appl. Phys., V.8, p.397-400.
- Mehta, P.P. and Nagpaul, K.K., 1971, Fission track ages of mica belts and some other Precambrian muscovites of India : Pure and Applied Geophysics, V.87, p.174-191.
- Merh, S.S., 1977, Structural studies in parts of Kumaun Himalaya: Him. Geol. V.7, p.26-42.
- Merh, S.S. and Vashi, N.M., 1965, Structure and metamorphism of the Ranikhet area of Almora district, Uttar Pradesh : Indian Mineralogist, V.6, p.55-66.
- Merril, R.B., Robertson, J.K. and Wyllie, P.J., 1970, Melting reactions in the system $\text{NaAlSi}_3\text{O}_8 - \text{KAlSi}_3\text{O}_8 - \text{SiO}_2$: Jour. Geol. V.78, p.558-569.
- Middlemiss, C.S., 1896, The geology of Hazara and the Black Mountain : Mem. Geol. Surv. India, V.26, p.1-302.
- Milner, H.B., 1962, Sedimentary petrography : Atten and Unwin, London, V.2, 715 p.
- Misch, P., 1949, Metasomatic grantization of batholithic dimensions : Am. Jour. Sci., V.247, p.209-245.
- Misch, P., 1971, Porphyroblasts and "crystallization force" some textural criteria : Bull. Geol. Soc. Am., V.82, p.245-251.
- Misra, R.C. and Bhattacharya A.R., 1976, The Central Crystalline zone of Northern Kumaun Himalaya. Its lithostratigraphy structure and tectonics with special reference to plate tectonics : Him. Geol., V.6, p.133-154.
- Misra, R.C., and Sharma R.P., 1966, Albite rims in granitic rocks of the Devi Dhura area, Dist. Almora U.P.: Bull. Geol. Soc. Ind., V.3(2), p.51-53.
- Mitchell, A.H.G., 1979, Guides to metal provinces in the Central Himalaya collision belt; the value of regional stratigraphic correlations and tectonic analogies : Mem. Geol. Soc. China, No.3, p.167-194.
- Mitchell, A.H.G., 1981, Phanerozoic plate boundaries in mainland SE Asia, the Himalayas and Tibet : Geol. Soc. London, V.138, p.109-122.
- Molnar, P. and Tapponnier, P., 1975, Cenozoic tectonics of Asia : effects of a continental collision : Science, N.Y., V.189, p.419-426.

- Moore, B.R. and Dennen, W.H., 1970, A geochemical trend in silicon-aluminium-iron ratios and the classification of elastic sediments : *Jour. Sed. Petrol.* V.40, p.1147-1152.
- Mukherjee, A., 1979, Inversion of metamorphic zoning in the Eastern Himalaya : In Verma, P.K., (Ed.), *Metamorphic Rock Sequences of the Eastern Himalaya*, K.P. Bagchi & Co., Calcutta, p.125-138.
- Mukhopadhyay, M.K. and Gangopadhyay P.K., 1971, Structural characteristics of rocks around Kalimpong, West Bengal; *Him.Geol.*, V.1, p.213-230.
- Nagpaul, K.K., 1981, Fission Track Geochronology of India : *Proc. Earth Planet Sci.* V.90, No.4, p.389-401.
- Nagpaul, K.K. and Lal, N., 1980, Age determination and uranium concentration by fission track studies.: Unpublished scientific report No.NBS(G)-182, Department of Physics, Kurukshetra University, Kurukshetra, 205p.
- Nagpal, M.K., Nagpaul, K.K. and Mehta, P.P., 1972, Uranium contents in minerals by fission track method : *Pure and Applied Geophysics*, V.102, p.153-160.
- Nagpaul, K.K., Gupta, M.L. and Mehta, P.P. 1973, Fission-Track Ages of some Himalayan granites : *Him. Geol.* V.3, p.249-261.
- Naha, K. and Ray, S.K., 1970, Metamorphism history of the Jutogh Series in the Simla Klippe, Lower Himalaya : *Contri. Mineral and Petrol.*, V.28, p.147-164.
- Naha, K. and Ray, S.K., 1971, Evidence of overthrusting in the metamorphic terrain of the Simla Himalayas : *Am. Jour. Sci.*, V.270, p.30-42.
- Narain, H., 1975, National report on the Geodetic and Gravitometric work done in India by various organizations and Institutions during the period 1971-74: Sixth General Assembly Meeting of I.U.G.C. at Grenoble France.
- Narayan Das, G.R., Parthasarthy, T.N. Taneja, P.C. and Perumal, N.U.A.S., 1979, Geology, structure and uranium mineralization in Kulu, Himachal Himalaya : *Jour. Geol. Soc. India*, V.20, p.95-102.
- Nesbitt, R.W. and Sun, S.S., 1976, Geochemistry Archean spinifex-textured peridotites and magnesian and low-magnesian tholeiites : *Earth Planet. Sc. Lett.*, V.31, p.433-453.
- Nilssen, B. and Smithson, S.E., 1965, Studies on the Precambrian Herefoss granite, I.K-feldspar obliquity: *Norsk.Gel. Tidssk.*, V.45, p.367-396.

- Ohta, Y. and Akiba, C. (Eds.), 1973, Geology of the Nepal Himalayas: Publication of the Himalayan Committee of Hokkaido University, Sapporo, Japan, 292 p.
- Orville, P.M., 1963, Alkali ion exchange between vapour and feldspar phases : Am. Jour. Sci., V.261, p.201-237.
- Orville, P.M., 1969, A model for metamorphic differentiation origin of thin layered amphibolites : Am. Jour. Sci. V.267, p.64-86.
- Pachauri, A.K., 1972, Stratigraphy, correlation and tectonics of the area around Purola, Uttarkashi and Dehradun Dists. (U.P.) : Him. Geol., V.2, p.371-387.
- Page, L.R., 1968, Devonian plutonic rocks in New England: In Zen, E. and White, W.S., Hadley, J.B. and Thompson, J.B., Jr., (Eds.), Studies of Appalachian Geology, Northern Maritime, Interscience, New York, p.371-383.
- Pande, I.C., 1956, Migmatites of Ramgarh, Distt. Nainital : Jour. Sci. Res. B.H.U., V.7, p.88-105.
- Pande, I.C., 1979, The Nanga Parbat-Namcha Barwa Region : In Verma, P.K. (Ed.), Introduction to Metamorphic Rock Sequences of the Eastern Himalaya, K.P. Bagchi & Co., Calcutta, p.3-20.
- Pande, I.C., Powar, K.B., and Das, B.K., 1963, The migmatites of Kumaun Hills, Uttar Pradesh, India : National Geographica Journal of India, V.IX, p.96-103.
- Pande, I.C. and Saxena, M.N., 1968, The birth and development of Himalaya : Publ. Centre of Advanced Study in Geology, V.4, p.1-19.
- Pande, I.C. and Viridi, N.S., 1970, On the Chareota window structure, District Mahasu, Himachal Pradesh : Jour. Geol. Soc. India, V.11, No.3, p.245-278.
- Pande, I.C. and Prasad, A.K., 1977, Petrometallogenetic series of magmatites and metallogeny in the Himalaya : Him. Geol. V.7, p.158-174.
- Pandey, B.K., Singh, V.P., Bhanot, V.B. and Mehta P.K., 1981, Rb-Sr geochronological studies of the gneissic rocks of the Ranikhet and Masi area of Almora Crystallines, Lesser Himalaya, Kumaun, U.P. (Abs), 12th Himalayan Geology Seminar, Dehradun.
- Pecher, A., 1975, The Main Central Thrust of the Nepal Himalaya and the related metamorphism in the Modi-Khola cross-section : Him. Geol. V.5, p.115-132.

- Pecher, A., 1977, Geology of the Nepal Himalaya : Deformation and petrography in the Main Central Thrust zone : *Eclog. Geol. Himalaya*, V.268, p.301-318.
- Pecher, A., and Le Fort, P., 1977, Origin and significance of the Lesser Himalaya augen gneisses : *Colloq. Int. CNRS No.268, Ecologie et Geologie de l'Himalaya, Sci. de la Terre*, Paris, p.319-329.
- Polder vaart, A., 1955, Chemistry of the Earth's Crust : *Geol. Soc. Am. Spec. Paper 62*, p.119-144.
- Powell, C. McA. and Conaghan, P.J., 1973, Polyphase Deformation in Phanerozoic Rocks of the Central Himalayan Gneiss, Northwest India. *Jour. Geol.* V.81, No.2, p.127-143.
- Powell, C. McA. and Conaghan, P.J., 1975, Tectonic models for the Tibetan Plateau : *Geology*, V.4, p.727-731.
- Prasad, A.K., Jiwan, J.S., and Gupta, B.C., 1980, Metabasites of Bhuntar-Manikaran area, Himachal Pradesh, their tectonomagmatic mineralogical and correlative significance : Publication of the Centre of Advanced Study in Geology, Department of Geology, Panjab University, Chandigarh, 8th Seminar Volume, No.12, p.254-270.
- Price, P.B. and Walker, R.M., 1963, Fossil tracks of charged particle tracks in mica and age of minerals : *Jour. Geophys. Res.*, V.68, p.4847-4862.
- Raju, B.N.V., Chabria, T., Prasad, R.N., Mahadevan, T.M. and Bhalla, N.S., 1981, Early Proterozoic Rb-Sr Isochron Age Central Crystalline Gneiss, Bhilangan Valley, District, Tehri, Uttar Pradesh (Abstract) : 12th Him. Geol. Seminar, Dehra Dun.
- Ramberg, H., 1949, The facies classification of rocks : a clue to the origin of quartzo-feldspathic massifs and veins : *Jour. Geol.*, V.57, p.18-54.
- Ramberg, H., 1952, The origin of metamorphic and metasomatic rocks : University of Chicago Press, Chicago, 317 p.
- Ramdohr, P. 1940, Die Erzminerale in gewöhnlichen magmatischen Gesteinen, Ab Landl, Preuss, Alld, Wiss, Math-naturw Klasse, No.2
- Rankama, K. and Sahama, Th. G., 1950, *Geochemistry* Chicago Press, 911 p.
- Ranga Rao, A (1972), Traverses in the Himalay of U.P. : *Geol. Survey of India, Misc. Publ. No.15*, p.31-44.

*

Rickard, M.J., 1961, A note on cleavages in crenulated rocks :
Geol. Mag., V.98(4), p.324-332.

- Rao, J.S.R.K. and Raju, R.D., 1977, X-ray studies on the structural state orthoclase content and Al-distribution in tetrahedra of potassium feldspars from Southern India: Jour. Geol. Soc. India. V.18, p.118-124.
- Ramsay, J.G., 1967, Folding and fracturing of rocks : McGraw-Hill, New York, 568 p.
- Ray, S., 1947, Zonal metamorphism in the Eastern Himalayas and some aspects of local geology : Quart. Jour. Geol. Min. Met. Soc. India, V.19, p.117-140.
- Ray, S.K., and Naha, K., 1971, Structural and metamorphic history of the "Simla Klippe" : a summary : Him. Geol. V.1, p.1-24.
- Reesor, J.E., 1965, Structural evolution and plutonism in Val halla gneiss complex, British Columbia; Geol. Surv. Con. Bull. 129, 128 p.
- *
Ringwood, A.E., 1975a, composition and Petrology of the Earth's Mantle : McGraw-Hill, New York.
- Ringwood, A.E., 1975b, Some aspects of the minor element chemistry of lunar mare basalts : The Moon 12, p.127-157.
- Ringwood, A.E., 1979, Origin of the Earth and the Moon : Springer-Verlag, New York, 295 p.
- Roedder, E., 1979, Fluid inclusions as samples of ore fluids: In Barnes, H.L., (Ed.), Geochemistry of hydrothermal ore deposits : John Wiley & Sons, Inc., p.684-737.
- Roper, P.J., 1972, Structural significance of "Button" or "fish-scab" texture in phyllonitic schist of the Brevard Zone, Northwestern South Carolina : Bull. Geol. Soc. Am., V.83, p.853-860.
- Saini, H.S., 1982, Radiometric geochronology of the Himalaya: Jour. Geol. Soc. India, V.23, p.290-293.
- Saini, H.S., Nagpaul, K.K. and Sharma, K.K., 1978, Fission track ages from Pandoh Baggi Tunnel area, Himachal Himalaya, and their tectonic interpretations : Tectonophysics, V.46, p.87-98.
- Saini, H.S., Waraich, R.S., Malhotra, N.K. and Nagpaul, K.K., 1979, Cooling and uplift rates and dating of dating of thrusts from Kinnaur, Himachal Himalaya : Him. Geol. V.9,
- Sarkar, S.N. and Shrish, 1976, Tectonic analysis of a part of the folded Baijnath Nappe and inner sedimentary Belt in the Baijnath Kausani-Someshwar Area, U.P. : Him. Geol. V.6, p.27-74.

- Saxena, M.N., 1971, The crystalline axis of the Himalaya : the Indian shield and continental drift : Tectonophysics, V.12, p.433-447.
- Schwan, W., 1980, Shortening structures in Eastern and North-western Himalayan rocks : Today and Tomorrow's Printers and Publishers, New Delhi, 62 p.
- Shackleton, R.M., 1981, Structure of Southern Tibet : report on a traverse from Lhasa to Kathmandu organized by Academia Sinica : Jour. Struct. Geol., V.3, No.1, p.97-105.
- Shah, S.K. and Sinha, A.K., 1974, Stratigraphy and tectonics of the "Tethyan" zone in a part of Western Kumaun Himalaya : Him. Geol., V.5, p.1-27.
- Shapiro, L., 1975, Rapid analysis of silicate carbonate and phosphate rock-revised edition, Geol. Surv. Bull. 1401, U.S.G. 71 p.
- Sharma, K.K., 1977, A contribution to the Geology of the Sutluj, Valley, Kinnaur, Himachal Pradesh, India : Colloq. Internat. du. C.N.R.S., No.268, Ecolo. Geol. de l' Himalaya, p.369-378.
- Sharma, K.K., Bal, K.D., Parshad, R., Lal, N. and Nagpaul, K.K., 1980, Paleo-uplift and cooling rates from various orogenic belts of India, as revealed by radiometric ages : Tectonophysics, V.70, p.135-158.
- Sharma, K.K., Sinha, A.K., Bagdararian, G.P. and Ch. Gukarian, R.S., 1978, Potassium-Argon dating of Dras volcanics Shyok volcanics and Ladakh Granite, Ladakh NW Himalaya : Him. Geol. V.8, p.288-295.
- Sharma, V.P., 1977, The stratigraphy and structure of parts of the Simla Himalaya : Mem. Geol. Surv. India, V.106, 488 p.
- Shaw, D.M. and Kudo, A.M., 1965, A test of the discriminant function in the amphibolite problem : Miner. Mag. V.34, p.423-435.
- Shelley, D., 1972, Porphyroblasts and "crystallization force". Some textural criteria discussion : Bull. Geol. Soc. Am., V.83, p.919-920.
- Shipulin, F.K., 1975, The geochemistry of chalcophile elements during magmatic processes : In Tugarsinov, A.T. (Ed.), Recent contribution to Geochemistry and Analytical chemistry, John Wiley and Sons, New York, p.318-323.

- Sighinolfi, G.P., 1971, Investigations into deep crustal levels : fractionation effects and geochemical trends related to high-grade metamorphism. *Geochim. Cosmochim. Acta.*, V.35, p.1005-1021.
- Sighinolfi, G.P., and Gorgoni, C., 1978, Chemical evolution of high-grade metamorphic rocks-anatexis and remotion of material from granulite terrains chemical Geology, V.22, p.157-176.
- Sinha, A.K., and Bagdosarian, G.P., 1976, Potassium-Argon dating of some magmatic and metamorphic rocks from Tethyan and lesser zones of Kumaun and Garhwal Indian Himalaya and its implication in the Himalayan tectogenesis : *Colloq. Int. CNRS No.268, Ecologie et Geologie de l'Himalaya, Sci. de la Terre, Paris*, p.387-393.
- Sinha Roy, S., 1973, Gondwana pebble Slate in the Rangit Valley tectonic window, Darjeeling Himalaya, and its significance: *Jour. Geol. Soc. India*, V,14, p.31-39.
- Sinha Roy, S., 1974, Polymetamorphism in Daling rocks from a part of the eastern Himalayas and some problems of Himalayan metamorphism : *Him. Geol.* V.4,
- Sinha Roy, S., 1975. Polymetamorphism in the Daling rocks from a part of Kalimpong hills, eastern Himalaya and some problems of Himalayan metamorphsim. *Him. Geol.* V.4, p.74-101.
- Sinha Roy, S., 1976, A possible Himalayan microcontinent : *Nature*, V.263, No.5573, p.117-120.
- Sinha Roy, S., 1977, Mylonitic microstructure and their bearing on the development of mylonites- an example from deformed trondhjemites of the Bergen Arc region, SW Norway : *Geol. Mag.*, V.114, p.445-458.
- Sinha Roy, S., 1978, Himalayan transverse faults and folds and their parallelism with subsurface structures of North Indian Plains Discussion: *Tectonophysics*, V.45, p.229-237.
- Sinha Roy, S., 1978, Eastern Tethys and microplates framed in Himalayan, Central and Southeast Asian Geology: *Proc. III Regional Conference on Geology and Mineral Resources of Southeast Asia, Bangkok*, p.165-171.
- Sinha Roy, S., 1980, Stratigraphic relations of the Lesser Himalayan Formations of Eastern Himalaya : In Valdiya, K.S. and Bhatia, S.B., (Eds.), *Stratigraphy and Correlations of Lesser Himalayan Formations*, Hindustan Publishing Corporation (India), Delhi, p.242-254,

- Sinha Roy, S., and Furnes, H., 1978, Geochemistry and geotectonic implication of basic volcanic rocks in the Lower Gondwana sequence (Upper Paleozoic) of the Sikkim Himalayas : Geol. Mag. V.115 (6), p.427-436.
- Sinha Roy, S., 1979, Structural Evolution of Basement (?) Gneisses in Eastern Sikkim : In Verma, P.K., (Ed.), Metamorphic Rock Sequences of the Eastern Himalaya, K.P. Bagchi & Co., Calcutta, p.43-66.
- Sinvhal, H., Agrawal, P.N., King, G.C.P. and Gaur, V.K., 1973, Interpretations of measured movements at a Himalayan (Nahan) thrust : Geophys. J. R. Astron. Soc., V.34, p.203.
- Snowden, P.A., and Snowden, D.V., 1981, Petrochemistry of the late Archean granites of the Chinamora batholith, Zimbabwe : Precambrian Research, V.16, p.103-129.
- Spry, A., 1969, Metamorphic Textures : Pergamon Press, Oxford, 350 p.
- Spry, A., 1972, Porphyroblasts and "crystallization force". Some textural criteria: discussion. Bull. Geol. Soc. Am., V.83, p.1201-1202.
- Srikantia, S.V. and Bhargava, O.N., 1974, The Salkhala and the Jutogh relationship in the Kashmir and Himachal Himalaya: A reappraisal : Him. Geol., V.4, p.394-413.
- Srikantia, S.V., and Sharma, R.P., 1976, Geology of the Shali belt and the adjoining areas : Mem. Geol. Surv. India, V.106, p.31-166.
- Stocklin, J., 1977, Structural correlation of the Alpine ranges between Iran and Central Asia : Mem. h. Ser. Soc. Geol. Fr., V.8, p.333-353.
- Stoliazka, F., 1866, Geological sections across the Himalayan mountains from Wangtu bridge on the River Sutluj to Sungdo on the Indus, with an account of the formations in Spiti, accompanied by a revision of all known fossils from that district : Mem. Geol. Surv. India, V.5, 153 p.
- St-Onge, M.R., 1981, "Normal" and "inverted" metamorphic isograds and their relation to syntectonic Proterozoic batholiths in the Wopmay Orogen, Northwest Territories, Canada : Tectonophysics, V.76, p.295-316.
- Storre, B. and Karotke, E., 1971, An experimental determination of Upper stability limit of muscovite + quartz in the range 7-20 Kb water pressure : Neues. Jahrb. Mineral Monatsh, p.237-240.

- Strachey, R., 1851, On the geology of part of the Himalaya and Tibet : Quart. Jour. Geol. London, V.7, p.292-310.
- Sugimura, A., 1968, Spatial relations of basaltic magmas in island arcs: In Hess, H.H. and Polder vaart, A., (Ed.), Basalt', V.2 p.
- Taron, P.B., 1979, Basic volcanic rocks of Uttar Pradesh and Himachal Pradesh, Lesser Himalaya - a review : Miscellaneous publications no.41 of Geological Survey of India, p.315-336.
- Tewari, A.P., 1970, Director Generals General Report for 1966-67: Rec. Geol. Surv. India. V.101, p.71-72.
- Tewari, A.P., Setti, D.N. and Seiz, J.F., 1972, The significance of Ghuttu Window to the north of the Main Central Thrust, Tehri Garhwal, U.P. Geol. Surv. India, Misc. Publ. No.15, p.195-206.
- Thakur, V.C. 1973, Some genetic significance on the development of foliation and lineation in the Dalhousie granite body and surrounding metasedimentary formations of the Chamba area of Himachal Pradesh : Recent Researches in Geology, Hindustan Publishing Corporation (India), Delhi, p.41-52.
- Thakur, V.C., 1977, the divergent isogrs of metamorphism in some parts of Higher Himalaya zone : Ecolg. geol., Himalaya, V.268, p.433-443.
- Thakur, V.C., 1980, Tectonics of the Central Crystallines of Western Himalaya : Tectonophysics, V.62, p.141-154.
- Thakur, V.C., 1981, An overview of thrusts and nappes of western Himalaya : Thrust and Nappe Tectonics, Geol. Soc. London, p.381-392.
- Toksoz, M.N. and Bird, P., 1977, Modelling of temperatures in continental convergence zones : Tectonophysics V.14, p.181-193. 41
- Troger, W.E., 1979, Optical Determination of Rock-forming Minerals : Part 1, E. Schweizerbartsche Verlagsbuchhandlung, Stuttgart, 188 p.
- Turekian, K.K., 1963, The chromium and nickel distribution in basaltic rocks and eclogites : Geochim. Cosmochim. Acta, V.27, p.835-846.
- Turner, F.J., 1968, Metamorphic Petrology, Mineralogical and Field Aspects : McGraw-Hill Book Company, New York, 403 p.

- Tuttle, O.F. and Bowen, N.L., 1958, Origin of granite in the light of experimental studies in the system $\text{NaAlSi}_3\text{O}_8$ - KAlSi_3O_8 - SiO_2 - H_2O : Mem. Geol. Soc. Am. V.74, p.1-153.
- Valdiya, K.S., 1962, An outline of the stratigraphy and structure of the southern part of the Pithoragarh District: Jour. Geol. Soc. India, V.3, p.27-48.
- Valdiya, K.S. and Gupta, V.J., 1972, A contribution to the geology of northeastern Kumaun with special reference to the Hercynian gap in Tethys Himalaya : Him. Geol. V.2, p.1-33.
- Valdiya, K.S., 1973, Lithological subdivision and tectonics of the "central crystalline zone" of Kumaun Himalaya : Proc. Semin. Geodyn. Himalayan Region, N.G.R.I., Hyderabad, p.204-205. (abstr.).
- Valdiya, K.S., 1976, Himalayan transverse faults and folds and their parallelism with subsurface structures of North Indian Plains : Tectonophysics, V.32, p.353-386.
- Valdiya, K.S., 1977, Structural set up of the Kumaun Lesser Himalaya : Proc. Colloqu Ecol. Himalaya, C.N.R.C. Paris, p.449-462.
- Valdiya, K.S., 1978, Extension and analogue of the Chail Nappe in Kumaun : Ind. Jour. Earth Sci., V.5, p.1-19.
- Valdiya, K.S., 1980, The two intracrustal boundary thrusts of the Himalaya : Tectonophysics, V.66, p.323-348.
- Valdiya, K.S., 1981, Geology of the Kumaun Lesser Himalaya, Wadia Inst. Himalayan Geol., Dehradun.
- Varadarajan, S., 1977, Potassium-Argon age of the metasites from the Bhim Tal - Bhawali area Nainital district, Kumaon Himalaya and its significance : in Tiwari, B.S. and Gupta, V.J., Recent Researches in Geology (Vol.3), Hindustan Publishing Corporation, New Delhi, p.233-251.
- Vaughan, D.J., 1976, Sedimentary geochemistry and mineralogy of the sulphides of lead-zinc, copper and iron, and their occurrence in sedimentary ore deposits : in Wolf, K.H. (Ed.), Handbook of stratiform and stratiform ore deposits : Elsevier, Amsterdam, p.351-358.
- Veevers, J.J., Jones J.G. and Talent J.A., 1971, Indo-Australian stratigraphy and the configuration and dispersal of Gondwanaland : Nature, V.229, No.5284, p.383-388.

- Veevers, J.J., Powell, C.McA. and Johnson, B.D., 1975, Greater India's place in Gondwanaland and in Asia : Earth Planet Sci. Lett. V.27, p.383-387.
- Veevers, J.J. Powell, C.McA. and Johnson B.D., 1980, Seafloor constraints on the reconstruction of Gondwanaland : Earth Planet Sci. Lett. V.51, p.435-444.
- Verma, P.K., (Ed.), 1979, Metamorphic rock sequences of the Eastern Himalaya : K.P. Bagchi & Co. Calcutta, 166 p.
- Vernon, R.H., 1977, Microfabric of mica aggregates in partly recrystallized biotite : Contrib. Mineral. Petrol. V.61, p.175-185.
- Viljoen, M.J. and Viljoen, R.P., 1969, The geology and geochemistry of the lower ultramafic unit of the Onverwacht group and a proposed new class of igneous rock : Spec. Publ. Geol. Soc. S.Africa, No.2, p.55-85.
- Virdi, N.S., 1976, Stratigraphy and structure of the area around Nirth, district Simla, Himachal Pradesh : Him. Geol. V.6, p.163-175.
- Vorontsov, A.Y. and Line N.G., 1966 Rubidium and lithium in the granitoids of the Bugulmin complex (Eastern Sayans) : Geochem. Internat. V.3, p.1108-1116.
- Vuagnat, M., 1949, Sur les pillow lavas dalradicnues de la penisule de Tayvallich (argyllshire): Schweiz Min. Petr. Mitt., V.29, p.524-536.
- Wadia, D.N., 1975, Geology of India : IV Ed., Tata McGraw Hill, New Delhi, 508 p.
- Wakhaloo, S.N. and Dhar, S.L., 1972, Metamorphism of pelitic rocks from Kishtwar area, Kashmir : Him. Geol. V.2, p.317-329.
- Walker, F. and Poldervaart, A., 1949, Karro dolerites of the Union of South Africa : Bull. Geol. Soc. Am., V.60, p.591-706.
- Walker, K.R., 1969, A mineralogical, petrological and geochemical investigation of the Palisades Sill, New Jersey : Geol. Soc. Am. Mem., No.115, p.175-187,
- Wedepohl, K.H.(Ed.) , 1969, Handbook of Geochemistry, V.I, Springer Verlag Berlin, 442 p.
- Winkler, H.G.F., 1976, Petrogenesis of metamorphic rocks (4th Edition) Springer-Verlag, New York, 1979, (5th Edition) Springer-Verlag, New York.

- Winkler, H.G.F., 1979, Petrogenesis of Metamorphic Rocks (5th Ed.) Springer-Verlag, New York,
- Wiseman, J.D.H., 1934, Central and southwest Highland epidiorites, A study in progressive metamorphism : Quart. Jour. Geol. Soc. V.190, p.354-417.
- Wright, T.L. and Stewart, D.B., 1968, X-ray and optical study of alkali feldspar : II determination of composition and structural state from refined unit-cell parameters and 2V : Am. Mineral, V.53, p.38-87.
- Wright, T.L., 1968, X-ray and optical study of alkali feldspars : II an X-ray metho for determining the composition and structural state from measurement of 20 values for three reflection: Am. Mineral., V.53, p.88-104.
- West, W.D., 1934, The Geology of the Himalaya : Curr. Sci., V.3, p.286-291-
- White, A.J.R., 1966, Genesis of migmatites from the Palmer Region of South Australia : Chem. Geol., V.1, p.165-200.
- Williams, P.F., Means, W.D. and Hobbs, B.E., 1977, Development of axial-plane slaty cleavage and schistosity in experimental and natural materials : Tectonophysics, V.42, p.139-158.
- Yoder, H.S., Jr., (Ed.), 1979, The Evolution of the Igneous Rocks : Princetone University Press, Princetone, New Jersey, 588 p.